ISSN 2307-8960 (online)

World Journal of *Clinical Cases*

World J Clin Cases 2019 June 26; 7(12): 1367-1534

Published by Baishideng Publishing Group Inc

World Journal of Clinical Cases

Contents

Semimonthly Volume 7 Number 12 June 26, 2019

World Journal of Clinical Cases
Volume 7 Number 12 June 26, 2019

Contents

NAME OF JOURNAL
World Journal of Clinical Cases

ISSN
ISSN 2307-8960 (online)

LAUNCH DATE
April 16, 2013

FREQUENCY
Semimonthly

EDITORS-IN-CHIEF
Dennis A Bloomfield, Sandro Vento

EDITORIAL BOARD MEMBERS
https://www.wjgnet.com/2307-8960/editorialboard.htm

EDITORIAL OFFICE
Jin-Lei Wang, Director

PUBLICATION DATE
June 26, 2019

INSTRUCTIONS TO AUTHORS
https://www.wjgnet.com/bpg/gerinfo/204

GUIDELINES FOR ETHICS DOCUMENTS
https://www.wjgnet.com/bpg/GerInfo/287

GUIDELINES FOR NON-NATIVE SPEAKERS OF ENGLISH
https://www.wjgnet.com/bpg/gerinfo/240

PUBLICATION MISCONDUCT
https://www.wjgnet.com/bpg/gerinfo/208

ARTICLE PROCESSING CHARGE
https://www.wjgnet.com/bpg/gerinfo/242

STEPS FOR SUBMITTING MANUSCRIPTS
https://www.wjgnet.com/bpg/GerInfo/239

ONLINE SUBMISSION
https://www.f6publishing.com

World Journal of Clinical Cases

Submit a Manuscript: https://www.f6publishing.com

World J Clin Cases 2019 June 26; 7(12): 1367-1382

DOI: 10.12998/wjcc.v7.i12.1367

ISSN 2307-8960 (online)

REVIEW

Biomarkers *vs* imaging in the early detection of hepatocellular carcinoma and prognosis

Lavinia Alice Balaceanu

ORCID number: Lavinia Alice Balaceanu (0000-0003-0441-3905).

Author contributions: Balaceanu LA conceived of, designed and performed the review of the literature, and wrote the manuscript.

Conflict-of-interest statement: The author declares no potential conflicts of interest in relation to this publication.

Manuscript source: Invited manuscript

Received: February 20, 2019
Peer-review started: February 20, 2019
First decision: March 11, 2019
Revised: April 7, 2019
Accepted: May 2, 2019
Article in press: May 3, 2019
Published online: June 26, 2019

P-Reviewer: Harmanci O, Gong Z, Suda T
S-Editor: Cui LJ

Lavinia Alice Balaceanu, Department of Internal Medicine, Carol Davila University of Medicine and Pharmacy, Sf. Ioan Clinical Emergency Hospital, Bucharest 42122, Romania

Corresponding author: Lavinia Alice Balaceanu, PhD, Associate Professor, Department of Internal Medicine, Carol Davila University of Medicine and Pharmacy, Sf. Ioan Clinical Emergency Hospital, Soseaua Vitan-Barzesti No. 13, Bucharest 42122, Romania. alice-balaceanu@yahoo.com
Telephone: +40-0213345190

Abstract

Hepatocellular carcinoma (HCC) is the 5th most frequently diagnosed cancer in the world, according to the World Health Organization. The incidence of HCC is between 3/100000 and 78.1/100000, with a high incidence reported in areas with viral hepatitis B and hepatitis C, thus affecting Asia and Africa predominantly. Several international clinical guidelines address HCC diagnosis and are structured according to the geographical area involved. All of these clinical guidelines, however, share a foundation of diagnosis by ultrasound surveillance and contrast imaging techniques, particularly computed tomography, magnetic resonance imaging, and sometimes contrast-enhanced ultrasound. The primary objective of this review was to systematically summarize the recent published studies on the clinical utility of serum biomarkers in the early diagnosis of HCC and for the prognosis of this disease.

Key words: Hepatocellular carcinoma; Biomarkers; Imaging; Ultrasonography; Computed tomography; Magnetic resonance imaging

Core tip: Hepatocellular carcinoma (HCC) is an important cause of morbidity and mortality worldwide. Current HCC screening and diagnostic guidelines are based on imaging techniques-ultrasonography for screening, and dynamic contrast-enhanced computed tomography, magnetic resonance, and ultrasound for diagnosis. The use of biomarkers is promising but the diverse aetiology and complex pathophysiological mechanisms of HCC make it difficult to find an ideal combination. This review systematically summarizes the existing data on the role of biomarkers in early diagnosis and prognosis of HCC, to promote efforts to find alternatives to the imaging investigations which are expensive and not always accepted by patients.

L-Editor: A
E-Editor: Wu YXJ

Citation: Balaceanu LA. Biomarkers *vs* imaging in the early detection of hepatocellular carcinoma and prognosis. *World J Clin Cases* 2019; 7(12): 1367-1382
URL: https://www.wjgnet.com/2307-8960/full/v7/i12/1367.htm
DOI: https://dx.doi.org/10.12998/wjcc.v7.i12.1367

INTRODUCTION

Hepatocellular carcinoma (HCC) is the 5th most frequently diagnosed cancer in the world, according to the World Health Organization (WHO)[1]. The incidence of HCC is between 3/100000 and 78.1/100000, with high incidence reported in areas with viral hepatitis B and hepatitis C, these being represented predominantly by the Asian and African geographic regions[1]. As such, the international clinical guidelines that are currently in use were generated according to the geographical area involved.

For HCC surveillance in general, persons with chronic hepatitis B virus (HBV) infection (HBV DNA level > 2000 IU/mL), HBV-related cirrhosis, family history of HCC or age over 40 years, the WHO guidelines recommend abdominal ultrasound and alpha-fetoprotein (AFP) measurement every 6 mo[2]. The same recommendations are given for patients with hepatitis C virus (HCV)-related cirrhosis[3].

The Canadian guidelines recommend ultrasound surveillance every 6 mo for high-risk groups, including individuals with HBV- or HCV-related cirrhosis, cirrhosis on fatty liver disease, or chronic carriers of HBV, as well as for non-cirrhotic patients[4]. If a liver nodule with a diameter of less than 1 cm is found, ultrasonography (US) will be repeated over 3 mo, in order to assess the increase in diameter or change in characteristics[4]. In the very early stage, the diagnosis could be done with radiologic techniques, such as 4-phase dynamic contrast-enhanced computed tomography (CT) scan or gadolinium-enhanced magnetic resonance imaging (MRI), or biopsy[4]. Contrast-enhanced US (CEUS) has the same sensitivity as dynamic contrast-enhanced CT or MRI in liver nodule diagnosis[4]. For indeterminate liver nodule, biopsy showing cellular characteristics and positive staining for glypican-3, glutamine synthetase, heat shock protein 70 and clathrin heavy chain are necessary[4]. Serum biomarkers such as AFP, AFP-L3 (the fucosylated component of AFP or lens culinaris agglutinin-reactive fraction of AFP) and des-gamma-carboxy prothrombin (DCP) are more useful in late-stage or aggressive HCC than in the early stage of small HCC, mainly because the biomarkers are not highly sensitive[4].

The American Association for the Study of Liver Diseases (commonly known as the AASLD) *guidelines* recommend 6-mo interval surveillance for cirrhotic patients, carried out by US with or without AFP detection[5]. For the HCC diagnostic evaluation, multiphasic CT or multiphasic MRI have similar performance[5]. The contrast agents used are extracellular (giving information about the liver nodule based on blood flow) or hepatobiliary (giving additional information about hepatocellular function)[5]. The selection of imaging method and contrast agent is made based upon the individual patient, MRI contraindications, and institutional factors[5]. In North America, multiphasic CEUS is not widely used, but it can be used for non-invasive HCC diagnosis[5]. If an indeterminate liver nodule has been discovered in a cirrhotic patient, it can be followed by imaging, with an alternative imaging procedure and/or an alternative contrast agent, or biopsy[5]. Large multicentre prospective studies are still needed, however, to identify non-imaging characteristics for predicting HCC progression as accurately as possible[5].

The American College of Gastroenterology (ACG) clinical guidelines recommend CT or MRI when a liver nodule is greater than 1 cm, with acoustic shadow detected by US, when AFP is elevated or rising in the absence of liver nodule, or with clinical suspicion of HCC[6].

For HCC screening, the National Comprehensive Cancer Network guidelines recommend 6-mo interval US for cirrhotic patients of any cause and for chronic hepatitis B patients, with or without AFP detection[7]. If US is inadequate, multiphasic contrast-enhanced CT or MRI are recommended[7].

The Australian guidelines include US and AFP as initial investigations in HCC surveillance[8]. HCC diagnosis is made based on findings from four-phase contrast-enhanced CT, contrast enhanced-MRI, CEUS in selected cases, and finally with PET and liver biopsy[8].

The European Association for the Study of the Liver (EASL) guidelines recommend ultrasonographic surveillance every 6 mo performed by experienced persons on individuals in high-risk populations[9]. In general, the AFP level varies in patients with

HBV- or HCV-related cirrhosis, either during flares of the infection, exacerbation of the cirrhotic state, or HCC progression[9]. For these reasons, AFP could produce false-positive results and is not used in surveillance programs[9]. As a diagnostic test, when added to ultrasound assessment, AFP has good sensitivity (with a 20 ng/mL cut-off) and good specificity (with a 200 ng/mL cut-off)[9]. These values were mostly obtained in patients with viral infection activity but cannot yet support the calculation of a cost-effective ratio for early HCC surveillance programs[9]. As to the clinical utility of the other biomarkers in the diagnosis or prognosis of the disease, they (*i.e.*, ALP-L3, DCP) are not recommended, alone or in combination, for early detection of HCC in surveillance programs[9]. For early diagnosis of HCC, the *EASL guidelines* recommend imaging techniques (multiphasic contrast-enhanced CT, dynamic contrast-enhanced MRI, or CEUS) for liver nodules of more than 1 cm diameter[9]. In small HCC, MRI with hepatobiliary contrast agents (*e.g.*, gadoxetic acid and gadobenate dimeglumine) has higher sensitivity than MRI with extracellular agents[9]. In non-cirrhotic cases, histological and immunohistological tests are used to confirm the HCC diagnosis[9].

The same recommendations are provided by the European Society for Medical Oncology (ESMO), with multiphasic contrast-enhanced CT or MRI for HCC diagnosis and no role for AFP in the diagnostic work-up[10].

The Japan guidelines recommend ultrasound examination with AFP measurement every 3-6 mo[11]. For cirrhotic patients, dynamic CT or dynamic MRI are recommended[11]. The three serum biomarkers AFP, AFP-L3 and DCP are used for definitive diagnosis of HCC or for the subsequent surveillance exams[11]. These biomarkers are also used to estimate the efficacy of treatment in HCC patients who presented elevated levels before treatment[11]. The response to treatment could be occasionally assessed, but with difficulty, by imaging techniques, with the associated changes (*e.g.*, lipiodol deposits, arterioportal shunt) compared to the serum biomarkers[11]. CEUS is recommended for estimating the residual tumours after percutaneous ablation therapy and transcatheter arterial chemoembolization[11].

The Asia-Pacific clinical practice guidelines recommend US only as a screening test and suggest it to not represent a diagnostic test[12]. When the screening test is positive, the diagnosis of HCC is made by dynamic CT, dynamic MRI, or gadolinium ethoxybenzyl diethylenetriamine pentaacetic acid (Gd-EOB-DTPA)-enhanced MRI[12]. From among the serum biomarkers, AFP with a level more than 200 ng/mL is used in combination with US in the surveillance programs[12]. Being a marker of necroinflammation and regeneration, AFP is elevated in active hepatitis and cirrhosis in the absence of HCC[12]. For that, in small HCC, AFP is not recommended as a confirmatory test[12]. Its level decreases with improvement of chronic hepatitis B activity and post-treatment with interferon treatment for chronic hepatitis C[12]. AFP-L3 seems to be more useful than AFP alone in differential diagnosis of HCC from benign nodules[12]. The role of DCP (also termed prothrombin induced by vitamin K absence II (PIVKA-II)) is still controversial in diagnostic performance for small HCC, as compared with AFP[12]. Serum glypican-3, as an HCC serum diagnostic biomarker, is also inconsistent[12]. Other serum biomarkers, such as Golgi protein 73 (GP73), osteopontin, microRNAs or circulating free DNA, are not yet applied in clinical practice, mainly due to the heterogeneous results of clinical trials and low cost-benefit[12]. No ideal combination of serum biomarkers has yet been found, as the increase in sensitivity is achieved with decreased specificity[12] (Table 1).

The International guidelines for CEUS recommendations cites dynamic CEUS as capable of evaluating the enhancement patterns of a liver nodule during arterial, portal venous and late phases, with the appearance being similar as that in contrast-enhanced CT and contrast-enhanced MRI[13].

CEUS has advantages over dynamic CT or MRI according to its features of providing a real-time evaluation of the arterial phase, applicability to renal failure patients, and its ability to diagnose malignant or non-malignant portal vein thrombosis, to select one or more nodules for biopsy from multiple nodules with different patterns, to localize small HCC for percutaneous ablation and to assess recurrence[4,13]. The post-vascular phase (also known as the Kupffer phase) can be evaluated with a specific ultrasonographic contrast agent, perfluorobutane, having a hydrogenated egg phospatidyl serine shell[13]. Enhancement defect can better characterize the HCC nodule[13]. Dependence on the operator's experience and a lower visibility of the sub-diaphragmatic segment of the liver, especially in liver steatosis, are the main disadvantages of CEUS[13] (Table 2).

LITERATURE SEARCH

A systematic literature search was carried out in the PubMed, Web of Science Core

Table 1 International guidelines for hepatocellular carcinoma surveillance programs

Guideline	Indications	AFP	Imaging	Period (mo)
WHO	HBV DNA > 2000 UI/mL, HCV cirrhosis	+	US	6
Canadian	Cirrhosis, HBV chronic carriers		US	6
AASLD	Cirrhosis	+/-	US	6
NCCN	Cirrhosis, HBV chronic hepatitis	+/-	US	6
Australian			US	
EASL			US	6
Japan	Cirrhosis	+	US/dynamic CT/MRI	3-6
Asia-Pacific		> 200 ng/mL	US	6

AASLD: American Association for the Study of Liver Diseases; CT: Computed tomography; EASL: European Association for the Study of the Liver; HBV: Hepatitis B virus; HCV: Hepatitis C virus; MRI: Magnetic resonance imaging; NCCN: National Comprehensive Cancer Network; US: Ultrasonography; WHO: World Health Organization.

Collection, Elsevier ScienceDirect and Google Scholar databases for the past 5 years, using the terms "hepatocellular carcinoma", "biomarkers hepatocellular carcinoma", and "imaging hepatocellular carcinoma". A total of 2318 articles and 720 reviews were found. The articles included in the study were limited to English full-text articles and reviews in humans, and excluding case reports or post-specific treatment (*i.e.*, chemotherapy or radiotherapy) studies.

AFP USED IN ALGORITHMS OR IN COMBINATION WITH OTHER BIOMARKERS

Genetic correction

Various authors have attempted to increase AFP sensitivity by different algorithms. The efficiency of serum AFP in primary HCC seems to be improved by genetic correction; for example, using the single-nucleotide polymorphisms rs12506899 and rs2251844, as shown in a Chinese study of elderly patients reported by Wang *et al*[14].

Age, biochemical laboratory tests, serial values of AFP

Tayob *et al*[15] used an algorithm based on patient age, findings of laboratory tests, and serial measurements of AFP levels for improving the rate of HCC detection in HCV-related cirrhosis. When AFP was incorporated in another algorithm along with levels of alanine aminotransferase (ALT), alkaline phosphatase, age and sex, the rate of HCC detection in HCV, HBV and non-viral liver disease was significantly enhanced, as shown by Wang *et al*[16].

AFP and DCP (PIVKA II)

Yu *et al*[17] found DCP sensitivity and specificity for HBV-related HCC to be greater than AFP. In that study, when DCP and AFP were used together as diagnostic biomarkers for HCC, their sensitivity and specificity were even greater. Chen *et al*[18] found that the various prediction algorithms including AFP and DCP had a higher efficacy for early HCC diagnosis in patients with liver cirrhosis. Fu *et al*[19] analysed the combination of DCP and AFP as biomarkers for primary HCC diagnosis, finding higher effects than with each biomarker alone. Qin *et al*[20] showed that a panel test comprised of AFP (cut-off of 10 ng/mL), DCP (cut-off of 4 ng/mL) and dickkopf-1 (cut-off of 2 ng/mL) had both a high sensitivity and specificity, superior to each biomarker alone. However, future studies are needed to assess the role of this panel in detecting early HCC and the cut-off levels for different stages of HCC[20].

In a meta-analysis, Chen *et al*[21] found that DCP had a better accuracy than AFP for detection of HCC, regardless of the tumour diameter, the patients' ethnicity (American, European, Asian, or African), or the aetiology of HCC (HBV-related or mixed). For the diagnosis of HCC associated with alcoholic and non-alcoholic fatty liver disease, AFP and DCP appeared to be the best combination of biomarkers in the study by Beale *et al*[22]. At a level of 15 ng/mL, AFP alone had a good sensitivity and a specificity of 100%[22]. Increasing AFP values during the course of liver disease should prompt a careful surveillance, while increased DCP levels prompt suspicion of larger tumours[22]. In monitoring of the evolution of hepatic cirrhosis associated with fatty liver disease, glypican-3, squamous cell carcinoma antigen-I, and follistatin have no benefit, according to this study[22].

Table 2 International guidelines for hepatocellular carcinoma diagnosis

Guideline	Liver nodule US	Biomarkers	Indications for biomarkers
Canadian	CT/MRI/CEUS	AFP, AFP-L3, DCP	Late stage/aggressive
AASLD	CT/MRI		
ACG	CT/MRI		
NCCN	CT/MRI		
Australian	CT/MRI/CEUS: Selected case		
EASL	CT/MRI/CEUS		
ESMO	CT/MRI		
Japan	CT/MRI	AFP, AFP-L3, DCP	Definitive diagnosis, efficacy of treatment
Asia-Pacific	CT/MRI/CEUS		

AFP: Alpha-fetoprotein; AFP-L3: Alpha-fetoprotein L3; AASLD: American Association for the Study of Liver Diseases; CEUS: Contrast-enhanced computed tomography; CT: Computed tomography; DCP: Des-gamma-carboxyprothrombin; EASL: European Association for the Study of the Liver; ESMO: European Society for Medical Oncology; MRI: Magnetic resonance imaging; NCCN: National Comprehensive Cancer Network; US: Ultrasonography.

AFP, AFP-L3, and DCP (PIVKA II)

Yu *et al*[23] reported that in early HCC, AFP-L3 has the best specificity and GP73 has the best sensitivity. The use of four combined biomarkers (AFP, AFP-L3, DCP, and GP73) in neural network models was shown to be capable of differentiating early HCC from liver cirrhosis[23]. Li *et al*[24] demonstrated that a panel test of AFP, AFP-L3 and PIVKA II with the GALAD scoring algorithm is better for early diagnosis of HCC than any of the biomarkers used alone. The utility of the triple combination of the biomarkers was also demonstrated by other authors, including Gao *et al*[25], Caviglia *et al*[26], Best *et al*[27], and Berhane *et al*[28]. Optimal follow-up was analysed by Oeda *et al*[29], as an independent factor of receipt of curative treatment. Wongjarupong *et al*[30] revealed an association between AFP, AFP-L3, DCP and tumour size, to predict the recurrence after liver transplant. Best *et al*[27] studied patients with HCC of different aetiology (*i.e.*, viral infection, and alcoholic and non-alcoholic steatohepatitis) and found an increased specificity for AFP (cut-off of 20 ng/mL) in non-viral HCC; AFP-L3 had an increased sensitivity in non-viral HCC, and DCP had an increased specificity in viral HCC. Combination of the three biomarkers improved the sensitivity, and the use of GALAD scores increased the specificity, including for early HCC diagnosis.

AFP and AFP-L3

Li *et al*[31] analysed a combination of high-level AFP, AFP-L3 and AFP-L3 to AFP ratio and ALT, as predictive factors for HCC in HBV cirrhotic patients, while GP73 level decreased after development of HCC. Kim *et al*[32] used multiple reaction monitoring-mass spectrometry and found serum AFP-L3 as the lower limit and producing less false-negative results.

AFP and osteopontin

Duarte-Salles *et al*[33] suggested a combination of osteopontin and AFP as the best predictors for HBV-related HCC. Ge *et al*[34] showed that osteopontin in combination with AFP and dickkopf-1 have an increased sensitivity in early diagnosis of HBV-related HCC; osteopontin alone had a lower specificity, being increased in chronic HBV hepatitis and liver cirrhosis.

AFP and neutrophil-to lymphocyte ratio

Xing *et al*[35] suggested combinations of AFP and neutrophil-to-lymphocyte ratio for diagnosis of HBV- and HCV-related HCC. Hu *et al*[36] identified AFP, neutrophil-to-lymphocyte ratio, tumour size, and tumour number were independent predictors of microvascular invasion in HCC, associated with HBV and HCV infection.

AFP and serum human endothelial cell-specific molecule-1

Youssef *et al*[37] revealed that serum level of human endothelial cell-specific molecule-1 (cut-off of 2967 pg/mL) had a high sensitivity and specificity in HCV-related HCC patients. In combination with AFP and vascular endothelial growth factor, it was also found to be a predictive factor for mortality.

Serum thioredoxin

Li *et al*[38] found a higher sensitivity and specificity for serum thioredoxin (cut-off level 20.5 ng/mL) in detecting early HCC compared to those for AFP; when the two were combined the sensitivity increased.

AFP, α-L-fucosidase (AFU), and 5'-nucleotidase (5'-NT)

In a small number of patients with primary HCC, Junna *et al*[39] found the combination of AFU, 5'-NT and AFP to have significantly elevated levels (*vs* a control group).

OTHER BIOMARKERS FOR EARLY DETECTION OF HCC IN AFP-NEGATIVE PATIENTS

Although GPC3, GP73, osteopontin, micro (mi)RNAs, MDK, DKK1, and VEGF play roles in the diagnosis, prognosis and treatment of HCC, Song *et al*[40] and Chiba *et al*[41] revealed the need for further studies before widespread use in clinical practice. In a study of cirrhotic patients with HBV-related HCC, Shu *et al*[42] showed levels of AFP-L3 and GP-3 to be insignificantly different from those in the control group, but the fucosylated PON1 level was significantly increased. For cirrhotic patients with low-level AFP (< 20 ng/mL), an algorithm based on clinical characteristics, AFP and fucosylated kininogen was proposed by Wang *et al*[43]. In a study of hepatitis B surface antigen (HBsAg)-positive patients, Guo *et al*[44] found the combination of AFP and serum CD14 (AFP/CD14 cut-off of 0.197 ng/mL) to have higher sensitivity and specificity in early diagnosis of HCC. Kim *et al*[45] shows that fibronectin can differentiate HCC from cirrhosis. Chen *et al*[46] found soluble intercellular adhesion molecule-1 to be highly associated with HCC development in patients with HBV, HCV, non-alcoholic fatty liver disease, and alcoholic or cryptogenic liver disease. In a small study, Badr *et al*[47] found the serum calcium channel α2δ1 subunit (cut-off of 14.22 ng/mL) to have a high sensitivity and specificity, suggesting its potential as a novel biomarker in early detection of HCC in HCV cirrhotic patients. Wang *et al*[48] revealed an increased specificity, but a low sensitivity, of serum autoantibodies to nucleophosmin 1, 14-3-3zeta and mouse double minute 2 homolog proteins. Tayaka *et al*[49] proposed the von Willebrand factor antigen as a predictive biomarker for HCC development in HBV and HCV chronic hepatitis. Finally, several cytokines with significantly increased levels in HCC (*e.g.*, IL-1β, IL-6, IL-10, IL-17A, IL-22, and IL-250) and others with lower levels (*e.g.*, IL-4 and IL-33) in peripheral blood were shown by *Shen et al*[50] to be specific for HCC.

No biomarker to date has been shown to have high accuracy in the early detection of HCC; although, some may have clinical utility in the near future, as revealed by Tsuchiya *et al*[51]. While it has been shown that combinations of biomarkers or algorithms that add other clinical variables increase sensitivity and specificity, randomized clinical trials are required to validate the optimal combinations, especially in early detection of HCC, as suggested by Tsuchiya *et al*[51], Khattab *et al*[52] and Lou *et al*[53].

DCP (PIVKA-II)

In a meta-analysis, Zhu *et al*[54] demonstrated that DCP had moderate accuracy in early HCC diagnosis. Moreover, the results indicated DCP level may be different depending on ethnicity, possibly due to the predominantly different aetiology of HCC (alcoholic cirrhosis *vs* HBV and HCV chronic hepatitis) between Caucasians and Asians[54].

MiRNAs

MiRNAs are non-coding, endogenous, small RNAs, released in the case of liver cell damage into peripheral blood. Although there are multiple published studies, we cannot yet establish a unitary vision of the best combination of miRNAs for early diagnosis of HCC. This may be due, at least in part, to the different aetiologies of HCC in various geographic areas and possibly to genetic polymorphisms. Some authors have reported miRNA as a single test or in combination with other biomarkers/biochemical tests useful in the early diagnosis of HCC. Xu *et al*[55] reported that serum exosomal hnRNPH1 mRNA (cut-off of 0.670) had a high sensitivity and specificity for HCC, suggesting its potential as an HCC diagnostic biomarker in regions of high HBV prevalence. In combination with AFP, these values were improved. However, the authors of this study were not able to compare RNA levels in patients with active

HBV infection *vs* inactive, compensated *vs* decompensated liver cirrhosis, or various stages of fibrosis[55].

In a small study, Balkan *et al*[56] found no difference in levels of miR-122 and miR-192 between the HCC group (mostly patients with HBV-related disease) and the control group (non-alcoholic fatty liver disease patients). In contrast, the miR-26 serum level was much lower in the HCC patients. Long *et al*[57] reported a higher sensitivity and specificity for miR-88 in the whole blood *vs* AFP for detection of early HCC, also HBV-related. Shi *et al*[58] found an association of mi-RNA-106b with HCC for early detection, but further trails are needed to determine the threshold value. Liu *et al*[59] reported miRNA-125b, AFP and tumour size to be predictors of microvascular invasion in patients with HCC, prior to surgery. Serum level of miR-4463 was reported by Hu *et al*[60] to be significantly higher in HCC patients, no matter the sex of the patients, the size of the nodule, the stage of the HCC, the pathological type, or the values of the other serum factor tests (*i.e.*, ALT, aspartate aminotransferase, total bilirubin, and HBsAg status). In that study the highest level of miRNAs was found in the group of patients with the lowest level of AFP and shorter survival time[60].

Other authors have reported combinations of miRNAs useful in the early diagnosis of HCC. As reported by An *et al*[61], miR-122 in combination with miR-375, miR-10a, and miR-423 could be used for diagnosis and prognosis of HCC. Jiang *et al*[62] reported a panel with miR-10b, miR-106b, miR-181a as biomarkers applicable to screening for HCC in Chinese patients. Xue *et al*[63] reported the success of another panel composed of eight miRNAs (miR-122, miR-125b, miR-145, miR-192, miR-194, miR-29a, miR-17-5p, miR-106a) with significantly increased levels in serum for patients with HCC (mostly associated with HBV infection). Liu *et al*[64] studied a combination of high serum miR-21 and mi-R106b and low serum mi-R224 levels and found a high sensitivity and specificity for HCC compared with cirrhotic levels, predominantly HBV-related. In a meta-analysis, Liao *et al*[65] revealed that serum miR-21 could be used as a co-biomarker in early detection of HCC, due to its high sensitivity and specificity. In another meta-analysis, by Ding *et al*[66], multiple serum miRNAs (miR-21, miR-199, and miR-122) had a relatively high accuracy in HCC diagnosis. Xu *et al*[67] showed that serum levels of miRNA-25, miRNA-375 and let-7f can play a role in diagnosis of HCC. Finally, high levels of serum exosomal miR-122, miR-148a and AFP were studied by Wang *et al*[68] and found to be adequate for HCC diagnosis and screening programs (Table 3).

In comparison to the predominant HCV aetiology, the HBV-related HCC has a different profile of altered miRNA expression. Mohamed *et al*[69] studied miR-23a and found a high sensitivity for HCC, mostly for HCV-related cases. Other authors have reported on a panel of miRNAs useful in the early diagnosis of HCV-related HCC. Motawi *et al*[70] reported a combination of serum miR-19a, miR-146a, miR-192 and miR-195 with increased accuracy in early detection of HCV-related HCC. Amr *et al*[71] reported miR-122 and miR-224 as early diagnostic serum biomarkers in HCV-related HCC. Elemeery *et al*[72] found that a panel of miRNAs composed of miR-214-5p, miR-375, miR-125b and miR-1269 had an increased sensitivity for the early detection of HCV-related HCC. Serum miR-939 and miR-595 were identified by Fornari *et al*[73] as independent factors for HCC, mostly involving HCV-related cases. In that same study, the serum level of miR-519d was found to be correlated with the tissue level of miR-519d in HCC[73].

Xue *et al*[63] reported miR-106a to be an independent factor of overall survival and prognosis, fitting with its role in promotion of tumorigenesis. Zhuang *et al*[74] detected serum miR-128-2 in most of the patients with HBV-associated HCC. Results from a study by Zhu *et al*[75] suggested the potential of miR-192-5p and miR-29a-3p as biomarkers for progression of HBV-related HCC and survival, with an inverse relationship. Similarly, the results from a study suggested miR-23a as a prognostic biomarker.

In a systematic review, Klingenberg *et al*[76] concluded that non-coding RNAs [miRNA and long non-coding (lnc) RNA] can be used for early diagnosis in HCC, due to high sensitivity and specificity; however, most of the studies analysed had included cases with only one or two HCC aetiologies. If an HBV-related HCC panel of miRNAs (including miR-122 and miR-21) was to be studied for its diagnostic biomarker potential, the miRNAs should also be investigated for their potential in diagnosis of HCC associated with non-alcoholic fatty liver disease, alcohol or HCV infection in large trials with the specific group patients, as demonstrated by Schütte *et al*[77].

Zhang *et al*[78] considered the multiple origins of miRNAs, the lack of standardized protocols for pro-analytical manipulation of samples in research, the physiologic processing that would occur after the point of analysis, the unknown miRNA binding proteins, and the lack of existing large studies on patients and control populations to support any single or combination of miRNAs in a panel for clinical application for the detection and prognosis of patients with HCC. Likewise, Loosen *et al*[79] cited the

Table 3 MicroRNAs in hepatocellular carcinoma

miRNA	Hepatitis virus	Ref.
For early diagnosis		
exosomal hnRNPH1 miR	HBV	Xu *et al*[55]
miR-26	HBV	Balkan *et al*[56]
miR-88	HBV	Long *et al*[57]
mi-R-106b		Shi *et al*[58]
miR-125b		Liu *et al*[59]
miR-4463		Hu *et al*[60]
miR-10a, miR-122, miR-375, miR-423	HBV	An *et al*[61]
miR-10b, miR-106b, miR-181a	HBV	Jiang *et al*[62]
miR-17-5p, miR-29a, miR-106a, miR-122, miR-125b, miR-145, miR-192, miR-194	HBV	Xue *et al*[63]
miR-21, mi-R106b, mi-R224	HBV	Liu *et al*[64]
miR-21		Liao *et al*[65]
miR-21, miR-122, miR-199		Ding *et al*[66]
miR-25, miR-375, let-7f		Xu *et al*[67]
miR-122, miR-148a, AFP	HBV	Wang *et al*[68]
miRNA-23a	HCV	Mohamed *et al*[69]
miR-19a, miR-146a, miR-192, and miR-195	HCV	Motawi *et al*[70]
miR-122, miR-224	HCV	Amr *et al*[71]
miR-125b, miR-214-5p, miR-375, miR-1269	HCV	Elemeery *et al*[72]
miR-595, miR-939	HCV	Fornari *et al*[73]
For overall survival and prognosis		
miR-106a	HBV	Xue *et al*[63]
miR-128-2	HBV	Zhuang *et al*[74]
miR-192-5p and miR-29a-3p	HBV	Zhu *et al*[75]
miR-23a	HCV	Mohamed *et al*[69]

HBV: Hepatitis B virus; HCV: Hepatitis C virus.

need for standardization of sample collection, analysis, and data normalization and quantification methods to generate findings to support the inclusion of miRNAs in a diagnostic algorithm applied in clinical practice.

LncRNAs

LncRNAs are non-protein-coding transcripts with more than 200 nucleotides. Yuan *et al*[80] showed that, among the circulating lncRNAs, LINC00152, RP11-160H22.5 and XLOC014172 in combination with AFP could be predictive biomarkers for HBV-related HCC. Wang *et al*[81] found the lncRNAs uc001ncr and AX800134 to have high accuracy in detection of HBV-related HCC, especially in the early stage and when the level of AFP is lower than 400 ng/mL. Tang *et al*[82] found three lncRNAs RP11–160H22.5, XLOC_014172 and LOC149086, that can predict the occurrence of HBV-related HCC. Zheng *et al*[83] showed that high expression of serum UCA I is associated with high-grade HCC and advanced TNM stage, suggesting the potential of this factor as a biomarker for screening. In another study, Xu *et al*[84] demonstrated that ENSG00000258332.1 (cut-off of 1.345) and LINC00635 (cut-off of 1.690) had high sensitivity and specificity for HBV-related HCC. When these biomarkers were combined with AFP level higher than 20 ng/mL, both the sensitivity and the sensibility were increased (Table 4).

A meta-analysis by Chen *et al*[85] found that a panel of serum or plasma lncRNAs including LINC00152, RP11-160H22.5, XLOC014172, LOC149086 or HULC, Linc00152 or uc001ncr, AX800134 or PVT1, and uc002mbe.2 had a higher accuracy in HCC than any single lncRNA or in tissue samples. In that meta-analysis, the sensitivity and the specificity of the collective lncRNA biomarkers were both higher for Asian patients than for African patients[85]. In another meta-analysis, Hao *et al*[86] identified multiple factors that influenced the accuracy of lncRNAs in detecting HCC. However, the various aetiologies around the world (*i.e.*, HCV infection in Africa and Egypt, and HBV infection in Asia) may underlie the observation of plasma lncRNAs having a lower accuracy than serum lncRNAs[86].

Table 4 LncRNAs in hepatocellular carcinoma

LncRNA	Hepatitis virus	Ref.
For early diagnosis		
LINC00152, RP11-160H22.5 and XLOC014172	HBV	Yuan *et al*[80]
uc001ncr and AX800134	HBV	Wang *et al*[81]
RP11–160H22.5, XLOC_014172 and LOC149086	HBV	Tang *et al*[82]
UCA I	HBV	Zheng *et al*[83]
ENSG00000258332.1, LINC00635	HBV	Xu *et al*[84]
LINC00152, RP11-160H22.5, XLOC014172, LOC149086 or HULC, Linc00152 or uc001ncr, AX800134 or PVT1, uc002mbe.2		Chen *et al*[85]
Predictors for poor prognosis		
BANCR		Qin *et al*[88]
XLOC_014172 and LOC149086	HBV	Tang *et al*[82]
UCA I	HBV	Zheng *et al*[83]

HBV: Hepatitis B virus; HCV: Hepatitis C virus; lncRNA: Long non-coding RNA.

Zheng *et al*[87] reported poor rates of survival (1.25-fold increased risk) and recurrence-free survival (1.66-fold increased risk) in patients with higher levels of lncRNAs, supporting the proposal of these factors to serve as predictive biomarkers for HCC prognosis. Indeed, Qin *et al*[88] found high levels of the plasma lnc-RNA BANCR in HCC patients and determined a correlation with poor prognosis. In the study by Tang *et al*[82], the secondary increase of lncRNAs XLOC_014172 and LOC149086 following surgical treatment was found to be predictive of metastasis. Finally, serum UCA I was proposed by Zheng *et al*[83] as another biomarker for prognostic evaluation.

PLASMA METABOLITES

HCC is characterized by aerobic glycolysis, increased consumption of glucose, and high levels of lactate. This type of metabolism persists immediately following surgery or transcatheter arterial chemoembolization, as demonstrated by Chen *et al*[89]. Kim *et al*[90] studied the molecular changes produced by alteration in the energy metabolism pathways that underlie the metabolomic and proteomic observations, in order to better determine their practical application in the early detection of HCC. The study by Di Poto *et al*[91] supported a proposal for the combination of plasma metabolites with other co-variates, such as AFP, in early detection of HCC in cirrhotic patients. Saito *et al*[92] studied the serum metabolomic profile in patients with HBV-related HCC compared to that in patients with HCV-related HCC, and found distinctions, especially for glutamic acid, methionine, and gamma-Glu-Gly-Gly. Similarly, the type of HBV or HCV infection and the metabolic profile of the patient have important roles in establishing the metabolomic panel as diagnostic and prognostic markers in HCC, as shown by Fitian *et al*[93]. Finally, Ferrin *et al*[94] studied the potential protein biomarkers in HCV-alcoholic patients and identified the complement component 4a as an independent predictor of HCC.

Kimhofer *et al*[95] analysed numerous studies of metabonomic and proteomic biomarkers in a comprehensive review. The metabonomic biomarkers that have been studied are bile acids, lysophosphatidylcholines, free fatty acids, carnitine and energy metabolism-related products, but the best panel of these for early detection of HCC need to be validated before inclusion in future guidelines[95]. Finally, Guo *et al*[96] showed that although there are technological advances, the study of metabolomics, particularly for that of HCC, is still in its infancy.

SERUM LIPIDS

Passos-Castilho *et al*[97] proposed seven lipids detected by spectrometry as predictive of HCV-related HCC, with high sensitivity and moderate specificity. In a later study, Passos-Castilho *et al*[98] proposed four lipids as independent predictor factors of HBV-related HCC in cirrhotic patients, with moderate sensitivity and specificity.

SERUM BIOMARKERS FOR PREDICTION PROGRESSION OF DISEASE, POOR PROGNOSIS, AND RECURRENCE

Margetts *et al*[99] found a neutrophil-to-lymphocyte ratio of > 3.15 to be associated with poor survival. In addition, the Systemic Immune-Inflammation Index score was found to be strongly correlated with tumour size. High neutrophil-to-lymphocyte ratio was also proposed by Zheng *et al*[100] as a predictive biomarker of poor survival and poor recurrence-free survival in HCC patients before treatment. That study also found the high neutrophil-to-lymphocyte ratio as well as the platelet-to-lymphocyte ratio to be independent predictive factors for survival and recurrence in HCC patients with curative and palliative treatment. Goyal *et al*[101] proposed the red blood cell distribution width useful when to be incorporated in a prognostic panel of other inflammatory biomarkers for outcomes after HCC surgery. Serum cartilage oligomeric matrix protein and interleukin-6 have been studied by Van Hees *et al*[102] and shown to be predictive factors of HBV-related HCC, but large-scale studies are needed to validate them for use in current practice. In another study, by Hong *et al*[103], autoantibodies against tumour-associated antigens appeared to be more useful in the prognosis of HCC than in its early diagnosis; again, large studies are needed to clarify their roles in the various stages of HCC. Finally, Sun *et al*[104] determined that the circulating tumour cells assay is not useful for HCC detection when used as the sole biomarker; however, it did show promise as a predictor of poor prognosis.

The serum antibodies anti-HSP 70 and anti-Eno-1 were shown by Yu *et al*[105] to be predictive of microvascular invasion in HBV-related HCC prior to surgical treatment, with anti-Eno-1 having a better sensitivity and specificity.

IMAGING DIAGNOSIS

Kuo *et al*[106] reported a higher cost-effectiveness ratio for ultrasound screening compared to bimodal biomarkers (AFP and US) for early detection of HCC in endemic areas. However, this assessment cannot be universally valid, especially if screening is performed in patients with cirrhosis and without specialized and well-trained staff. A meta-analysis by Hanna *et al*[107] showed that CEUS has the same sensitivity as contrast-enhanced CT or gadolinium-enhanced MRI in diagnosis of HCC and that it is useful for supplementary characterization of the liver nodules detected by US.

Although dynamic CEUS has an important role in the diagnosis and characterization of small liver tumours, the ultrasonographic differential diagnosis between HCC and intrahepatic cholangiocellular carcinoma is difficult, sometimes having the same hypervascularization and washout pattern, as shown by Van Beers *et al*[108]. This does not happen with contrast-enhanced MRI or CT performed with small-molecular-weight agents, for both intravascular and extravascular extracellular space distribution[107]. Westwood *et al*[109] performed a systematic review to review imaging techniques and found that the sulphur hexafluoride microbubble used as contrast agent in US seems to have the same performance as contrast-enhanced-CT or MRI for diagnosis of focal liver lesions. However, it is necessary to standardize dynamic CEUS and generate clear criteria for comparing the three methods in the same patient[108,109]. Yao *et al*[110] proposed radiomic analysis in multi-modal US to determine the best to obtain a better differential diagnosis between benign and malign liver tumours, with a good prediction of microvascular invasion and Ki-67 and PD-1 expression.

The best sensitivity (85.6%) and positive predictive value (94.2%) in the imaging diagnosis of HCC has been reported for MRI with gadoxetate as the contrast agent, according to meta-analysis findings from Hanna *et al*[107]. In that study, the MRI with gadoxetate rates were followed by MRI with other contrast agents, contrast enhanced-CT, and US without contrast agent respectively. Although CEUS seems to have high sensitivity and positive predictive value, reference standards are required for proper comparison of the three contrast-enhanced imaging methods (MRI, CT, and US)[107]. In a comprehensive review, Ippolito *et al*[111] revealed the differences in contrast agents used in dynamic contrast-enhanced MRI perfusion according to application by different researchers and depending upon the intended purpose. For diagnosing and evaluating early HCC characteristics, gadobenate-dimeglumine or gadolinium ethoxybenzyl diethylenetriaminepentaacetic acid (Gd-EOB-DTPA) is recommended[111]. For prognosticating the disease, gadodiamide is recommended[111]. For investigating treatment response, Gd-EOB-DTPA, dadobenate-dimeglumine, gadopentetate-dimeglumine or gadodiamide are recommended[111].

According to European Society of Gastrointestinal and Abdominal Radiology (commonly known as ESGAR) consensus, Neri *et al*[112] revealed that MRI with Gd-

EOB-DTPA as the contrast agent is the best technique for characterization of focal lesions with diameter equal to or greater than 10 mm in a cirrhotic liver. The dual renal and hepatocyte elimination of Gd-EOB-DTPA makes it useful as a contrast agent for both perfusion imaging in the early phase and for hepatocyte imaging in the late phase[112]. Through dynamic contrast-enhanced MRI with Gd-EOB-DTPA, morphological and functional data can be obtained[112]. These features are particularly useful for HCC in cirrhotic liver, in late hepatic arterial phase (*i.e.*, hepatic artery and portal vein enhancement) and hepatobiliary phase (*i.e.*, delayed by reduced hepatic function)[112]. If MRI combines Gd-EOB-DTPA as a contrast agent with a diffusion weighted imaging technique, additional qualitative and quantitative data can be obtained on the degree of HCC differentiation, microvascular invasion, or response to treatment[111].

Functional MRI (*i.e.*, magnetic resonance elastography, diffusion-weighted MRI, or T1-weighted dynamic contrast-enhanced MRI) provides additional quantitative and qualitative information that is extremely useful both in HCC early diagnosis and in prognosis and response to treatment; these techniques are expected to find application on a large scale in clinical practice in the near future[111,112].

Tanabe *et al*[113] showed that the time interval between imaging investigations should be determined according to the initial LI-RADS staging. Because ultrasonographic nodules smaller than 2 cm in cirrhotic patients may be included in MRI investigations as initial LI-RADS stages and subsequently determined to be early HCC, Darnell *et al*[114] proposed an active work-up, including biopsy, for optimal HCC management. Yang *et al*[115] analysed some methods as dual-input two-compartment pharmacokinetic models of dynamic contrast-enhanced MRI to determine which could better predict microvascular characteristics of HCC. The dual-input extended Tofts model could better measure the extravascular extracellular space volume ratio, while the dual-input two-compartment exchange model could better predict the microvascular permeability. These data will be very useful for personalized treatment but need standardization and further large trials.

Kavanaugh *et al*[116] suggested that the complex cellular mechanisms involved in HCC growth determine a higher detection rate of small tumours by (4S)-4-(3-[^{18}F]fluoropropyl)-L-glutamic acid (^{18}F-FSPG) positron emission tomography (PET)-CT compared to 11C-acetate PET-CT; the former does not reach 100%, however, as not all HCCs express the x_c-transporter (gene symbol SLC7A11). Cho *et al*[117] revealed the utility of fluorine-18 fluorodeoxyglucose (^{18}F-FDG) PET-CT in early or intermediate HCC, in management of the disease (*i.e.*, hepatic resection or liver transplant), but it was found to not be useful in very early-stage HCC without extrahepatic metastases. Of note, accumulation of the ^{18}F-FDG radiotracer in inflammatory liver lesions is one of the limitations of this method for its use in the diagnosis of a hepatic nodule as HCC[117].

CONCLUSION

All clinical guidelines for diagnosis of HCC are based on ultrasound surveillance and contrast imaging techniques (*i.e.*, CT, MRI, and sometimes CEUS). Although there have been important advances in our understanding of the roles of various biomarkers in certain stages of the disease, especially in combinations, large studies involving certain population groups are needed before biomarkers can be introduced into clinical practice on a large scale. The different predominant aetiologies of certain geographical areas (*i.e.*, high incidence of HBV, HCV, alcoholic and non-alcoholic fatty liver disease, cryptogenic disease) make it difficult to find a unique combination of biomarkers for the diagnosis of HCC. Nonetheless, imaging techniques still play a leading role in both HCC surveillance and diagnosis.

REFERENCES

1 **Mak LY**, Cruz-Ramón V, Chinchilla-López P, Torres HA, LoConte NK, Rice JP, Foxhall LE, Sturgis EM, Merrill JK, Bailey HH, Méndez-Sánchez N, Yuen MF, Hwang JP. Global Epidemiology, Prevention, and Management of Hepatocellular Carcinoma. *Am Soc Clin Oncol Educ Book* 2018; **38**: 262-279 [PMID: 30231359 DOI: 10.1200/EDBK_200939]

2 **Geneva: World Health Organization**. Guidelines for the Prevention, Care and Treatment of Persons with Chronic Hepatitis B Infection. [PMID: 26225396]

3 **Geneva: World Health Organization**. WHO Guidelines Approved by the Guidelines Review Committee. Guidelines for the Screening Care and Treatment of Persons with Chronic Hepatitis C Infection: Update Version. [PMID: 27227200]

4 **Burak KW**, Sherman M. Hepatocellular carcinoma: Consensus, controversies and future directions. A report from the Canadian Association for the Study of the Liver Hepatocellular Carcinoma Meeting. *Can J*

Gastroenterol Hepatol 2015; **29**: 178-184 [PMID: 25965437]
5 **Heimbach JK**, Kulik LM, Finn RS, Sirlin CB, Abecassis MM, Roberts LR, Zhu AX, Murad MH, Marrero JA. AASLD guidelines for the treatment of hepatocellular carcinoma. *Hepatology* 2018; **67**: 358-380 [PMID: 28130846 DOI: 10.1002/hep.29086]
6 **Marrero JA**, Ahn J, Rajender Reddy K; Americal College of Gastroenterology. ACG clinical guideline: the diagnosis and management of focal liver lesions. *Am J Gastroenterol* 2014; **109**: 1328-1347; quiz 1348 [PMID: 25135008 DOI: 10.1038/ajg.2014.213]
7 **Benson AB**, D'Angelica MI, Abbott DE, Abrams TA, Alberts SR, Saenz DA, Are C, Brown DB, Chang DT, Covey AM, Hawkins W, Iyer R, Jacob R, Karachristos A, Kelley RK, Kim R, Palta M, Park JO, Sahai V, Schefter T, Schmidt C, Sicklick JK, Singh G, Sohal D, Stein S, Tian GG, Vauthey JN, Venook AP, Zhu AX, Hoffmann KG, Darlow S. NCCN Guidelines Insights: Hepatobiliary Cancers, Version 1.2017. *J Natl Compr Canc Netw* 2017; **15**: 563-573 [PMID: 28476736]
8 Optimal cancer care pathway for people with hepatocellular carcinoma. Available from: www.cancer.org.au/ocp
9 **European Association for the Study of the Liver**. European Association for the Study of the Liver. EASL Clinical Practice Guidelines: Management of hepatocellular carcinoma. *J Hepatol* 2018; **69**: 182-236 [PMID: 29628281 DOI: 10.1016/j.jhep.2018.03.019]
10 **Vogel A**, Cervantes A, Chau I, Daniele B, Llovet J, Meyer T, Nault JC, Neumann U, Ricke J, Sangro B, Schirmacher P, Verslype C, Zech CJ, Arnold D, Martinelli E; ESMO Guidelines Committee. Hepatocellular carcinoma: ESMO Clinical Practice Guidelines for diagnosis, treatment and follow-up. *Ann Oncol* 2018; **29**: iv238-iv255 [PMID: 30285213 DOI: 10.1093/annonc/mdy308]
11 **Kokudo N**, Hasegawa K, Akahane M, Igaki H, Izumi N, Ichida T, Uemoto S, Kaneko S, Kawasaki S, Ku Y, Kudo M, Kubo S, Takayama T, Tateishi R, Fukuda T, Matsui O, Matsuyama Y, Murakami T, Arii S, Okazaki M, Makuuchi M. Evidence-based Clinical Practice Guidelines for Hepatocellular Carcinoma: The Japan Society of Hepatology 2013 update (3rd JSH-HCC Guidelines). *Hepatol Res* 2015; 45 [PMID: 25625806 DOI: 10.1111/hepr.12464]
12 **Omata M**, Cheng AL, Kokudo N, Kudo M, Lee JM, Jia J, Tateishi R, Han KH, Chawla YK, Shiina S, Jafri W, Payawal DA, Ohki T, Ogasawara S, Chen PJ, Lesmana CRA, Lesmana LA, Gani RA, Obi S, Dokmeci AK, Sarin SK. Asia-Pacific clinical practice guidelines on the management of hepatocellular carcinoma: a 2017 update. *Hepatol Int* 2017; **11**: 317-370 [PMID: 28620797 DOI: 10.1007/s12072-017-9799-9]
13 **Claudon M**, Dietrich CF, Choi BI, Cosgrove DO, Kudo M, Nolsøe CP, Piscaglia F, Wilson SR, Barr RG, Chammas MC, Chaubal NG, Chen MH, Clevert DA, Correas JM, Ding H, Forsberg F, Fowlkes JB, Gibson RN, Goldberg BB, Lassau N, Leen EL, Mattrey RF, Moriyasu F, Solbiati L, Weskott HP, Xu HX. Guidelines and good clinical practice recommendations for contrast enhanced ultrasound (CEUS) in the liver--update 2012: a WFUMB-EFSUMB initiative in cooperation with representatives of AFSUMB, AIUM, ASUM, FLAUS and ICUS. *Ultraschall Med* 2013; **34**: 11-29 [PMID: 23129518 DOI: 10.1055/s-0032-1325499]
14 **Wang K**, Bai Y, Chen S, Huang J, Yuan J, Chen W, Yao P, Miao X, Wang Y, Liang Y, Zhang X, He M, Yang H, Guo H, Wei S. Genetic correction of serum AFP level improves risk prediction of primary hepatocellular carcinoma in the Dongfeng-Tongji cohort study. *Cancer Med* 2018; **7**: 2691-2698 [PMID: 29696820 DOI: 10.1002/cam4.1481]
15 **Tayob N**, Richardson P, White DL, Yu X, Davila JA, Kanwal F, Feng Z, El-Serag HB. Evaluating screening approaches for hepatocellular carcinoma in a cohort of HCV related cirrhosis patients from the Veteran's Affairs Health Care System. *BMC Med Res Methodol* 2018; **18**: 1 [PMID: 29301497 DOI: 10.1186/s12874-017-0458-6]
16 **Wang M**, Devarajan K, Singal AG, Marrero JA, Dai J, Feng Z, Rinaudo JA, Srivastava S, Evans A, Hann HW, Lai Y, Yang H, Block TM, Mehta A. The Doylestown Algorithm: A Test to Improve the Performance of AFP in the Detection of Hepatocellular Carcinoma. *Cancer Prev Res (Phila)* 2016; **9**: 172-179 [PMID: 26712941 DOI: 10.1158/1940-6207.CAPR-15-0186]
17 **Yu R**, Ding S, Tan W, Tan S, Tan Z, Xiang S, Zhou Y, Mao Q, Deng G. Performance of Protein Induced by Vitamin K Absence or Antagonist-II (PIVKA-II) for Hepatocellular Carcinoma Screening in Chinese Population. *Hepat Mon* 2015; **15**: e28806 [PMID: 26300931 DOI: 10.5812/hepatmon.28806v2]
18 **Chen H**, Zhang Y, Li S, Li N, Chen Y, Zhang B, Qu C, Ding H, Huang J, Dai M. Direct comparison of five serum biomarkers in early diagnosis of hepatocellular carcinoma. *Cancer Manag Res* 2018; **10**: 1947-1958 [PMID: 30022853 DOI: 10.2147/CMAR.S167036]
19 **Fu J**, Li Y, Li Z, Li N. Clinical utility of decarboxylation prothrombin combined with α-fetoprotein for diagnosing primary hepatocellular carcinoma. *Biosci Rep* 2018; 38 [PMID: 29717027 DOI: 10.1042/BSR20180044]
20 **Qin QF**, Weng J, Xu GX, Chen CM, Jia CK. Combination of serum tumor markers dickkopf-1, DCP and AFP for the diagnosis of primary hepatocellular carcinoma. *Asian Pac J Trop Med* 2017; **10**: 409-413 [PMID: 28552111 DOI: 10.1016/j.apjtm.2017.03.016]
21 **Chen J**, Wu G, Li Y. Evaluation of Serum Des-Gamma-Carboxy Prothrombin for the Diagnosis of Hepatitis B Virus-Related Hepatocellular Carcinoma: A Meta-Analysis. *Dis Markers* 2018; **2018**: 8906023 [PMID: 30402170 DOI: 10.1155/2018/8906023]
22 **Beale G**, Chattopadhyay D, Gray J, Stewart S, Hudson M, Day C, Trerotoli P, Giannelli G, Manas D, Reeves H. AFP, PIVKAII, GP3, SCCA-1 and follisatin as surveillance biomarkers for hepatocellular cancer in non-alcoholic and alcoholic fatty liver disease. *BMC Cancer* 2008; **8**: 200 [PMID: 18638391 DOI: 10.1186/1471-2407-8-200]
23 **Yu Y**, Song J, Zhang R, Liu Z, Li Q, Shi Y, Chen Y, Chen J. Preoperative neutrophil-to-lymphocyte ratio and tumor-related factors to predict microvascular invasion in patients with hepatocellular carcinoma. *Oncotarget* 2017; **8**: 79722-79730 [PMID: 29108352 DOI: 10.18632/oncotarget.19178]
24 **Li B**, Li B, Guo T, Sun Z, Li X, Li X, Chen L, Zhao J, Mao Y. Artificial neural network models for early diagnosis of hepatocellular carcinoma using serum levels of α-fetoprotein, α-fetoprotein-L3, des-γ-carboxy prothrombin, and Golgi protein 73. *Oncotarget* 2017; **8**: 80521-80530 [PMID: 29113322 DOI: 10.18632/oncotarget.19298]
25 **Gao J**, Song P. Combination of triple biomarkers AFP, AFP-L3, and PIVAKII for early detection of hepatocellular carcinoma in China: Expectation. *Drug Discov Ther* 2017; **11**: 168-169 [PMID: 28757516 DOI: 10.5582/ddt.2017.01036]
26 **Caviglia GP**, Abate ML, Petrini E, Gaia S, Rizzetto M, Smedile A. Highly sensitive alpha-fetoprotein, Lens culinaris agglutinin-reactive fraction of alpha-fetoprotein and des-gamma-carboxyprothrombin for

hepatocellular carcinoma detection. *Hepatol Res* 2016; **46**: E130-E135 [PMID: 26082262 DOI: 10.1111/hepr.12544]

27 **Best J**, Bilgi H, Heider D, Schotten C, Manka P, Bedreli S, Gorray M, Ertle J, van Grunsven LA, Dechêne A. The GALAD scoring algorithm based on AFP, AFP-L3, and DCP significantly improves detection of BCLC early stage hepatocellular carcinoma. *Z Gastroenterol* 2016; **54**: 1296-1305 [PMID: 27936479 DOI: 10.1055/S-0042-119529]

28 **Berhane S**, Toyoda H, Tada T, Kumada T, Kagebayashi C, Satomura S, Schweitzer N, Vogel A, Manns MP, Benckert J, Berg T, Ebker M, Best J, Dechêne A, Gerken G, Schlaak JF, Weinmann A, Wörns MA, Galle P, Yeo W, Mo F, Chan SL, Reeves H, Cox T, Johnson P. Role of the GALAD and BALAD-2 Serologic Models in Diagnosis of Hepatocellular Carcinoma and Prediction of Survival in Patients. *Clin Gastroenterol Hepatol* 2016; **14**: 875-886.e6 [PMID: 26775025 DOI: 10.1016/j.cgh.2015.12.042]

29 **Oeda S**, Iwane S, Takasaki M, Furukawa NE, Otsuka T, Eguchi Y, Anzai K. Optimal Follow-up of Patients with Viral Hepatitis Improves the Detection of Early-stage Hepatocellular Carcinoma and the Prognosis of Survival. *Intern Med* 2016; **55**: 2749-2758 [PMID: 27725532 DOI: 10.2169/internalmedicine.55.6730]

30 **Wongjarupong N**, Negron-Ocasio GM, Chaiteerakij R, Addissie BD, Mohamed EA, Mara KC, Harmsen WS, Theobald JP, Peters BE, Balsanek JG, Ward MM, Giama NH, Venkatesh SK, Harnois DM, Charlton MR, Yamada H, Algeciras-Schimnich A, Snyder MR, Therneau TM, Roberts LR. Model combining pre-transplant tumor biomarkers and tumor size shows more utility in predicting hepatocellular carcinoma recurrence and survival than the BALAD models. *World J Gastroenterol* 2018; **24**: 1321-1331 [PMID: 29599607 DOI: 10.3748/wjg.v24.i12.1321]

31 **Li B**, Li B, Guo T, Sun Z, Li X, Li X, Wang H, Chen W, Chen P, Mao Y. The Clinical Values of Serum Markers in the Early Prediction of Hepatocellular Carcinoma. *Biomed Res Int* 2017; **2017**: 5358615 [PMID: 28540298 DOI: 10.1155/2017/5358615]

32 **Kim H**, Sohn A, Yeo I, Yu SJ, Yoon JH, Kim Y. Clinical Assay for AFP-L3 by Using Multiple Reaction Monitoring-Mass Spectrometry for Diagnosing Hepatocellular Carcinoma. *Clin Chem* 2018; **64**: 1230-1238 [PMID: 29875214 DOI: 10.1373/clinchem.2018.289702]

33 **Duarte-Salles T**, Misra S, Stepien M, Plymoth A, Muller D, Overvad K, Olsen A, Tjønneland A, Baglietto L, Severi G, Boutron-Ruault MC, Turzanski-Fortner R, Kaaks R, Boeing H, Aleksandrova K, Trichopoulou A, Lagiou P, Bamia C, Pala V, Palli D, Mattiello A, Tumino R, Naccarati A, Bueno-de-Mesquita HB, Peeters PH, Weiderpass E, Quirós JR, Agudo A, Sánchez-Cantalejo E, Ardanaz E, Gavrila D, Dorronsoro M, Werner M, Hemmingsson O, Ohlsson B, Sjöberg K, Wareham NJ, Khaw KT, Bradbury KE, Gunter MJ, Cross AJ, Riboli E, Jenab M, Hainaut P, Beretta L. Circulating Osteopontin and Prediction of Hepatocellular Carcinoma Development in a Large European Population. *Cancer Prev Res (Phila)* 2016; **9**: 758-765 [PMID: 27339170 DOI: 10.1158/1940-6207.CAPR-15-0434]

34 **Ge T**, Shen Q, Wang N, Zhang Y, Ge Z, Chu W, Lv X, Zhao F, Zhao W, Fan J, Qin W. Diagnostic values of alpha-fetoprotein, dickkopf-1, and osteopontin for hepatocellular carcinoma. *Med Oncol* 2015; **32** (3): 59 [PMID: 25652109 DOI: 10.1007/s12032-014-0367-z]

35 **Xing H**, Zheng YJ, Han J, Zhang H, Li ZL, Lau WY, Shen F, Yang T. Protein induced by vitamin K absence or antagonist-II versus alpha-fetoprotein in the diagnosis of hepatocellular carcinoma: A systematic review with meta-analysis. *Hepatobiliary Pancreat Dis Int* 2018; **17**: 487-495 [PMID: 30257796 DOI: 10.1016/j.hbpd.2018.09.009]

36 **Hu J**, Wang N, Yang Y, Ma L, Han R, Zhang W, Yan C, Zheng Y, Wang X. Diagnostic value of alpha-fetoprotein combined with neutrophil-to-lymphocyte ratio for hepatocellular carcinoma. *BMC Gastroenterol* 2018; **18**: 186 [PMID: 30545306 DOI: 10.1186/s12876-018-0908-6]

37 **Youssef AA**, Issa HA, Omar MZ, Behiry EG, Elfallah AA, Hasaneen A, Darwish M, Ibrahim DB. Serum human endothelial cell-specific molecule-1 (endocan) and vascular endothelial growth factor in cirrhotic HCV patients with hepatocellular carcinoma as predictors of mortality. *Clin Exp Gastroenterol* 2018; **11**: 431-438 [PMID: 30538523 DOI: 10.2147/CEG.S171339]

38 **Li J**, Cheng ZJ, Liu Y, Yan ZL, Wang K, Wu D, Wan XY, Xia Y, Lau WY, Wu MC, Shen F. Serum thioredoxin is a diagnostic marker for hepatocellular carcinoma. *Oncotarget* 2015; **6**: 9551-9563 [PMID: 25871387 DOI: 10.18632/oncotarget.3314]

39 **Junna Z**, Gongde C, Jinying X, Xiu Z. Serum AFU, 5'-NT and AFP as Biomarkers for Primary Hepatocellular Carcinoma Diagnosis. *Open Med (Wars)* 2017; **12**: 354-358 [PMID: 29043300 DOI: 10.1515/med-2017-0051]

40 **Song PP**, Xia JF, Inagaki Y, Hasegawa K, Sakamoto Y, Kokudo N, Tang W. Controversies regarding and perspectives on clinical utility of biomarkers in hepatocellular carcinoma. *World J Gastroenterol* 2016; **22**: 262-274 [PMID: 26755875 DOI: 10.3748/wjg.v22.i1.262]

41 **Chiba T**, Suzuki E, Saito T, Ogasawara S, Ooka Y, Tawada A, Iwama A, Yokosuka O. Biological features and biomarkers in hepatocellular carcinoma. *World J Hepatol* 2015; **7**: 2020-2028 [PMID: 26261691 DOI: 10.4254/wjh.v7.i16.2020]

42 **Shu H**, Li W, Shang S, Qin X, Zhang S, Liu Y. Diagnosis of AFP-negative early-stage hepatocellular carcinoma using Fuc-PON1. *Discov Med* 2017; **23**: 163-168 [PMID: 28472609]

43 **Wang M**, Sanda M, Comunale MA, Herrera H, Swindell C, Kono Y, Singal AG, Marrero J, Block T, Goldman R, Mehta A. Changes in the Glycosylation of Kininogen and the Development of a Kininogen-Based Algorithm for the Early Detection of HCC. *Cancer Epidemiol Biomarkers Prev* 2017; **26**: 795-803 [PMID: 28223431 DOI: 10.1158/1055-9965.EPI-16-0974]

44 **Guo J**, Jing R, Zhong JH, Dong X, Li YX, Liu YK, Huang TR, Zhang CY. Identification of CD14 as a potential biomarker of hepatocellular carcinoma using iTRAQ quantitative proteomics. *Oncotarget* 2017; **8**: 62011-62028 [PMID: 28977922 DOI: 10.18632/oncotarget.18782]

45 **Kim H**, Park J, Kim Y, Sohn A, Yeo I, Jong Yu S, Yoon JH, Park T, Kim Y. Serum fibronectin distinguishes the early stages of hepatocellular carcinoma. *Sci Rep* 2017; **7**: 9449 [PMID: 28842594 DOI: 10.1038/s41598-017-09691-3]

46 **Chen VL**, Le AK, Podlaha O, Estevez J, Li B, Vutien P, Chang ET, Rosenberg-Hasson Y, Pflanz S, Jiang Z, Ge D, Gaggar A, Nguyen MH. Soluble intercellular adhesion molecule-1 is associated with hepatocellular carcinoma risk: multiplex analysis of serum markers. *Sci Rep* 2017; **7**: 11169 [PMID: 28894136 DOI: 10.1038/s41598-017-10498-5]

47 **Amhimmid Badr S**, Waheeb Fahmi M, Mahmoud Nomir M, Mohammad El-Shishtawy M. Calcium channel α2δ1 subunit as a novel biomarker for diagnosis of hepatocellular carcinoma. *Cancer Biol Med* 2018; **15**: 52-60 [PMID: 29545968 DOI: 10.20892/j.issn.2095-3941.2017.0167]

48 **Wang T**, Liu M, Zheng SJ, Bian DD, Zhang JY, Yao J, Zheng QF, Shi AM, Li WH, Li L, Chen Y, Wang

JH, Duan ZP, Dong L. Tumor-associated autoantibodies are useful biomarkers in immunodiagnosis of α-fetoprotein-negative hepatocellular carcinoma. *World J Gastroenterol* 2017; **23**: 3496-3504 [PMID: 28596685 DOI: 10.3748/wjg.v23.i19.3496]

49 **Takaya H**, Kawaratani H, Tsuji Y, Nakanishi K, Saikawa S, Sato S, Sawada Y, Kaji K, Okura Y, Shimozato N, Kitade M, Akahane T, Moriya K, Namisaki T, Mitoro A, Matsumoto M, Fukui H, Yoshiji H. von Willebrand factor is a useful biomarker for liver fibrosis and prediction of hepatocellular carcinoma development in patients with hepatitis B and C. *United European Gastroenterol J* 2018; **6**: 1401-1409 [PMID: 30386613 DOI: 10.1177/2050640618779660]

50 **Shen J**, Wu H, Peng N, Cai J. An eight cytokine signature identified from peripheral blood serves as a fingerprint for hepatocellular cancer diagnosis. *Afr Health Sci* 2018; **18**: 260-266 [PMID: 30602951 DOI: 10.4314/ahs.v18i2.9]

51 **Tsuchiya N**, Sawada Y, Endo I, Saito K, Uemura Y, Nakatsura T. Biomarkers for the early diagnosis of hepatocellular carcinoma. *World J Gastroenterol* 2015; **21**: 10573-10583 [PMID: 26457017 DOI: 10.3748/wjg.v21.i37.10573]

52 **Khattab M**, Fouad M, Ahmed E. Role of biomarkers in the prediction and diagnosis of hepatocellular carcinoma. *World J Hepatol* 2015; **7**: 2474-2481 [PMID: 26483869 DOI: 10.4254/wjh.v7.i23.2474]

53 **Lou J**, Zhang L, Lv S, Zhang C, Jiang S. Biomarkers for Hepatocellular Carcinoma. *Biomark Cancer* 2017; **9**: 1-9 [PMID: 28469485 DOI: 10.1177/1179299X16684640]

54 **Zhu R**, Yang J, Xu L, Dai W, Wang F, Shen M, Zhang Y, Zhang H, Chen K, Cheng P, Wang C, Zheng Y, Li J, Lu J, Zhou Y, Wu D, Guo C. Diagnostic Performance of Des-γ-carboxy Prothrombin for Hepatocellular Carcinoma: A Meta-Analysis. *Gastroenterol Res Pract* 2014; **2014**: 529314 [PMID: 25165471 DOI: 10.1155/2014/529314]

55 **Xu H**, Dong X, Chen Y, Wang X. Serum exosomal hnRNPH1 mRNA as a novel marker for hepatocellular carcinoma. *Clin Chem Lab Med* 2018; **56**: 479-484 [PMID: 29252188 DOI: 10.1515/cclm-2017-0327]

56 **Balkan A**, Gulsen MT, Kaya B. Serum microRNA-26, microRNA-122 and microRNA-192 expressions in hepatocellular carcinoma. *Acta Medica Mediterranea* 2017; **33**: 165 [DOI: 10.19193/0393-6384_2017_1_025]

57 **Long XR**, Zhang YJ, Zhang MY, Chen K, Zheng XFS, Wang HY. Identification of an 88-microRNA signature in whole blood for diagnosis of hepatocellular carcinoma and other chronic liver diseases. *Aging (Albany NY)* 2017; **9**: 1565-1584 [PMID: 28657540 DOI: 10.18632/aging.101253]

58 **Shi BM**, Lu W, Ji K, Wang YF, Xiao S, Wang XY. Study on the value of serum miR-106b for the early diagnosis of hepatocellular carcinoma. *World J Gastroenterol* 2017; **23**: 3713-3720 [PMID: 28611524 DOI: 10.3748/wjg.v23.i20.3713]

59 **Liu M**, Wang L, Zhu H, Rong W, Wu F, Liang S, Xu N, Wu J. A Preoperative Measurement of Serum MicroRNA-125b May Predict the Presence of Microvascular Invasion in Hepatocellular Carcinomas Patients. *Transl Oncol* 2016; **9**: 167-172 [PMID: 27267832 DOI: 10.1016/j.tranon.2016.03.002]

60 **Hu T**, Li J, Zhang C, Lv X, Li S, He S, Yan H, Tan Y, Lei M, Wen M, Zuo J. The potential value of microRNA-4463 in the prognosis evaluation in hepatocellular carcinoma. *Genes Dis* 2017; **4**: 116-122 [PMID: 30258914 DOI: 10.1016/j.gendis.2017.03.003]

61 **An Y**, Gao S, Zhao WC, Qiu BA, Xia NX, Zhang PJ, Fan ZP. Novel serum microRNAs panel on the diagnostic and prognostic implications of hepatocellular carcinoma. *World J Gastroenterol* 2018; **24**: 2596-2604 [PMID: 29962816 DOI: 10.3748/wjg.v24.i24.2596]

62 **Jiang L**, Cheng Q, Zhang BH, Zhang MZ. Circulating microRNAs as biomarkers in hepatocellular carcinoma screening: a validation set from China. *Medicine (Baltimore)* 2015; **94**: e603 [PMID: 25761179 DOI: 10.1097/MD.0000000000000603]

63 **Xue X**, Zhao Y, Wang X, Qin L, Hu R. Development and validation of serum exosomal microRNAs as diagnostic and prognostic biomarkers for hepatocellular carcinoma. *J Cell Biochem* 2019; **120**: 135-142 [PMID: 30238497 DOI: 10.1002/jcb.27165]

64 **Liu HN**, Wu H, Chen YJ, Tseng YJ, Bilegsaikhan E, Dong L, Shen XZ, Liu TT. Serum microRNA signatures and metabolomics have high diagnostic value in hepatocellular carcinoma. *Oncotarget* 2017; **8**: 108810-108824 [PMID: 29312570 DOI: 10.18632/oncotarget.22224]

65 **Liao Q**, Han P, Huang Y, Wu Z, Chen Q, Li S, Ye J, Wu X. Potential Role of Circulating microRNA-21 for Hepatocellular Carcinoma Diagnosis: A Meta-Analysis. *PLoS One* 2015; **10**: e0130677 [PMID: 26114756 DOI: 10.1371/journal.pone.0130677]

66 **Ding Y**, Yan JL, Fang AN, Zhou WF, Huang L. Circulating miRNAs as novel diagnostic biomarkers in hepatocellular carcinoma detection: a meta-analysis based on 24 articles. *Oncotarget* 2017; **8**: 66402-66413 [PMID: 29029522 DOI: 10.18632/oncotarget.18949]

67 **Xu J**, Li J, Zheng TH, Bai L, Liu ZJ. MicroRNAs in the Occurrence and Development of Primary Hepatocellular Carcinoma. *Adv Clin Exp Med* 2016; **25**: 971-975 [PMID: 28028963 DOI: 10.17219/acem/36460]

68 **Wang Y**, Zhang C, Zhang P, Guo G, Jiang T, Zhao X, Jiang J, Huang X, Tong H, Tian Y. Serum exosomal microRNAs combined with alpha-fetoprotein as diagnostic markers of hepatocellular carcinoma. *Cancer Med* 2018; **7**: 1670-1679 [PMID: 29573235 DOI: 10.1002/cam4.1390]

69 **Mohamed AA**, Ali-Eldin ZA, Elbedewy TA, El-Serafy M, Ali-Eldin FA, AbdelAziz H. MicroRNAs and clinical implications in hepatocellular carcinoma. *World J Hepatol* 2017; **9**: 1001-1007 [PMID: 28878865 DOI: 10.4254/wjh.v9.i23.1001]

70 **Motawi TK**, Shaker OG, El-Maragh SA, Senousy MA. Serum MicroRNAs as Potential Biomarkers for Early Diagnosis of Hepatitis C Virus-Related Hepatocellular Carcinoma in Egyptian Patients. *PLOS One* 2015; **10**: e0137706 [PMID: 26352740 DOI: 10.1371/journal.pone.0137706]

71 **Amr KS**, Elmawgoud Atia HA, Elazeem Elbnhawy RA, Ezzat WM. Early diagnostic evaluation of miR-122 and miR-224 as biomarkers for hepatocellular carcinoma. *Genes Dis* 2017; **4**: 215-221 [PMID: 30258925 DOI: 10.1016/j.gendis.2017.10.003]

72 **Elemeery MN**, Badr AN, Mohamed MA, Ghareeb DA. Validation of a serum microRNA panel as biomarkers for early diagnosis of hepatocellular carcinoma post-hepatitis C infection in Egyptian patients. *World J Gastroenterol* 2017; **23**: 3864-3875 [PMID: 28638226 DOI: 10.3748/wjg.v23.i21.3864]

73 **Fornari F**, Ferracin M, Trere D, Milazzo M, Marinelli S, Galassi M, Venerandi L, Pollutri D, Patrizi C, Borghi A, Foschi FG, Stefanini GF, Negrini M, Bolondi L, Gramantieri L. Circulating microRNAs, miR-939, miR-595, miR-519d and miR-494, Identify Cirrhotic Patients with HCC. *PLOS One* 2015; **10**: e0141448 [PMID: 26509672 DOI: 10.1371/journal.pone.0141448]

74 **Zhuang L**, Xu L, Wang P, Meng Z. Serum miR-128-2 serves as a prognostic marker for patients with hepatocellular carcinoma. *PLoS One* 2015; **10**: e0117274 [PMID: 25642945 DOI:

10.1371/journal.pone.0117274]
75 **Zhu HT**, Hasan AM, Liu RB, Zhang ZC, Zhang X, Wang J, Wang HY, Wang F, Shao JY. Serum microRNA profiles as prognostic biomarkers for HBV-positive hepatocellular carcinoma. *Oncotarget* 2016; **7**: 45637-45648 [PMID: 27317768 DOI: 10.18632/oncotarget.10082]
76 **Klingenberg M**, Matsuda A, Diederichs S, Patel T. Non-coding RNA in hepatocellular carcinoma: Mechanisms, biomarkers and therapeutic targets. *J Hepatol* 2017; **67**: 603-618 [PMID: 28438689 DOI: 10.1016/j.jhep.2017.04.009]
77 **Schütte K**, Schulz C, Link A, Malfertheiner P. Current biomarkers for hepatocellular carcinoma: Surveillance, diagnosis and prediction of prognosis. *World J Hepatol* 2015; **7**: 139-149 [PMID: 25729470 DOI: 10.4254/wjh.v7.i2.139]
78 **Zhang YC**, Xu Z, Zhang TF, Wang YL. Circulating microRNAs as diagnostic and prognostic tools for hepatocellular carcinoma. *World J Gastroenterol* 2015; **21**: 9853-9862 [PMID: 26379392 DOI: 10.3748/wjg.v21.i34.9853]
79 **Loosen SH**, Schueller F, Trautwein C, Roy S, Roderburg C. Role of circulating microRNAs in liver diseases. *World J Hepatol* 2017; **9**: 586-594 [PMID: 28515844 DOI: 10.4254/wjh.v9.i12.586]
80 **Yuan W**, Sun Y, Liu L, Zhou B, Wang S, Gu D. Circulating LncRNAs Serve as Diagnostic Markers for Hepatocellular Carcinoma. *Cell Physiol Biochem* 2017; **44**: 125-132 [PMID: 29130980 DOI: 10.1159/000484589]
81 **Wang K**, Guo WX, Li N, Gao CF, Shi J, Tang YF, Shen F, Wu MC, Liu SR, Cheng SQ. Serum LncRNAs Profiles Serve as Novel Potential Biomarkers for the Diagnosis of HBV-Positive Hepatocellular Carcinoma. *PLoS One* 2015; **10**: e0144934 [PMID: 26674525 DOI: 10.1371/journal.pone.0144934]
82 **Tang J**, Jiang R, Deng L, Zhang X, Wang K, Sun B. Circulation long non-coding RNAs act as biomarkers for predicting tumorigenesis and metastasis in hepatocellular carcinoma. *Oncotarget* 2015; **6**: 4505-4515 [PMID: 25714016 DOI: 10.18632/oncotarget.2934]
83 **Zheng ZK**, Pang C, Yang Y, Duan Q, Zhang J, Liu WC. Serum long noncoding RNA urothelial carcinoma-associated 1: A novel biomarker for diagnosis and prognosis of hepatocellular carcinoma. *J Int Med Res* 2018; **46**: 348-356 [PMID: 28856933 DOI: 10.1177/0300060517726441]
84 **Xu H**, Chen Y, Dong X, Wang X. Serum Exosomal Long Noncoding RNAs ENSG00000258332.1 and LINC00635 for the Diagnosis and Prognosis of Hepatocellular Carcinoma. *Cancer Epidemiol Biomarkers Prev* 2018; **27**: 710-716 [PMID: 29650788 DOI: 10.1158/1055-9965.EPI-17-0770]
85 **Chen S**, Zhang Y, Wu X, Zhang C, Li G. Diagnostic Value of lncRNAs as Biomarker in Hepatocellular Carcinoma: An Updated Meta-Analysis. *Can J Gastroenterol Hepatol* 2018; **2018**: 8410195 [PMID: 30410873 DOI: 10.1155/2018/8410195]
86 **Hao QQ**, Chen GY, Zhang JH, Sheng JH, Gao Y. Diagnostic value of long noncoding RNAs for hepatocellular carcinoma: A PRISMA-compliant meta-analysis. *Medicine (Baltimore)* 2017; **96**: e7496 [PMID: 28700498 DOI: 10.1097/MD.0000000000007496]
87 **Zheng C**, Liu X, Chen L, Xu Z, Shao J. lncRNAs as prognostic molecular biomarkers in hepatocellular carcinoma: a systematic review and meta-analysis. *Oncotarget* 2017; **8**: 59638-59647 [PMID: 28938667 DOI: 10.18632/oncotarget.19559]
88 **Qin Y**, Wu J, Ke Z, Xu J. Expression of plasma lncRNABANCR in hepatocellular carcinomaand its diagnostic and prognostic significance. *Int J Clin Med* 2017; **10**: 11984-11990
89 **Chen Y**, Zhou J, Li J, Feng J, Chen Z, Wang X. Plasma metabolomic analysis of human hepatocellular carcinoma: Diagnostic and therapeutic study. *Oncotarget* 2016; **7**: 47332-47342 [PMID: 27322079 DOI: 10.18632/oncotarget.10119]
90 **Kim JU**, Shariff MI, Crossey MM, Gomez-Romero M, Holmes E, Cox IJ, Fye HK, Njie R, Taylor-Robinson SD. Hepatocellular carcinoma: Review of disease and tumor biomarkers. *World J Hepatol* 2016; **8**: 471-484 [PMID: 27057305 DOI: 10.4254/wjh.v8.i10.471]
91 **Di Poto C**, Ferrarini A, Zhao Y, Varghese RS, Tu C, Zuo Y, Wang M, Nezami Ranjbar MR, Luo Y, Zhang C, Desai CS, Shetty K, Tadesse MG, Ressom HW. Metabolomic Characterization of Hepatocellular Carcinoma in Patients with Liver Cirrhosis for Biomarker Discovery. *Cancer Epidemiol Biomarkers Prev* 2017; **26**: 675-683 [PMID: 27913395 DOI: 10.1158/1055-9965.EPI-16-0366]
92 **Saito T**, Sugimoto M, Okumoto K, Haga H, Katsumi T, Mizuno K, Nishina T, Sato S, Igarashi K, Maki H, Tomita M, Ueno Y, Soga T. Serum metabolome profiles characterized by patients with hepatocellular carcinoma associated with hepatitis B and C. *World J Gastroenterol* 2016; **22**: 6224-6234 [PMID: 27468212 DOI: 10.3748/wjg.v22.i27.6224]
93 **Fitian AI**, Cabrera R. Disease monitoring of hepatocellular carcinoma through metabolomics. *World J Hepatol* 2017; **9**: 1-17 [PMID: 28105254 DOI: 10.4254/wjh.v9.i1.1]
94 **Ferrín G**, Rodríguez-Perálvarez M, Aguilar-Melero P, Ranchal I, Llamoza C, Linares CI, González-Rubio S, Muntané J, Briceño J, López-Cillero P, Montero-Álvarez JL, de la Mata M. Plasma protein biomarkers of hepatocellular carcinoma in HCV-infected alcoholic patients with cirrhosis. *PLoS One* 2015; **10**: e0118527 [PMID: 25789864 DOI: 10.1371/journal.pone.0118527]
95 **Kimhofer T**, Fye H, Taylor-Robinson S, Thursz M, Holmes E. Proteomic and metabonomic biomarkers for hepatocellular carcinoma: a comprehensive review. *Br J Cancer* 2015; **112**: 1141-1156 [PMID: 25826224 DOI: 10.1038/bjc.2015.38]
96 **Guo W**, Tan HY, Wang N, Wang X, Feng Y. Deciphering hepatocellular carcinoma through metabolomics: from biomarker discovery to therapy evaluation. *Cancer Manag Res* 2018; **10**: 715-734 [PMID: 29692630 DOI: 10.2147/CMAR.S156837]
97 **Passos-Castilho AM**, Lo Turco E, Ferraz ML, Matos C, Silva I, Parise E, Pilau E, Gozzo F, Granato C. Plasma lipidomic fingerprinting to distinguish among hepatitis C-related hepatocellular carcinoma, liver cirrhosis, and chronic hepatitis C using MALDI-TOF mass spectrometry: a pilot study. *J Gastrointestin Liver Dis* 2015; **24**: 43-49 [PMID: 25822433 DOI: 10.15403/jgld.2014.1121.pas]
98 **Passos-Castilho AM**, Carvalho VM, Cardozo KH, Kikuchi L, Chagas AL, Gomes-Gouvêa MS, Malta F, de Seixas-Santos Nastri AC, Pinho JR, Carrilho FJ, Granato CF. Serum lipidomic profiling as a useful tool for screening potential biomarkers of hepatitis B-related hepatocellular carcinoma by ultraperformance liquid chromatography-mass spectrometry. *BMC Cancer* 2015; **15**: 985 [PMID: 26680993 DOI: 10.1186/s12885-015-1995-1]
99 **Margetts J**, Ogle LF, Chan SL, Chan AWH, Chan KCA, Jamieson D, Willoughby CE, Mann DA, Wilson CL, Manas DM, Yeo W, Reeves HL. Neutrophils: driving progression and poor prognosis in hepatocellular carcinoma? *Br J Cancer* 2018; **118**: 248-257 [PMID: 29123264 DOI: 10.1038/bjc.2017.386]
100 **Zheng J**, Cai J, Li H, Zeng K, He L, Fu H, Zhang J, Chen L, Yao J, Zhang Y, Yang Y. Neutrophil to

Lymphocyte Ratio and Platelet to Lymphocyte Ratio as Prognostic Predictors for Hepatocellular Carcinoma Patients with Various Treatments: a Meta-Analysis and Systematic Review. *Cell Physiol Biochem* 2017; **44**: 967-981 [PMID: 29179180 DOI: 10.1159/000485396]

101 **Goyal H**, Hu ZD. Prognostic value of red blood cell distribution width in hepatocellular carcinoma. *Ann Transl Med* 2017; **5**: 271 [PMID: 28758097 DOI: 10.21037/atm.2017.06.30]

102 **Van Hees S**, Michielsen P, Vanwolleghem T. Circulating predictive and diagnostic biomarkers for hepatitis B virus-associated hepatocellular carcinoma. *World J Gastroenterol* 2016; **22**: 8271-8282 [PMID: 27729734 DOI: 10.3748/wjg.v22.i37.8271]

103 **Hong Y**, Huang J. Autoantibodies against tumor-associated antigens for detection of hepatocellular carcinoma. *World J Hepatol* 2015; **7**: 1581-1585 [PMID: 26085917 DOI: 10.4254/wjh.v7.i11.1581]

104 **Sun C**, Liao W, Deng Z, Li E, Feng Q, Lei J, Yuan R, Zou S, Mao Y, Shao J, Wu L, Zhang C. The diagnostic value of assays for circulating tumor cells in hepatocellular carcinoma: A meta-analysis. *Medicine (Baltimore)* 2017; **96**: e7513 [PMID: 28723763 DOI: 10.1097/MD.0000000000007513]

105 **Yu YQ**, Wang L, Jin Y, Zhou JL, Geng YH, Jin X, Zhang XX, Yang JJ, Qian CM, Zhou DE, Liu DR, Peng SY, Luo Y, Zheng L, Li JT. Identification of serologic biomarkers for predicting microvascular invasion in hepatocellular carcinoma. *Oncotarget* 2016; **7**: 16362-16371 [PMID: 26918350 DOI: 10.18632/oncotarget.7649]

106 **Kuo MJ**, Chen HH, Chen CL, Fann JC, Chen SL, Chiu SY, Lin YM, Liao CS, Chang HC, Lin YS, Yen AM. Cost-effectiveness analysis of population-based screening of hepatocellular carcinoma: Comparing ultrasonography with two-stage screening. *World J Gastroenterol* 2016; **22**: 3460-3470 [PMID: 27022228 DOI: 10.3748/wjg.v22.i12.3460]

107 **Hanna RF**, Miloushev VZ, Tang A, Finklestone LA, Brejt SZ, Sandhu RS, Santillan CS, Wolfson T, Gamst A, Sirlin CB. Comparative 13-year meta-analysis of the sensitivity and positive predictive value of ultrasound, CT, and MRI for detecting hepatocellular carcinoma. *Abdom Radiol (NY)* 2016; **41**: 71-90 [PMID: 26830614 DOI: 10.1007/s00261-015-0592-8]

108 **Van Beers BE**, Daire JL, Garteiser P. New imaging techniques for liver diseases. *J Hepatol* 2015; **62**: 690-700 [PMID: 25457198 DOI: 10.1016/j.jhep.2014.10.014]

109 **Westwood M**, Joore M, Grutters J, Redekop K, Armstrong N, Lee K, Gloy V, Raatz H, Misso K, Severens J, Kleijnen J. Contrast-enhanced ultrasound using SonoVue® (sulphur hexafluoride microbubbles) compared with contrast-enhanced computed tomography and contrast-enhanced magnetic resonance imaging for the characterisation of focal liver lesions and detection of liver metastases: a systematic review and cost-effectiveness analysis. *Health Technol Assess* 2013; **17**: 1-243 [PMID: 23611316 DOI: 10.3310/hta17160]

110 **Yao Z**, Dong Y, Wu G, Zhang Q, Yang D, Yu JH, Wang WP. Preoperative diagnosis and prediction of hepatocellular carcinoma: Radiomics analysis based on multi-modal ultrasound images. *BMC Cancer* 2018; **18**: 1089 [PMID: 30419849 DOI: 10.1186/s12885-018-5003-4]

111 **Ippolito D**, Inchingolo R, Grazioli L, Drago SG, Nardella M, Gatti M, Faletti R. Recent advances in non-invasive magnetic resonance imaging assessment of hepatocellular carcinoma. *World J Gastroenterol* 2018; **24**: 2413-2426 [PMID: 29930464 DOI: 10.3748/wjg.v24.i23.2413]

112 **Neri E**, Bali MA, Ba-Ssalamah A, Boraschi P, Brancatelli G, Alves FC, Grazioli L, Helmberger T, Lee JM, Manfredi R, Martì-Bonmatì L, Matos C, Merkle EM, Op De Beeck B, Schima W, Skehan S, Vilgrain V, Zech C, Bartolozzi C. ESGAR consensus statement on liver MR imaging and clinical use of liver-specific contrast agents. *Eur Radiol* 2016; **26**: 921-931 [PMID: 26194455 DOI: 10.1007/s00330-015-3900-3]

113 **Tanabe M**, Kanki A, Wolfson T, Costa EA, Mamidipalli A, Ferreira MP, Santillan C, Middleton MS, Gamst AC, Kono Y, Kuo A, Sirlin CB. Imaging Outcomes of Liver Imaging Reporting and Data System Version 2014 Category 2, 3, and 4 Observations Detected at CT and MR Imaging. *Radiology* 2016; **281**: 129-139 [PMID: 27115054 DOI: 10.1148/radiol.2016152173]

114 **Darnell A**, Forner A, Rimola J, Reig M, García-Criado Á, Ayuso C, Bruix J. Liver Imaging Reporting and Data System with MR Imaging: Evaluation in Nodules 20 mm or Smaller Detected in Cirrhosis at Screening US. *Radiology* 2015; **275**: 698-707 [PMID: 25658038 DOI: 10.1148/radiol.15141132]

115 **Yang JF**, Zhao ZH, Zhang Y, Zhao L, Yang LM, Zhang MM, Wang BY, Wang T, Lu BC. Dual-input two-compartment pharmacokinetic model of dynamic contrast-enhanced magnetic resonance imaging in hepatocellular carcinoma. *World J Gastroenterol* 2016; **22**: 3652-3662 [PMID: 27053857 DOI: 10.3748/wjg.v22.i13.3652]

116 **Kavanaugh G**, Williams J, Morris AS, Nickels ML, Walker R, Koglin N, Stephens AW, Washington MK, Geevarghese SK, Liu Q, Ayers D, Shyr Y, Manning HC. Utility of [18F] FSPG PET to Image Hepatocellular Carcinoma: First Clinical Evaluation in a US Population. *Mol Imaging Biol* 2016; **18**: 924-934 [PMID: 27677886 DOI: 10.1007/s11307-016-1007-0]

117 **Cho Y**, Lee DH, Lee YB, Lee M, Yoo JJ, Choi WM, Cho YY, Paeng JC, Kang KW, Chung JK, Yu SJ, Lee JH, Yoon JH, Lee HS, Kim YJ. Does 18F-FDG positron emission tomography-computed tomography have a role in initial staging of hepatocellular carcinoma? *PLoS One* 2014; **9**: e105679 [PMID: 25153834 DOI: 10.1371/journal.pone.0105679]

World Journal of Clinical Cases

Submit a Manuscript: https://www.f6publishing.com

World J Clin Cases 2019 June 26; 7(12): 1383-1392

DOI: 10.12998/wjcc.v7.i12.1383

ISSN 2307-8960 (online)

ORIGINAL ARTICLE

Basic Study

Study on gene expression patterns and functional pathways of peripheral blood monocytes reveals potential molecular mechanism of surgical treatment for periodontitis

Jin-Ji Ma, Hong-Mei Liu, Xiang-Hua Xu, Li-Xin Guo, Qing Lin

ORCID number: Jin-Ji Ma (0000-0002-3409-7387); Hong-Mei Liu (0000-0002-6130-1005); Xiang-Hua Xu (0000-0003-1793-1728); Li-Xin Guo (0000-0003-0168-139X); Qing Lin (0000-0001-7741-367X).

Author contributions: Ma JJ and Liu HM contributed equally to this work. Ma JJ, Liu HM, and Xu XH designed the research; Ma JJ, Liu HM, and Guo LX performed the research; Xu XH and Lin Q analyzed the data; Ma JJ, Liu HM, and Lin Q wrote the paper.

Institutional review board statement: This study was reviewed and approved by the Institutional Review Board of Jinan Stomatological Hospital.

Conflict-of-interest statement: The authors declare no conflict of interest.

Data sharing statement: No additional data are available.

ARRIVE guidelines statement: The authors have read the ARRIVE guidelines, and the manuscript was prepared and revised according to the ARRIVE guidelines.

Jin-Ji Ma, Jinan Stomatological Hospital Gaoxin Branch, Jinan 250001, Shandong Province, China

Hong-Mei Liu, Li-Xin Guo, Qing Lin, Department of Endodontics, Jinan Stomatological Hospital, Jinan 250001, Shandong Province, China

Xiang-Hua Xu, Department of Stomatology, Shandong Provincial Hospital, Jinan 250001, Shandong Province, China

Corresponding author: Qing Lin, BSc, Attending Doctor, Department of Endodontics, Jinan Stomatological Hospital, No. 101, Jingliu Road, Jinan 250001, Shandong Province, China.
cunl69338@163.com
Telephone: +86-531-86261570
Fax: +86-531-86261570

Abstract

BACKGROUND

Periodontitis is a chronic inflammation of periodontal supporting tissue caused by local factors. Periodontal surgery can change the gene expression of peripheral blood mononuclear cells. However, little is known about the potential mechanism of surgical treatment for periodontitis.

AIM

To explore the potential molecular mechanism of surgical treatment for periodontitis.

METHODS

First, based on the expression profiles of genes related to surgical treatment for periodontitis, a set of expression disorder modules related to surgical treatment for periodontitis were obtained by enrichment analysis. Subsequently, based on crosstalk analysis, we proved that there was a significant crosstalk relationship between module 3 and module 5. Finally, based on predictive analysis of multidimensional regulators, we identified a series of regulatory factors, such as endogenous genes, non-coding RNAs (ncRNAs), and transcription factors, which have potential regulatory effects on periodontitis.

RESULTS

A total of 337 genes related to surgical treatment for periodontitis were obtained, and 3896 genes related to periodontitis were amplified. Eight expression modules

Manuscript source: Unsolicited manuscript

Received: March 21, 2019
Peer-review started: March 23, 2019
First decision: April 18, 2019
Revised: April 23, 2019
Accepted: May 1, 2019
Article in press: May 1, 2019
Published online: June 26, 2019

P-Reviewer: Vieyra JP, Gurav AN
S-Editor: Dou Y
L-Editor: Wang TQ
E-Editor: Wu YXJ

of periodontitis were obtained, involving the aggregation of 2672 gene modules. These modules are mainly involved in G-protein coupled receptor signaling pathway, coupled to cyclic nucleotide second messenger, and adenylate cyclase-modulating G-protein coupled receptor signaling pathway. In addition, eight endogenous genes (including *EGF*, *RPS27A*, and *GNB3*) were screened by network connectivity analysis. Finally, based on this set of potential dysfunction modules, 94 transcription factors (including NFKB1, SP1, and STAT3) and 1198 ncRNAs (including MALAT1, CRNDE, and ANCR) were revealed. These core regulators are thought to be involved in the potential molecular mechanism of periodontitis after surgical treatment.

CONCLUSION
Based on the results of this study, we can show biologists and pharmacists a new idea to reveal the potential molecular mechanism of surgical treatment for periodontitis, and provide valuable reference for follow-up treatment programs.

Key words: Peripheral blood mononuclear cells; Gene expression; Dysregulation module; Potential molecular mechanism; Gene expression pattern

Core tip: Based on the expression pattern and function of genes in peripheral blood mononuclear cells of periodontitis patients, key genes (including *EGF*, *RPS27A, GNB3, etc*.) were identified. Further, transcription factors (including NFKB1, SP1, STAT3, *etc*.,) and non-coding RNAs (including MALAT1, CRNDE, and ANCR) that significantly regulated gene co-expression modules were identified. Exploring the relationships between genes and regulators may reveal the potential molecular mechanism of surgical treatment for periodontitis.

Citation: Ma JJ, Liu HM, Xu XH, Guo LX, Lin Q. Study on gene expression patterns and functional pathways of peripheral blood monocytes reveals potential molecular mechanism of surgical treatment for periodontitis. *World J Clin Cases* 2019; 7(12): 1383-1392
URL: https://www.wjgnet.com/2307-8960/full/v7/i12/1383.htm
DOI: https://dx.doi.org/10.12998/wjcc.v7.i12.1383

INTRODUCTION

Periodontitis is a highly prevalent inflammatory disease in dental support tissues. It is caused by the growth of bacteria in the biofilm on the surface of teeth. As a mature periodontitis disease, it is characterized by progressive destruction of the supporting tissues of teeth. Periodontitis is a multifactorial disease. The susceptibility and severity of periodontitis are influenced by the polymorphism of immune response related genes, and are also determined by environmental and genetic factors[1,2]. Relevant studies have shown that periodontal diseases are associated with various systemic diseases, including cardiovascular diseases such as stroke and atherosclerosis[3,4]. Many data show that periodontitis affects 20% of the world's population. The prevalence of periodontitis in adults is 35%, and it increases with age, reaches a peak in the 45-50 age group[5-7]. Periodontitis has a variety of risk factors, which may cause plaque, dental calculi, diabetes, and other diseases, and has multiple negative impacts on the quality of life of patients[5,8]. Therefore, many scholars actively explore the pathogenesis of periodontitis. It is well known that bacterial infection is the main cause of periodontal disease, and the bacterial colonization of actinomycetes and *Porphyromonas gingivalis* is the main cause of periodontitis[9,10]. On the one hand, the change of immune response in diabetic patients may cause periodontitis[11]. On the other hand, the severity of periodontal disease may also be related to the expression of multiple metalloproteinase genes in the oral mucosal epithelium[12]. Recent studies have shown that periodontitis, a chronic inflammatory oral infection, may have a profound impact on human health[13]. As far as the potential relationship between periodontitis and systemic diseases is concerned, the changes of immune cell function induced by periodontitis may cause lipid metabolism disorder through the mechanism related to inflammatory cytokines, which has a serious negative impact on

the health of whole body cells[13].

After understanding some of the pathogenesis of periodontitis, scholars around the world are actively studying the corresponding treatment mechanisms and inhibition methods. For example, according to van Winkelhoff *et al*[14], mechanical periodontal therapy combined with metronidazole and amoxicillin is effective for subgingival inhibition of actinomycete infection in patients with severe periodontitis. In addition, triclosan and copolymer toothpaste were found to be able to effectively control the development of plaque and gingivitis, thereby inhibiting the occurrence of periodontitis[15]. Relevant studies have shown that periodontitis is essentially an inflammatory reaction in periodontal attachment caused by bacteria[16]. Periodontal infection is not only related to chronic inflammation, but also to oxidative stress in severe periodontitis and its treatment[17]. YKL-40, as a chitin-binding glycoprotein, may be an inflammatory marker of periodontitis, which has been confirmed by Kido *et al*[18]. On the one hand, as one of the biomarkers of periodontitis, pulp-like cell-1 may play an important role in the association between periodontal infection and systemic inflammatory response[19]. On the other hand, the increased inflammatory response of higher serum C-reactive protein level may be as important as the promotion of periodontitis[20].

Previous data show that periodontal therapy can change the gene expression pattern of peripheral blood monocytes[21]. Therefore, we can think that the gene expression of peripheral blood mononuclear cells also has a feedback regulation effect on periodontal therapy. Therefore, in our study, we proposed a comprehensive analysis method based on the gene expression patterns and functional pathways of peripheral blood mononuclear cells. It combined co-expression analysis and enrichment analysis of functional pathways, and focused on predicting a series of core non-coding RNAs (ncRNAs) and transcription factors to reveal the potential molecular mechanism of surgical treatment for periodontitis.

MATERIALS AND METHODS

Function modules related to co-expression analysis and recognition

First, the gene expression profiles of 3896 related genes in periodontitis were analyzed by weighted gene co-expression network analysis (WGCNA)[22] and the gene modules of co-expression were searched. Second, the weighted value of correlation coefficient was used to calculate the correlation coefficient between any two genes (Person Coefficient) by taking the N power of the correlation coefficient. The connection between genes in the network obeys scale-free networks, which makes the algorithm more biologically meaningful. Then, a hierarchical clustering tree was constructed by the correlation coefficient between genes. Different branches of the clustering tree represent different gene modules, and different colors represent different modules.

Analysis of crosstalk and internal driving force among modules

First, Python was used to program the human protein interaction network (score > 950) in String to generate 1000 random networks[23] while keeping the network size and the degree of each node unchanged. Second, according to the number of interaction pairs between significant modules obtained by random network statistics, the number of interaction pairs between modules was compared with the number of interaction pairs in random background. When the number of interaction pairs between modules was larger than that of interaction pairs in random background, it was called crosstalk. The method of calculating significant crosstalk was as follows: Under the background of random network, the number of interaction pairs between modules in N random networks was larger than that in real networks. The formula of calculating P-value is: $P = n/N$ (in this work, $N = 1000$). When a P-value was <0.05, there was a crosstalk interaction among modules. Then, Cytoscape[24] was used to display the significant crosstalk to visually observe the complex regulatory relationship between modules. In addition, Cytoscape was used for display and network analysis (including connectivity calculation). Finally, the genes with the greatest connectivity was screened and considered as the core molecule to regulate the progress of the module and identified as the intrinsic gene. These endogenous genes may represent potential key molecules in the effect of surgical treatment on periodontitis.

Functional and pathway enrichment analysis

Exploring the function and signal pathway of genes is often an effective means to study the molecular mechanism of disease, while the function and pathway of module gene participation can characterize the dysfunction mechanism of modules in

the process of disease occurrence. Therefore, we used R language Cluster profiler package[25] to analyze the enrichment of GO function (pvalue Cutoff = 0.01, qvalueCutoff = 0.01) and KEGG pathway (pvalueCutoff = 0.05, qvalueCutoff = 0.2), respectively. According to the function and pathway of module gene participation, it was identified as a functional disorder module related to periodontitis.

Identification of transcription factors and ncRNAs that have regulatory effects on modules

First, we downloaded all human transcription factor target data in TRRUST V2 database[26], and obtained 116 interaction pairs of 94 transcription factors. Then, human ncRNA-protein data (score > 0.5) were downloaded from RAID 2.0 database[27], and 1678 interaction pairs involving 1198 ncRNAs were obtained. Then, pivot analysis based on these interaction data was performed to identify the regulatory effects of these transcription factors and ncRNAs on the modules. Pivot analysis refers to searching for at least two interacting drivers with the module in the target pair and calculating the significance of the interaction between the driver and the module according to the hypergeometric test. Transcription factors and ncRNAs with a P-value < 0.01 were the pivots of the significant regulatory module. Finally, the pivots were identified as the core pivots by statistical analysis.

RESULTS

Synergistic expression of periodontitis-related genes in the pathogenesis of periodontitis

Because the regulatory mechanism of periodontitis-related genes and the synergistic relationship between genes are not clear, we conducted in-depth research. First, a total of 337 genes related to surgical treatment of periodontitis was integrated into several databases. Second, we amplified 337 related genes and got 3896 related genes. We analyzed the WGCNA co-expression of the amplified genes and observed the expression of these genes in 15 patients with periodontitis. We found that eight groups of genes expressed synergistically in the group based on cohesion. Finally, these eight groups of genes were identified as eight functional modules, involving 2672 clusters of module genes (Figure 1). These functional modules may participate in different functions and pathways, representing different regulatory mechanisms to mediate the occurrence and development of periodontitis.

Interaction between dysfunctional modules

The intergenic regulation has always been complex and changeable. Similarly, the relationships between modules are complex and diverse. The interaction between modules is the pivot to maintain the relationship between modules and the whole world, and is also the key to exploring the function of modules. Exploring the crosstalk relationship between modules is helpful to deepen our understanding of the potential dysfunction mechanism of module regulation of periodontitis. Therefore, we conducted crosstalk analysis among modules based on the relationship between module genes. The results showed that there was a complex interaction between modules 2, 3, 4, 5, 6, 7, and 8, while other modules had simple crosstalk (Figure 2). This crosstalk may represent the driving force between modules, which together regulate the potential molecular mechanism of peripheral blood monocytes in the surgical treatment of periodontitis.

Functional and pathway enrichment analysis and identification of dysfunctional modules

Studying the function and pathway of gene involvement is an important means to identify its mediated pathogenesis. In order to study the possible dysfunction caused by module gene disorder, we analyzed the enrichment of function and pathway of each module. The results showed that most of the functional modules were enriched in periodontitis-related functions and pathways. GO function and KEGG pathway enrichment analyses were carried out on the eight functional modules. A total of 45887 functions and 1796 KEGG pathway enrichment results were obtained. Among them, there are 5950 molecular functions, 3976 cell components, and 35691 biological processes in which these genes participate (Figure 3, Table 1). It is worth noting that G-protein coupled receptor signaling pathway, coupled to cyclic nucleotide second messenger, and adenylate cyclase-modulating G-protein coupled receptor signaling pathway, which are significantly involved, may be identified as the core signaling pathways involved in the potential disorder mechanism of periodontitis. From the above data, we can find that these signaling pathways may be closely related to the

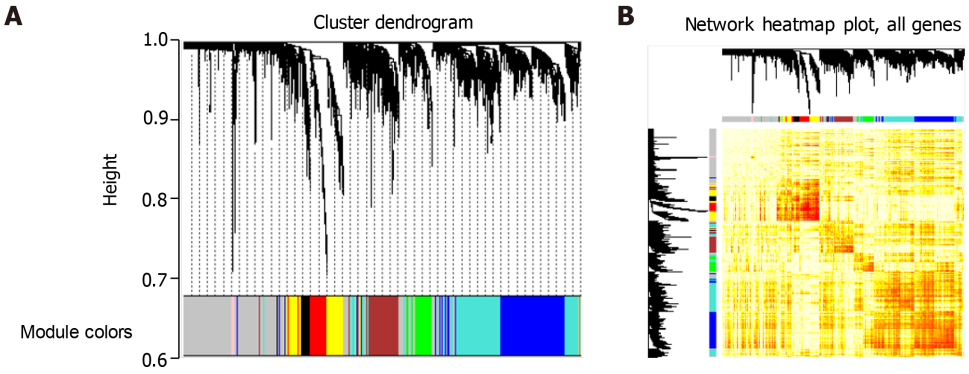

Figure 1 Clustering module for synergistic expression of genes related to periodontitis. A: According to the co-expression relationship of differentially expressed genes, eight modules are clustered, and one color represents one module; B: Thermogram of modular gene expression in samples. Genes associated with periodontitis are expressed in groups intuitively in disease samples.

molecular mechanism of periodontitis in the surgical treatment of peripheral blood monocytes.

Identification of key regulatory factors driving the development of periodontitis

Further, our study of 2672 modular genes revealed that there were also target interactions among these genes. In-depth study of gene interaction within the module was then performed to calculate its connectivity and screen each module with the highest connectivity of the intrinsic genes. Eight endogenous genes including *EGF*, *RPS27A*, and *GNB3* were screened from eight dysfunction modules. In addition, besides the module-driven genes, there were also key regulatory factors such as ncRNAs and transcription factors, which also play an indispensable role in the potential molecular mechanism of periodontitis. Scientific prediction of ncRNAs regulating dysfunction module genes is helpful for us to explore the post-transcriptional regulation mechanism of periodontitis. To this end, pivot analysis based on the targeting relationship between ncRNAs and genes was carried out to predict ncRNA regulators causing module dysfunction. We identified 198 ncRNAs that had significant regulatory effects on modules, involving 1678 ncRNA-module interaction pairs. Statistical analysis of the results showed that MALAT1 had a significant regulatory relationship with six dysfunction modules and may play an important role in the potential molecular mechanism of periodontitis, so it was identified as the core ncRNA. ANCR also plays an important role in the molecular mechanism of periodontitis. In addition, other ncRNAs may also play a role in driving the potential molecular mechanism of periodontitis. Similarly, transcription factors are equally important in regulating gene transcription. Many studies have shown that disordered expression of transcription factors may lead to the occurrence of various diseases. The dysfunction of periodontitis is also closely related to the dysfunction of transcription factors, which is also reflected in the regulation of dysfunction module by transcription factors. Therefore, we used pivot analysis to predict the module according to the regulation of genes by transcription factors. The results showed that there were 94 transcription factors involving 116 pivot-module interaction pairs. Statistical analysis of these transcription factors showed that NFKB1, SP1, and STAT3 had significant regulatory effects on 6 and 4 dysfunction modules, respectively, and they are likely to participate in the potential molecular mechanism of surgical treatment for periodontitis. These data suggest that transcription factors may play an important role in the molecular mechanism of surgical treatment of periodontitis. These transcription factors, which have significant regulatory effects on multiple dysfunction modules, have been identified as the core transcription factors driving the development of periodontitis.

DISCUSSION

It is well known that periodontitis is a multifactorial disease. Studies have shown that some clinical variability of periodontitis may be caused by genetic factors[28]. As a high-risk inflammatory disease, periodontitis is considered a potential risk factor for systemic diseases such as cardiovascular diseases[20]. Therefore, scholars around the world are actively exploring the detailed and specific pathogenesis and treatment mechanism of periodontitis. In this study, we investigated the gene expression

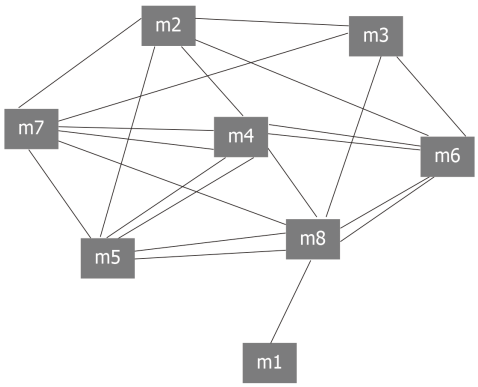

Figure 2 Crosstalk relationship between periodontitis modules.

patterns and functional pathways of peripheral blood mononuclear cells to reveal the potential molecular mechanism of the effect of surgical treatment on periodontitis. We proposed a comprehensive approach, which first integrated 3896 genes related to periodontitis and carried out co-expression analysis. Finally, eight functional modules with synergistic expression were identified, involving 2672 module gene clusters. Based on the results of functional enrichment, we also obtained that these modules are significantly involved in G-protein coupled receptor signaling pathway, coupled to cyclic nucleotide second messenger, and adenylate cyclase-modulating G-protein coupled receptor signaling pathway. Among them, adenylate cyclase has been found to be significantly involved in many signaling pathways, which also indicates that adenylate cyclase plays an important role in the signaling pathway in periodontitis. According to the research of Petrovich *et al*[29], the decrease of adenylate cyclase activity increases with the severity of periodontal pathological process, so it may play an important role in the pathogenesis of periodontitis. In addition, we also found that fibroblasts are also an important functional pathway involved in periodontitis, which is involved in the derivation of osteoclasts, contributing to the loss of attachment and destruction of periodontal ligaments and leading to periodontitis[30].

On the other hand, we identified the transcription factors involved in these dysfunctional modules for periodontitis-related genes, and obtained 94 transcription factors involving 116 pivot-module interaction pairs. Statistical analysis of these transcription factors revealed that NFKB1 had significant regulatory effects on five functional modules, which may be the core transcription factor involved in the potential molecular mechanism of surgical treatment for periodontitis. NFKB1 has been found to be involved in immune responses, cell proliferation, and other processes. NFKB1 is an important molecule involved in osteoclast differentiation, so inhibition of its growth can be used to treat periodontitis and various bone and joint diseases [31]. Both SP1 and STAT3 have regulatory effects on the four functional modules. Transcription factor SP1 has been found in a large number of cases of periodontitis, indicating that it plays an important role in causing periodontitis[1]. The expression of STAT3 was inhibited in gingival epithelial cells of patients with diabetic periodontitis. Therefore, down-regulation of STAT3 signaling could improve diabetic periodontitis to some extent, which was confirmed by Wang *et al*[32]. These transcription factors can be considered as core transcription factors regulating the potential molecular mechanism of surgical treatment for periodontitis.

In addition, ncRNAs have been considered as important regulators of disease occurrence and development. We conducted pivot analysis based on the targeting relationship between ncRNAs and genes. The prediction results showed that there were 1198 ncRNAs that had significant regulatory effects on modules, including 1678 ncRNA-module interaction pairs. Statistical analysis of the results showed that MALAT1 had a significant regulatory relationship with six dysfunction modules, which were considered as key regulators of periodontitis. According to Ziebolz *et al*[33], MALAT1 can participate in the pathogenesis of periodontitis through a variety of pathways, including cytokine-cytokine receptor, adhesion molecule, and chemokine signal transduction pathway[2]. In addition, ANCR has been found to play an important role in regulating the osteogenic differentiation of periodontitis. In that study, ANCR has been found to regulate two functional modules[33]. At the same time, we screened a series of genes with the greatest connectivity, which were considered as the core driving molecules and identified as intrinsic genes. In total, there were eight endogenous genes, which may represent the potential key disorders in periodontitis treated by surgery. Analysis of these eight endogenous genes showed that EGF is an

Table 1 Biological functions and signal pathway of gene participation (excerpts)

ID	Description	*P*-value	Count
GO:0007631	Feeding behavior	1.49E-13	26
GO:0070371	ERK1 and ERK2 cascade	2.32E-13	46
GO:0070372	Regulation of ERK1 and ERK2 cascade	5.73E-13	44
GO:0050878	Regulation of body fluid levels	2.12E-12	57
GO:0097485	Neuron projection guidance	2.44E-12	38
GO:0007411	Axon guidance	8.41E-12	37
GO:0035567	Non-canonical Wnt signaling pathway	2.61E-11	28
GO:0007218	Neuropeptide signaling pathway	3.08E-11	23
GO:2000027	Regulation of organ morphogenesis	4.06E-11	36
GO:0019932	Second-messenger-mediated signaling	5.57E-11	43
GO:0009410	Response to xenobiotic stimulus	5.72E-11	38
GO:0051047	Positive regulation of secretion	8.82E-11	46
GO:1903532	Positive regulation of secretion by cell	9.27E-11	44
GO:0019373	Epoxygenase P450 pathway	1.21E-10	11
GO:1905330	Regulation of morphogenesis of an epithelium	2.75E-10	29
hsa04080	Neuroactive ligand-receptor interaction	7.10E-22	68
hsa00982	Drug metabolism - cytochrome P450	5.57E-09	21
hsa00980	Metabolism of xenobiotics by cytochrome P450	1.62E-08	21
hsa04020	Calcium signaling pathway	4.82E-08	34
hsa00830	Retinol metabolism	4.97E-08	19
hsa05204	Chemical carcinogenesis	6.96E-08	21
hsa04630	JAK-STAT signaling pathway	9.51E-08	31
hsa04060	Cytokine-cytokine receptor interaction	3.93E-07	44
hsa04024	cAMP signaling pathway	3.95E-07	34
hsa04913	Ovarian steroidogenesis	4.34E-07	15
hsa04713	Circadian entrainment	1.21E-06	21
hsa04151	PI3K-Akt signaling pathway	2.21E-06	48
hsa00590	Arachidonic acid metabolism	2.89E-06	16
hsa04650	Natural killer cell mediated cytotoxicity	6.05E-06	24
hsa04724	Glutamatergic synapse	6.17E-06	22

inhibitory factor for cell apoptosis[34]. According to the research results of many scholars, it can be shown that EGF has the effect of bone catabolism, which may stimulate osteoclast formation and tooth movement, and has a certain regulatory effect on the occurrence and development of periodontitis[35].

Based on the results of this study, we obtained several key functional modules of surgical treatment for periodontitis. These modules provide many proven periodontitis-related genes and candidate factors to be tested, which provide a theoretical basis for further study of periodontitis. We have also predicted a series of potential regulatory factors; these core regulatory factors may become the focus of future research on periodontitis.

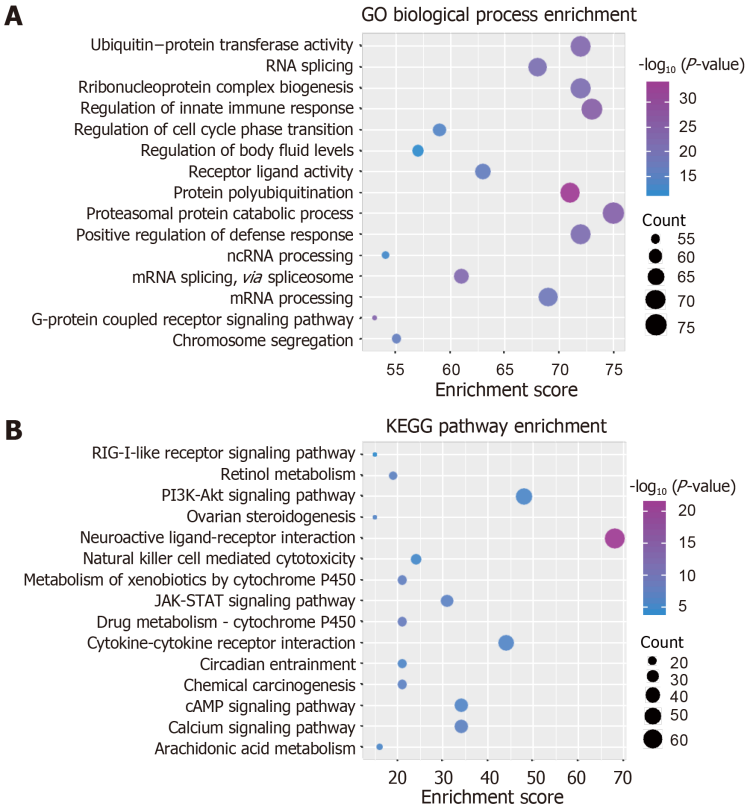

Figure 3 Functional and pathway identification of gene participation in surgical treatment for periodontitis. A: GO functional enrichment analysis of module genes (excerpts). The darker the color, the stronger the significance of enrichment. The larger the circle, the larger the proportion of module genes in GO functional entry genes; B: KEGG pathway enrichment analysis of module genes. The darker the color, the stronger the significance of enrichment. The larger the circle, the larger the proportion of module genes to KEGG pathway entry genes.

ARTICLE HIGHLIGHTS

Research background

Periodontal diseases are associated with various systemic diseases, including cardiovascular diseases such as stroke and atherosclerosis, which seriously affect the quality of life for patients.

Research motivation

At present, little is known about the potential mechanism of surgical treatment for periodontitis.

Research objectives

To explore the mechanism of surgical treatment for periodontitis based on the gene expression of peripheral blood mononuclear cells.

Research methods

Co-expression analysis, enrichment analysis, crosstalk analysis, and pivot regulatory factor prediction

Research results

A total of 337 genes related to periodontitis were clustered into 8 co-expression modules. These genes are mainly involved in G-protein coupled receptor signaling pathway, coupled to cyclic nucleotide second messenger, and adenylate cyclase-modulating G-protein coupled receptor signaling pathway. In addition, 94 transcription factors (including NFKB1, SP1, and STAT3) and 1198 ncRNAs (including MALAT1, CRNDE, and ANCR) regulatory module genes were identified.

Research conclusions

The key factors we have identified affect the recovery of periodontitis after surgery through a variety of biological processes and signaling pathways

Research perspectives

The results of this study provide a new theoretical basis and individualized treatment direction for follow-up treatment.

REFERENCES

1 **Larsson L**, Thorbert-Mros S, Rymo L, Berglundh T. Interleukin-10 genotypes of the -1087 single nucleotide polymorphism influence sp1 expression in periodontitis lesions. *J Periodontol* 2011; **82**: 1376-1382 [PMID: 21309719 DOI: 10.1902/jop.2011.100623]

2 **Peng W**, Deng W, Zhang J, Pei G, Rong Q, Zhu S. Long noncoding RNA ANCR suppresses bone formation of periodontal ligament stem cells via sponging miRNA-758. *Biochem Biophys Res Commun* 2018; **503**: 815-821 [PMID: 29913147 DOI: 10.1016/j.bbrc.2018.06.081]

3 **Schenkein HA**, Sabatini R, Koertge TE, Brooks CN, Purkall DB. Anti-cardiolipin from periodontitis patients induces MCP-1 production by human umbilical vein endothelial cells. *J Clin Periodontol* 2013; **40**: 212-217 [PMID: 23281818 DOI: 10.1111/jcpe.12043]

4 **Behle JH**, Papapanou PN. Periodontal infections and atherosclerotic vascular disease: an update. *Int Dent J* 2006; **56**: 256-262 [PMID: 16972401 DOI: 10.1111/j.1875-595X.2006.tb00110.x]

5 **van Winkelhoff AJ**, Winkel EG, Vandenbroucke-Grauls CM. [Periodontitis: a hidden chronic infection]. *Ned Tijdschr Geneeskd* 2001; **145**: 557-563 [PMID: 11293993]

6 **Schaefer AS**, Richter GM, Nothnagel M, Laine ML, Rühling A, Schäfer C, Cordes N, Noack B, Folwaczny M, Glas J, Dörfer C, Dommisch H, Groessner-Schreiber B, Jepsen S, Loos BG, Schreiber S. A 3' UTR transition within DEFB1 is associated with chronic and aggressive periodontitis. *Genes Immun* 2010; **11**: 45-54 [PMID: 19829306 DOI: 10.1038/gene.2009.75]

7 **Horning GM**, Hatch CL, Lutskus J. The prevalence of periodontitis in a military treatment population. *J Am Dent Assoc* 1990; **121**: 616-622 [PMID: 2229742 DOI: 10.14219/jada.archive.1990.0221]

8 **Preshaw PM**, Alba AL, Herrera D, Jepsen S, Konstantinidis A, Makrilakis K, Taylor R. Periodontitis and diabetes: a two-way relationship. *Diabetologia* 2012; **55**: 21-31 [PMID: 22057194 DOI: 10.1007/s00125-011-2342-y]

9 **Kumar RS**, Prakash S. Impaired neutrophil and monocyte chemotaxis in chronic and aggressive periodontitis and effects of periodontal therapy. *Indian J Dent Res* 2012; **23**: 69-74 [PMID: 22842253 DOI: 10.4103/0970-9290.99042]

10 **Novak MJ**, Novak KF. Early-onset periodontitis. *Curr Opin Periodontol* 1996; **3**: 45-58 [PMID: 8624569]

11 **Kranthi J**, Sudhakar K, Kulshrestha R, Raju PK, Razdan A, Srinivasa Ts. Comparison of the serum immunoglobulin IgM level in diabetic and nondiabetic patients with chronic periodontitis. *J Contemp Dent Pract* 2013; **14**: 814-818 [PMID: 24685780 DOI: 10.5005/jp-journals-10024-1408]

12 **Kinoshita N**, Awano S, Yoshida A, Soh I, Ansai T. Periodontal disease and gene-expression levels of metalloendopeptidases in human buccal mucosal epithelium. *J Periodontal Res* 2013; **48**: 606-614 [PMID: 23360525 DOI: 10.1111/jre.12045]

13 **Iacopino AM**, Cutler CW. Pathophysiological relationships between periodontitis and systemic disease: recent concepts involving serum lipids. *J Periodontol* 2000; **71**: 1375-1384 [PMID: 10972656 DOI: 10.1902/jop.2000.71.8.1375]

14 **van Winkelhoff AJ**, Tijhof CJ, de Graaff J. Microbiological and clinical results of metronidazole plus amoxicillin therapy in Actinobacillus actinomycetemcomitans-associated periodontitis. *J Periodontol* 1992; **63**: 52-57 [PMID: 1313103 DOI: 10.1902/jop.1992.63.1.52]

15 **Seymour GJ**, Palmer JE, Leishman SJ, Do HL, Westerman B, Carle AD, Faddy MJ, West MJ, Cullinan MP. Influence of a triclosan toothpaste on periodontopathic bacteria and periodontitis progression in cardiovascular patients: a randomized controlled trial. *J Periodontal Res* 2017; **52**: 61-73 [PMID: 26932733 DOI: 10.1111/jre.12369]

16 **Tucker R**. Periodontitis and pregnancy. *J R Soc Promot Health* 2006; **126**: 24-27 [PMID: 16478012 DOI: 10.1177/1466424006061170]

17 **D'Aiuto F**, Nibali L, Parkar M, Patel K, Suvan J, Donos N. Oxidative stress, systemic inflammation, and severe periodontitis. *J Dent Res* 2010; **89**: 1241-1246 [PMID: 20739696 DOI: 10.1177/0022034510375830]

18 **Kido J**, Bando Y, Bando M, Kajiura Y, Hiroshima Y, Inagaki Y, Murata H, Ikuta T, Kido R, Naruishi K, Funaki M, Nagata T. YKL-40 level in gingival crevicular fluid from patients with periodontitis and type 2 diabetes. *Oral Dis* 2015; **21**: 667-673 [PMID: 25740558 DOI: 10.1111/odi.12334]

19 **Bostanci N**, Oztürk VÖ, Emingil G, Belibasakis GN. Elevated oral and systemic levels of soluble triggering receptor expressed on myeloid cells-1 (sTREM-1) in periodontitis. *J Dent Res* 2013; **92**: 161-165 [PMID: 23242230 DOI: 10.1177/0022034512470691]

20 **Pejcic A**, Kesic LJ, Milasin J. C-reactive protein as a systemic marker of inflammation in periodontitis. *Eur J Clin Microbiol Infect Dis* 2011; **30**: 407-414 [PMID: 21057970 DOI: 10.1007/s10096-010-1101-1]

21 **Papapanou PN**, Sedaghatfar MH, Demmer RT, Wolf DL, Yang J, Roth GA, Celenti R, Belusko PB, Lalla E, Pavlidis P. Periodontal therapy alters gene expression of peripheral blood monocytes. *J Clin Periodontol* 2007; **34**: 736-747 [PMID: 17716309 DOI: 10.1111/j.1600-051X.2007.01113.x]

22 **Langfelder P**, Horvath S. WGCNA: an R package for weighted correlation network analysis. *BMC Bioinformatics* 2008; **9**: 559 [PMID: 19114008 DOI: 10.1186/1471-2105-9-559]

23 **Hopf TA**, Green AG, Schubert B, Mersmann S, Schärfe CPI, Ingraham JB, Toth-Petroczy A, Brock K, Riesselman AJ, Palmedo P, Kang C, Sheridan R, Draizen EJ, Dallago C, Sander C, Marks DS. The EVcouplings Python framework for coevolutionary sequence analysis. *Bioinformatics* 2018 [PMID: 30304492 DOI: 10.1093/bioinformatics/bty862]

24 **Carlin DE**, Demchak B, Pratt D, Sage E, Ideker T. Network propagation in the cytoscape cyberinfrastructure. *PLoS Comput Biol* 2017; **13**: e1005598 [PMID: 29023449 DOI: 10.1371/journal.pcbi.1005598]

25 **Yu G**, Wang LG, Han Y, He QY. clusterProfiler: an R package for comparing biological themes among gene clusters. *OMICS* 2012; **16**: 284-287 [PMID: 22455463 DOI: 10.1089/omi.2011.0118]

26 **Han H**, Cho JW, Lee S, Yun A, Kim H, Bae D, Yang S, Kim CY, Lee M, Kim E, Lee S, Kang B, Jeong D, Kim Y, Jeon HN, Jung H, Nam S, Chung M, Kim JH, Lee I. TRRUST v2: an expanded reference database of human and mouse transcriptional regulatory interactions. *Nucleic Acids Res* 2018; **46**: D380-D386 [PMID: 29087512 DOI: 10.1093/nar/gkx1013]

27 **Yi Y**, Zhao Y, Li C, Zhang L, Huang H, Li Y, Liu L, Hou P, Cui T, Tan P, Hu Y, Zhang T, Huang Y, Li X, Yu J, Wang D. RAID v2.0: an updated resource of RNA-associated interactions across organisms. *Nucleic Acids Res* 2017; **45**: D115-D118 [PMID: 27899615 DOI: 10.1093/nar/gkw1052]

28 **Grigoriadou ME**, Koutayas SO, Madianos PN, Strub JR. Interleukin-1 as a genetic marker for periodontitis: review of the literature. *Quintessence Int* 2010; **41**: 517-525 [PMID: 20490394]

29 **Petrovich IuA**, Podorozhnaia RP, Genesina TI, Beloklitskaia GF. [Adenylate cyclase and guanylate

cyclase in the saliva of healthy persons and in periodontitis]. *Stomatologiia (Mosk)* 1991; 30-33 [PMID: 1685812]

30 **Beklen A**, Al-Samadi A, Konttinen YT. Expression of cathepsin K in periodontitis and in gingival fibroblasts. *Oral Dis* 2015; **21**: 163-169 [PMID: 24661326 DOI: 10.1111/odi.12230]

31 **Jimi E**, Fukushima H. [NF-κB signaling pathways and the future perspectives of bone disease therapy using selective inhibitors of NF-κB]. *Clin Calcium* 2016; **26**: 298-304 [PMID: 26813510]

32 **Wang Q**, Li H, Xie H, Fu M, Guo B, Ding Y, Li W, Yu H. 25-Hydroxyvitamin D3 attenuates experimental periodontitis through downregulation of TLR4 and JAK1/STAT3 signaling in diabetic mice. *J Steroid Biochem Mol Biol* 2013; **135**: 43-50 [PMID: 23333931 DOI: 10.1016/j.jsbmb.2013.01.008]

33 **Li S**, Liu X, Li H, Pan H, Acharya A, Deng Y, Yu Y, Haak R, Schmidt J, Schmalz G, Ziebolz D. Integrated analysis of long noncoding RNA-associated competing endogenous RNA network in periodontitis. *J Periodontal Res* 2018; **53**: 495-505 [PMID: 29516510 DOI: 10.1111/jre.12539]

34 **Vaahtokari A**, Aberg T, Thesleff I. Apoptosis in the developing tooth: association with an embryonic signaling center and suppression by EGF and FGF-4. *Development* 1996; **122**: 121-129 [PMID: 8565823]

35 **Alves JB**, Ferreira CL, Martins AF, Silva GA, Alves GD, Paulino TP, Ciancaglini P, Thedei G, Napimoga MH. Local delivery of EGF-liposome mediated bone modeling in orthodontic tooth movement by increasing RANKL expression. *Life Sci* 2009; **85**: 693-699 [PMID: 19796647 DOI: 10.1016/j.lfs.2009.09.010]

World Journal of Clinical Cases

Submit a Manuscript: https://www.f6publishing.com

World J Clin Cases 2019 June 26; 7(12): 1393-1402

DOI: 10.12998/wjcc.v7.i12.1393

ISSN 2307-8960 (online)

ORIGINAL ARTICLE

Case Control Study

Clinical differentiation of acute appendicitis and right colonic diverticulitis: A case-control study

Yosuke Sasaki, Fumiya Komatsu, Naoyasu Kashima, Takahiro Sato, Ikutaka Takemoto, Sho Kijima, Tadashi Maeda, Takamasa Ishii, Taito Miyazaki, Yoshiko Honda, Nagato Shimada, Yoshihisa Urita

ORCID number: Yosuke Sasaki (0000-0002-5290-4875); Fumiya Komatsu (0000-0003-3011-1089); Naoyasu Kashima (0000-0003-4650-432X); Takahiro Sato (0000-0003-4678-1095); Ikutaka Takemoto (0000-0002-3020-7972); Sho Kijima (0000-0001-9599-8405); Tadashi Maeda (0000-0002-9475-8909); Takamasa Ishii (0000-0002-7218-043X); Taito Miyazaki (0000-0001-7239-8677); Yoshiko Honda (0000-0002-9939-1587); Nagato Shimada (0000-0002-1482-9405); Yoshihisa Urita (0000-0003-1740-0572).

Author contributions: Sasaki Y designed the research, collected data, and wrote the manuscript; Komatsu F and Kashima N collected data with Sasaki Y; Takemoto I and Kijima S assisted with data collection; Ishii T supervised data collection; Sato T, Maeda T, and Miyazaki T provided supervision and discussion as experts of infectious diseases; Honda Y and Shimada N provided supervision and discussion as surgeons; and Urita Y supervised the research and supervised statistical analyses.

Institutional review board statement: The ethics committee of Toho University Medical Center Omori Hospital approved the study's protocol (M17057).

Informed consent statement: The center's ethics committee approved waiver of individual informed consent subject to public announcement of the research

Yosuke Sasaki, Fumiya Komatsu, Naoyasu Kashima, Takahiro Sato, Ikutaka Takemoto, Sho Kijima, Tadashi Maeda, Takamasa Ishii, Taito Miyazaki, Yoshiko Honda, Nagato Shimada, Yoshihisa Urita, Department of General Medicine and Emergency Care, Toho University School of Medicine, Ota-ku, Tokyo 143-8541, Japan

Corresponding author: Yosuke Sasaki, MD, PhD, Assistant Professor, Department of General Medicine and Emergency Care, Toho University School of Medicine, Omori Hospital, 6-11-1 Omori-Nishi, Ota-Ku, Tokyo 143-8541, Japan. yousuke.sasaki@med.toho-u.ac.jp
Telephone: +81-3-37624151
Fax: +81-3-37656518

Abstract

BACKGROUND

Acute right colonic diverticulitis (ARCD) is an important differential diagnosis of acute appendicitis (AA) in Asian countries because of the unusually high prevalence of right colonic diverticula. Due to qualitative improvement and the high penetration rate of computed tomography (CT) scanning in Japan, differentiation of ARCD and AA mainly depends on this modality. But cost, limited availability, and concern for radiation exposure make CT scanning problematic. Differential findings of ARCD from AA are based on several small studies that used univariate comparisons from Korea and Taiwan. Previous studies on clinical and laboratory differences between AA and ARCD are limited.

AIM

To determine clinical differences between AA and ARCD for differentiation of these two diagnoses by creating a logistic regression model.

METHODS

We performed an exploratory single-center retrospective case-control study evaluating 369 Japanese patients (age ≥ 16 years), 236 (64.0%) with AA and 133 (36.0%) with ARCD, who were hospitalized between 2012 and 2016. Diagnoses were confirmed by CT images. We compared age, sex, onset-to-visit interval, epigastric/periumbilical pain, right lower quadrant (RLQ) pain, nausea/vomiting, diarrhea, anorexia, medical history, body temperature, blood pressure, heart rate, RLQ tenderness, peritoneal signs, leukocyte count, and levels of serum creatinine, serum C-reactive protein (CRP), and serum alanine aminotrans-ferase. We subsequently performed logistic regression analysis for differentiating AA from ARCD based on the results of the univariate analyses.

because of the retrospective and noninvasive study design. Comprehensive consents were obtained by all participants.

Manuscript source: Unsolicited manuscript

Received: March 12, 2019
Peer-review started: March 13, 2019
First decision: March 19, 2019
Revised: April 13, 2019
Accepted: May 10, 2019
Article in press: May 11, 2019
Published online: June 26, 2019

P-Reviewer: Augustin G, Wijaya R
S-Editor: Wang JL
L-Editor: A
E-Editor: Xing YX

RESULTS

In the AA and ARCD groups, median ages were 35.5 and 41.0 years, respectively (p=0.011); median onset-to-visit intervals were 1 [interquartile range (IQR): 0-1] and 2 (IQR: 1-3) days, respectively ($P < 0.001$); median leukocyte counts were 12600 and 11500/mm^3, respectively ($P = 0.002$); and median CRP levels were 1.1 (IQR: 0.2-4.1) and 4.9 (IQR: 2.9-8.5) mg/dL, respectively ($P < 0.001$). In the logistic regression model, odds ratios (ORs) were significantly high in nausea/vomiting (OR: 3.89, 95%CI: 2.04-7.42) and anorexia (OR: 2.13, 95%CI: 1.06-4.28). ORs were significantly lower with a longer onset-to-visit interval (OR: 0.84, 95%CI: 0.72-0.97), RLQ pain (OR: 0.28, 95%CI: 0.11-0.71), history of diverticulitis (OR: 0.034, 95%CI: 0.005-0.20), and CRP level > 3.0 mg/dL (OR: 0.25, 95%CI: 0.14-0.43). The regression model showed good calibration, discrimination, and optimism.

CONCLUSION

Clinical findings can differentiate AA and ARCD before imaging studies; nausea/vomiting and anorexia suggest AA, and longer onset-to-visit interval, RLQ pain, previous diverticulitis, and CRP level > 3.0 mg/dL suggest ARCD.

Key words: Abdominal pain; Acute abdomen; Appendicitis; Clinical difference; C-reactive protein; Diverticulitis; Right lower quadrant pain

Core tip: Right colonic diverticulitis is an important differential diagnosis of appendicitis in Asian countries because of the unusually high prevalence of right colonic diverticula; however, studies reporting clinical differentiation between appendicitis and right colonic diverticulitis are still limited. Our case-control study using a logistic regression model shows that nausea/vomiting [odds ratio (OR): 3.89] and anorexia (OR: 2.13) suggest that appendicitis is more likely. On the other hand, longer onset-to-visit interval (OR: 0.84), right lower quadrant pain (OR: 0.28), history of diverticulitis (OR: 0.034), and CRP level > 3.0 mg/dL (OR: 0.25) suggest that right colonic diverticulitis is more likely.

Citation: Sasaki Y, Komatsu F, Kashima N, Sato T, Takemoto I, Kijima S, Maeda T, Ishii T, Miyazaki T, Honda Y, Shimada N, Urita Y. Clinical differentiation of acute appendicitis and right colonic diverticulitis: A case-control study. *World J Clin Cases* 2019; 7(12): 1393-1402
URL: https://www.wjgnet.com/2307-8960/full/v7/i12/1393.htm
DOI: https://dx.doi.org/10.12998/wjcc.v7.i12.1393

INTRODUCTION

Because of the unusually high prevalence of right colonic diverticulosis in Asian countries[1-3], acute right colonic diverticulitis (ARCD) is a very important differential diagnosis of acute appendicitis (AA) in Asian countries[4,5]. Thanks to qualitative improvement and the high penetration rate of computed tomography (CT) scanning in Japan[6], differentiation of ARCD and AA mainly depends on this modality. However, cost, limited availability in primary care settings[7], and concern for radiation exposure in young patients[8] make CT scanning problematic. Although prolonged pain, initial right lower quadrant (RLQ) pain, lack of migration of pain, leukocytosis, nausea/vomiting, constipation, and systemic toxic signs have been proposed as differential findings of ARCD from AA[4,9-12], these findings are based on several small studies using univariate comparisons from Korea and Taiwan[9-12]; we could not find any previous published studies from Japan or confounder-adjusted studies. Therefore, this study aimed to reveal useful clinical differentiation points between AA and ARCD using a logistic regression model that adjusted for confounders based on Japanese data. Given the limitations of CT scanning described above[7,8], evidence on the clinical differences between ARCD and AA may be useful to clinicians.

MATERIALS AND METHODS

Design and patients

In this exploratory single-center retrospective case-control study, we evaluated medical records from patients of the Toho University Medical Center Omori Hospital, which has 948 beds and is located in Tokyo, Japan. The ethics committee of Toho University Medical Center Omori Hospital approved the study's protocol (M17057). Patients were enrolled if they were ≥ 16 years old and hospitalized for AA or ARCD between January 2012 and December 2016. All patients were Japanese (immigrants or tourists were not included). Diagnoses were confirmed by CT scans in all cases and for both groups. We included both simple and complicated appendicitis in the AA group. Patients with a history of appendectomy were excluded. We included both simple and complicated right colonic diverticulitis in the ARCD group.

Study variables

The patients' medical records were searched to collect data from their first visit, such as age, sex, time interval from the onset of symptoms until the time of the visit (onset-to-visit interval), epigastric/periumbilical pain, RLQ pain, nausea/vomiting, diarrhea, anorexia, medical history (of previous AA treated without appendectomy, previous acute diverticulitis (including any parts of the colon), diabetes, hypertension, hyperlipidemia, liver cirrhosis, hemodialysis, chronic lung diseases, malignant tumors, immunosuppressant use, and antiplatelet use), body temperature, blood pressure, heart rate, RLQ tenderness, peritoneal signs, leukocyte count, levels of serum creatinine, serum C-reactive protein (CRP), and serum alanine aminotransferase (ALT), and findings of CT and ultrasonography at admission. Body temperature was measured at the axilla with an electric thermometer (Terumo, Tokyo, Japan). We reviewed whether the patients had a history of acute appendicitis that was treated without appendectomy because previous appendicitis is a well-known risk factor of recurrent appendicitis if appendectomy was not performed[13]. Although ALT has not been reported as a potential confounder in any previous studies, we collected and evaluated the ALT level to ensure that liver function abnormality was not a confounder in this study.

Categorization of contentious variables

All continuous variables except for onset-to-visit interval were categorized for statistical analyses as follows. Fever was defined as an axillary measured body temperature ≥ 38.0°C[9]. Shock was defined as systolic blood pressure < 12.0 kPa (< 90 mmHg)[14]. Tachycardia was defined as heart rate ≥ 100 beats per minute. Leukocytosis was defined as a leukocyte count > 11000/mm^3[15]. Elevated liver enzyme was defined as ALT > 29 IU/L[16]. Renal dysfunction was defined as a serum creatinine level > 1.2 mg/dL because of difficulty with retrospectively obtaining the estimated glomerular filtration ratio. Because we could not find previous studies that defined a specific cut-off of age groups, we divided the patients into age groups based on the median age of the patients as follows: young, ≤ 40 years and old, > 40 years; we did not use receiver operator characteristic (ROC) analysis of age for predicting ARCD because it was poorly accurate [area under the curve (AUC) was 0.41]. CRP was categorized as low: ≤ 3.0 mg/dL or high: > 3.0 mg/dL because ROC analysis of CRP for predicting ARCD showed that a CRP level of 3.0 mg/dL had the best corrective classification as much as 71.0% (AUC, 0.76; sensitivity, 75.2%; specificity, 68.6%; Figure 1).

Statistical analyses

Univariate comparisons: We compared all evaluated patient characteristics with AA and ARCD to select candidates of independent variables of logistic regression. The chi-square test was used for all dichotomous/categorical variables, while the Wilcoxon rank-sum test was used for continuous variables because of their skewed distributions.

Logistic regression model: Logistic regression analysis was subsequently performed based on the results of the univariate analyses. As mentioned above, we converted all continuous variables, except for onset-to-visit interval, into categorized variables for logistic regression. We examined the variance inflation factors (VIF) to evaluate multicollinearity of the regression model.

Discrimination, calibration, and internal validation of the regression model: We performed discrimination of the regression model by creating an ROC curve. We also calibrated the model using the Hosmer-Lemeshow (HL) goodness of fit test. Finally, we performed internal validation by bootstrap methods with 100 samples for 5 times.

All statistical analyses were performed using Stata/IC software (version 15.1; Stata Corp., College Station, TX, USA). A *P*-value < 0.05 was considered statistically significant. The statistical methods of this study were reviewed by Takuhiro Moro-

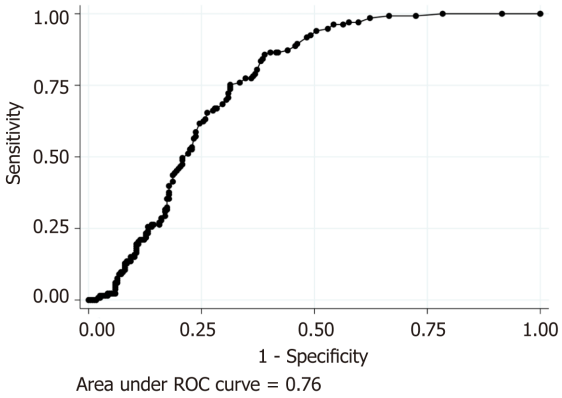

Figure 1 Receiver operating characteristic curve of C-reactive protein for predicting acute right colonic diverticulitis. C-reactive protein (CRP) was categorized as low: ≤ 3.0 mg/dL or high: > 3.0 mg/dL because receiver operating characteristic analysis of CRP for predicting acute right colonic diverticulitis shows that a CRP level of 3.0 mg/dL has the best corrective classification as much as 71.0% (area under curve, 0.76; sensitivity, 75.2%; specificity, 68.6%). ROC: Receiver operating characteristic.

mizato from the Internal Medicine Department, Renal and Rheumatology Division of the Okinawa Nanbu Medical Center and Children's Medical Center.

The manuscript was written according to the STROBE Statement—checklist of items.

RESULTS

The 369 eligible patients consisted of 236 patients (64.0%) with AA and 133 patients (36.0%) with ARCD. The median age was 38 years and 212 patients (57.5%) were men. Patient characteristics and the results of the univariate analyses are shown in Table 1. In 236 patients with AA, 38 patients (16.1%) were diagnosed with complicated appendicitis. On the other hand, 10/133 patients (7.5%) with ARCD were diagnosed with complicated right colonic diverticulitis. In 41 patients with a history of appendicitis, only 6 patients with a history of appendectomy were excluded before the study because conservative treatment for AA was the *de facto* standard treatment for appendicitis in our hospital; 32 and 3 patients with a history of appendicitis were eventually included in the AA group and ARCD group, respectively ($P < 0.001$, Table 1). The univariate analyses revealed that patients aged > 40 years were significantly less prevalent in the AA group; the median ages were 35.5 years [interquartile range (IQR), 25.0-50.5 years] in the AA group and 41.0 years (IQR, 31.0-51.0 years) in the ARCD group ($P = 0.011$). The onset-to-visit interval was 1 day longer in the ARCD group; the median interval was 1 d (IQR, 0-1) in the AA group and 2 d (IQR, 1-3) in the ARCD group ($P < 0.001$). The numbers of patients with epigastric/periumbilical pain, nausea/vomiting, anorexia, and history of unresected appendicitis were significantly higher in the AA group. Conversely, the numbers of patients with RLQ pain, history of diverticulitis, leukocytosis, and high CRP levels were significantly higher in the ARCD group. Median leukocyte counts in the AA and ARCD groups were 12600/mm^3 (IQR, 10100-15200) and 11500/mm^3 (IQR, 9500-13500), respectively ($P = 0.002$). Median CRP levels in the AA and ARCD groups were 1.1 mg/dL (IQR, 0.2-4.1) and 4.9 mg/dL (IQR, 2.9-8.5), respectively ($P < 0.001$). Although RLQ pain was significantly prevalent in the ARCD group (AA 72.5% *vs* ARCD 94.0%, $P < 0.001$), the prevalence of RLQ tenderness was not different between the groups (AA 97.5% *vs* ARCD 95.5%, $P = 0.31$). In 65 patients with AA without RLQ pain, 61 (93.9%) had RLQ tenderness. Prevalence of fever (body temperature ≥ 38.0°C) was not significantly different between the AA and ARCD groups (AA 14.4% *vs* ARCD 15.0%, $P = 0.87$). Because the definition of fever differs among previous studies[9,11,17], we also evaluated the prevalence of fever with the definition of fever as a body temperature > 37.2°C[11] or > 37.3°C[17]. However, all results showed that the prevalence of fever was not significantly different between AA and ARCD ($P = 0.77$-0.78).

On the basis of the results of univariate analysis, we performed logistic regression analysis to compare AA and ARCD using the following ten factors as explanatory factors: Age, onset-to-visit interval, epigastric/periumbilical pain, RLQ pain, nausea/vomiting, anorexia, history of unresected appendicitis, history of acute appendicitis, leukocytosis (leukocyte >11000/mm^3), and high CRP level (> 3.0 mg/dL). As shown

Table 1 Patient characteristics *n* (%)

Characteristics	Appendicitis (*n* = 236)	Diverticulitis (*n* = 133)	*P*-value
Age > 40 (yr)	96.0 (40.7)	70.0 (52.6)	0.027[a]
Age (years)	35.5 [25-50.5]	41.0 [31.0-51.0]	0.011[a]
Male sex	129 (54.7)	83 (62.4)	0.149
Onset-to-visit interval (d)	1 [0-1]	2 [1-3]	< 0.001[a]
Epigastric/periumbilical pain	119 (50.4)	47 (35.3)	0.005[a]
RLQ pain	171 (72.5)	125 (94.0)	< 0.001[a]
Nausea/vomiting	123 (52.1)	19 (14.3)	< 0.001[a]
Diarrhea	46 (19.5)	25 (18.8)	0.871
Anorexia	64 (27.1)	21 (15.8)	0.013[a]
History of unresected appendicitis	32 (13.6)	3 (2.3)	< 0.001[a]
History of diverticulitis	2 (0.9)	22 (16.5)	< 0.001[a]
Diabetes mellitus	11 (4.7)	2 (1.5)	0.114
Hypertension	24 (10.2)	14 (10.5)	0.914
Dyslipidemia	21 (8.9)	15 (11.3)	0.459
Liver cirrhosis	0	1 (0.8)	0.182
Hemodialysis	0	1 (0.8)	0.182
Chronic lung diseases	2 (0.9)	1 (0.8)	0.922
Malignancy	1 (0.4)	2 (1.5)	0.267
Immunosuppressant use	1 (0.4)	3 (2.3)	0.103
Antiplatelet use	0	0	N/A
Fever	34 (14.4)	20 (15.0)	0.869
Shock	6 (2.5)	3 (2.3)	0.864
RLQ tenderness	230 (97.5)	127 (94.5)	0.306
Peritoneal signs	137 (58.1)	72 (54.1)	0.466
Leukocytosis	159 (67.4)	72 (54.1)	0.012[a]
Leukocyte count ($10^3/mm^3$)	12.6 [10.1-15.2]	11.5 [9.3-13.5]	0.002[a]
High CRP level (> 3.0 mg/dL)	74 (31.4)	98 (73.7)	< 0.001[a]
CRP level (mg/dL)	1.1 [0.2-4.1]	4.9 [2.9-8.5]	< 0.001[a]
Creatinine level > 1.2 (mg/dL)	7 (3.0)	5 (3.8)	0.68
ALT level > 29 (IU/L)	38 (16.1)	24 (18.1)	0.632

[a]*P* value < 0.05. AA: Acute appendicitis; ALT: Alanine aminotransferase; ARCD: Acute right colonic diverticulitis; CRP: C-reactive protein; N/A: Not applicable; RLQ: Right lower quadrant.

in Table 2 and Figure 2, the logistic regression revealed that nausea/vomiting and anorexia had significantly high odds ratios (ORs), suggesting that AA is more likely. On the other hand, longer onset-to-visit interval, RLQ pain, history of diverticulitis, and high CRP level had significantly low ORs, suggesting that ARCD is more likely. Age, epigastric/periumbilical pain, history of unresected appendectomy, and leukocytosis were not significant. The regression model showed good calibration (HL chi-square: 8.14, $P = 0.42$) and good discrimination (AUC = 0.86, Figure 3), and there was no multicollinearity because the VIF of all explanatory variables were 1.2 or less and the mean VIF was 1.10. Optimism, as calculated by the bootstrap method, was 0.00003.

DISCUSSION

Previous studies have reported prolonged pain and higher age as predictors of ARCD and nausea/vomiting and leukocytosis as predictors of AA; most of our results were consistent with the results of previous studies[9-12]. On the other hand, history of diverticulitis, RLQ pain, and high serum CRP levels have not been previously established as predictors of ARCD.

In order to discuss the clinical differences of AA and ARCD, we would like to begin with discussing the association between clinical findings and the pathophysiologies of AA and ARCD, especially the differences between them, because we think that

Table 2 Logistic regression for differentiating acute appendicitis from acute right colonic diverticulitis

	OR [95%CI]	*P*-value
Age >40 (yr)	0.62 [0.35-1.08]	0.093
Onset-to-visit interval (d)	0.84 [0.72-0.97]	0.021[a]
Epigastric/periumbilical pain	1.14 [0.65-2.00]	0.64
RLQ pain	0.28 [0.11-0.71]	0.007[a]
Nausea/vomiting	3.89 [2.04-7.42]	< 0.001[a]
Anorexia	2.13 [1.06-4.28]	0.033[a]
History of unresected appendicitis	3.09 [0.82-11.63]	0.095
History of diverticulitis	0.034 [0.0059-0.20]	< 0.001[a]
Leukocytosis	1.50 [0.86-2.60]	0.15
High CRP level (>3.0 mg/dL)	0.25 [0.14-0.43]	< 0.001[a]

[a]*P*-value < 0.05. CRP: C-reactive protein; OR: Odds ratio; RLQ: Right lower quadrant.

clinical differences are based on differences in pathologies of AA (localized peritonitis following intraluminal pressure elevation of the appendix) and diverticulitis (localized peritonitis due to microperforation of the affected diverticulum).

While contradicting evidence has been proposed[18], most cases of AA are traditionally thought to be initiated by elevation of the intraluminal pressure of the appendix (with concurrent inflammation), which can be caused by luminal obstruction associated with fecalith, enlarged lymphoid tissue, barium, worms, tumors, or appendiceal ulcer due to unknown etiology[18,19]. These conditions cause poorly localized visceral epigastric/periumbilical pain that is conducted by slow-conducting C fibers that enter the spinal cord at T8-T10[19,20]. Anorexia, nausea, and vomiting soon follow as the distension exacerbates[21]. Persistent elevation of intraluminal pressure of the appendix causes ischemia and subsequently proceeds to necrosis of the appendix and localized peritonitis around the adjacent parietal peritoneum, which cause somatic pain localized to the RLQ that is conducted by A delta fibers (fast-conducting and unilateral)[19]. Previous studies comparing AA and ARCD reported that the prevalence of the migration of pain in AA was 39.2%-82.0%, which is a significantly higher prevalence than that in ARCD (15.4%-54.0%)[9-11]. Another review on AA reported that the sensitivity and specificity of the migration for the diagnosis of AA were 64% and 82%, respectively[21]. Although we lacked the prevalence of the migration of pain in the present study, our result indicating a significantly high OR of nausea/vomiting and anorexia in the logistic regression model for differentiating AA from ARCD is compatible with the generally accepted pathophysiology described above and that discussed in previous studies. In four previous studies, two studies showed a significantly high proportion of nausea/vomiting in AA cases; the proportions were 8%-16% in ARCD groups and 32%-72% in AA groups[10,12]. The proportions were insignificant in the other two studies[9,11].

On the other hand, acute diverticulitis is thought to be caused by localized peritonitis around the diverticulum due to micro-macroperforation from invasion or ischemia of the affected diverticulum *via* fecalith[22,23]. Therefore, acute diverticulitis generally presents as "localized peritonitis" without the preceding phase of symptoms caused by visceral nerve stimulation. This difference of pathophysiology from AA may explain the reason why our study showed that RLQ pain, a typical symptom of localized peritonitis around ascending colonic diverticula, was more prevalent in ARCD at the time of visit while some patients with AA visited the hospital due to other symptoms associated with elevated intraluminal pressure, such as nausea/vomiting or epigastric/periumbilical pain before complaining of RLQ pain. The results of comparing the prevalence of RLQ pain between AA and ARCD patients differs among previous studies[9,11,12]. Our logistic regression model showed a significantly lower OR, implying that RLQ pain was a better predictor of ARCD.

Although a previous study showed that ARCD had prolonged symptoms compared to AA (ARCD 68.4 ± 23.3 h *vs* AA 29.8 ± 20.2 h, $P < 0.01$)[9], we could not find the cause of the difference. We think that rapid progression of AA may explain the shorter onset-to-visit interval in AA cases; approximately 90% of patients with AA reportedly developed localized inflammation or necrosis within 24 h after onset of symptoms[24]. Namely, rapid exacerbation and changing symptoms might motivate patients to visit the hospital early.

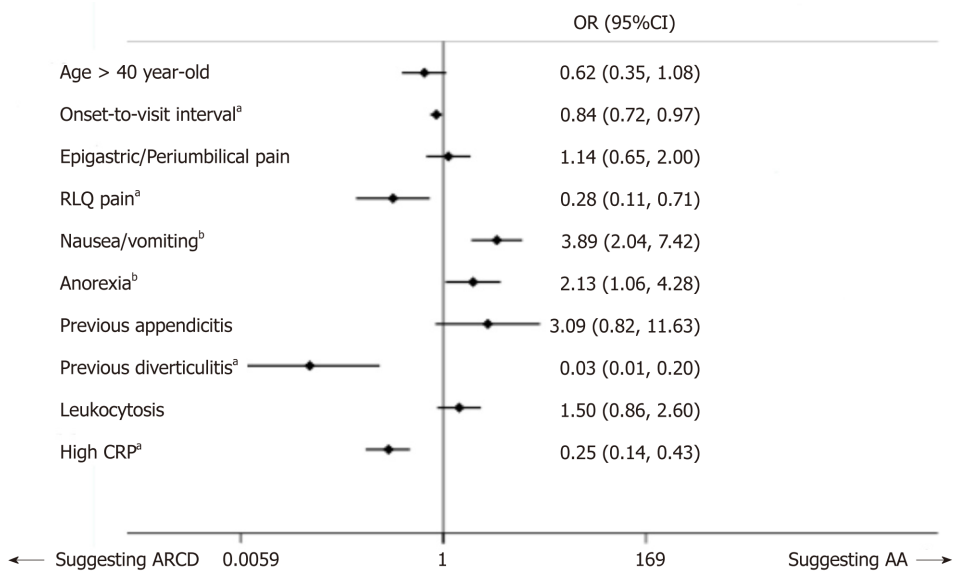

Figure 2 Forest plot of the logistic regression model for differentiating acute appendicitis from acute right colonic diverticulitis. [a]Longer onset-to-visit interval, right lower quadrant pain, history of diverticulitis, and high serum C-reactive protein level (>3.0 mg/dL) at the time of visit have significantly low odds ratios (ORs), which suggests that acute right colonic diverticulitis (ARCD) is more likely rather than acute appendicitis (AA) (left side of the figure). [b]Nausea/vomiting and anorexia have significantly high ORs, which suggests that AA is more likely rather than ARCD (right side of the figure). AA: Acute appendicitis; ARCD: Acute right colonic diverticulitis; CRP: C-reactive protein; OR: Odds ratio; RLQ: Right lower quadrant.

Diagnostic ability of CRP in AA patients has been extensively studied[25]. Although it is frequently elevated, recent reviews have concluded that serum CRP has insufficient diagnostic utility of simple appendicitis, especially in the early phase[8,25]. Some studies showed that an elevated CRP level and persistent elevation of the CRP level reportedly serve as predictors of perforated appendicitis or appendicitis complicated with an intra-abdominal abscess[8,25]. On the other hand, recent reviews concluded that the CRP level is associated with diverticulitis severity[26]. Similar to appendicitis, the CRP level was also significantly higher in patients who required surgery or cases with perforated diverticulitis compared to mild or simple diverticulitis[27]. Although previous studies suggested that lack of systemic signs of toxicity and fever make ARCD more likely compared to AA[4,11], they did not mention CRP. Therefore, to the best of our knowledge, this is the first study to discuss differences of CRP between appendicitis and diverticulitis. We think our result aligned with previously explained CRP elevation in proportion to progression and severity of peritonitis or intra-abdominal inflammation[8,28]. Namely, the CRP value was lower in the AA group because it included patients with simple appendicitis who had a low CRP level due to the absence of peritoneal inflammation, while most patients with ARCD had an elevated CRP level associated with peritonitis. Considering the chronological elevation of CRP levels in AA[8,29], a longer onset-to-visit interval may confound the higher CRP at the time of visit in ARCD cases. However, our logistic regression indicated that the CRP level was independent from the onset-to-visit interval.

Previous studies have proposed leukocytosis as an important differential factor of AA rather than ARCD based on univariate analyses[9,10,12]. Our study also showed a higher leukocyte count in the AA group than in the ARCD group. However, it was not a significant predictive factor in our logistic regression model (Table 2 and Figure 2).

We believe that our findings will provide new evidence on the utility of CRP and leukocytosis for diagnosing acute abdomen. However, considering the inconsistent clinical significance of CRP for diagnosing acute abdomen in previous studies and the discrepancy of significance of leukocytosis between previous studies and the present study, a cautious attitude is required when applying our results to individual patients. We will separately discuss the heterogeneity of cases (simple and complicated) in the present study in the following paragraphs about our study limitations.

Similar to a previous study[9], our univariate comparison showed that a higher median age of patients in the ARCD group was comparable to that in the AA group. Yet, it was insignificant in logistic regression. Increase of diverticulosis in proportion to patients' age[23] and higher prevalence of AA in younger patients[21] may explain the

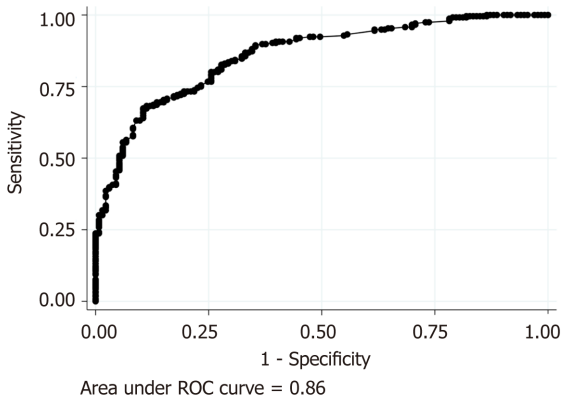

Figure 3 Receiver operating characteristic curve of the logistic regression model for differentiating acute appendicitis from acute right colonic diverticulitis. Receiver operating characteristic curve of the regression model for differentiating acute appendicitis from acute right colonic diverticulitis shows good discrimination, with an area under the curve as high as 0.86, as shown above. ROC: Receiver operating characteristic.

difference of age. On the other hand, the age of the patients with ARCD is reportedly younger than the age of patients with left colonic diverticulitis[5]. Given that our study included only patients with ARCD, this age difference among the site of diverticulum may explain the insignificance in our logistic regression.

Our study has some limitations. First, because the present study was a retrospective case-control study that used medical records, we could not collect some previously reported important information, such as parameters included in the Alvarado score[17], *e.g.*, migration of abdominal pain or neutrophilia/left shift, despite previous studies clearly showing a high prevalence of pain migration and higher Alvarado score in AA compared to ARCD[9,11,12]. Furthermore, because the patient groups in the present study were limited to patients with AA and ARCD instead of including all patients with differential diagnoses of RLQ pain, our results should be cautiously applied to patients with RLQ pain.

As mentioned earlier, we diagnosed AA and ARCD based on the findings of CT because it has been the most common diagnostic tool of AA and ARCD in Japanese clinical practice thanks to the fact that CT is the most available modality[6]. We believe that we could appropriately diagnose AA and ARCD by CT because its respective sensitivities and specificities are reportedly 90%-100% and 91%-99% for diagnosing AA[20], and 94% and 99% for diagnosing colonic diverticulitis[30]. Of note, we lacked the confirmation of diverticula by colonoscopy or barium enema examination in the present retrospective study.

Second, the cut-off value of the CRP level in our study can be regarded as arbitrarily defined because it was not previously defined. However, we determined 3.0 mg/dL as the cut-off value based on the result of ROC analysis (Figure 1) because of the lack of commonly used cut-off values of the CRP level; the cut-off values for diagnosing AA or ARCD vary widely between 3.0 and 20 mg/dL depending on the study[8,25-27].

Third, we included 38 (16.1%) patients with complicated appendicitis in the AA group. As discussed, symptoms, physical findings, and laboratory data of uncomplicated cases should be different from those of complicated appendicitis; complicated appendicitis should manifest similarly to ARCD because of the progression of peritonitis. Thus, the mixed results in the AA group might affect the study results. We initially considered dividing the AA group into simple appendicitis and complicated appendicitis groups, as done in a previous study[10]. However, we eventually took priority in examining our simple question, "Does this patient have appendicitis or diverticulitis?" Therefore, we eventually included all cases in one AA group, regardless of complications/stages. We will evaluate the clinical differences of simple and complicated appendicitis in a separate clinical study. We also included 10 (7.5%) patients with complicated right colonic diverticulitis in the ARCD group. Although we took priority in examining appendicitis or diverticulitis in the present study, further studies on the clinical difference of simple and complicated ARCD are required. Because this study included potentially different cases in the same groups, we have to be cautious in applying our results to individual cases. Because previous studies focused on differences between each single parameter[9-12], further multivariable analysis or scoring system studies that address the limitations of the present study are warranted.

In conclusion, our logistic regression model for differentiating AA from ARCD showed that nausea/vomiting and anorexia increase the probability of AA rather than ARCD. Conversely, longer onset-to-visit interval, RLQ pain, history of diverticulitis, and CRP level > 3.0 mg/dL at the time of visit increase the probability of ARCD rather than AA (Figure 2). Because of the lack of previous studies on the clinical differences between AA and ARCD (especially from Japan), and the cost, limited availability, and concern for radiation exposure of CT scanning, we believe that our findings provide important evidence for many physicians managing acute abdominal pain.

ACKNOWLEDGEMENTS

We acknowledge the excellent assistance of the staff of Harvard Medical School Introduction to Clinical Research Training Japan and Okinawa Asia Clinical Investigation Synergy (OACIS). Moreover, we thank Dr. Takuhiro Moromizato (Internal Medicine Department, Renal and Rheumatology Division at the Okinawa Nanbu Medical Center and Children's Medical Center) for providing assistance and reviewing the statistical analysis.

ARTICLE HIGHLIGHTS

Research background

Because of the high prevalence of right colonic diverticulosis in Asian countries, acute right colonic diverticulitis (ARCD) is an important differential diagnosis of acute appendicitis (AA) in Asian countries. However, studies on the clinical differentiation of AA and ARCD are limited.

Research motivation

Given the cost, limited availability in primary care settings and concern for radiation exposure in young patients of computed tomography (CT) scan, evidence on the clinical differentiation of ARCD and AA based on history, physical signs, and easily available laboratory data will be useful for clinicians who care for Asian patients with acute abdomen.

Research objective

This study aimed to reveal clinical findings, such as symptoms, physical signs, and widely available laboratory data that are useful for differentiating AA from ARCD.

Research methods

We performed a single-center retrospective case-control study that evaluated 236 patients with AA and 133 patients with ARCD, who were hospitalized in Toho University Medical Center Omori Hospital between 2012 and 2016. We compared patients' characteristics, symptoms, physical signs, and widely available laboratory data. We performed logistic regression for clinical differentiation between AA and ARCD.

Research results

Median ages were 35.5 and 41.0 years in the AA and ARCD groups, respectively (P = 0.011). Median onset-to-visit intervals were 1 and 2 days in the AA and ARCD groups, respectively (P < 0.001). Prevalences of epigastric/periumbilical pain, nausea/vomiting, anorexia, and history of unresected appendicitis were significantly higher in the AA group, whereas RLQ pain and history of diverticulitis were more prevalent in the ARCD group. Median leukocyte counts in the AA and ARCD groups were 12600 and 11500/mm^3, respectively (P = 0.002). Median CRP levels in the AA and ARCD groups were 1.1 and 4.9 mg/dL, respectively (P < 0.001). The logistic regression model showed a significantly high odds ratio (OR) in nausea/vomiting (OR: 3.89) and anorexia (OR: 2.13). ORs were significantly lower with a longer onset-to-visit interval (OR: 0.84), RLQ pain (OR: 0.28), history of diverticulitis (OR: 0.034), and CRP level > 3.0 mg/dL (OR: 0.25), suggesting that ARCD was more likely.

Research conclusions

Our logistic regression model for differentiating AA from ARCD showed that nausea/vomiting and anorexia increase the probability of AA rather than ARCD. Conversely, longer onset-to-visit interval, RLQ pain, history of diverticulitis, and CRP level > 3.0 mg/dL at the time of visit increase the probability of ARCD rather than AA. Our study suggests that clinical findings can differentiate AA and ARCD based on clinical information in advance of imaging studies.

Research perspectives

Given the lack of previous study on clinical differences between AA and ARCD, and the cost, limited availability, and concern for radiation exposure of CT scanning, our findings will provide useful evidence for physicians managing Asian patients with acute abdomen.

REFERENCES

1 **Markham NI**, Li AK. Diverticulitis of the right colon--experience from Hong Kong. *Gut* 1992; **33**: 547-549 [PMID: 1582600 DOI: 10.1016/0002-9610(61)90653-5]
2 **Narasaka T**, Watanabe H, Yamagata S, Munakata A, Tajima T. Statistical analysis of diverticulosis of the colon. *Tohoku J Exp Med* 1975; **115**: 271-275 [PMID: 1129775 DOI: 10.1620/tjem.115.271]
3 **Chan CC**, Lo KK, Chung EC, Lo SS, Hon TY. Colonic diverticulosis in Hong Kong: distribution pattern and clinical significance. *Clin Radiol* 1998; **53**: 842-844 [PMID: 9833789 DOI: 10.1016/S0009-9260(98)80197-9]
4 **Lee IK**. Right colonic diverticulitis. *J Korean Soc Coloproctol* 2010; **26**: 241-245 [PMID: 21152224 DOI: 10.3393/jksc.2010.26.4.241]
5 **Matsushima K**. Management of right-sided diverticulitis: A retrospective review from a hospital in Japan. *Surg Today* 2010; **40**: 321-325 [PMID: 20339986 DOI: 10.1007/s00595-008-4055-5]
6 **Organisation for Economic Cooperation and Development**. Health at a Glance 2017: OECD indicators; 2017. Available from: https://www.oecd-ilibrary.org/social-issues-migration-health/health-at-a-glance-2017_health_glance-2017-en
7 **Wu HP**, Lin CY, Chang CF, Chang YJ, Huang CY. Predictive value of C-reactive protein at different cutoff levels in acute appendicitis. *Am J Emerg Med* 2005; **23**: 449-453 [PMID: 16032609 DOI: 10.1016/j.ajem.2004.10.013]
8 **March B**, Leigh L, Brussius-Coelho M, Holmes M, Pockney P, Gani J. Can CRP velocity in right iliac fossa pain identify patients for intervention? A prospective observational cohort study. *Surgeon* 2018 [PMID: 30309747 DOI: 10.1016/j.surge.2018.08.007]
9 **Chen SC**, Chang KJ, Wei TC, Yu SC, Wang SM. Can cecal diverticulitis be differentiated from acute appendicitis? *J Formos Med Assoc* 1994; **93**: 263-265 [PMID: 7920071]
10 **Shin JH**, Son BH, Kim H. Clinically distinguishing between appendicitis and right-sided colonic diverticulitis at initial presentation. *Yonsei Med J* 2007; **48**: 511-516 [PMID: 17594161 DOI: 10.3349/ymj.2007.48.3.511]
11 **Lee IK**, Kim SH, Lee YS, Kim HJ, Lee SK, Kang WK, Ahn CH, Oh ST, Jeon HM, Kim JG, Kim EK, Chang SK. Diverticulitis of the right colon: Tips for preoperative diagnosis and treatment strategy. *J Korean Soc Coloproctol* 2007; **23**: 223-231 [DOI: 10.3393/jksc.2007.23.4.223]
12 **Lee IK**, Jung SE, Gorden DL, Lee YS, Jung DY, Oh ST, Kim JG, Jeon HM, Chang SK. The diagnostic criteria for right colonic diverticulitis: prospective evaluation of 100 patients. *Int J Colorectal Dis* 2008; **23**: 1151-1157 [PMID: 18704462 DOI: 10.1007/s00384-008-0512-2]
13 **Salminen P**, Tuominen R, Paajanen H, Rautio T, Nordström P, Aarnio M, Rantanen T, Hurme S, Mecklin JP, Sand J, Virtanen J, Jartti A, Grönroos JM. Five-Year Follow-up of Antibiotic Therapy for Uncomplicated Acute Appendicitis in the APPAC Randomized Clinical Trial. *JAMA* 2018; **320**: 1259-1265 [PMID: 30264120 DOI: 10.1001/jama.2018.13201]
14 **Edelman DA**, White MT, Tyburski JG, Wilson RF. Post-traumatic hypotension: should systolic blood pressure of 90-109 mmHg be included? *Shock* 2007; **27**: 134-138 [PMID: 17224786 DOI: 10.1097/01.shk.0000239772.18151.18]
15 **Riley LK**, Rupert J. Evaluation of Patients with Leukocytosis. *Am Fam Physician* 2015; **92**: 1004-1011 [PMID: 26760415]
16 **Kwo PY**, Cohen SM, Lim JK. ACG Clinical Guideline: Evaluation of Abnormal Liver Chemistries. *Am J Gastroenterol* 2017; **112**: 18-35 [PMID: 27995906 DOI: 10.1038/ajg.2016.517]
17 **Alvarado A**. A practical score for the early diagnosis of acute appendicitis. *Ann Emerg Med* 1986; **15**: 557-564 [PMID: 3963537 DOI: 10.1016/S0196-0644(86)80993-3]
18 **Arnbjörnsson E**, Bengmark S. Role of obstruction in the pathogenesis of acute appendicitis. *Am J Surg* 1984; **147**: 390-392 [PMID: 6322604 DOI: 10.1016/0002-9610(84)90174-0]
19 **Silen W**, Longo DL, Fauci AS, Kasper DL, Hauser SL, Jameson JL. Acute appendicitis and peritonitis. Longo DL, Fauci AS, Kasper DL, Hauser SL, Jameson JL. *Harrison's principles of internal medicine. 18th ed*. New York: McGraw-Hill 2012; 2516-2519
20 **Birnbaum BA**, Wilson SR. Appendicitis at the millennium. *Radiology* 2000; **215**: 337-348 [PMID: 10796905 DOI: 10.1148/radiology.215.2.r00ma24337]
21 **Wagner JM**, McKinney WP, Carpenter JL. Does this patient have appendicitis? *JAMA* 1996; **276**: 1589-1594 [PMID: 8918857 DOI: 10.1001/jamaoto.2015.0540]
22 **Gearhart SL**, Longo DL, Fauci AS, Kasper DL, Hauser SL, Jameson JL. Diverticular disease and common anorectal disorders. Longo DL, Fauci AS, Kasper DL, Hauser SL, Jameson JL. *Harrison's principles of internal medicine*. New York: McGraw-Hill 2012; 2502–2510
23 **Touzios JG**, Dozois EJ. Diverticulosis and acute diverticulitis. *Gastroenterol Clin North Am* 2009; **38**: 513-525 [PMID: 19699411 DOI: 10.1016/j.gtc.2009.06.004]
24 **Temple CL**, Huchcroft SA, Temple WJ. The natural history of appendicitis in adults. A prospective study. *Ann Surg* 1995; **221**: 278-281 [PMID: 7717781]
25 **Shogilev DJ**, Duus N, Odom SR, Shapiro NI. Diagnosing appendicitis: evidence-based review of the diagnostic approach in 2014. *West J Emerg Med* 2014; **15**: 859-871 [PMID: 25493136 DOI: 10.5811/westjem.2014.9.21568]
26 **Tan JP**, Barazanchi AW, Singh PP, Hill AG, Maccormick AD. Predictors of acute diverticulitis severity: A systematic review. *Int J Surg* 2016; **26**: 43-52 [PMID: 26777741 DOI: 10.1016/j.ijsu.2016.01.005]
27 **Käser SA**, Fankhauser G, Glauser PM, Toia D, Maurer CA. Diagnostic value of inflammation markers in predicting perforation in acute sigmoid diverticulitis. *World J Surg* 2010; **34**: 2717-2722 [PMID: 20645093 DOI: 10.1007/s00268-010-0726-7]
28 **Kechagias A**, Sofianidis A, Zografos G, Leandros E, Alexakis N, Dervenis C. Index C-reactive protein predicts increased severity in acute sigmoid diverticulitis. *Ther Clin Risk Manag* 2018; **14**: 1847-1853 [PMID: 30323607 DOI: 10.2147/TCRM.S160113]
29 **Clyne B**, Olshaker JS. The C-reactive protein. *J Emerg Med* 1999; **17**: 1019-1025 [PMID: 10595891 DOI: 10.1016/S0736-4679(99)00135-3]
30 **Laméris W**, van Randen A, Bipat S, Bossuyt PMM, Boermeester MA, Stoker J. Graded compression ultrasonography and computed tomography in acute colonic diverticulitis: Meta-analysis of test accuracy. *Eur Radiol* 2008; **18**: 2498-2511 [PMID: 18523784 DOI: 10.1007/s00330-008-1018-6]

World Journal of Clinical Cases

Submit a Manuscript: https://www.f6publishing.com

World J Clin Cases 2019 June 26; 7(12): 1403-1409

DOI: 10.12998/wjcc.v7.i12.1403

ISSN 2307-8960 (online)

ORIGINAL ARTICLE

Retrospective Study

Feasibility of prostatectomy without prostate biopsy in the era of new imaging technology and minimally invasive techniques

Nian-Zeng Xing, Ming-Shuai Wang, Qiang Fu, Fei-Ya Yang, Chang-Ling Li, Ya-Jian Li, Su-Jun Han, Ze-Jun Xiao, Hao Ping

ORCID number: Nian-Zeng Xing (0000-0003-4370-3008); Ming-Shuai Wang (0000-0003-3667-2856); Qiang Fu (0000-0002-1666-0009); Fei-Ya Yang (0000-0002-7793-8772); Chang-Ling Li (0000-0001-9480-6838); Ya-Jian Li (0000-0002-7053-8717); Su-Jun Han (0000-0002-4322-0228); Ze-Jun Xiao (0000-0002-3186-7905); Hao Ping (0000-0003-2912-0965).

Author contributions: All authors helped to perform the study; Xing NZ and Wang MS are co-first authors; Xing NZ contributed to study conception and design and manuscript writing; Wang MS contributed to study design, manuscript writing, and data analysis; Yang FY, Li YJ, Han SJ, Xiao ZJ, and Li CL contributed to data collection and manuscript writing; Ping H and Fu Q contributed to manuscript writing and data analysis.

Institutional review board statement: As the retrospective study and data analysis were performed anonymously, this study was exempt from the ethical approval.

Informed consent statement: Patients were not required to give informed consent to the study because the analysis used anonymous clinical data that were obtained after each patient agreed to treatment by written consent.

Conflict-of-interest statement: All authors declare no conflicts of interest related to this article.

Data sharing statement: No

Nian-Zeng Xing, Fei-Ya Yang, Chang-Ling Li, Ya-Jian Li, Su-Jun Han, Ze-Jun Xiao, Department of Urology, National Cancer Center/National Clinical Research Center for Cancer/Cancer Hospital, Chinese Academy of Medical Sciences and Peking Union Medical College, Beijing 100021, China

Ming-Shuai Wang, Institute of Urology, Capital Medical University, Department of Urology, Beijing Chaoyang Hospital, Capital Medical University, Beijing 100020, China

Qiang Fu, Department of Urology, Shandong Provincial Hospital, Jinan 250021, Shandong Province, China

Hao Ping, Department of Urology, Beijing Tongren Hospital, Capital Medical University, Beijing 100005, China

Corresponding author: Nian-Zeng Xing, MD, PhD, Chairman, Professor, Surgeon, Director, Department of Urology, National Cancer Center/National Clinical Research Center for Cancer/Cancer Hospital, Chinese Academy of Medical Sciences and Peking Union Medical College, No. 17, Pan Jia Yuan Nan Li, Chaoyang District, Beijing 100021, China. xingnianzeng@hotmail.com

Telephone: +86-18612023952

Abstract

BACKGROUND

Routinely, after receiving prostate specific antigen (PSA) testing and digital rectum examination, patients with suspected prostate cancer are required to undergo prostate biopsy. However, the ability of ultrasound-guided prostate biopsy to detect prostate cancer is limited. Nowadays, a variety of diagnostic methods and more sensitive diagnostic methods, such as multi-parameter prostate magnetic resonance imaging (mpMRI) and prostate-specific membrane antigen positron emission tomography/computed tomography (PSMA PET/CT) can be applied clinically. Furthermore, laparoscopic/robot-assisted prostatectomy is also a safe and effective procedure for the treatment of benign prostatic hyperplasia. So maybe it is time to reconsider the necessary to perform prostate biopsy before radical prostatectomy.

AIM

To explore the feasibility of radical prostatectomy without prostate biopsy in the era of new imaging technology and minimally invasive techniques.

METHODS

additional data are available.

Manuscript source: Unsolicited manuscript

Received: February 17, 2019
Peer-review started: February 18, 2019
First decision: April 18, 2019
Revised: April 25, 2019
Accepted: May 10, 2019
Article in press: May 11, 2019
Published online: June 26, 2019

P-Reviewer: Morling JR, Sis B
S-Editor: Wang JL
L-Editor: Wang TQ
E-Editor: Xing YX

From June 2014 to November 2018, 11 cases of laparoscopic radical prostatectomy without prostate biopsy were performed at the three tertiary medical centers involved in this study. All patients received prostate magnetic resonance imaging and prostate cancer was suspected, including six patients with positive ^{68}Ga-PSMA PET/CT results. Laparoscopic radical prostatectomy and pelvic lymph node dissection were performed for all patients.

RESULTS

All surgeries were accomplished successfully. The mean age was 69 ± 7.7 year, the mean body mass index was 24.7 ± 1.6 kg/m^2, the range of serum PSA was 4.3 to >1000 ng/mL, and the mean prostate volume was 40.9 ± 18.3 mL. The mean operative time was 96 ± 23.3 min, the mean estimated blood loss was 90 ± 90.9 mL, and the median duration of catheter placement was 14 d. The final pathology confirmed that all specimens were prostate cancer except one case of benign prostatic hyperplasia. No major complications occurred in 90 d postoperatively.

CONCLUSION

The current practice of mandating a prostatic biopsy before prostatectomy should be reconsidered in the era of new imaging technology and minimally invasive techniques. Radical prostatectomy could be carried out without the evidence of malignancy. Large-sample randomized controlled trials are definitely required to confirm the feasibility of this new concept.

Key words: Prostate cancer; Biopsy; Prostatectomy; Magnetic resonance imaging; Prostate-specific membrane antigen positron emission tomography/computed tomography

Core tip: The ability of ultrasound-guided prostate biopsy to detect prostate cancer is limited. Maybe prostate biopsy can be exempt before surgery when multi-parameter prostate magnetic resonance imaging and prostate-specific membrane antigen positron emission tomography/computed tomography are both positive. The current practice of mandating a prostatic biopsy before prostatectomy should be reconsidered in the era of new imaging technology and minimally invasive techniques.

Citation: Xing NZ, Wang MS, Fu Q, Yang FY, Li CL, Li YJ, Han SJ, Xiao ZJ, Ping H. Feasibility of prostatectomy without prostate biopsy in the era of new imaging technology and minimally invasive techniques. *World J Clin Cases* 2019; 7(12): 1403-1409
URL: https://www.wjgnet.com/2307-8960/full/v7/i12/1403.htm
DOI: https://dx.doi.org/10.12998/wjcc.v7.i12.1403

INTRODUCTION

Prostate cancer is one of the most common malignancies worldwide. The current methods for diagnosing prostate cancer include digital rectal examination (DRE), serum prostate specific antigen (PSA), transrectal prostate ultrasound, and magnetic resonance imaging (MRI). Routinely, after receiving one or more of these tests, patients with suspected prostate cancer are required to undergo prostate biopsy. However, the sensitivity of ultrasound-guided prostate biopsy is approximately 48%[1]. While clinically insignificant cancers are often detected, clinically significant cancers are sometimes missed after prostate biopsy[2,3]. Transrectal ultrasound guided (TRUS)-biopsy also carries significant morbidity and can cause life-threatening sepsis[4]. Nowadays, we have a variety of diagnostic methods and more sensitive diagnostic methods, such as multi-parameter prostate magnetic resonance imaging (mpMRI) and prostate-specific membrane antigen positron emission tomography /computed tomography (PSMA PET/CT). The reported sensitivity of mpMRI for the detection of clinically significant disease was 93% (95%CI: 88%-96%)[1], and ^{68}Gallium-PSMA PET/CT had a 100% detection rate for index lesions at radical prostatectomy[5]. Furthermore, laparoscopic/robot-assisted prostatectomy is also a safe and effective procedure for the treatment of benign prostatic hyperplasia[6]. To take all the above-mentioned factors together, we hypothesized that it might be no longer necessary to

perform prostate biopsy before radical prostatectomy.

In this study, we summarized 11 cases of radical prostatectomy without prostate biopsy from three tertiary hospitals to explore the feasibility of radical prostatectomy without prostate biopsy.

MATERIALS AND METHODS

Clinical data

Between June 2014 and December 2018, five, three, and three cases of laparoscopic radical prostatectomy were performed without prostate biopsy before surgery at National Cancer Center/Cancer Hospital of Chinese Academy of Medical Sciences, Beijing Chaoyang Hospital Affiliated to Capital Medical University, and Shandong Provincial Hospital, respectively. All surgeries were performed by the same surgeon who had high volume experience of laparoscopic surgeries. All patients received serum PSA test, digital rectal examination, transrectal prostatic ultrasound, and MRI of the prostate, and six of them received ^{68}Ga-PSMA PET/CT examination. Informed consent was obtained before surgery to fully communicate with patients and family members, and to explain possible surgical risks especially postoperative pathology. Data were collected, including patient demographics, perioperative outcomes, pathological results, and complications. Postoperative complications were graded using the Clavien classification method, and the complications were classified into minor (Clavien grade I-II) and major (Clavien grade III-V)[7].

Surgical technique

All surgeries were carried out using an extraperitoneal approach and five trocar technique as we described before[8]. After creating a working space via an extraperitoneal approach, the prostate, bladder, and endopelvic fascia were exposed. The endopelvic fascia was incised on both sides, and blunt dissection was performed towards the apex of the prostate. The puboprostatic ligaments were preserved, and the dorsal venous complex was ligated using a 2/0 v-lok suture. The bladder neck was carefully dissected and preserved followed by dissection of the seminal vesicles and incision of the Denonvillier's fascia. The prostatic pedicles were clipped close to the prostate and cut with cold scissors step by step. Apical dissection of the prostate and division of the urethra were then performed. The urethra was cut at the middle between the external urethral sphincter and the apex of the prostate with cold scissors. Bilateral pelvic lymph node dissection was performed in all patients. All specimens were removed in a retrieval endobag.

The "sandwich" reconstruction technique was utilized during the urethrovesical anastomosis[8]. First, the posterior reconstruction was accomplished by two-layer suturing including the Denonvillier's fascia with the median dorsal raphe (MDR) and the posterior wall of the bladder with the MDR. The second step of the reconstruction was the urethrovesical anastomosis. The third step was anterior reconstruction consisting of reattachment of the puboprostatic ligaments with the detrusor apron of the bladder.

RESULTS

All surgeries were successfully accomplished without open conversion. The patient characteristics and pathologic outcomes are shown in Table 1.

The mean age was 69 ± 7.7 year and the mean BMI was 24.7 ± 1.6 kg/m^2. The range of serum PSA was 4.3 to >1000 ng/mL and the mean prostate volume was 40.9 ± 18.3 mL. The mean operative time was 96 ± 23.3 min, the mean estimated blood loss was 90 ± 90.9 mL, and no patient required transfusion. The median time of catheter retention was 14 d. No major complications occurred in 90 d postoperatively.

The pathological results showed ten cases of prostatic adenocarcinoma and one case of benign prostatic hyperplasia. The pathologic tumor stage revealed pT2aN0 (1 case), pT2bN0 (1 case), pT2cN0 (3 cases), pT2cN1 (1 case), pT3aN0 (3 cases), and pT3bN0 (1 case) (Figure 1). One patient developed pelvic lymph node metastasis (16/22) and no lymph node metastasis was found in other patients. There were two cases with a Gleason score of (3 + 3 = 6) points, two with a score of (3 + 4 = 7) points, one with a score of (4 + 3 = 7) points, one with a score of (4 + 4 = 8) points, and four with a score ≥ 9 points. Two cases had positive margins at the prostatic base.

Table 1 Patient characteristics and pathologic outcomes

Case	Age (yr)	BMI (kg/m²)	Maximum PSA (ng/mL)	Prostate volume	MRI	PET/CT	Bone scan	Pathology tumor stage	Gleason score	Positive lymph nodes
1	61	25.4	8.6	40	+	/	/	T3aN0	3 + 4 = 7	0
2	71	25.3	>1000	23	+	/	+	T3bN0	4 + 5 = 9	0
3	62	24.5	>1000	30	+	/	+	T2cN1	5 + 4 = 9	16/22
4	76	25.3	18.3	80	+	/	/	T2cN0	4 + 3 = 7	0
5	79	22.4	41.2	20	+	+	/	T2cN0	5 + 5 = 10	0
6	80	23.3	15.2	46	+	/	/	Benign prostatic hyperplasia		0
7	73	23.4	27.7	31	+	+	/	T3aN0	4 + 4 = 8	0
8	56	23.2	9.2	41	+	+	/	T2aN0	3 + 3 = 6	0
9	69	26.6	22	47	+	+	/	T3aN0	4 + 5 = 9	0
10	67	24.5	4.3	27	+	+	/	T2bN0	3 + 4 = 7	0
11	65	27.6	15.9	65	+	+	/	T2cN0	3+ 3 = 6	0

+: Positive. /: not receiving the test; BMI: Body mass index; PSA: Prostatic specific antigen; MRI: Magnetic resonance imaging; PET/CT: Positron emission tomography and computed tomography.

DISCUSSION

Prostate biopsy to exclude cancer has been part of clinical practice since the beginning of the 20th century. The introduction of PSA and ultrasound into clinical practice in the 1980s and the evolution of mpMRI in the early 21st century have driven the prostate biopsy into a more scientific-based procedure. Current practice mandates a prostate biopsy before radical prostatectomy, despite many complications such as urosepsis, urinary retention, and hematuria *etc*[9]. On the other hand, renal tumors are treated completely differently. When a renal tumor was highly suspected to be malignant by CT or MRI imaging, radical nephrectomy or partial nephrectomy is routinely carried out clinically. Renal tumor biopsy is not mandated before surgery currently[10].

Compared to radical nephrectomy and partial nephrectomy, the procedure of radical prostatectomy is more difficult and postoperative complications seriously affect the quality of life, such as urinary incontinence and erectile dysfunction. However, with accumulation of surgical experience, improvement of surgical techniques, and advancement of surgical equipment, minimally invasive radical prostatectomy has shorter operative time, less trauma, and faster recovery, and the early continence and erectile function recover faster than before[11-13]. Our previous data also showed that patients' early urinary continence rate and quality of life were significantly improved after laparoscopic radical prostatectomy with the "sandwich" urethrovesical anastomosis technique[8].

The use of mpMRI and the PI-RADS prostate cancer scoring system has significantly improved the diagnostic accuracy of clinically significant prostate cancer[14,15]. And there is evidence that mpMRI tends to detect higher risk disease and systematically overlooks low-risk disease[1,14]. Ahmed *et al*[1] found that the sensitivity of mpMRI for the detection of clinically significant disease was 93% (95%CI: 88%-96%), which was significantly superior to the sensitivity of TRUS biopsy (48%; 95%CI: 42%-55%). One meta-analysis showed that the pooled sensitivity and specificity of mpMRI for prostate cancer detection are 74% and 88%, respectively[16]. Assessment of lymph node involvement can be performed by both CT and mpMRI, but both have a very low sensitivity[17].

The use of PSMA PET/CT further enhances the accuracy of diagnosing prostate cancer, not only to assess primary lesions but also to assess metastases. Berger *et al*[5] compared the accuracy of ^{68}Ga-PSMA PET/CT and mpMRI in assessing prostate cancer and found that ^{68}Ga-PSMA PET/CT had a 100% detection rate for index lesions at radical prostatectomy. Six patients in our study underwent ^{68}Ga-PSMA PET/CT and the detection rate was 100%, which was confirmed by final pathology. Besides primary lesion, PSMA PET/CT also had a high specificity and moderate sensitivity for lymph node metastasis detection for patient with intermediate- to high-risk prostate cancer[18]. It is more accurate than morphologic imaging for detection of lymph node metastasis[19]. Until now, no prospective study accesses the oncologic efficacy of PSMA PET/CT guided lymph node dissection compared to conventional

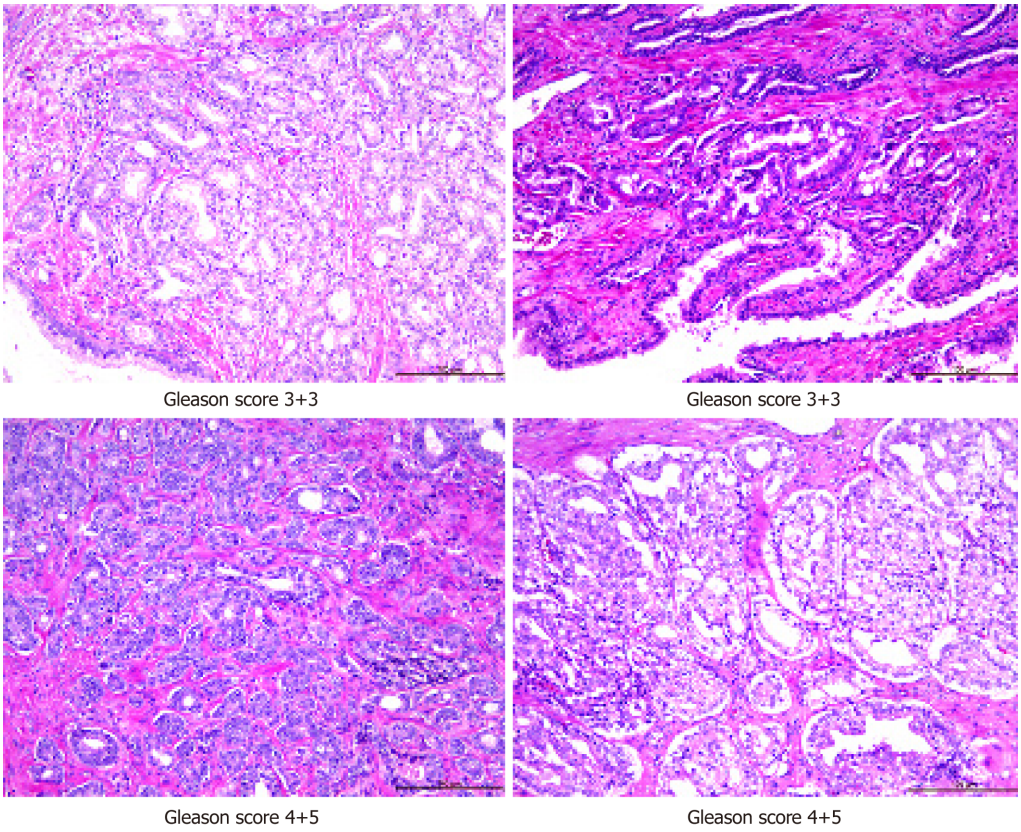

Figure 1 Pathological images of prostate cancer.

strategy.

One lesion by lesion analysis showed that combination of ^{68}Ga-PSMA PET/CT and multiparameter MRI can improve the detection of clinically significant prostate cancer[20]. We recommend every patient being suspected of having prostate cancer to receive mpMRI and PSMA PET/CT which could help surgeons to detect clinically significant prostate cancer, and prostate biopsy can be exempt before surgery when both imaging tests are positive.

The critical concern for radical prostatectomy without biopsy is overtreatment if the pathology turns to be benign. However, the prostate is not a vital organ for the elder man. Rather it may lead to risks such as benign prostate hyperplasia and prostate cancer which influence the quality of life. Surgery is an optional treatment modality for both benign prostate hyperplasia and prostate cancer. While benign prostate hyperplasia is mostly operated by the transurethra procedure, laparoscopic and robot-assisted laparoscopic surgeries are also indicated in some patients. One meta-analysis study showed that open, laparoscopic, and robot-assisted laparoscopic surgeries can safely complete simple prostatectomy[21]. One study comparing transurethral holmium laser enucleation of the prostate with robot-assisted simple prostatectomy showed that both procedures can effectively treat benign prostatic hyperplasia[22]. Although the transurethral laser ablation procedure had shorter operation time, less blood loss, and shorter hospital stay, there was no significant difference in the major complications or postoperative urinary continence. One of our cases was benign prostate hyperplasia. The patient was very satisfied with the treatment since he recovered very well without major complications, while his lower urinary tracts symptoms disappeared. Therefore, it is acceptable even the final pathology is benign for some patients who received radical prostatectomy.

In summary, the current practice of mandating a prostatic biopsy before prostatectomy should be reconsidered in the era of new imaging technology and minimally invasive techniques. Radical prostatectomy could be carried out without the evidence of malignancy. Large-sample randomized controlled trials are definitely required to confirm the feasibility of this new concept.

ARTICLE HIGHLIGHTS

Research background
Prostate cancer is one of the most common malignant tumors. When the total PSA and/or digital rectum examination are positive, prostate biopsy is routinely proposed to patients. However, the detection ability of the transrectal ultrasound guided (TRUS) prostate biopsy is limited. While clinically insignificant cancers are often detected, clinically significant cancers are sometimes missed after prostate biopsy. TRUS-biopsy also carries significant morbidity and can cause life-threatening sepsis. The reported sensitivity of multi-parameter prostate magnetic resonance imaging for the detection of clinically significant disease was 93% (95%CI 88-96), and ^{68}Gallium-prostate-specific membrane antigen positron emission tomography/computed tomography had a 100% detection rate for index lesions at radical prostatectomy.

Research motivation
Nowadays, many imaging techniques with a very high detection rate for prostate cancer are applied clinically. Some patients are afraid of prostate biopsy, and they really want to remove the prostate immediately when they were told that they might have prostate cancer. For elder men, laparoscopic/robot-assisted prostatectomy is also a safe and effective procedure for the treatment of benign prostatic hyperplasia. So it might be no longer necessary to perform prostate biopsy before radical prostatectomy.

Research objectives
The main objective of the study was to explore the feasibility of radical prostatectomy without prostate biopsy in the era of new imaging technology and minimally invasive techniques.

Research methods
A retrospective study was designed. The cases of laparoscopic radical prostatectomy without prostate biopsy before surgery were collected at the three medical centers involved in this study between June 2014 and December 2018. The perioperative outcomes and pathology results were analyzed.

Research results
All surgeries were successfully accomplished without open conversion. The pathological results showed ten cases of prostatic adenocarcinoma and one case of benign prostatic hyperplasia. Lower urinary tract symptoms disappeared when the patient with benign prostatic hyperplasia underwent laparoscopic radical prostatectomy.

Research conclusions
The current practice of mandating a prostatic biopsy before prostatectomy should be reconsidered in the era of new imaging technology and minimally invasive techniques. Radical prostatectomy could be carried out without the evidence of malignancy.

Research perspectives
It might be no longer necessary to perform prostate biopsy before radical prostatectomy. However, large-sample randomized controlled trials are definitely required to confirm the feasibility of this new concept.

REFERENCES

1 **Ahmed HU**, El-Shater Bosaily A, Brown LC, Gabe R, Kaplan R, Parmar MK, Collaco-Moraes Y, Ward K, Hindley RG, Freeman A, Kirkham AP, Oldroyd R, Parker C, Emberton M; PROMIS study group. Diagnostic accuracy of multi-parametric MRI and TRUS biopsy in prostate cancer (PROMIS): a paired validating confirmatory study. *Lancet* 2017; **389**: 815-822 [PMID: 28110982 DOI: 10.1016/S0140-6736(16)32401-1]

2 **Caverly TJ**, Hayward RA, Reamer E, Zikmund-Fisher BJ, Connochie D, Heisler M, Fagerlin A. Presentation of Benefits and Harms in US Cancer Screening and Prevention Guidelines: Systematic Review. *J Natl Cancer Inst* 2016; **108**: djv436 [PMID: 26917630 DOI: 10.1093/jnci/djv436]

3 **Abraham NE**, Mendhiratta N, Taneja SS. Patterns of repeat prostate biopsy in contemporary clinical practice. *J Urol* 2015; **193**: 1178-1184 [PMID: 25444971 DOI: 10.1016/j.juro.2014.10.084]

4 **Loeb S**, Vellekoop A, Ahmed HU, Catto J, Emberton M, Nam R, Rosario DJ, Scattoni V, Lotan Y. Systematic review of complications of prostate biopsy. *Eur Urol* 2013; **64**: 876-892 [PMID: 23787356 DOI: 10.1016/j.eururo.2013.05.049]

5 **Berger I**, Annabattula C, Lewis J, Shetty DV, Kam J, Maclean F, Arianayagam M, Canagasingham B, Ferguson R, Khadra M, Ko R, Winter M, Loh H, Varol C. 68Ga-PSMA PET/CT vs. mpMRI for locoregional prostate cancer staging: correlation with final histopathology. *Prostate Cancer Prostatic Dis* 2018; **21**: 204-211 [PMID: 29858591 DOI: 10.1038/s41391-018-0048-7]

6 **Nestler S**, Bach T, Herrmann T, Jutzi S, Roos FC, Hampel C, Thüroff JW, Thomas C, Neisius A. Surgical treatment of large volume prostates: a matched pair analysis comparing the open, endoscopic (ThuVEP) and robotic approach. *World J Urol* 2018 [PMID: 30515596 DOI: 10.1007/s00345-018-2585-z]

7 **Dindo D**, Demartines N, Clavien PA. Classification of surgical complications: a new proposal with evaluation in a cohort of 6336 patients and results of a survey. *Ann Surg* 2004; **240**: 205-213 [PMID: 15273542]

8 **Liao X**, Qiao P, Tan Z, Shi H, Xing N. "Total reconstruction" of the urethrovesical anastomosis contributes to early urinary continence in laparoscopic radical prostatectomy. *Int Braz J Urol* 2016; **42**: 215-222 [PMID: 27256174 DOI: 10.1590/S1677-5538.IBJU.2014.0666]

9 **Halpern JA**, Sedrakyan A, Dinerman B, Hsu WC, Mao J, Hu JC. Indications, Utilization and Complications Following Prostate Biopsy: New York State Analysis. *J Urol* 2017; **197**: 1020-1025

[PMID: 27856226 DOI: 10.1016/j.juro.2016.11.081]
10 **Ljungberg B**, Bensalah K, Canfield S, Dabestani S, Hofmann F, Hora M, Kuczyk MA, Lam T, Marconi L, Merseburger AS, Mulders P, Powles T, Staehler M, Volpe A, Bex A. EAU guidelines on renal cell carcinoma: 2014 update. *Eur Urol* 2015; **67**: 913-924 [PMID: 25616710 DOI: 10.1016/j.eururo.2015.01.005]
11 **Sooriakumaran P**, Pini G, Nyberg T, Derogar M, Carlsson S, Stranne J, Bjartell A, Hugosson J, Steineck G, Wiklund PN. Erectile Function and Oncologic Outcomes Following Open Retropubic and Robot-assisted Radical Prostatectomy: Results from the LAParoscopic Prostatectomy Robot Open Trial. *Eur Urol* 2018; **73**: 618-627 [PMID: 28882327 DOI: 10.1016/j.eururo.2017.08.015]
12 **Coughlin GD**, Yaxley JW, Chambers SK, Occhipinti S, Samaratunga H, Zajdlewicz L, Teloken P, Dunglison N, Williams S, Lavin MF, Gardiner RA. Robot-assisted laparoscopic prostatectomy versus open radical retropubic prostatectomy: 24-month outcomes from a randomised controlled study. *Lancet Oncol* 2018; **19**: 1051-1060 [PMID: 30017351 DOI: 10.1016/S1470-2045(18)30357-7]
13 **Yaxley JW**, Coughlin GD, Chambers SK, Occhipinti S, Samaratunga H, Zajdlewicz L, Dunglison N, Carter R, Williams S, Payton DJ, Perry-Keene J, Lavin MF, Gardiner RA. Robot-assisted laparoscopic prostatectomy versus open radical retropubic prostatectomy: early outcomes from a randomised controlled phase 3 study. *Lancet* 2016; **388**: 1057-1066 [PMID: 27474375 DOI: 10.1016/S0140-6736(16)30592-X]
14 **Turkbey B**, Brown AM, Sankineni S, Wood BJ, Pinto PA, Choyke PL. Multiparametric prostate magnetic resonance imaging in the evaluation of prostate cancer. *CA Cancer J Clin* 2016; **66**: 326-336 [PMID: 26594835 DOI: 10.3322/caac.21333]
15 **Weinreb JC**, Barentsz JO, Choyke PL, Cornud F, Haider MA, Macura KJ, Margolis D, Schnall MD, Shtern F, Tempany CM, Thoeny HC, Verma S. PI-RADS Prostate Imaging - Reporting and Data System: 2015, Version 2. *Eur Urol* 2016; **69**: 16-40 [PMID: 26427566 DOI: 10.1016/j.eururo.2015.08.052]
16 **Godley KC**, Syer TJ, Toms AP, Smith TO, Johnson G, Cameron D, Malcolm PN. Accuracy of high b-value diffusion-weighted MRI for prostate cancer detection: a meta-analysis. *Acta Radiol* 2018; **59**: 105-113 [PMID: 28376634 DOI: 10.1177/0284185117702181]
17 **Li L**, Wang L, Feng Z, Hu Z, Wang G, Yuan X, Wang H, Hu D. Prostate cancer magnetic resonance imaging (MRI): multidisciplinary standpoint. *Quant Imaging Med Surg* 2013; **3**: 100-112 [PMID: 23630657 DOI: 10.3978/j.issn.2223-4292.2013.03.03]
18 **van Leeuwen PJ**, Emmett L, Ho B, Delprado W, Ting F, Nguyen Q, Stricker PD. Prospective evaluation of 68Gallium-prostate-specific membrane antigen positron emission tomography/computed tomography for preoperative lymph node staging in prostate cancer. *BJU Int* 2017; **119**: 209-215 [PMID: 27207581 DOI: 10.1111/bju.13540]
19 **Rauscher I**, Maurer T, Beer AJ, Graner FP, Haller B, Weirich G, Doherty A, Gschwend JE, Schwaiger M, Eiber M. Value of 68Ga-PSMA HBED-CC PET for the Assessment of Lymph Node Metastases in Prostate Cancer Patients with Biochemical Recurrence: Comparison with Histopathology After Salvage Lymphadenectomy. *J Nucl Med* 2016; **57**: 1713-1719 [PMID: 27261524 DOI: 10.2967/jnumed.116.173492]
20 **Chen M**, Zhang Q, Zhang C, Zhao X, Marra G, Gao J, Lv X, Zhang B, Fu Y, Wang F, Qiu X, Guo H. Combination of 68Ga-PSMA PET/CT and multiparameter MRI improves the detection of clinically significant prostate cancer: a lesion by lesion analysis. *J Nucl Med* 2018 [PMID: 30552201 DOI: 10.2967/jnumed.118.221010]
21 **Ferretti M**, Phillips J. Prostatectomy for benign prostate disease: open, laparoscopic and robotic techniques. *Can J Urol* 2015; **22** Suppl 1: 60-66 [PMID: 26497345]
22 **Zhang MW**, El Tayeb MM, Borofsky MS, Dauw CA, Wagner KR, Lowry PS, Bird ET, Hudson TC, Lingeman JE. Comparison of Perioperative Outcomes Between Holmium Laser Enucleation of the Prostate and Robot-Assisted Simple Prostatectomy. *J Endourol* 2017; **31**: 847-850 [PMID: 28637364 DOI: 10.1089/end.2017.0095]

World Journal of Clinical Cases

Submit a Manuscript: https://www.f6publishing.com

World J Clin Cases 2019 June 26; 7(12): 1410-1420

DOI: 10.12998/wjcc.v7.i12.1410

ISSN 2307-8960 (online)

ORIGINAL ARTICLE

Retrospective Study

Safety and efficacy of transfemoral intrahepatic portosystemic shunt for portal hypertension: A single-center retrospective study

Yu Zhang, Fu-Quan Liu, Zhen-Dong Yue, Hong-Wei Zhao, Lei Wang, Zhen-Hua Fan, Fu-Liang He

ORCID number: Yu Zhang (0000-0001-9895-175X); Fu-Quan Liu (0000-0003-1972-7712); Zhen-Dong Yue (0000-0001-5403-8336); Hong-Wei Zhao (0000-0001-5657-1839); Lei wang (0000-0003-4080-1630); Zhen-Hua Fan (0000-0001-5417-1997); Fu-Liang He (0000-0003-1643-1465).

Author contributions: Liu FQ designed the research; Yue ZD, Zhao HW, Wang L, Fan ZH and He FL performed the research; Zhang Y analyzed the data and wrote the paper; Liu FQ critically revised the manuscript for important intellectual content.

Supported by Capital Health Development Scientific Research Project, No. 2018-1-2081.

Institutional review board statement: All patients involved in this study gave their informed consent. Institutional review board approval of our hospital was obtained for this study.

Informed consent statement: Written informed consent was waived from all subjects in this study.

Conflict-of-interest statement: The authors of this manuscript declare no relationships with any companies, whose products or services may be related to the subject matter of the article.

Yu Zhang, Fu-Quan Liu, Zhen-Dong Yue, Hong-Wei Zhao, Lei Wang, Zhen-Hua Fan, Fu-Liang He, Department of Interventional Therapy, Peking University Ninth School of Clinical Medicine, Beijing Shijitan Hospital and Capital Medical University, Beijing 100010, China

Corresponding author: Fu-Quan Liu, BCPS, MD, Director, Professor, Department of Interventional Therapy, Peking University Ninth School of Clinical Medicine, Beijing Shijitan Hospital and Capital Medical University, No. 10 Tie Yi Road, Yangfangdian, Haidian District, Beijing 100010, China. lfuquan@aliyun.com
Telephone: +86-13701179758

Abstract

BACKGROUND

Transfemoral intrahepatic portosystemic shunt (TFIPS) can be performed to treat portal hypertension. However, few studies have evaluated the safety and efficacy of this technique.

AIM

To retrospectively evaluate the safety and clinical outcomes of TFIPS and compare them with those of typical transjugular intrahepatic portosystemic shunt (TIPS).

METHODS

This retrospective study was approved by our hospital ethics committee. From November 2012 to November 2015, 19 patients who underwent successful TFIPS placement were included. In addition, 21 patients treated with TIPS during the same period were selected as controls. Data collected included the success rate and complications of TIPS and TFIPS. Continuous data were expressed as the mean ± SD and were compared using the Student's *t* test. All categorical data were expressed as count (percentage) and were compared using the χ^2 test or Fisher's exact test. The Kaplan–Meier method was used to calculate cumulative survival rate and survival curves.

RESULTS

Baseline characteristics were comparable between the two groups. The success rate of TFIPS and TIPS was 95% (19/20) and 100% (21/21), respectively. Effective portal decompression and free antegrade shunt flow was completed in all patients. The portal pressure gradient prior to TIPS and TFIPS placement was 23.91 ± 4.64 mmHg and 22.61 ± 5.39 mmHg, respectively, and it was significantly decreased to 10.85 ± 3.33 mmHg and 10.84 ± 3.33 mmHg after stent placement, respectively. Time–to-event calculated rates of shunt patency at one and two

Manuscript source: Unsolicited manuscript

Received: March 8, 2019
Peer-review started: March 8, 2019
First decision: April 18, 2019
Revised: April 28, 2019
Accepted: May 11, 2019
Article in press: May 11, 2019
Published online: June 26, 2019

P-Reviewer: Alexopoulou A, Garbuzenko DV
S-Editor: Wang JL
L-Editor: Filipodia
E-Editor: Wang J

years in the TFIPS and TIPS groups were not statistically different (94.7% *vs* 95.2% and 94.7% *vs* 90.5%, respectively). *De nova* hepatic encephalopathy was 27.5% (11/40) with five patients in the TFIPS group (26.3%) and six patients (28.6%) in the TIPS group experiencing it (P = 0.873). The cumulative survival rates were similar between the two groups: 94.7% and 94.7% at 1 and 2 years, respectively, in the TFIPS group *vs* 100% and 95.2% at 1 and 2 years, respectively, in the TIPS group (P = 0.942).

CONCLUSION
TFIPS may be a valuable adjunct to traditional approaches in patients with portal hypertension.

Key words: Transjugular intraheptic portosystemic shunt; Transfemoral intraheptic portosystemic shunt; Portal hypertension; Variceal bleeding

Core tip: Transjugular intrahepatic portosystemic shunt is currently an accepted therapy and has proved beneficial in the treatment of portal hypertension and their complications. However, exceptionally challenging anatomy may require unorthodox salvage techniques, such as transfemoral intrahepatic portosystemic shunt (TFIPS). Because of the rare use of TFIPS, there are few clinical trials that have assessed the safety and effectiveness of TFIPS. In this retrospective study, we describe the TFIPS procedure in detail and evaluate the safety and clinical outcomes of TFIPS and compare them with those of typical transjugular intrahepatic portosystemic shunt. The TFIPS procedure is feasible and efficacy in patients with unorthodox anatomy between the hepatic vein and the portal vein bifurcation.

Citation: Zhang Y, Liu FQ, Yue ZD, Zhao HW, Wang L, Fan ZH, He FL. Safety and efficacy of transfemoral intrahepatic portosystemic shunt for portal hypertension: A single-center retrospective study. *World J Clin Cases* 2019; 7(12): 1410-1420
URL: https://www.wjgnet.com/2307-8960/full/v7/i12/1410.htm
DOI: https://dx.doi.org/10.12998/wjcc.v7.i12.1410

INTRODUCTION

Portal hypertension (PH) is a common clinical symptom and is mainly caused by chronic liver diseases. A recent epidemiological study suggested that in Europe, PH caused around 150000 deaths per year, and the mortality rate was equal to or greater than that due to breast cancer[1]. Transjugular intrahepatic portosystemic shunt (TIPS) is currently an accepted therapy and has proved beneficial in the treatment of complications of PH, such as gastrointestinal variceal bleeding and refractory ascites[2,3]. With the wide acceptance of polytetrafluoroethylene-covered stents, there has been a significant improvement in long-term TIPS patency[4-7].

Published rates of the technical success of TIPS creation are extremely high, ranging from 90% to 100%[8]. Despite the variance in hepatic vascular anatomy, almost all patients can be successfully treated with standard access (the right jugular vein), standard equipment and standard imaging. Exceptionally challenging anatomy may need new unconventional techniques, for example left hepatic vein–to–left portal vein shunts, direct inferior vena cava (IVC)–to–portal vein (PV) shunts[9] or percutaneous mesocaval shunts[10]. Besides abnormal hepatic vascular anatomy, central venous occlusions or anatomic anomalies, such as those due to pacemaker-related instrumentation or previous dialysis, can also be challenging and may require the use of unorthodox alternative methods of the venous route. One study[11] reported the least common approach, through the femoral vein that involved the use of an accessory hepatic vein to create a shunt. However, because of the rare use of transfemoral intrahepatic portosystemic shunt (TFIPS) there are few clinical trials that have assessed the safety and effectiveness of TFIPS. Thus, we report our experience on the successful creation of TFIPS in 19 patients.

The aim of this study was to compare the effectiveness and clinical outcomes of TIPS with TFIPS in the treatment of symptomatic PH and to determine the safety and

efficacy of TFIPS in these patients.

MATERIALS AND METHODS

This retrospective study was carried out in compliance with the Declaration of Helsinki of the World Medical Association and was approved by Shijitan Hospital Ethics Committee. Due to the retrospective nature of the study, informed consent was waived.

Patient selection

From a retrospectively collected database of patients who underwent successful TFIPS placement from November 2012 to November 2015, a total of 20 patients with cirrhosis were selected. One patient was excluded due to massive hemorrhage leading to the failure of TFIPS. Eventually, 19 patients who underwent successful TFIPS placement were included in this study. In addition, 21 patients with cirrhosis treated with TIPS during the same period were selected as controls from a historical cohort.

Perioperative management

Before undergoing TFIPS/TIPS for PH, all patients underwent contrast-enhanced multiphasic computed tomography (CT) and/or gadoxetic acid-enhanced liver magnetic resonance imaging. Liver cirrhosis was diagnosed by liver biopsy or unequivocal clinical, laboratory (liver function, blood coagulation, routine blood tests) and morphologic liver characteristics on CT and/or magnetic resonance imaging. Gastroscopy was performed to exclude bleeding caused by ulcers and other diseases. Coagulation function, the number of platelets and a reduction in jaundice were adjusted to adapt to the TFIPS/ TIPS procedure.

TFIPS technique

This procedure was performed after intravenous sedation, where propofol and remifentanil were infused using a target controlled infusion system. The right femoral vein access was achieved using a 10F sheath (Radifocus, Terumo, Leuven, Belgium). A snare (Amplatz Goose Neck Snare Kit, EV3, United States) with a loop diameter of 1 cm was then placed into the right hepatic vein (RHV) and left open in the lumen. Subsequently, a puncture in the abdominal wall was made *via* the snare loop into the PV with the appropriate position and angle obtained under CT guidance. Using a 18G puncture needle, a 0.035" guidewire (Radifocus, Terumo, Leuven, Belgium) was then advanced all the way to the PV and subsequently to the splenic vein. The puncture needle was then gently retracted, and the guidewire was pulled back into the femoral approach by retracting the snare. Consequently, an access from the right femoral vein through the RHV into the PV and splenic vein was achieved.

Additional steps were similar to the standard TIPS procedure and were performed under fluoroscopic guidance. Firstly, an 8/10 mm balloon catheter (Wanda, Boston Scientific, Galway, Ireland) was used to expand the shunt. The shunt was secured with a covered stent (8 or 10 mm, Fluency, Bard, United States) and further extended to the HV with a bare stent (8 or 10 mm, ELuminexx, Bard, United States). Portal vein pressure (PVP) was measured post-dilatation with an 8 mm balloon catheter. A pigtail catheter was used for photography, and a pressure transducer system (Combitrans, Braun Melsungen, Germany) with a multichannel monitor (Sirecust, Siemens, Germany) was used to measure hemodynamic parameters. The varicosed vein was then embolized after shunting. All measurements were performed at least three times.

TIPS technique

TIPS stent (8 mm or 10 mm, Fluency, Bard, United States) was inserted as previously described[12]. Briefly, an intrahepatic tract was punctured in the right internal jugular vein, which was between the right or middle HV and the PV.

Postoperative management

Conventional observations and treatment were performed after TIPS/TFIPS. Each patient was asked to remain in bed for 24 h after the procedure. Prophylactic antibiotics were administered as previously described. Subcutaneous injection of low molecular weight heparin (5000 IU, 2 times/d) was administered for 5 d after the procedure and then changed to warfarin for at least one year. Patients receiving anticoagulant therapy were closely monitored for blood coagulation dysfunction every 2 wk, and the international normalized ratio was maintained at between 2 and 3. Intravenous injection of branched chain amino acids (250-500 mL, once/d) and oral lactulose (15-30 mL, 2-3 times/d) were routinely administered to prevent hepatic encephalopathy (HE). Oral bicyclol tablets (25 mg, 3 times/d) were routinely

administered as a liver protection strategy.

Follow-up

Systemic examinations were performed in all patients at 1, 3, 6, 9 and 12 mo after the procedure, followed by annual re-examinations. Detailed medical history and symptoms were recorded. These examinations included liver function, coagulation, blood ammonia, routine blood tests, color ultrasonography, esophagography, CT and gastroscopy. When color ultrasonography suggested stenosis of the shunt channel, aggravation of varicosity, or gastrointestinal bleeding, refractory hydrothorax or ascites, imaging of the shunt channel was repeated, and the PVP was measured. If the blood flow in the shunt channel was normal, whereas the PVP increased or stenosis/occlusion of the shunt channel was identified, balloon dilation of the shunt channel and re-stenting was performed.

Statistical analysis

Baseline demographic, clinical and laboratory characteristics were retrieved from clinical records. The following pre-TIPS/TFIPS clinical data were analyzed: age, sex, cause of liver cirrhosis, Child-Pugh score, MELD score, previous upper gastrointestinal hemorrhage, portal pressure gradient (PPG) before and after TIPS creation, and the diameter of the stent-graft used. The Child-Pugh and MELD scores were also calculated on the basis of data obtained on the day of TIPS /TFIPS creation.

Quantitative data are shown as means and standard deviations and were compared using the paired *t* test. Qualitative variables are expressed as absolute and relative frequencies and were compared using the χ^2 test or Fisher's exact test. Statistical analysis was performed using the SPSS software (version 20.0, SPSS Inc., United States) and GraphPad Prism software (version 7.0 Graphpad Software Inc., United States). The Kaplan–Meier method was used to calculate cumulative survival rate and survival curves. $P < 0.05$ was considered statistically significant.

RESULTS

Patient characteristics

Nineteen patients (male/female, 17/2; age, 46.3 ± 13 years) were included in the TFIPS group. Because of the spatial relationship between the HV or the IVC and the main branches of the intrahepatic PV being unorthodox, TIPS could not be performed in 16 cases (Figure 1 and Figure 2). Due to complete occlusion of the bilateral jugular vein and/or superior vena cava, TIPS could not be performed in 3 cases (Figure 3). Twenty-one patients (male/female, 18/3; age, 45.7 ± 12 years) were included in the TIPS group. The mean follow-up period was 20 (range: 7-34) mo and 22 (range, 9-35) mo in the TFIPS and TIPS groups, respectively. Baseline characteristics in the two groups were comparable and are shown in Table 1.

Technical success

The successful creation of a shunt between the HV and the intrahepatic branch of the PV was defined as a technical success[13]. The technical success rate of TFIPS and TIPS was 95% (19/20) and 100% (21/21), respectively. Polytetrafluoroethylene–covered stents were used in most TIPS creations. Seventeen patients in the TFIPS group and seventeen patients in the TIPS group were treated for variceal bleeding with adjunctive variceal embolization. One patient in the TFIPS group failed this procedure due to failure to puncture the PV. Intraperitoneal bleeding was observed following puncture of the PV in one case in the TFIPS group, and a covered stent was successfully used to stop bleeding. The mean procedure time in the TFIPS group was 110.0 ± 12.11 min and was 74.11 ± 5.12 min in the TIPS group ($P < 0.001$).

Hemodynamic changes

Hemodynamic success refers to the successful post-TIPS reduction of the portosystemic gradient below a threshold indicated for the clinical setting[14]. Effective portal decompression and free antegrade shunt flow was completed in all patients. No statistically significant differences were observed between the two groups in terms of PVP and PPG before and after surgery (Figure 4). Detailed hemodynamic changes are shown in Table 2. The PPG prior to TIPS and TFIPS placement was 23.91 ± 4.64 mmHg and 22.61 ± 5.39 mmHg, respectively. PPG decreased significantly to 10.85 ± 3.33 mmHg and 10.84 ± 3.33 mmHg after stent placement in the TIPS and TFIPS groups, respectively.

Clinical effects

TIPS are well described as an effective treatment for variceal bleeding and refractory

Table 1 Patient characteristics

Index	TFIPS, *n* = 19	TIPS, *n* = 21	t/χ^2	*P* value
Gender, male/female	17/2	18/3	0.019	0.889
Age in yr, mean ± SD	46.3 ± 13	45.7 ± 12	0.942	0.349
Duration of follow-up in mo	20 (7-34)	22 (9-35)		
Etiology as viral/other	15/4	16/5	0.213	0.725
Child-Pugh stage, *n*			0.043	0.979
Stage A	5	5		
Stage B	13	15		
Stage C	1	1		
Child-Pugh score	7.31 ± 1.60	6.88 ± 1.90	0.77	0.446
MELD score	11.62 ± 3.22	10.87 ± 2.24	0.862	0.394
Gastrointestinal bleeding, yes/no	18/1	20/1	0.005	0.942
Refractory ascites, yes/no	1/18	1/20	0.005	0.942
Blood ammonia	33.01 ± 17.89	34.33 ± 13.15	0.268	0.790
Previous splenectomy and devascularization, yes/no	3/16	4/17	0.049	0.826
Previous sclerotherapy, yes/no	17/2	19/2	0.169	0.681

MELD: Model for end-stage liver disease; TFIPS: Transfemoral intrahepatic portosystemic shunt; TIPS: Transjugular intrahepatic portosystemic shunt.

ascites. The overall clinical success rate was 92.1% (35/38) for variceal bleeding and 100% (2/2) for ascites. The subgroup clinical failure rate is shown in Table 2. Rebleeding occurred due to recurrent PV thrombosis developed in one patient, and shunt dysfunction developed in two patients.

Follow-up and shunt patency

All shunts were patent on Doppler ultrasonography immediately after their creation (24-36 h). Three patients (1 in the TFIPS group *vs* 2 in the TIPS group) exhibited shunt dysfunction, and these patients underwent shunt revision (stent placement). Two patients developed recurrent gastrointestinal bleeding. Time-to-event calculated rates of shunt patency at one and two years in the TFIPS and TIPS groups were not statistically different (94.7% *vs* 95.2% and 94.7% *vs* 90.5%, respectively).

HE and hepatic myelopathy

De nova HE was observed in 27.5% (11/40) of patients. Five patients in the TFIPS group (26.3%) and six patients (28.6%) in the TIPS group experienced HE ($P = 0.873$). Data grading the severity of HE using the West Haven criteria[15] are shown in Table 3. The percentages of severest grade HE episodes were not statistically different between the two groups. Time-to-event (Kaplan-Meier) *de nova* HE analysis is shown in Figure 5A and there were no significant differences between the two groups [log-rank $P = 0.993$, hazard ratio: 1.01, 95% confidence interval: 0.31–3.29]. No symptoms of hepatic myelopathy were observed in any of the patients.

Survival

Overall 2-year survival rate after TIPS/TFIPS creation was 95% (38/40). The subgroup survival rate was shown in Table 3. One patient in the TIPS group underwent transplant within 12 mo of TIPS creation and survived the 2-year follow-up period. One patient died in the TFIPS group due to recurrent variceal bleeding. Time-to-event (Kaplan-Meier) survival analysis was shown in Figure 5B and there were no significant differences between the two groups (log-rank $P = 0.942$, hazard ratio: 1.11, 95% confidence interval: 0.56–14.48).

DISCUSSION

TIPS is an effective method for decompressing PVP; thus, preventing bleeding from gastroesophageal varices and reducing the symptoms of ascites[16-18]. The standard procedure is feasible when the right or middle HV and the right PV can be aligned along a straight imaginary intrahepatic tract within the liver parenchyma[19]. In some cases, the liver may be distorted and the location of porta hepatis may be more cranially than usual. These anatomic variations are sometimes seen in cases with a

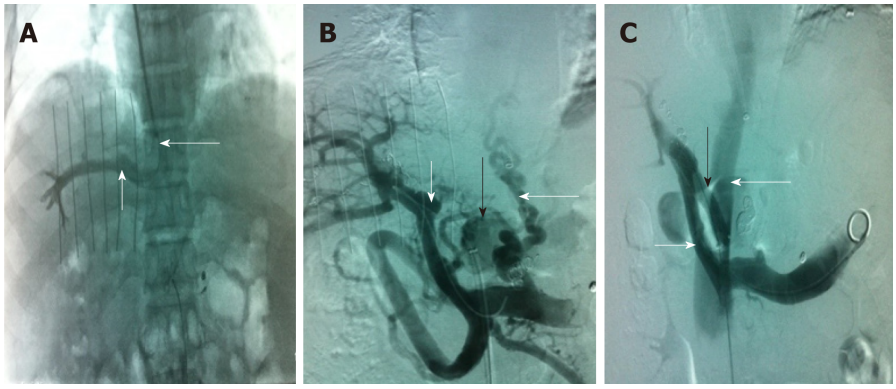

Figure 1 Transjugular intrahepatic portosystemic shunt. A: Venography of the right hepatic vein *via* jugular vein catheterization showed that the sharp angles/spatial relationship between the inferior vena cava (long white arrow) and the right hepatic vein (short white arrow) were inappropriate; thus, conventional transjugular intrahepatic portosystemic shunt could not be performed; B: Puncture of the intrahepatic portal vein through the inferior vena cava *via* femoral vein access and venography. The venogram showed the portal vein (short white arrow), lateral branch (black arrow) and varicose vein (long white arrow); C: The shunt (black arrow) between the portal vein (short white arrow) and the inferior vena cava (long white arrow) was successfully created. Subsequently, the varicose veins and collateral vessels disappeared completely.

small, shrunken cirrhotic liver and the standard TIPS procedure may be impossible in these cases. Despite the fact that there are many studies describing techniques to enable PV imaging and access, TIPS shunt placement may be technically difficult or impossible in certain patients for a variety of anatomic reasons[11,20-22] and may be a valuable contingency plan after an unsuccessful TIPS creation. For example, transcaval TIPS was performed in a patient with acute Budd-Chiari syndrome and a thrombosed mesocaval shunt and stenosis of the IVC[22], and a method known as the "gun-sight" approach[23] can create a portocaval shunt in patients with HVs unsuitable for conventional TIPS creation.

The right jugular vein access is the standard approach for TIPS, which usually makes it much easier to puncture the RHV. The orientation of the liver may change due to liver cirrhosis. An acute angle between the IVC and the RHV may form, and the distance between the RPV and the RHV may be decreased[20]. The TFIPS creation is an alternative technique that may successfully circumvent these anatomic constraints. Importantly, the TFIPS procedure provides a new route for the creation of an intrahepatic portosystemic shunt. The RHV is located using the right femoral vein. Furthermore, the route to the portal system is created by trans-mesenteric access. As a consequence, the liver parenchymal shunt tract was created by puncturing from the PV to RHV. Technically, it is much easier to puncture the PV under the guidance of ultrasound. After puncturing the PV, the PV can not only be visualized by direct PV angiography, but a catheter can also be inserted. By using a lateral comparison, depending on the different spatial relationship between the HV and the PV, lateral revision of the puncture needle in an arc, not across the catheter, can prevent puncture of the liver, allows better puncture accuracy and improves the success rate of TFIPS.

In the present study, the TFIPS procedure was performed as a curative treatment in 19 patients who were unable to undergo conventional TIPS. The safety and clinical outcomes of TFIPS were determined. The results showed that in patients with PH, TFIPS was an effective measure in reducing the PPG compared with TIPS. Furthermore, TFIPS was not associated with a higher incidence and severity of HE or other unfavorable outcomes such as procedure-related mortality. In fact, the mean PPG before and after TFIPS was not statistically different from that seen in TIPS. The addition of the TFIPS technique for salvage cases allowed us to achieve a 100% technical success rate, regardless of venous patency.

There are various treatment methods for variceal bleeding, which depend on liver function, patient anatomy and local expertise. Recommended societal guidelines[24] cite a 95% technical and 90% clinical success rate for TIPS creation when performed in patients with patent hepatic and portal veins. Our technical success and clinical success rates are close to those in the above report. In our institution, TFIPS creation is not the default primary intervention for PH, making the results more likely to be achievable in "real-world" practice in which the TIPS procedure is more likely to remain the default intervention. In this setting, TFIPS creation appears to be a safe, expedient and effective treatment for patients with acute variceal hemorrhage who are poor anatomic candidates for conventional TIPS creation or who have undergone

Figure 2 Computed tomography and transjugular intrahepatic portosystemic shunt. A: Inferior vena cava stent (black long arrow); B: Liver caudate lobe is much bigger due to congestion, which makes the portal vein (black short arrow) become nearer to the abdominal wall. The acute angle between the inferior vena cava and internal portal vein is unorthodox; C: Puncture of the intrahepatic portal vein through the inferior vena cava *via* femoral vein access and venography. The venogram showed the portal vein (short white arrow) and the varicose vein (long white arrow); D: A Scoop channel between the portal vein (short white arrow) and the inferior vena cava (long white arrow) was successfully established with the stent (black arrow). The varicose veins disappeared completely.

an unsuccessful TIPS creation. Despite salvage circumstances, outcomes were comparable to the expected outcomes after conventional TIPS creation. However, there is a learning curve for the physician. Furthermore, increased setup time and additional equipment required in a crowded procedure room may also discourage routine use. We suggest using TFIPS for the second attempt if regular TIPS is unsuccessful through the right jugular access route.

The limitations of the present report include its retrospective design, a single center and small sample size. Furthermore, some patients were suggested to attend institutions for routine examination, where clinical data were available, but postoperative imaging or endoscopy may not have been routinely performed; thus, assessment for complete variceal eradication was limited. The follow-up period was 12 and 24 mo, and as such the long-term durability of salvage TFIPS is unknown.

In conclusion, our research demonstrated that TFIPS sufficiently decompressed PH and prevented variceal rebleeding compared with TIPS. The use of TFIPS did not decrease HE rates compared with TIPS and no survival benefit was observed. However, TFIPS appears to be a safe, expedient and effective treatment for patients who are poor anatomic candidates for standard TIPS creation or who have undergone an unsuccessful TIPS creation.

Table 2 Hemodynamic changes

Index	TFIPS, *n* = 19	TIPS, *n* = 21	t/χ^2	*P* value
Pre-operation PVP, mmHg	35.00 ± 6.05	34.01 ± 4.70	0.578	0.566
Post-operation PVP, mmHg	21.43 ± 2.83	20.98 ± 3.65	0.429	0.670
Mean decreased PVP differential, mmHg	13.57 ± 6.70	13.03 ± 5.44	0.281	0.780
Pre-operation PPG, mmHg	23.91 ± 4.64	22.61 ± 5.39	0.814	0.421
Post-operation PPG, mmHg	10.85 ± 3.33	10.84 ± 3.33	0.095	0.925
Mean decreased PPG differential, mmHg	13.07 ± 5.26	11.87 ± 5.10	0.728	0.471
PPG ≤ 12 mmHg, *n* (%)	13 (68.4)	14 (66.7)	0.014	0.906
PPG reduction ≥ 50%, *n* (%)	19 (100)	21 (100)	-	-

PVP: Portal vein pressure; PPG: Portal pressure gradient; TFIPS: Transfemoral intrahepatic portosystemic shunt; TIPS: Transjugular intrahepatic portosystemic shunt.

Table 3 Comparison of clinical effects

Index	TFIPS group, *n* = 19		TIPS group, *n* = 21		t/χ^2		*P* value	
	12 mo	24 mo	12 mo	24 mo	12 mo	24 mo	12 mo	24 mo
Child-Pugh score	5.45 ± 1.60	6.32 ± 1.60	6.45 ± 1.50	7.11 ± 1.60	0.042	0.061	0.852	0.813
MELD score	10.31 ± 1.44	11.52 ± 1.43	11.12 ± 1.55	11.14 ± 1.79	0.487	0.624	0.794	0.527
Blood ammonia	83.6 ± 39.4	87.3 ± 33.1	85.7 ± 23.4	88.2 ± 29.6	0.758	0.518	0.246	0.238
Variceal rebleeding, *n* (%)	1 (5.3)	1 (5.3)	1 (4.8)	2 (9.5)	0.005	0.261	0.942	0.609
RS, *n*	0	0	0	0	0	1	0	1
Shunt patency	18 (94.7)	18 (94.7)	20 (95.2)	19 (90.5)	0.005	0.261	0.942	0.609
HE, *n* (%)	4 (21.1)	5 (26.3)	4 (19.0)	6 (28.6)	0.025	0.025	0.874	0.873
grade of HE, *n*					0.107	0.166	0.948	0.573
I	2	2	1	2				
II	1	2	2	3				
III	1	1	1	1				
IV	0	0	0	0				
HM, *n*	0	0	0	0	0	1	0	1
Survival, *n* (%)	18 (94.7)	18 (94.7)	21(100)	20 (95.2)	0	0.001	1	0.981

MELD: Model for end-stage liver disease; RS: Refractory ascites; HE: Hepatic encephalopathy; HM: Hepatic myelopathy; TFIPS: Transfemoral intrahepatic portosystemic shunt; TIPS: Transjugular intrahepatic portosystemic shunt.

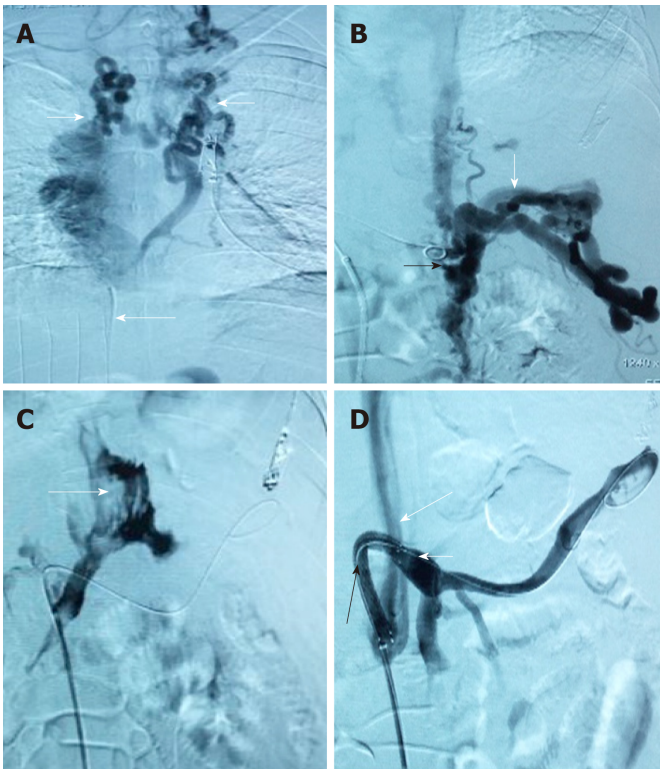

Figure 3 Due to complete occlusion of the bilateral jugular vein and/or superior vena cava, transjugular intrahepatic portosystemic shunt could not be performed in 3 cases. A: Venogram *via* jugular vein access indicated that cavernous transformation of the bilateral jugular vein (white short arrow) and superior vena cava was occluded (long white arrow). Thus, conventional transjugular intrahepatic portosystemic shunt could not be performed; B: Puncture of the intrahepatic portal vein through the inferior vena cava *via* femoral vein access and venography. The venogram showed the angiography catheter in the portal vein (black arrow) and portal vein blood flow reflux into the hepatic varicose veins (long white arrow); C: The venogram showed that the contrast agent infiltrated the abdominal cavity (long white arrow) when the hepatic vein was punctured *via* the inferior vena cava; D: A semi-arc shunt between the portal vein (short white arrow) and the inferior vena cava (long white arrow) was successfully created using the covered stent (black arrow). Subsequently, the varicose veins disappeared completely.

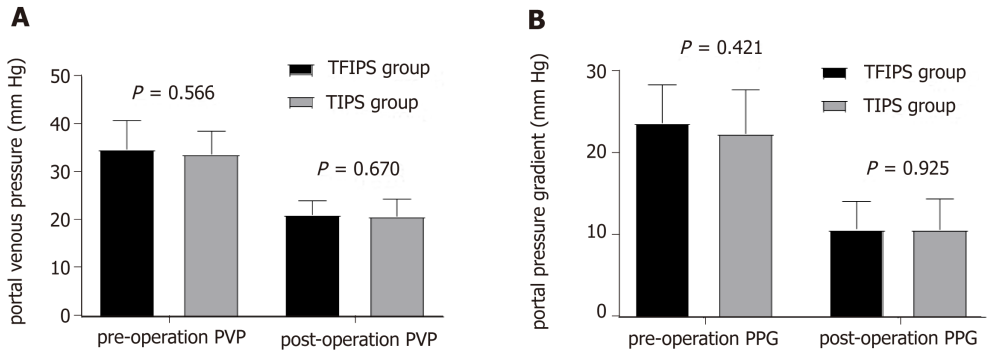

Figure 4 No statistically significant differences were observed between the two groups in terms of portal vein pressure and portal pressure gradient before and after surgery. PVP: Portal vein pressure; PPG: Portal pressure gradient; TFIPS: Transfemoral intrahepatic portosystemic shunt; TIPS: Transjugular intrahepatic portosystemic shunt.

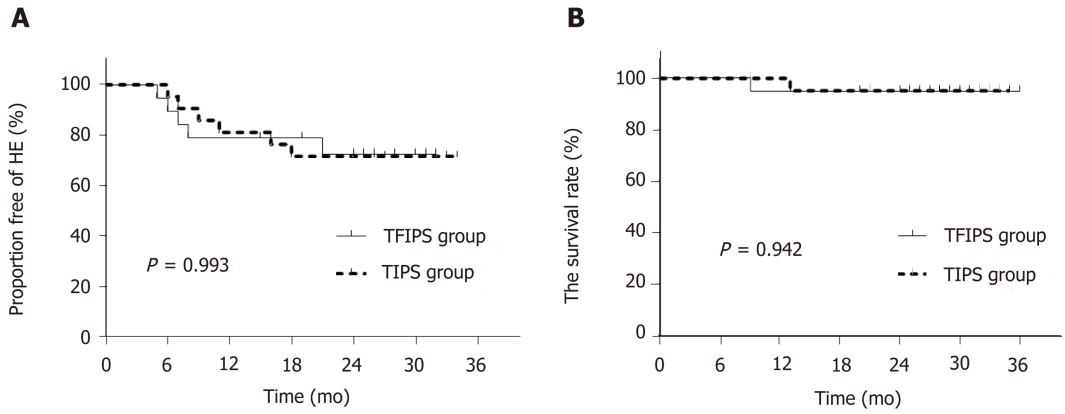

Figure 5 Time-to-event (Kaplan-Meier) *de novo* hepatic encephalopathy analysis. There were no significant differences between the two groups. TFIPS: Transfemoral intrahepatic portosystemic shunt; TIPS: Transjugular intrahepatic portosystemic shunt.

ARTICLE HIGHLIGHTS

Research background

Transjugular intrahepatic portosystemic shunts (TIPS) have been used successfully for the treatment of portal hypertension and their complications, such as bleeding varices and refractory ascites. TIPS creation is a percutaneous image-guided procedure in which a decompressive channel is created between a hepatic vein and an intrahepatic branch of the portal vein to reduce portal vein pressure.

Research motivation

TIPS are currently used for the treatment of complications of portal hypertension. With advances in materials, many experimental and clinical studies have been indicated that using covered stent grafts, especially polytetrafluoroethylene covered stent graft, could improve the long-term patency of TIPS. In most situations, a shunt between the hepatic and portal veins can be successfully connected from an internal jugular vein access. Rarely, occlusion of the central veins, hepatic veins, or the vena cava precludes a conventional approach. We used an unconventional procedure called transfemoral intrahepatic portosystemic shunt (TFIPS) to treat portal hypertension and compare this procedure to the traditional approach. In the future, further studies are needed to verify our results.

Research objectives

The main objective was to evaluate the safety and clinical outcomes of TFIPS and compare them with those of TIPS. If TFIPS procedure is as safe and effective as typical TIPS, we should use TFIPS in the patients who are not suitable for the traditional TIPS.

Research methods

In this one center retrospective study,the subjects were patients diagnosed with portal hypertension who underwent TFIPS (19 patients) because of anatomic reasons and TIPS (21 patients). Patient characteristics, technical success rate, hemodynamic changes, the incidence of shunt stenosis, the incidence of hepatic encephalopathy, hepatic myelopaphy (HM) and the survival rate were compared between the two groups.

Research results

This study showed that TFIPS is as effective as TIPS in decompressing portal venous pressure. The TFIPS procedure time is obviously longer than TIPS. There was no significant difference in the incidence of shunt stenosis, hepatic encephalopathy, hepatic myelopaphy and the survival time.

Research conclusions

We found that the TFIPS is as effective as TIPS in treating portal hypertension without increasing the complications of TIPS procedure. TFIPS may be a valuable adjunct to traditional approaches in patients with portal hypertension.

Research perspectives

Because this study used a single-center retrospective design and included relatively few patients, further investigations, such as a multi-center randomized controlled study, are needed. In addition, due to the increased time used in TFIPS procedure, methods to reduce procedure time are needed.

REFERENCES

1 **Blachier M**, Leleu H, Peck-Radosavljevic M, Valla DC, Roudot-Thoraval F. The burden of liver disease in Europe: a review of available epidemiological data. *J Hepatol* 2013; **58**: 593-608 [PMID: 23419824 DOI: 10.1016/j.jhep.2012.12.005]

2 **Rössle M**, Richter GM, Nöldge G, Palmaz JC, Wenz W, Gerok W. New non-operative treatment for variceal haemorrhage. *Lancet* 1989; **2**: 153 [PMID: 2567908]

3 **Rössle M**. TIPS: 25 years later. *J Hepatol* 2013; **59**: 1081-1093 [PMID: 23811307 DOI: 10.1016/j.jhep.2013.06.014]

4 **Bureau C**, Garcia-Pagan JC, Otal P, Pomier-Layrargues G, Chabbert V, Cortez C, Perreault P, Péron JM, Abraldes JG, Bouchard L, Bilbao JI, Bosch J, Rousseau H, Vinel JP. Improved clinical outcome using polytetrafluoroethylene-coated stents for TIPS: results of a randomized study. *Gastroenterology* 2004; **126**: 469-475 [PMID: 14762784]

5 **Riggio O**, Ridola L, Angeloni S, Cerini F, Pasquale C, Attili AF, Fanelli F, Merli M, Salvatori FM. Clinical efficacy of transjugular intrahepatic portosystemic shunt created with covered stents with different diameters: results of a randomized controlled trial. *J Hepatol* 2010; **53**: 267-272 [PMID: 20537753 DOI: 10.1016/j.jhep.2010.02.033]

6 **Weber CN**, Nadolski GJ, White SB, Clark TW, Mondschein JI, Stavropoulos SW, Shlansky-Goldberg RD, Trerotola SO, Soulen MC. Long-Term Patency and Clinical Analysis of Expanded Polytetrafluoroethylene-Covered Transjugular Intrahepatic Portosystemic Shunt Stent Grafts. *J Vasc Interv Radiol* 2015; **26**: 1257-65; quiz 1265 [PMID: 25990133 DOI: 10.1016/j.jvir.2015.04.005]

7 **Wang L**, Xiao Z, Yue Z, Zhao H, Fan Z, Zhao M, He F, Dai S, Qiu B, Yao J, Lin Q, Dong X, Liu F. Efficacy of covered and bare stent in TIPS for cirrhotic portal hypertension: A single-center randomized trial. *Sci Rep* 2016; **6**: 21011 [PMID: 26876503 DOI: 10.1038/srep21011]

8 **Boyer TD**, Haskal ZJ; American Association for the Study of Liver Diseases. The role of transjugular intrahepatic portosystemic shunt in the management of portal hypertension. *Hepatology* 2005; **41**: 386-400 [PMID: 15660434 DOI: 10.1002/hep.20559]

9 **Petersen B**, Binkert C. Intravascular ultrasound-guided direct intrahepatic portacaval shunt: midterm follow-up. *J Vasc Interv Radiol* 2004; **15**: 927-938 [PMID: 15361560 DOI: 10.1097/01.RVI.0000133703.35041.42]

10 **Nyman UR**, Semba CP, Chang H, Hoffman C, Dake MD. Percutaneous creation of a mesocaval shunt. *J Vasc Interv Radiol* 1996; **7**: 769-773 [PMID: 8897349]

11 **LaBerge JM**, Ring EJ, Gordon RL. Percutaneous intrahepatic portosystemic shunt created via a femoral vein approach. *Radiology* 1991; **181**: 679-681 [PMID: 1947081 DOI: 10.1148/radiology.181.3.1947081]

12 **Yao J**, Zuo L, An G, Yue Z, Zhao H, Wang L, Liu F. Risk Factors for Hepatic Encephalopathy after Transjugular Intrahepatic Portosystemic Shunt in Patients with Hepatocellular Carcinoma and Portal Hypertension. *J Gastrointestin Liver Dis* 2015; **24**: 301-307 [PMID: 26405702 DOI: 10.15403/jgld.2014.1121.243.yao]

13 **Haskal ZJ**, Rees CR, Ring EJ, Saxon R, Sacks D. Reporting standards for transjugular intrahepatic portosystemic shunts. Technology Assessment Committee of the SCVIR. *J Vasc Interv Radiol* 1997; **8**: 289-297 [PMID: 9084000]

14 **Dariushnia SR**, Haskal ZJ, Midia M, Martin LG, Walker TG, Kalva SP, Clark TW, Ganguli S, Krishnamurthy V, Saiter CK, Nikolic B; Society of Interventional Radiology Standards of Practice Committee. Quality Improvement Guidelines for Transjugular Intrahepatic Portosystemic Shunts. *J Vasc Interv Radiol* 2016; **27**: 1-7 [PMID: 26614596 DOI: 10.1016/j.jvir.2015.09.018]

15 **Wijdicks EF**. Hepatic Encephalopathy. *N Engl J Med* 2016; **375**: 1660-1670 [PMID: 27783916 DOI: 10.1056/NEJMra1600561]

16 **Heinzow HS**, Lenz P, Köhler M, Reinecke F, Ullerich H, Domschke W, Domagk D, Meister T. Clinical outcome and predictors of survival after TIPS insertion in patients with liver cirrhosis. *World J Gastroenterol* 2012; **18**: 5211-5218 [PMID: 23066315 DOI: 10.3748/wjg.v18.i37.5211]

17 **Merli M**, Salerno F, Riggio O, de Franchis R, Fiaccadori F, Meddi P, Primignani M, Pedretti G, Maggi A, Capocaccia L, Lovaria A, Ugolotti U, Salvatori F, Bezzi M, Rossi P. Transjugular intrahepatic portosystemic shunt versus endoscopic sclerotherapy for the prevention of variceal bleeding in cirrhosis: a randomized multicenter trial. Gruppo Italiano Studio TIPS (G.I.S.T.). *Hepatology* 1998; **27**: 48-53 [PMID: 9425916 DOI: 10.1002/hep.510270109]

18 **Narahara Y**, Kanazawa H, Fukuda T, Matsushita Y, Harimoto H, Kidokoro H, Katakura T, Atsukawa M, Taki Y, Kimura Y, Nakatsuka K, Sakamoto C. Transjugular intrahepatic portosystemic shunt versus paracentesis plus albumin in patients with refractory ascites who have good hepatic and renal function: a prospective randomized trial. *J Gastroenterol* 2011; **46**: 78-85 [PMID: 20632194 DOI: 10.1007/s00535-010-0282-9]

19 **Liang HL**, Liu WC, Huang JS, Chen MC, Lai KH, Pan HB, Chen CK. TIPS in patients with cranial porta hepatis: ultrasound-guided transhepatic portohepatic-portocaval puncture in single needle pass. *AJR Am J Roentgenol* 2011; **196**: 914-918 [PMID: 21427345 DOI: 10.2214/AJR.10.4623]

20 **Hausegger KA**, Tauss J, Karaic K, Klein GE, Uggowitzer M. Use of the left internal jugular vein approach for transjugular portosystemic shunt. *AJR Am J Roentgenol* 1998; **171**: 1637-1639 [PMID: 9843303 DOI: 10.2214/ajr.171.6.9843303]

21 **Sze DY**, Magsamen KE, Frisoli JK. Successful transfemoral creation of an intrahepatic portosystemic shunt with use of the Viatorr device. *J Vasc Interv Radiol* 2006; **17**: 569-572 [PMID: 16567683 DOI: 10.1097/01.rvi.0000200054.73714.e1]

22 **Lee KH**, Lee DY, Won JY, Park SJ, Kim JK, Yoon W. Transcaval transjugular intrahepatic portosystemic shunt: preliminary clinical results. *Korean J Radiol* 2003; **4**: 35-41 [PMID: 12679632 DOI: 10.3348/kjr.2003.4.1.35]

23 **Haskal ZJ**, Duszak R, Furth EE. Transjugular intrahepatic transcaval portosystemic shunt: the gun-sight approach. *J Vasc Interv Radiol* 1996; **7**: 139-142 [PMID: 8773989]

24 **Haskal ZJ**, Martin L, Cardella JF, Cole PE, Drooz A, Grassi CJ, McCowan TC, Meranze SG, Neithamer CD, Oglevie SB, Roberts AC, Sacks D, Silverstein MI, Swan TL, Towbin RB, Lewis CA; Society of Cardiovascular & Interventional Radiology, Standards of Practice Committee. Quality improvement guidelines for transjugular intrahepatic portosystemic shunts. SCVIR Standards of Practice Committee. *J Vasc Interv Radiol* 2001; **12**: 131-136 [PMID: 11265875]

World Journal of Clinical Cases

Submit a Manuscript: https://www.f6publishing.com

World J Clin Cases 2019 June 26; 7(12): 1421-1429

DOI: 10.12998/wjcc.v7.i12.1421

ISSN 2307-8960 (online)

ORIGINAL ARTICLE

Observational Study

Impact of gastroesophageal reflux disease on the quality of life of Polish patients

Rafał Gorczyca, Piotr Pardak, Anna Pękala, Rafał Filip

ORCID number: Rafał Gorczyca (0000-0002-3334-557X); Piotr Pardak (0000-0001-8489-781X); Anna Pękala (0000-0001-6779-1909); Rafał Filip (0000-0002-5954-151X).

Author contributions: Gorczyca R and Filip R designed the study, performed the data collection and statistical analyses; Filip R, Pardak P and Pękala A performed data interpretation and drafted the manuscript; All authors read and approved the final manuscript.

Institutional review board statement: The study protocol was approved by the Institutional Ethic Committee at the Institute of Rural Health in Lublin, Poland.

Informed consent statement: All patients gave their written informed consent prior to study inclusion.

Conflict-of-interest statement: There are no conflicts of interest to report for any of the authors.

STROBE statement: The authors have read the STROBE Statement-checklist of items, and the manuscript was prepared and revised according to the STROBE Statement-checklist of items.

Rafał Gorczyca, Department of Clinical Endoscopy, Institute of Rural Health, Lublin 20-080, Poland

Piotr Pardak, Anna Pękala, Rafał Filip, Department of Gastroenterology with IBD Unit of Clinical Hospital 2, University of Rzeszów, Rzeszów 35-301, Poland

Corresponding author: Piotr Pardak, MD, Doctor, Department of Gastroenterology with IBD Unit of Clinical Hospital 2, University of Rzeszów, Lwowska 60, Rzeszów 35-301, Poland.
piotrpardak@wp.pl
Telephone: +48-17-8664607
Fax: +48-17-8664702

Abstract

BACKGROUND

Gastro-esophageal reflux disease (GERD) is a serious health and social problem leading to a considerable decrease in the quality of life of patients. Among the risk factors associated with reflux symptoms and that decrease the quality of life are stress, overweight and an increase in body weight. The concept of health-related quality of life (HRQL) covers an expanded effect of the disease on a patient's wellbeing and daily activities and is one of the measures of widely understood quality of life. HRQL is commonly measured using a self-administered, disease-specific questionnaires.

AIM

To determine the effect of reflux symptoms, stress and body mass index (BMI) on the quality of life.

METHODS

The study included 118 patients diagnosed with reflux disease who reported to an outpatient department of gastroenterology or a specialist hospital ward for planned diagnostic tests. Assessment of the level of reflux was based on the frequency of 5 typical of GERD symptoms. HRQL was measured by a 36-item Short Form Health Survey (SF-36) and level of stress using the 10-item Perceived Stress Scale. Multi-variable relationships were analyzed using multiple regression.

RESULTS

Eleven models of analysis were performed in which the scale of the SF-36 was included as an explained variable. In all models, the same set of explanatory variables: Gender, age, reflux symptoms, stress and BMI, were included. The

Manuscript source: Unsolicited manuscript

Received: January 3, 2019
Peer-review started: January 3, 2019
First decision: January 30, 2019
Revised: April 22, 2019
Accepted: May 2, 2019
Article in press: May 2, 2019
Published online: June 26, 2019

P-Reviewer: Viswanath YKS
S-Editor: Ji FF
L-Editor: Filipodia
E-Editor: Wang J

frequency of GERD symptoms resulted in a decrease in patients' results according to 6 out of 8 SF-36 scales- except for mental health and vitality scales. Stress resulted in a decrease in patient function in all domains measured using the SF-36. Age resulted in a decrease in physical function and in overall assessment of self-reported state of health. An increasing BMI exerted a negative effect on physical fitness and limitations in functioning resulting from this decrease.

CONCLUSION
In GERD patients, HRQL is negatively determined by the frequency of reflux symptoms and by stress, furthermore an increasing BMI and age decreases the level of physical function.

Key words: Gastroesophageal reflux disease; Stress; Psychological factors; Health-related quality of life; Obesity

Core tip: Gastro-esophageal reflux disease is a serious health problem leading to a decrease in the quality of life. This study determines the effect of reflux symptoms, stress and body mass index (commonly known as BMI) on the quality of life measured by a 36-item Short Form Health Survey. We demonstrate that in patients with gastro-esophageal reflux, stress decreases the quality of life to a higher degree than the frequency of reflux symptoms. Age and increasing BMI result in decreased physical function. Therefore, the patient's stress level should be considered in the diagnosis and therapy, as well as an assessment of the progress of treatment.

Citation: Gorczyca R, Pardak P, Pękala A, Filip R. Impact of gastroesophageal reflux disease on the quality of life of Polish patients. *World J Clin Cases* 2019; 7(12): 1421-1429
URL: https://www.wjgnet.com/2307-8960/full/v7/i12/1421.htm
DOI: https://dx.doi.org/10.12998/wjcc.v7.i12.1421

INTRODUCTION

Gastro-esophageal reflux disease (GERD) is a serious health and social problem, considering the frequency and specificity of symptoms, causing an increase in absenteeism rate, consequently creating a financial burden for health care, and above all, leading to a considerable decrease in the quality of life of patients. According to a 1999 study, reflux disease symptoms occurred every day in 7%-10%, and once a week in nearly 20% of the population in highly developed countries[1]. In 2003 in Poland, based on Carlsson's questionnaire, reflux disease was diagnosed in more than 34% of patients aged over 15 who reported to a family physician[2]. A special problem for patients is the noxiousness of symptoms at the phase of aggravation of the disease and frequent recurrences after successful therapy. A decrease in perceived quality of life is symptomatic of GERD[3-5]. The Montreal definition describes GERD as a condition that develops when the reflux of stomach contents causes troublesome symptoms and/or complications. The symptoms are considered troublesome when they occur more frequently than once a week because only then they cause a decrease in the perceived quality of life[3,4].

The concept of health-related quality of life (HRQL) covers an expanded effect of the disease on a patient's wellbeing and daily activities. To date, there is no commonly accepted definition of this concept, and the basic problem is the specification of contents of the domains of activities to which this definition refers. In practice, HRQL should refer to contents included in a given measurement instrument[5-7]. HRQL is commonly measured using a self-administered questionnaire completed by patients. Disease-specific and general questionnaires are distinguished. The first provide information concerning disorders and limitations typical of a given disease. However, this limits the possibility to compare the quality of life between patients suffering from different diseases. General (generic) questionnaires provide comparability of results, measure the respondent's functioning within several basic spheres (domains), which are general enough in that they concern many types of diseases, and may also,

within a certain scope, be reasonably measured in healthy individuals. The HRQL is one of the measures of widely understood quality of life (QOL), which covers many spheres of activity beyond the area of health and disease, but often related with it, such as interpersonal relationships in a family, social and financial problems[8]. The etiopathogenesis of GERD is multi-factorial and, in the case of individual patients, is difficult to determine unequivocally. Among the risk factors with a documented relation to reflux symptoms are, among others, stress[9-11], being overweight and obesity[11,12]. Here, stress will be understood in a narrower sense as a psychological distress, *i.e*. the state of strong or long-term psychological tension, connected with low mood, emotions of fear and anxiety or aggression. The relationship between stress and reflux symptoms and quality of life has been well documented. In a cross-sectional controlled population study conducted among the Norwegian population that included nearly 59000 respondents[13], the relationship was assessed between psychiatric disorders (anxiety, depression) and reflux symptoms. It was observed that anxiety and depression correlated to a 3- 4-fold increase in the risk of occurrence of reflux symptoms. In a study of reflux disease patients conducted by Nojkova *et al*[14], patients who had reflux symptoms and concomitant symptoms of psychological distress, showed a significantly lower quality of life and more severe reflux symptoms at the beginning of therapy compared to those without symptoms of distress. In a repeated study, after the completion of therapy with a proton pump inhibitor (rabeprazole at a dose 20 mg/d) patients with distress continued to show a lower quality of life and higher intensity of reflux symptoms than those without distress, despite an improvement in both groups.

Although there is clear evidence for a relationship between stress and reflux symptoms, a randomized experimental study did not confirm the effect of stress on the number of reflux episodes measured using 24-h esophageal pH monitoring, despite the fact that the group subjected to stress perceived an increased intensity of symptoms in subjective evaluations[15]. While undertaking attempts to explain the relationship between experiencing reflux symptoms and stress, the researchers refer to the presence of a strong relationship between the degree of emotional tension accompanying stress and a decreased threshold of pain sensitivity. It was also observed that patients with reflux disease emphasize the inability to control pain and the randomness with which pain occurs. At the same time, they are strongly convinced that there is a relationship between their psychological condition and the intensity of the complaints experienced[16,17]. An important study that cast light on the relationship between stress and the heartburn symptoms was by Farré *et al*[18] examining the effect of stress on the esophageal mucosa of rats. The researchers traced changes in the esophageal mucosa using electron microscopy and concluded that strong stress may result in an increase in permeability of the esophageal mucosa. They also observed an enhanced effect between stress and exposure of the esophageal mucosa to acid, leading to increased permeability and dilatation of intracellular spaces. Additionally, obesity and being overweight are related to GERD. Epidemiological studies demonstrate that a high percentage of GERD patients are overweight or obese[19-21], and in a population of nurses, Jakobson *et al*[22] observed a nearly linear increase in GERD risk ratio with an increase in body mass index (BMI). One factor that correlated with GERD symptoms was lower esophageal sphincter pressure and higher intragastric pressure[20,23]. Simultaneously, an increase in body weight is negatively correlated with the level of HRQL, both in the case of somatically healthy individuals[24] and in the case of a number of diseases where, apart from the symptoms of the main disease, it is an additional factor that decreases patient HRQL[25-28].

Aim

The primary goal of the study was to determine the independent effect of reflux symptoms, stress and increasing BMI on the quality of life of patients using the SF-36 questionnaire.

MATERIALS AND METHODS

The study protocol was approved by the Institutional Ethic Committee at the Institute of Rural Health in Lublin, Poland. Assessment of the level of reflux symptoms was based on five symptoms considered typical of GERD. The frequency of each symptom was rated by the respondent on the 5-point Likert-type scale. These were: (1) Heartburn after meals (scores from 0- never to 4- after every meal/almost after every meal); (2) Heartburn in a lying position (scores from 0- never to 4- always/almost always); (3) Waking from sleep due to heartburn (scores from 0- never to 4- every

night/almost every night); (4) Regurgitation; and (5) Acid reflux (scores from 0- never to 4- always/almost always). The sum of ratings was transformed into a 0-100 range. The transformed score represents the percentage of the possible maximum score achieved. It was taken as a measure of the overall level of reflux symptoms (ORS). Reliability measured using Cronbach's alpha homogeneity coefficient for ORS was 0.83, which suggests a good level of homogeneity of the scale.

HRQL was measured by a generic questionnaire, 36-item Short Form Health Survey (SF-36), which measures the quality of life across eight domains: (1) Physical function (PF); (2) Role limitations due to physical problems (RP); (3) Bodily pain (BP); (4) General health perceptions (GH); (5) Vitality (Vt); (6) Social function (SF); (7) Role limitations due to emotional problems (RE); and (8) Mental health perceptions (MH). In addition, single item scale Health Transition (HT) identifies perceived change in health in the last year. Based on eight basic scales, two standardized summary scales are calculated: Physical Component Summary (PCS) and Mental Component Summary (MCS), which represent the physical and mental dimensions of HRQL, respectively. Calculating the results within these two dimensions, the authors of the test provided the values of factor score coefficients for eight individual scales of the test in each dimension, calculated based on a validation study in the United States. Stress levels were measured using the S. Kohen 10-item Perceived Stress Scale (PSS-10) as adapted by Juczyński and Ogińska-Bulik[29].

Study population

The study included 127 patients aged 19-64 diagnosed with reflux disease at various phases of treatment, who reported to a specialist outpatient department of gastroenterology or a specialist hospital ward for planned diagnostic tests. Each patient who met the preliminary criteria of age and health status and expressed consent to participate in the study participated in a research session carried out by a psychologist. The study was conducted with each patient individually or in small groups of up to four patients. Ultimately, the results of 118 patients, 43 (36.4%) males and 75 (63.6%) females, were considered in the analyses.

Statistical analysis

Statistical analyses were performed using the statistical package SPSS v.22. The results of eight SF-36 scales were expressed in the form of transformed scores, *i.e*. the percentage of the row score to the maximum possible score in the given scale. For each of the eight scales, the value 0 was assigned to the worst and 100 to the best quality of functioning. Standardized results according to the PCS and MCS scales were converted, according to the instruction, into T-scores, with the mean 50 and standard deviation 10. Evaluations of changes in the state of health remained in raw form, *i.e*. according to the 5-point scale within the range of values from 1-5. Multivariable relationships were analyzed using multiple regression. Eleven models of analysis were performed in which the subsequent scale of the SF-36 was included as an explained variable. In all models, the same set of explanatory variables (gender, age, GERD symptoms (ORS), stress (PSS-10), and BMI) was included. Analyses were performed using the backward elimination technique, the final effect of which is leaving in the model only the set of variables that have a significant effect on the explained variable.

RESULTS

In the examined population, females were older than males ($P = 0.004$): Mean age 48.4 ± 12.09 and 41.8 ± 13.21, respectively. Also, females had a lower BMI compared to males: 24.7 ± 4.51 and 26.0 ± 3.37), respectively ($P = 0.034$). However, the two groups did not significantly differ according to the frequency of GERD symptoms (mean value for the examined population was 45.0 ± 25.26), nor by the mean value of any of the SF-36 scales and the stress level. The age group < 50 had a lower BMI value (24.0 ± 3.78, within the normal range) than the age group > 50 years (26.4 ± 4.25, overweight, $P = 0.003$). These groups did not differ by the level of GERD symptoms or by stress level. In the HRQL examination, the older group showed a generally lower level of PF than the younger group (PCS: 41.7 ± 7.92 and 47.6 ± 6.33, respectively, $P < 0.0001$). In the case of detailed scales, significant differences were noted to the disadvantage of the older group in the scales: PF, RP, BP, GH, and also in the RE scale (Table 1).

The frequency of GERD symptoms resulted in a decrease in patients' results according to six out of eight F-36 scales. Only in two scales, MH and Vt, the effect of GERD symptoms was insignificant. Consequently, a significant decrease in the results under the effect of symptoms was observed according to both PSC and MSC summary scales.

Table 1 Mean values of variables analyzed in the study population in general and according to gender and age

Variable	Sex			Age			Total, *n* = 118
	M, *n* = 43	F, *n* = 75	Sig.	< 50 yr, *n* = 62	≥ 50 yr, *n* = 56	Sig.	
Age	41.8 (13.21)	48.4 (12.09)	0.0044	NA	NA	NA	46.0 (12.86)
BMI	26.0 (3.37)	24.7 (4.51)	0.034	24.0 (3.78)	26.4 (4.25)	0.003	25.2 (4.17)
GERD symptoms	47.6 (26.4)	43.6 (24.65)	0.43	44.4 (23.24)	45.7 (27.53)	0.75	45.0 (25.26)
Stress	19.9 (6.87)	18.8 (3.79)	0.65	18.5 (4.98)	20.0 (5.2)	0.13	19.2 (5.13)
PF	79.8 (19.88)	78.7 (17.69)	0.54	87.1 (12.66)	70.3 (19.85)	0.000001	79.1 (18.44)
RP	60.3 (29.06)	61.7 (22.12)	0.88	67.1 (24.59)	54.6 (23.43)	0.011	61.2 (24.76)
BP	51.3 (29.45)	42.8 (21.18)	0.12	50.4 (25.41)	40.9 (23.19)	0.027	45.9 (24.74)
GH	53.0 (20.46)	52.4 (16.44)	0.96	58.9 (18.51)	45.7 (14.5)	0.00003	52.6 (17.92)
Vt	47.7 (17.31)	51.1 (17.19)	0.42	51.7 (16.29)	47.7 (18.14)	0.21	49.8 (17.23)
SF	62.5 (23.31)	64.0 (24.05)	0.74	65.3 (24)	61.4 (23.39)	0.35	63.5 (23.69)
RE	65.5 (29.07)	68.8 (24.05)	0.70	74.5 (24.97)	60.0 (25)	0.0022	67.6 (25.92)
MH	56.5 (18.47)	55.5 (17.18)	0.49	57.4 (17.15)	54.2 (18.06)	0.39	55.9 (17.59)
HT	3.5 (1.03)	3.4 (0.84)	0.62	3.3 (0.84)	3.6 (0.97)	0.12	3.4 (0.91)
PCS	45.7 (8.69)	44.3 (7.07)	0.42	47.6 (6.33)	41.7 (7.92)	0.000068	44.8 (7.69)
MCS	39.1 (11.47)	40.4 (10.38)	0.73	40.9 (10.78)	38.9 (10.74)	0.39	39.9 (10.76)

NA: Not applicable; BMI: Body mass index; GERD: Gastro-esophageal reflux disease; PF: Physical functioning; RP: Physical problems; BP: Bodily pain; GH: General health perceptions; Vt: Vitality; SF: Social functioning; RE: Role limitations due to emotional problems; MH: Mental health perceptions; HT: Health Transition; PCS: Physical Component Summary; MCS: Mental Component Summary.

Stress resulted in a decrease in patient function in all domains and dimensions measured using the SF-36. PF decreased as age increased, according to the results of both PF scale and PCS. Age was also the factor resulting in a decrease in overall assessment of self-reported state of health (GH). An increasing BMI exerted a negative effect on physical fitness (PF) and limitations in functioning resulting from this decrease (RP). Notably, it also caused limitations in social relations that resulted from emotional disorders (RE) (Table 2).

DISCUSSION

In the present study of the quality of life of patients with GERD, the control group was not considered. To compensate for this deficiency, the results of our studies using SF-36 (Lublin) were compared with the results obtained in a random sample of 8801 inhabitants of Great Britain drawn from General Practitioner Records held by the Health Authorities for Berkshire, Buckinghamshire, Northamptonshire, and Oxfordshire (GBS), and the subpopulation of chronically ill patients in this sample (GBS-longstanding illness)[30]. The sample covered 8,801 patients aged 18-64, including 43.4% of males and 55.6% of females. The groups (GBS and Lublin) were not significantly different according to age or gender (Figure 1).

Patients from Lublin showed a lower quality of life in all eight domains compared to GBS (significance of differences was analyzed using t-Student test). Compared to the GBS long-standing illness, they did not significantly differ according to the PF and Vt scales. The highest difference between the quality of the assessed domains was observed for BP. It occupied the lowest position in the Lublin population, while it was ranked 30 scores higher in the GB sample. Similarly, in American studies[31], 533 adults with a history of heartburn symptoms showed a lower quality of functioning in all eight domains compared to the general United States population.

Regression analysis demonstrated that stress and reflux complaints were two separate sources of the effect on HRQL in the general measures of physical and psychological functioning, as well as individual domains considered in SF-36. The strength of the effect of stress is especially noteworthy, as stress was the factor that decreased the HRQL in all domains and spheres (PCS, MCS). In the Vt and MH domains, stress remained the only variable that caused deterioration of the results. It is difficult to unequivocally refer to the dominant position of stress in the examined group, especially considering the fact that the sample selection for the study was not random, and it cannot be excluded that it favored more frequent occurrence among respondents distressed over the general GERD patient population[32]. The effect of

Table 2 Effect of selected variables on health-related quality of life measured using SF-36

Variable explained (percent of variability explained[1])	Explanatory variables[2]	Beta	Sig.
PF (41%)	Stress	-0.37	0.000002
	Age	-0.31	0.000097
	BMI	-0.24	0.0022
	GERD Symptoms	-0.15	0.045
RP (36%)	Stress	-0.47	< 0.000001
	BMI	-0.26	0.0006
	GERD Symptoms	-0.18	0.022
BP (29%)	Stress	-0.41	0.000002
	GERD Symptoms	-0.25	0.002
	Sex (1 = M, 2 = F)	-0.17	0.028
GH (37%)	Stress	-0.43	< 0.000001
	Age	-0.31	0.00005
	GERD Symptoms	-0.17	0.028
Vt (45%)	Stress	-0.67	< 0.000001
SF (32%)	Stress	-0.49	< 0.000001
	GERD Symptoms	-0.21	0.010
RE (44%)	Stress	-0.56	< 0.000001
	GERD Symptoms	-0.21	0.004
	BMI	-0.20	0.005
MH (59%)	Stress	-0.77	< 0.000001
PCS (30%)	Stress	-0.29	0.00041
	Age	-0.35	0.000017
	GERD Symptoms	-0.22	0.0061
MCS (53%)	Stress	-0.68	< 0.000001
	GERD Symptoms	-0.13	0.047

[1]Adjusted R square × 100;
[2]Variables: Stress, age, PF and BP were transformed to minimize their skewness. PF: Physical functioning; RP: Physical problems; BP: Bodily pain; GH: General health perceptions; Vt: Vitality; BMI: Body mass index; GERD: Gastro-esophageal reflux disease; SF: Social functioning; RE: Role limitations due to emotional problems; MH: Mental health perceptions; PCS: Physical Component Summary; MCS: Mental Component Summary.

stress on the domains of PF might have been partly an artifact of the method of measuring functioning in this sphere. SF-36 does not measure the actual level of PF, but the subjective self-evaluations of patients. These self-evaluations, under the effect of long-term stress accompanied by low mood and overall self-esteem, might have been subject to a disproportional decrease in actual fitness. The use of objective measures of the quality of PF would be a desired supplementation to the study. Notably, HRQL measurement using SF-36 questionnaire does not consider a several domains of functioning that are potentially important for the quality of life, such as intimate relations and sexual activity. Among patients with GERD, impaired sexual activity and avoidance of intimacy due to the disease is often observed[33]. On the other hand, SF-36 omits a widely-handled spiritual sphere- beliefs and religious activity, participation in culture- reading, interests and artistic activity.

Apart from stress and reflux complaints, increasing BMI had a limited effect on HRQL. This resulted in a decrease in the quality of life in the PF and RP domains. However, it increased the probability of occurrence of situations when emotional disorders lead to problems in relations with others and limitations in the frequency of social contacts (RE). In a survey of more than 3000 adults, Carr and Friedman[34] did not observe any deterioration in the quality of relations with others as BMI increased, except for severely obese people who experienced a higher level of tension and less support in family relations. Nevertheless, in a randomized British study, a negative effect of BMI was confirmed on the level of social functioning of females[35].

Correlation analyses do not allow for conclusions to be drawn concerning the cause-effect relationships between variables. Correlation and regression coefficients provide quantitative estimations of common variability of the analyzed variables, while determination of the directions of relationships between variables is of a non-statistic character and is based mainly on essential knowledge concerning relations in a given domain. Hence, conclusions drawn from correlation analyses do not possess

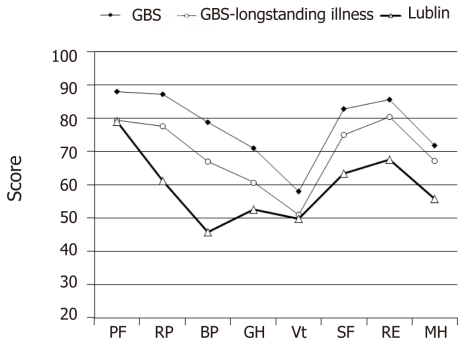

Figure 1 Mean scores for the 8 scales of SF-36 for GB samples and Lublin sample. PF: Physical functioning; RP: Physical problems; BP: Bodily pain; GH: General health perceptions; Vt: Vitality; SF: Social functioning; RE: Role limitations due to emotional problems; MH: Mental health perceptions; GBS: General Practitioner Records held by the Health Authorities for Berkshire, Buckinghamshire, Northamptonshire, and Oxfordshire.

the status of hypotheses, but rather the accuracy of which strengthens the scientific plausibility of the correlations revealed. Properly planned longitudinal studies may provide the ultimate solution.

The level of HRQL in patients with GERD is negatively determined by both the frequency of reflux symptoms and, to an even higher degree, by stress. An increasing BMI, irrespective of reflux symptoms, stress, and age, decreases the level of PF of GERD patients. It also leads to an increase in limitations in functioning ascribed to emotional disorders. The patient's stress level should be considered in diagnosis and therapy, as well as an assessment of treatment progress.

ARTICLE HIGHLIGHTS

Research background

Gastro-esophageal reflux disease (GERD) is a common and serious health problem leading to a decrease in the quality of life of patients. The concept of health-related quality of life (HRQL) covers an expanded effect of the disease on a patient's wellbeing and daily activities. This study evaluates the effect of GERD symptoms and factors that cause decrease in quality of life, such as stress level, age and body weight.

Research motivation

Since GERD leads to a considerable decrease in the quality of life, we conducted an observational study to assess the importance of its impact on the eight domains of life (physical functioning (PF), role limitations due to physical problems, bodily pain (BP), general health perceptions, vitality (Vt), social functioning, role limitations due to emotional problems and mental health perceptions) measured in a generic questionnaire. Moreover, we evaluated the importance of stress, excessive weight and age on the above-mentioned domains.

Research objectives

The research objective was to determine the independent effect of reflux symptoms, age, stress and increasing body mass index (BMI) on the quality of life of patients using the SF-36 questionnaire.

Research methods

A total of 118 patients diagnosed with reflux disease who reported to an outpatient department of gastroenterology or a specialist hospital ward for planned diagnostic tests were recruited. Assessment of the level of reflux was based on five typical GERD symptoms, HRQL was measured by a 36-item Short Form Health Survey and level of stress using the 10-item Perceived Stress Scale. Multi-variable relationships were analyzed using multiple regression. The results of our study were compared with the results obtained in a random sample of 8801 inhabitants of Great Britain drawn from General Practitioner Records held by the Health Authorities for Berkshire, Buckinghamshire, Northamptonshire, and Oxfordshire and the subpopulation of chronically ill patients in this sample.

Research results

In the examined population, the frequency of reflux symptoms resulted in a decrease in patients' results according to six out of eight SF-36 scales-except for mental health and Vt scales. Stress resulted in a decrease in patient function in all domains measured using the SF-36. Age resulted in a decrease in PF and in an overall assessment of self-reported state of health. An increasing BMI exerted a negative effect on physical fitness and limitations in functioning resulting from this decrease. When compared to the GBS group, patients from our study showed a lower

quality of life in all eight life domains. In turn, compared to the GBS-longstanding illness group, they did not significantly differ according to the PF and Vt scales. The largest difference between the quality of the assessed domains was observed for BP, which in the Lublin population occupied the lowest position, lower by 30 scores than in GB sample.

Research conclusions

The level of HRQL in GERD patients is negatively determined by both the frequency of reflux symptoms and, to an even higher degree, by stress. An increasing BMI, irrespective of reflux symptoms, stress, and age, decreases the level of PF of GERD patients. It also leads to an increase in limitations in functioning ascribed to emotional disorders. The patient's stress level should be considered in the diagnosis and therapy, as well as in the assessment of treatment progress.

Research perspectives

In our study, the stress level reported by the patient turned out to be more important for HRQL than the severity of gastroesophageal reflux disease. Future studies assessing the impact of diseases on HRQL should take into account factors that are not symptoms of the disease. Moreover, in assessing the effectiveness of treatment, we should take into account the improvement of HRQL as well as the reduction of disease-related symptoms.

REFERENCES

1 **Orlando RC**. *Reflux esophagitis*. In: Yamada T, Alpers DH, Owyang C, Powell DW, Laine L (eds.). Textbook of gastroenterology. Lippincott Williams Wilkins, Philadelphia 1999; 1235–1263
2 **Reguła J**. Epidemiologia choroby refluksowej w Polsce. Materiały IX Warszawskich Spotkań Gastroenterologicznych. Wydawnictwo Goldprint, Warszawa. 2003; 22-25
3 An evidence-based appraisal of reflux disease management--the Genval Workshop Report. *Gut* 1999; **44** Suppl 2: S1-16 [PMID: 10741335 DOI: 10.1136/gut.44.2008.S1]
4 **Vakil N**, van Zanten SV, Kahrilas P, Dent J, Jones R; Global Consensus Group. The Montreal definition and classification of gastroesophageal reflux disease: a global evidence-based consensus. *Am J Gastroenterol* 2006; **101**: 1900-1920; quiz 1943 [PMID: 16928254 DOI: 10.1111/j.1572-0241.2006.00630.x]
5 **Revicki DA**, Zodet MW, Joshua-Gotlib S, Levine D, Crawley JA. Health-related quality of life improves with treatment-related GERD symptom resolution after adjusting for baseline severity. *Health Qual Life Outcomes* 2003; **1**: 73 [PMID: 14641914 DOI: 10.1186/1477-7525-1-73]
6 **Chmielik A**, Ciszecki J. Assessment of health-related quality of life. *New Medicine* 2004; **3**: 74-76
7 **Marcinkowska M**, Malecka-Panas E. Rola czynników psychologicznych w patogenezie chorób czynnościowych przewodu pokarmowego. *Przew Lek* 2007; **1**: 56-75
8 **Kalinowska E**, Tarnowski W, Banasiewicz J. Metody pomiaru jakości życia u chorych z chorobą refluksową przełyku. *Gastroenterologia Polska* 2005; **12**: 531-536
9 **Jansson C**, Wallander MA, Johansson S, Johnsen R, Hveem K. Stressful psychosocial factors and symptoms of gastroesophageal reflux disease: a population-based study in Norway. *Scand J Gastroenterol* 2010; **45**: 21-29 [PMID: 19961344 DOI: 10.3109/00365520903401967]
10 **Chen M**, Xiong L, Chen H, Xu A, He L, Hu P. Prevalence, risk factors and impact of gastroesophageal reflux disease symptoms: a population-based study in South China. *Scand J Gastroenterol* 2005; **40**: 759-767 [PMID: 16118911 DOI: 10.1080/00365520510015610]
11 **Locke GR**, Talley NJ, Fett SL, Zinsmeister AR, Melton LJ. Risk factors associated with symptoms of gastroesophageal reflux. *Am J Med* 1999; **106**: 642-649 [PMID: 10378622 DOI: 10.1016/S0002-9343(99)00121-7]
12 **Nilsson M**, Johnsen R, Ye W, Hveem K, Lagergren J. Obesity and estrogen as risk factors for gastroesophageal reflux symptoms. *JAMA* 2003; **290**: 66-72 [PMID: 12837713 DOI: 10.1001/jama.290.1.66]
13 **Jansson C**, Nordenstedt H, Wallander MA, Johansson S, Johnsen R, Hveem K, Lagergren J. Severe gastro-oesophageal reflux symptoms in relation to anxiety, depression and coping in a population-based study. *Aliment Pharmacol Ther* 2007; **26**: 683-691 [PMID: 17697202 DOI: 10.1111/j.1365-2036.2007.03411.x]
14 **Nojkov B**, Rubenstein JH, Adlis SA, Shaw MJ, Saad R, Rai J, Weinman B, Chey WD. The influence of co-morbid IBS and psychological distress on outcomes and quality of life following PPI therapy in patients with gastro-oesophageal reflux disease. *Aliment Pharmacol Ther* 2008; **27**: 473-482 [PMID: 18194508 DOI: 10.1111/j.1365-2036.2008.03596.x]
15 **Wright CE**, Ebrecht M, Mitchell R, Anggiansah A, Weinman J. The effect of psychological stress on symptom severity and perception in patients with gastro-oesophageal reflux. *J Psychosom Res* 2005; **59**: 415-424 [PMID: 16310024 DOI: 10.1016/j.jpsychores.2005.05.012]
16 **Kamolz T**, Granderath FA, Bammer T, Pasiut M, Pointner R. Psychological intervention influences the outcome of laparoscopic antireflux surgery in patients with stress-related symptoms of gastroesophageal reflux disease. *Scand J Gastroenterol* 2001; **36**: 800-805 [PMID: 11495073 DOI: 10.1080/00365520117106]
17 **Kalinowska E**. Jakość życia a zaburzenia osobowości u pacjentów z chorobą refluksową przełyku leczonych chirurgicznie. *Postępy Nauk Medycznych* 2007; **20**: 430-438
18 **Farré R**, De Vos R, Geboes K, Verbecke K, Vanden Berghe P, Depoortere I, Blondeau K, Tack J, Sifrim D. Critical role of stress in increased oesophageal mucosa permeability and dilated intercellular spaces. *Gut* 2007; **56**: 1191-1197 [PMID: 17272649 DOI: 10.1136/gut.2006.113688]
19 **El-Serag H**. The association between obesity and GERD: a review of the epidemiological evidence. *Dig Dis Sci* 2008; **53**: 2307-2312 [PMID: 18651221 DOI: 10.1007/s10620-008-0413-9]
20 **Friedenberg FK**, Xanthopoulos M, Foster GD, Richter JE. The association between gastroesophageal reflux disease and obesity. *Am J Gastroenterol* 2008; **103**: 2111-2122 [PMID: 18796104 DOI: 10.1111/j.1572-0241.2008.01946.x]
21 **Hampel H**, Abraham NS, El-Serag HB. Meta-analysis: obesity and the risk for gastroesophageal reflux

disease and its complications. *Ann Intern Med* 2005; **143**: 199-211 [PMID: 16061918 DOI: 10.7326/0003-4819-143-3-200508020-00006]
22 **Jacobson BC**, Somers SC, Fuchs CS, Kelly CP, Camargo CA. Body-mass index and symptoms of gastroesophageal reflux in women. *N Engl J Med* 2006; **354**: 2340-2348 [PMID: 16738270 DOI: 10.1056/NEJMoa054391]
23 **Kouklakis G**, Moschos J, Kountouras J, Mpoumponaris A, Molyvas E, Minopoulos G. Relationship between obesity and gastroesophageal reflux disease as recorded by 3-hour esophageal pH monitoring. *Rom J Gastroenterol* 2005; **14**: 117-121 [PMID: 15990929]
24 **Han TS**, Tijhuis MA, Lean ME, Seidell JC. Quality of life in relation to overweight and body fat distribution. *Am J Public Health* 1998; **88**: 1814-1820 [PMID: 9842379 DOI: 10.2105/AJPH.88.12.1814]
25 **de Oliveira Ferreira N**, Arthuso M, da Silva R, Pedro AO, Pinto Neto AM, Costa-Paiva L. Quality of life in women with postmenopausal osteoporosis: correlation between QUALEFFO 41 and SF-36. *Maturitas* 2009; **62**: 85-90 [PMID: 19100693 DOI: 10.1016/j.maturitas.2008.10.012]
26 **Gülbay BE**, Acican T, Onen ZP, Yildiz OA, Bagçioğlu A, Arslan F, Köse K. Health-related quality of life in patients with sleep-related breathing disorders: relationship with nocturnal parameters, daytime symptoms and comorbid diseases. *Respiration* 2008; **75**: 393-401 [PMID: 17596681 DOI: 10.1159/000104865]
27 **Kalantar-Zadeh K**, Kopple JD, Block G, Humphreys MH. Association among SF36 quality of life measures and nutrition, hospitalization, and mortality in hemodialysis. *J Am Soc Nephrol* 2001; **12**: 2797-2806 [PMID: 11729250 DOI: 10.1089/089277901317203100]
28 **Sforza E**, Janssens JP, Rochat T, Ibanez V. Determinants of altered quality of life in patients with sleep-related breathing disorders. *Eur Respir J* 2003; **21**: 682-687 [PMID: 12762357 DOI: 10.1183/09031936.03.00087303]
29 **Juczyński Z**, Ogińska-Bulik N. *Narzędzia pomiaru stresu i radzenia sobie ze stresem*. Warszawa: Pracownia Testów Psychologicznych 2009;
30 **Jenkinson C**, Stewart-Brown S, Petersen S, Paice C. Assessment of the SF-36 version 2 in the United Kingdom. *J Epidemiol Community Health* 1999; **53**: 46-50 [PMID: 10326053 DOI: 10.1136/jech.53.1.46]
31 **Revicki DA**, Wood M, Maton PN, Sorensen S. The impact of gastroesophageal reflux disease on health-related quality of life. *Am J Med* 1998; **104**: 252-258 [PMID: 9552088 DOI: 10.1016/S0002-9343(97)00354-9]
32 **Lee ML**, Yano EM, Wang M, Simon BF, Rubenstein LV. What patient population does visit-based sampling in primary care settings represent? *Med Care* 2002; **40**: 761-770 [PMID: 12218767 DOI: 10.1097/00005650-200209000-00006]
33 **Liker H**, Hungin P, Wiklund I. Managing gastroesophageal reflux disease in primary care: the patient perspective. *J Am Board Fam Pract* 2005; **18**: 393-400 [PMID: 16148249 DOI: 10.3122/jabfm.18.5.393]
34 **Carr D**, Friedman MA. Body Weight and the Quality of Interpersonal Relationships. *Soc Psychol Q* 2006; **69**: 127-149 [DOI: 10.1177/019027250606900202]
35 **Tyrrell J**, Jones SE, Beaumont R, Astley CM, Lovell R, Yaghootkar H, Tuke M, Ruth KS, Freathy RM, Hirschhorn JN, Wood AR, Murray A, Weedon MN, Frayling TM. Height, body mass index, and socioeconomic status: mendelian randomisation study in UK Biobank. *BMJ* 2016; **352**: i582 [PMID: 26956984 DOI: 10.1136/bmj.i582]

World Journal of Clinical Cases

Submit a Manuscript: https://www.f6publishing.com

World J Clin Cases 2019 June 26; 7(12): 1430-1443

DOI: 10.12998/wjcc.v7.i12.1430

ISSN 2307-8960 (online)

SYSTEMATIC REVIEWS

Non-*albicans Candida* prosthetic joint infections: A systematic review of treatment

Christos Koutserimpas, Stylianos G Zervakis, Sofia Maraki, Kalliopi Alpantaki, Argyrios Ioannidis, Diamantis P Kofteridis, George Samonis

ORCID number: Christos Koutserimpas (0000-0002-1398-9626); Stylianos G Zervakis (0000-0002-8785-3780); Sofia Maraki (0000-0002-8553-0849); Kalliopi Alpantaki (0000-0003-0185-8474); Argyrios Ioannidis (0000-0003-0230-5302); Diamantis P Kofteridis (0000-0001-7603-2592); George Samonis (0000-0001-5857-9703).

Author contributions: Koutserimpas C, Zervakis SG, Alpantaki K and Samonis G designed the research; Zervakis SG, Maraki S and Kofteridis DP performed the research; Koutserimpas C and Ioannidis A contributed new reagents/analytic tools; Koutserimpas C and Ioannidis A analyzed the data; Koutserimpas C, Zervakis SG, Alpantaki K and Samonis G wrote the paper.

Conflict-of-interest statement: The authors declare no conflict of interest.

PRISMA 2009 Checklist statement: PRISMA 2009 Checklist statement is provided.

Christos Koutserimpas, Department of Orthopaedics and Traumatology, "251" Hellenic Air Force General Hospital of Athens, Athens 11525, Greece

Stylianos G Zervakis, Diamantis P Kofteridis, George Samonis, Department of Internal Medicine, University Hospital of Heraklion, Crete, Heraklion 71110, Greece

Sofia Maraki, Department of Clinical Microbiology and Microbial Pathogenesis, University Hospital of Heraklion, Crete, Heraklion 71110, Greece

Kalliopi Alpantaki, Department of Materials Science and Technology, University of Crete, Heraklion, Heraklion 71110, Greece

Argyrios Ioannidis, Department of General Surgery, "Sismanoglion" General Hospital of Athens, Athens 15126, Greece

Corresponding author: Christos Koutserimpas, MD, Doctor, Department of Orthopaedics and Traumatology, "251" Hellenic Air Force General Hospital of Athens, P. Kanellopoulou Av., Athens 11525, Greece. chrisku91@hotmail.com
Telephone: +30-694-8712130

Abstract

BACKGROUND

Non-*albicans Candida* prosthetic joint infections (PJIs) are rare. Optimal treatment involves a two-stage revision surgery in combination with an antifungal agent. However, no clear guidelines have been developed regarding the agent or treatment duration. Hence, a broad range of antifungal and surgical treatments have been reported so far.

AIM

To clarify treatment of non-*albicans Candida* PJIs.

METHODS

A literature review of all existing non-*albicans Candida* PJIs cases through April 2018 was conducted. Information was extracted about demographics, comorbidities, responsible species, duration and type of antifungal treatment, type of surgical treatment, time between initial arthroplasty and symptom onset, time between symptom onset and definite diagnosis, outcome of the infection and follow-up.

RESULTS

A total of 83 cases, with a mean age of 66.3 years, were located. The causative

Manuscript source: Invited manuscript

Received: January 22, 2019
Peer-review started: January 23, 2019
First decision: March 10, 2019
Revised: March 16, 2019
Accepted: April 19, 2019
Article in press: April 19,2019
Published online: June 26, 2019

P-Reviewer: Li J
S-Editor: Ji FF
L-Editor: Filipodia
E-Editor: Xing YX

yeast isolated in most cases was *C. parapsilosis* (45 cases; 54.2%), followed by *C. glabrata* (18 cases; 21.7%). The mean Charlson comorbidity index was 4.4 ± 1.5. The mean time from arthropalsty to symptom onset was 27.2 ± 43 mo, while the mean time from symptom onset to culture-confirmed diagnosis was 7.5 ± 12.5 mo. A two stage revision arthroplasty (TSRA), when compared to one stage revision arthroplasty, had a higher success rate (96% *vs* 73%, $P = 0.023$). Fluconazole was the preferred antifungal agent (59; 71%), followed by amphotericin B (41; 49.4%).

CONCLUSION
The combination of TSRA and administration of prolonged antifungal therapy after initial resection arthroplasty is suggested on the basis of limited data.

Key words: Fungal prosthetic joint infection; Knee arthroplasty infection; Hip arthroplasty infection; Antifungal treatment; Non-*albicans Candida* prosthetic joint infections

Core tip: Non-*albicans Candida* prosthetic joint infections (PJIs) are rare, and no clear guidelines exist regarding the treatment of these infections. The purpose of this study was to clarify, by reviewing current published cases, the treatment options of non-*albicans Candida* PJIs and, possibly, to improve the medical and surgical care of such cases. A literature review of all existing non-*albicans Candida* PJIs cases through April 2018 was conducted. The combination of two stage revision arthroplasty and administration of prolonged antifungal therapy after initial resection arthroplasty is suggested on the basis of limited data.

Citation: Koutserimpas C, Zervakis SG, Maraki S, Alpantaki K, Ioannidis A, Kofteridis DP, Samonis G. Non-*albicans Candida* prosthetic joint infections: A systematic review of treatment. *World J Clin Cases* 2019; 7(12): 1430-1443
URL: https://www.wjgnet.com/2307-8960/full/v7/i12/1430.htm
DOI: https://dx.doi.org/10.12998/wjcc.v7.i12.1430

INTRODUCTION

Prosthetic joint infection (PJI) is a severe complication of joint surgery, involving the joint prostheses and contiguous tissue, representing a main cause of total arthroplasty failure[1]. A plethora of microorganisms have been held responsible for these infections, such as Gram-positive and negative bacteria, while fungal microorganisms are considered rare causes. Fungal PJIs occur in about 1-2% of all cases, while the most common spread type seems to be hematogenous[2].

Optimal treatment is considered the two stage revision surgery in combination with an antifungal agent. However, no clear guidelines have yet been developed regarding the agent and treatment duration. Hence, a broad range of antifungal and surgical treatments have been reported so far[3,4].

Candida spp represent the most common fungal pathogens for PJIs, with *Candida albicans* being the most prevalent species. However, over the last years, the incidence of non-*albicans Candida* PJIs has increased[4,5]. The purpose of this study was to clarify, by reviewing current published cases, the treatment options of non-*albicans Candida* PJIs in order to potentially improve the medical and surgical care of such cases.

MATERIALS AND METHODS

A search of PubMed and MEDLINE databases was performed to identify all existing articles reporting the management of non-*albicans Candida* PJIs cases through April 2018. Isolated and combined terms of "fungal prosthetic joint infection", "fungal arthroplasty infection", "fungal hip arthroplasty infection", "fungal knee arthroplasty infection", "fungal shoulder arthroplasty infection", as well as terms including each non-*albicans Candida* species (*e.g.*, "*candida glabrata* joint infection", "*candida parapsilosis* joint infection, *etc*) were used. The citations in each article were reviewed to locate

additional references that were not retrieved during the initial search.

The present review is limited to papers published in English, peer-reviewed journals. Furthermore, cases without information about management and treatment were excluded. The data extracted from these studies included age, gender, affected joint, responsible non-*albicans Candida* species, duration and type of antifungal treatment, type of surgical treatment, time between initial arthroplasty and symptom onset, time between symptom onset and definite diagnosis (culture), outcome of the infection and follow-up of each case. Charlson Comorbidity score was calculated, when possible, by two independent investigators based on the information provided from each report.

Data were recorded and analyzed using Microsoft Excel 2010 (Microsoft Corporation, Redmond, Washington). Two-sided Fisher's exact tests were used to compare success rates between groups. Statistical analyses were carried out at the 5% level of significance.

RESULTS

Table 1 highlights the findings from the electronic search, covering a 39 year period ending in 2018. A total of 83 non-*albicans Candida* PJIs were identified[4,6-47]. A total of 46 cases (55.4%) were female patients, thirty-six male (43.4%), while in one case the gender was not clarified. The mean age of the study population was 66.3 years [standard deviation (SD) = 10.2]. The affected joint was the knee in 52 cases (62.6%), the hip in 29 (35%) and the shoulder in two (2.4%). Two of the knee prosthetic joint cases were bilateral. The mean Charlson comorbidity index of patients was 4.4 (SD = 1.5).

The mean time from initial arthroplasty implantation surgery to symptom onset was 27.2 mo (SD = 43), while the mean time from symptom onset to culture-confirmed diagnosis was 7.5 mo (SD = 12.5). Regarding the causative non-*albicans Candida* species, the most frequently isolated one was *C. parapsilosis*, found in 45 cases (54.2%), followed by *C. glabrata* in 18 (21.7%), *C. tropicalis* in ten (12%), *C pelliculosa* in three (3.6%) and *C. lusitanae* in two (2.4%), while *C. famata*, *C. lipolytica*, *C. utilis*, *C. guilliermondii* and *C. freyschussii* had caused one case each (1.2%) (Figure 1).

Regarding surgical treatment, in the majority of the described cases (44 cases; 53%) a two stage revision arthroplasty (TSRA) was performed, followed by resection arthroplasty (RA) (18 cases; 22%), one stage revision arthroplasty (OSRA) (eight cases; 9.6%), arthrodesis (five cases; 6%), debridement (three cases; 3.6%) and amputation (two cases; 2.4%). In three cases (3.6%), there was no surgical treatment (Figure 2). TSRA exhibited a success rate of 96%, RA a rate of ≥ 61% [in 7 cases information about the infection outcome was not provided (studies 8, 31, 32, 46, 60, 62, 66 in Table 1)], OSRA a rate of 73%, debridement a rate of 75%, amputation a rate of 100%, while no surgical treatment has shown a success rate of 60%. TSRA when compared to OSRA had a higher success rate (96% *vs* 73%; *P*-value = 0.023).

Regarding the preferred antifungal agent, 38 cases (45.8%) were treated with a single drug, 29 (34.9%) with two, 12 (14.5%) with more than two, while one case did not receive antifungal treatment [(1.2%); case 17 in Table 1; the antifungal agent was not reported in case 32].

Fluconazole was used in most cases [59; (71%), in 31 of them (52.5%) as monotherapy], followed by amphotericin B [41; (49.4%), in 4 (9.8%) as monotherapy], flucytosine [13; (15.7%), in 1 (7.7%) as monotherapy], caspofungin [7; (8.4%), in 1 (14.3%) as monotherapy], voriconazole [7; (8.4%), in 2 (28.6%) as monotherapy], ketoconazole [5; (6%), none as monotherapy], itraconazole [3; (3.6%), none as monotherapy] and anidulafungin [l; (1.2%), not as monotherapy]. The final outcome was successful in 74 cases (89.2%).

The majority of patients with *C. parapsilosis* PJIs were treated with fluconazole [30 cases; (66.7%), in 22 (73.3%) as monotherapy], followed by amphotericin B [19; (42.2%), none as monotherapy], flucytosine [8; (17.8%), in 1 (12.5%) as monotherapy], ketoconazole [3; (6.7%), none as monotherapy], while voriconazole and itraconazole were used in 1 case each (none as monotherapy). Outcome was successful in 40 cases (88.9%).

The majority of cases with *C. glabrata* PJIs were treated with amphotericin B [8; (44.4%), in 1 (12.5%) as monotherapy], followed by fluconazole [7; (38.9%), in 3 (42.9%) as monotherapy]. Caspofungin and voriconazole were used in 5 cases (27.8%) each, in 1 (20%) case each as monotherapy. Furthermore, three (16.7%) patients received flucytosine (none as monotherapy), two (11.1%) itraconazole (none as monotherapy) and one (5.6%) anidulafungin (not as monotherapy). Outcome was successful in 17 cases (94.4%), while one patient (case number 11 in Table 1) passed

Table 1 Non-*albicans Candida* prosthetic joint infection cases

Ref.	Year	Fungus	Gender	Age	Joint	Charlson comorbidity index	Antifungal treatment	Surgical treatment	Treatment duration	Outcome	Follow-up in mo	Time from implantation to symptoms onset in mo	Time from symptoms onset to definite diagnosis by culture, in mo
Koutserimpas *et al*[6]	2018	*C. glabrata*	Female	68	Knee	4	Anidulafungin / Voriconazole	TSRA	28 wk	Successful	-	180	0.5
Geng *et al*[7]	2016	*C. glabrata*	Male	78	Hip	4	Fluconazole / Amphotericin B / Caspofungin	Spacer implantation (failure)/ RA	26 wk	Successful		11	34.8
Klatte *et al*[8]	2014	*C. glabrata*	Female	81	Hip	4	Flucytosine / Amphotericin. B / Fluconazole	OSRA	-	Successful		8	-
Zhu *et al*[9]	2014	*C. glabrata*	Male	44	Hip	-	Amphotericin B / Voriconazole	No	6 wk	Successful	3	-	5
Anagnostakos *et al*[10]	2012	*C. glabrata*	Female	51	Hip	6	Fluconazole	TSRA	6 wk	Successful	70	-	-
Anagnostakos *et al*[10]	2012	*C. glabrata*	Male	78	Hip	6	Fluconazole	TSRA	6 wk	Successful	15	-	-
Bartalesi *et al*[11]	2012	*C. glabrata*	Female	60	Hip	-	Voriconazole / Caspofungin + Amphotericin B	TSRA	6 wk	Successful	48	-	-
Hall *et al*[12]	2012	*C. glabrata*	Female	60	Hip	4	Caspofungin	RA	6 wk	-	-	< 0.5	0.2
Dumaine *et al*[13]	2008	*C. glabrata*	-	72	Knee	5	Caspofungin + Flucytosine / Fluconazole + Flucytosine	Arthrodesis	16 wk	Successful	15	-	-
Lejko-Zupanc *et al*[14]	2005	*C. glabrata*	Male	74	Hip	5	Amphotericin B + Fluconazole / Caspofungin	RA	→ 3 wk	Successful	36	72	-
Fabry *et al*[15]	2005	*C. glabrata*	Female	74	Knee	6	Voriconazole	2x Debridement	32 wk	Death from unrelated causes while on therapy	24	72	-
Gaston *et al*[16]	2004	*C. glabrata*	Female	42	Knee	4	Voriconazole / Amphotericin B	Amputation (above knee)	8 wk	Successful	6	264	-

Açikgöz *et al*[17]	2002	*C. glabrata*	Female	70	Knee	-	Fluconazole	Arthrodesis	-	Successful	7.5	9	6
Ramamo-han *et al*[18]	2001	*C. glabrata*	Female	65	Hip	-	Amphotericin B + Flucytosine	TSRA	7 wk	Successful	24	48	-
Selmon *et al*[19]	1998	*C. glabrata*	Female	75	Knee	5	Amphotericin B/Itraconazole + Fluconazole	OSRA	> 8 wk	Successful	48	84	-
Nayeri *et al*[20]	1997	*C. glabrata*	Female	62	Hip	4	Amphotericin B+ Flucytosine / Itraconazole + Flucytosine	OSRA	11 wk	Successful	22	60	-
Darouiche *et al*[21]	1989	*C. glabrata*	Female	69	Hip	-	Amphotericin B	RA	1 wk	Successful	-	27	0.5
Goodman *et al*[22]	1983	*C. glabrata*	Female	69	Hip	3	-	RA	-	Successful	12	27	-
Geng *et al*[7]	2016	*C. parapsilosis*	Male	67	Knee	3	Fluconazole	TSRA	10 wk	Successful	48	3	-
Wang *et al*[23]	2015	*C. parapsilosis*	Female	67	Knee	4	Fluconazole	TSRA	10 wk	Successful	27	-	-
Wang *et al*[23]	2015	*C. parapsilosis*	Male	74	Knee	5	Fluconazole	TSRA	8 wk	Successful	30	-	-
Wang *et al*[23]	2015	*C. pasapsilosis*	Female	71	Knee	4	Fluconazole	TSRA	6 wk	Successful	62	-	-
Klatte *et al*[8]	2014	*C. parapsilosis*	Male	69	Knee	8	Flucytosine+ Amphotericin. B	OSRAx3 (Failure the first 2 times)	-	Successful	19	1	-
Klatte *et al*[8]	2014	*C. parapsilosis*	Female	82	Knee	4	Flucytosine+ Amphotericin. B	OSRA	-	Successful		2	-
Klatte *et al*[8]	2014	*C. parapsilosis*	Male	46	Knee	1	Flucytosine+ Amphotericin. B	OSRA	-	Successful		6	-
Ueng *et al*[24]	2013	*C. parapsilosis*	Male	62	Knee	4	Fluconazole	TSRA	-	Successful	≥ 24	4.5	1.5
Ueng *et al*[24]	2013	*C. parapsilosis*	Male	77	Knee	-	Fluconazole	TSRA	-	Successful	≥ 24	4	3
Ueng *et al*[24]	2013	*C. parapsilosis*	Male	66	Hip	-	Fluconazole	TSRA	-	Successful	≥ 24	2	1
Ueng *et al*[24]	2013	*C. parapsilosis*	Male	76	Knee	8	Fluconazole	TSRA	-	Successful	≥ 24	33	2
Ueng *et al*[24]	2013	*C. parapsilosis*	Male	36	Knee	-	Fluconazole	TSRA	-	Successful	≥ 24	74	2
Ueng *et al*[24]	2013	*C. parapsilosis*	Male	66	Hip	4	Fluconazole	RA	-	-	-	2	2
Kuiper *et al*[25]	2013	*C. parapsilosis*	Male	58	Hip	-	None	RA/refused further treatment	-	Refused further treatment	8	-	-
Chiu *et al*[26]	2013	*C. parapsilosis*	Male	71	Hip	5	Fluconazole	RA	40 wk	Successful	24	48	-
Hwang *et al*[4]	2012	*C. parapsilosis*	Female	71	Knee	-	Amphotericin B / Fluconazole	TSRA	≥ 6 wk	Successful	46	-	-

Hwang *et al*[4]	2012	*C. parapsilosis*	Female	76	Knee	-	Amphotericin B / Fluconazole	TSRA	≥ 6 wk	Successful	56	-	-
Hwang *et al*[4]	2012	*C. parapsilosis*	Female	76	Knee	-	Amphotericin B / Fluconazole	TSRA	≥ 6 wk	Successful	67	-	-
Hwang *et al*[4]	2012	*C. parapsilosis*	Female	72	Knee	-	Fluconazole	TSRA	≥ 6 wk	Successful	73	-	-
Hwang *et al*[4]	2012	*C. parapsilosis*	Female[1]	61[1]	Bilateral Knee	-	Amphotericin B / Fluconazole	TSRA	≥ 6 wk	Successful	65	-	-
Hwang *et al*[4]	2012	*C. parapsilosis*	Female[1]	61[1]	Bilateral Knee	-	Amphotericin B / Fluconazole	TSRA	≥ 6 wk	Successful	46	-	-
Hwang *et al*[4]	2012	*C. parapsilosis*	Female	67	Knee	-	Amphotericin B / Fluconazole	TSRA	≥ 6 wk	Successful	65	-	-
Hwang *et al*[4]	2012	*C. parapsilosis*	Female	68	Knee	-	Fluconazole,	TSRA	≥ 6 wk	Successful	69	-	-
Hwang *et al*[4]	2012	*C. parapsilosis*	Female	68	Knee	-	Fluconazole,	TSRA	≥ 6 wk	Successful	42	-	-
Hwang *et al*[4]	2012	*C. parapsilosis*	Female	67	Knee	-	Amphotericin B / Fluconazole	TSRA	≥ 6 wk	Successful	49	-	-
Hwang *et al*[4]	2012	*C. parapsilosis*	Female	60	Knee	-	Amphotericin B / Fluconazole	TSRA	≥ 6 wk	Successful	41	-	-
Hwang *et al*[4]	2012	*C. parapsilosis*	Female	73	Knee	-	Amphotericin B / Fluconazole	TSRA	≥ 6 wk	Successful	52	-	-
Anagnostakos *et al*[10]	2012	*C. parapsilosis*	Male	67	Knee	-	Fluconazole	RA	6 wk	-	-	-	-
Dutronc *et al*[27]	2010	*C. parapsilosis*	Male	66	Hip	5	Fluconazole	TSRA	24 wk	Successful	-	0	-
Dutronc *et al*[27]	2010	*C. parapsilosis*	Female	77	Hip	4	Ampotericin B + fluorocytosine / Fluconazole	RA	38 wk	Successful	-	5	-
Antony *et al*[28]	2008	*C. parapsilosis*	Female	67	Shoulder	3	Voriconazole / Fluconazole	TSRA	-	Successful	6	-	-
Antony *et al*[28]	2008	*C. parapsilosis*	Female	67	Hip	3	Fluconazole	TSRA	-	Successful	-	-	-
Yang *et al*[29]	2001	*C. parapsilosis*	Female	68	Knee	3	Fluconazole	TSRA	10 wk	Successful	48	0	16
Bruce *et al*[30]	2001	*C. parapsilosis*	Female	51	Hip	-	Fluconazole	TSRA	-	Successful	84	36	36
Brooks[31]	1998	*C. parapsilosis*	Male	64	Knee	5	Amphotericin B/Fluconazole	Debridement	28 wk	Successful	24	15	4
Wada *et al*[32]	1998	*C. parapsilosis*	Male	77	Knee	4	Fluconazole	Debridement	28 wk	Successful	36	0.5	0.5
Cushing *et al*[33]	1997	*C. parapsilosis*	Female	73	Knee	-	Fluconazole	No	> 24 wk	Successful	12	1	-
Fukasawa *et al*[34]	1997	*C. parapsilosis*	Female	80	Knee	-	Fluconazole	Debridement	53 wk	Successful	24		2

White *et al*[35]	1995	*C. parapsilosis*	Female	64	Knee	-	Fluconazole/Amphotericin B / Itraconazole	RA	20 wk	Successful	-	0	9
Tunkel *et al*[36]	1993	*C. parapsilosis*	Male	37	Knee	6	Amphotericin B / Ketoconazole / Fluconazole	TSRA (Failure) /Amputation (Successful)	-	Successful	7	4	0
Paul *et al*[37]	1992	*C. pasapsilosis*	Male	63	Knee	-	Amphotericin + fluorocytosine / ketoconazole	Arthrodesis	9 wk	Successful	24	3	4
Lim *et al*[38]	1986	*C. parapsilosis*	Male	35	Knee	-	Fluorocytosine	Arthrodesis	-	-	-	0	6
Younkin *et al*[39]	1984	*C. parapsilosis*	Female	75	Hip	-	Fluorocytosine+ Amphotericin B	TSRA	6 wk	Successful	24	0	60
Lichtman[40]	1983	*C. parapsilosis*	Male	59	Shoulder	-	Amphotericin B / ketoconazole	RA	Indefinite (> 58 d)	-	-	20	9
MacGregor *et al*[41]	1979	*C. parapsilosis*	Male	64	Knee	-	Amphotericin B + Fluorocytosine	Non-surgical (failure)/ then RA	21 wk	Successful	12	27	5
Sebastian *et al*[42]	2017	*C. tropicalis*	Male	53	Hip	3	Fluconazole	TSRA	28 wk	Successful	NR	24	0
Reddy *et al*[43]	2013	*C. tropicalis*	Female	62	Knee	3	Fluconazole	TSRA	30 wk	Successful	24	22.5	1.5
Ueng *et al*[24]	2013	*C. tropicalis*	Male	67	Hip	-	Fluconazole	RA	-	-	-	15	1
Lidder *et al*[44]	2013	*C. tropicalis*	Female	76	Hip	-	Amphotericin B	RA	24 wk	Successful	24	36	15
Azam *et al*[45]	2008	*C. tropicalis*	Male	73	Hip	6	Caspofungin / Fluconazole	TSRA	≥ 9 wk, (Caspofungin 1 wk, fluconazole ≥ 8 wk)	Successful	12	108	-
Wyman *et al*[46]	2002	*C. tropicalis*	Male	62	Knee		Fluconazole / Amphotericin B	TSRA	18 wk	Successful	36	0.25	6
Darouiche *et al*[21]	1989	*C. tropicalis*	Male	72	Hip	4	Amphotericin B / ketoconazole	Debridement (failure)/ RA	12 wk	Successful	36	0.5	1
Lambertus *et al*[47]	1988	*C. tropicalis*	Male	61	Hip	3	Amphotericin B	RA	-	Successful	24	6	6
Lambertus *et al*[47]	1988	*C. tropicalis*	Male	65	Hip	-	Amphotericin B / ketoconazole	RA/ arthrodesis	>24 wk	Successful	14	4	4
73.Goodman *et al*[30]	1983	*C. tropicalis*	Female	59	Knee	-	Amphotericin B	TSRA (failure)/ RA	6 wk	Successful	12	3	6
Hwang *et al*[4]	2012	*C. pelliculosa*	Female	67	Knee	-	Fluconazole	TSRA	≥ 6 wk	Successful	56	-	-
Hwang *et al*[4]	2012	*C. pelliculosa*	Female	64	Knee	-	Amphotericin B / fluconazole	TSRA	≥ 6 wk	Successful	35	-	-

Hwang *et al*[4]	2012	*C. pelliculosa*	Male	75	Knee	-	Amphotericin B / fluconazole	TSRA	≥ 6 wk	Successful	34	-	-
Klatte *et al*[8]	2014	*C. lusitaniae*	Male	74	Knee	6	Voriconazole	OSRA	-	Successful		12	-
Hwang *et al*[4]	2012	*C. lusitaniae*	Female	66	Knee	-	Amphotericin B / fluconazole	TSRA	≥ 6 wk	Successful	43	-	-
Hwang *et al*[4]	2012	*C. famata*	Female	83	Knee	-	Amphotericin B / fluconazole	TSRA	≥ 6 wk	Successful	33	-	-
Anagnostakos *et al*[10]	2012	*C. lipolytica*	Male	77	Hip	7	Fluconazole	TSRA	6 wk	Successful	22	-	-
Wang *et al*[23]	2015	*C. utilis*	Female	56	Knee	2	Fluconazole	TSRA	6 wk	Successful	24	-	5
Dutronc *et al*[27]	2010	*C. guillermondii*	Male	76	Knee	4	Amphotericin B+ fluorocytosine / Fluconazole	None	14 wk (2 wkAMB+ 5FC, then 3 mo FZ)	Failure	-	0	-
Geng *et al*[7]	2016	*C. freyschussii*	Female	58	Knee	2	Fluconazole / Caspofungin	TSRA	10 wk	Successful	55	<0.25	

Patient demographics, antifungal treatment, its duration, as well as infection outcome and follow-up period are presented.
[1]Bilateral PJI in the same patient; -: Not reported or unclear. TSRA: Two stage revision arthroplasty; OSRA: One stage revision arthroplasty; RA: Resection arthroplasty.

away from unrelated causes.

The majority of *C. tropicalis* PJIs were treated with amphotericin B [6; (60%), in 3 (50%) as monotherapy], followed by fluconazole [5; (50%), in 3 (60%) as monotherapy], ketoconazole [2; (20%), none as monotherapy] and caspofungin [1; (10%), not as monotherapy]. Outcome was successful in 9 cases (90%; case number 66 in Table 1, treated with fluconazole as monotherapy, did not provide information about outcome).

All patients suffering from *C. pelliculosa* PJI received fluconazole [3 cases; (100%), 1 (33.3%) as monotherapy], while 2 of them (66.7%) received amphotericin B (none as monotherapy). All patients (100%) were treated successfully. Both patients suffering from *C.lusitaniae* were treated successfully. Voriconazole was used as monotherapy in 1 case (50%), while amphotericin B and fluconazole were used in the other.

One patient suffering from *C. famata* was successfully treated with amphotericin B and fluconazole, while fluconazole as monotherapy was successfully used for the treatment of each case of *C. lipolytica* and *C. utilis* PJI. One case of *C. freyschussii* was successfully treated with fluconazole and caspofungin. A case of *C. guilliermondii* infection received amphotericin B, fluorocytosine and fluconazole, however, the result was failure. The mean antifungal treatment duration was 12.8 wk (SD = 10.9), while the mean follow-up of these cases was 33.3 mo (SD = 19.6).

DISCUSSION

Fungal invasive infections, such as PJIs, due to *Candida* species have been acknowledged as a major cause of morbidity and mortality. These infections have been associated with progress in medical modalities, and is some cases have been considered iatrogenic[3,4]. *Candida* PJIs are relative rare, since only case reports or small case series have been reported so far. *Candida albicans* is the most prevalent species. However, the incidence of invasive candidiasis and PJIs due to non-*albicans Candida* is increasing[5,48]. Optimal treatment of these infections remains unclear, since no certain guidelines exist for the antifungal, as well as for the surgical treatments[48]. It is, therefore, of paramount importance to report such cases and to obtain a better understanding of treatment options and outcomes of these infections. The present study is an effort to review, in a systematic way, the non-*albicans Candida* PJI cases

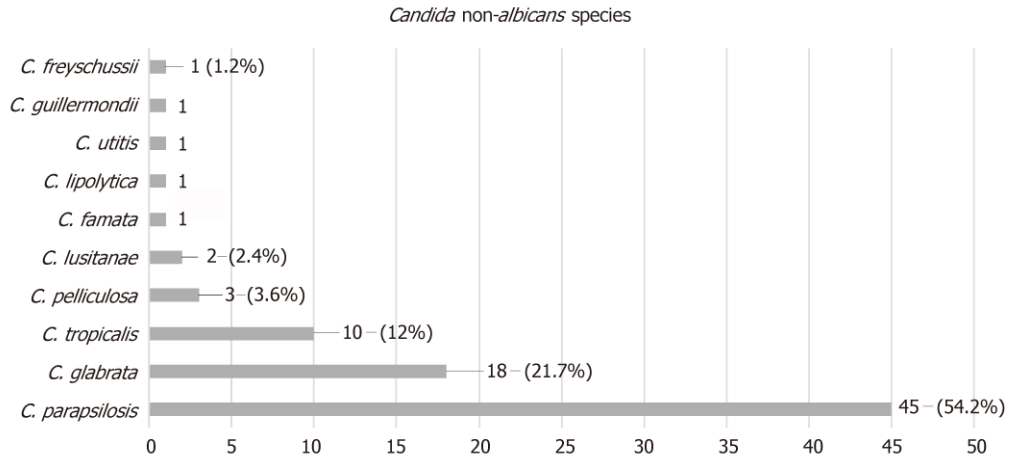

Figure 1 Prosthetic joint infection causative non-*albicans Candida* species.

DISCUSSION

Fungal invasive infections, such as PJIs, due to *Candida* species have been acknowledged as a major cause of morbidity and mortality. These infections have been associated with progress in medical modalities, and is some cases have been considered iatrogenic[3,4]. *Candida* PJIs are relative rare, since only case reports or small case series have been reported so far. *Candida albicans* is the most prevalent species. However, the incidence of invasive candidiasis and PJIs due to non-*albicans Candida* is increasing[5,48]. Optimal treatment of these infections remains unclear, since no certain guidelines exist for the antifungal, as well as for the surgical treatments[48]. It is, therefore, of paramount importance to report such cases and to obtain a better understanding of treatment options and outcomes of these infections. The present study is an effort to review, in a systematic way, the non-*albicans Candida* PJI cases described in the literature. The study focuses on the preferred antifungal agent, the optimal surgical treatment, and the duration of therapy.

The electronic search has revealed a total of 83 patients with non-*albicans Candida* PJI. Their mean age was 66.3 years. Although *Candida* PJI is still considered rare, its incidence is expected to rise, due to the increasing number of joint arthroplasty surgeries performed worldwide[2,48].

Several risk factors have been identified for invasive candidiasis, such as immunosuppression, long-term antimicrobial use and systemic disease[3,4,5,48]. Such a patient profile has been illustrated by the relatively high mean Charlson comorbidity index of the present study's population, found to be 4.4.

Candida PJI is most commonly considered of hematogenous origin[2,6,48]. The mean time between initial arthroplasty surgery and symptomatology onset in the study population was 27.2 mo, while it ranged from immediately after surgery to 264 mo. It is of note that in 13 cases [15.7%; cases 8, 23, 47, 51, 54, 55, 57, 60, 61, 69, 70, 82, 83 (Table 1)] this time was found to be less than 1 mo. Therefore, in these cases the spread should be considered perioperative.

It is also of interest that the mean time between symptomatology onset and definite (culture-based) diagnosis was 7.5 mo, ranging from immediately after onset to 60 mo. This could be attributed to the fact that the main symptoms of *Candida* PJI are non-specific, which mainly include pain and swelling[1-5,48]. The symptomatology onset may be mild, insidious and slowly progressive. Therefore, diagnosis may be delayed due to low suspicion index.

The most frequently isolated non-*albicans Candida* spp was *C. parapsilosis*, found in 45 cases (54.2%), followed by *C. glabrata* in 18 (21.7%), *C. tropicalis* in 10 (12%), *C pelliculosa* in 3 (3.6%), *C. lusitanae* in 2 (2.4%) and 1 case each (1.2%) of PJI caused by *C. famata*, *C. lipolytica*, *C. utitis*, *C. guillermondii* and *C. freyschussii*.

In the present study, *C. parapsilosis* was found to be the predominant pathogen causing PJIs, as compared to other non-*albicans Candida* species. *C. parapsilosis* prevalence has dramatically increased over the last 3 decades. Infections due to this pathogen are more frequently associated with prosthetic devices, indwelling catheters and hyperalimentation solutions. The pathogenesis of the infection depends on the expression of virulence factors, including adherence to host cells and tissues, biofilm formation and secretion of extracellular hydrolytic enzymes[5,49].

The treatment of *C. parapsilosis* PJIs has proven to be successful in 88.9% of the

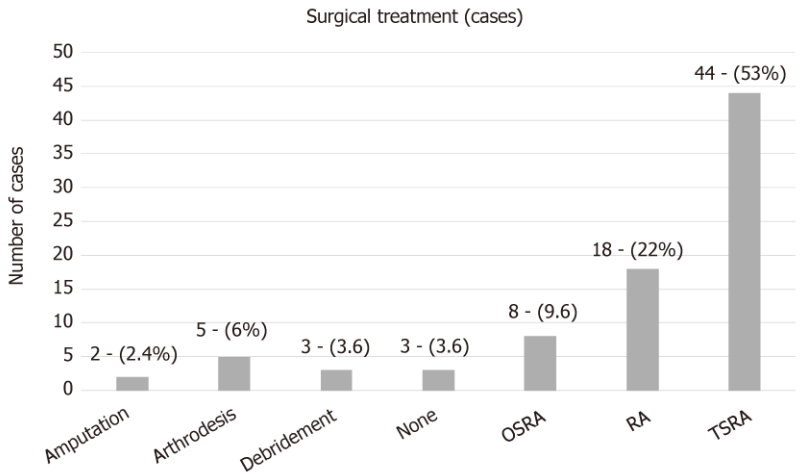

Figure 2 Surgical treatment for non-*albicans Candida* prosthetic joint infection. TSRA: Two stage revision arthroplasty; OSRA: One stage revision arthroplasty; RA: Resection arthroplasty.

studied cases. This is probably due to the fact that echinocandines were not used for the treatment of such cases, taking into account that *C. parapsilosis*' MICs are usually elevated to echinocandins, as compared to other *Candida* spp[50].

Treatment of *C. glabrata* PJIs has been successful in 94.4% of the studied cases. This is probably due to the fact that an azole compound has rarely been used for treatment and, in the limited number of cases when an azole was used, the drug has been given in combination with another antifungal, taking into account that *C. glabrata* is often resistant to azoles[50]. In most cases of *C. tropicalis* PJIs, treatment has been successful, since either single antifungal agents or combinations are known to be effective against this *Candida* spp.

All cases of *C. pelliculosa* PJIs have been treated successfully due to the use of effective agents. *C. lusitaniae* is intrinsically resistant to amphotericin B[50,51]. One case received this agent in combination with fluconazole, while the other one was treated with voriconazole as monotherapy. Hence, finally, the 2 cases caused by *C. lusitanae* were successfully treated.

The cases of *C. famata*, *C. lypolitica* and *C. utilis* were successfully treated with the antifungals given. It is of note that the single case of *C. guillermondii*, although treated with a combination of antifungals, resulted in failure. For successful treatment, it is of the utmost importance to carry out susceptibility testing to obtain accurate MIC values following *Candida* isolation, taking into account that different *Candida* species are characterized by intrinsic resistance to certain antifungal compounds. Regarding the preferred antifungal agent, fluconazole was used in most cases [59; (71%), in 31 of them (52.5%) as monotherapy], followed by amphotericin B [41; (49.4%), in 4 (9.8%) as monotherapy]. Fluconazole has been rarely associated with severe hepatotoxicity. Therefore, liver function tests should be performed regularly during prolonged fluconazole therapy[50,51]. Amphotericin B is an effective broad spectrum agent. However, it is relatively toxic and its side effects, including renal dysfunction, may restrict its long-term use, which is essential in PJI cases[6]. Echinocandines are the most recently developed anti-Candida agents. Although C. parapsilosis strains mostly exhibit high MICs, these agents can often be clinically effective due to their immunomodulatory properties and the fact that they successfully penetrate biofilms[52].

The mean duration of antifungal treatment in the study population was 12.8 wk, while it ranged from 1 to 53 wk. One case (case 32 in Table 1) did not receive any antifungal treatment. Guidelines for the treatment of osteoarticular infections from *Candida* spp exist. However, no clear recommendations are available for the treatment of such PJIs[6,48]. Therefore, the treatment duration is mainly based on the clinical and laboratory findings of each case.

Several options for surgical treatment have also been described. In the study population, in most cases (44 cases; 53%) a TSRA was performed, followed by RA (18 cases; 22%), OSRA (8 cases; 9.6%), arthrodesis (5 cases; 6%), debridement (3 cases; 3.6%) and amputation (2 cases; 2.4%).Three cases did not receive surgical treatment (3.6%; case 4, 55 and 82 in Table 1). RA, arthrodesis, amputation and debridement are usually considered alternative options to arthroplasty exchange. TSRA had a statistically significant higher success rate when compared to OSRA (96% *vs* 73%; *P*-

value = 0.023). Therefore, it seems more proper that TSRA should be considered as the optimal surgical intervention.

The present review has shown that non-*albicans Candida* PJIs represent a dangerous reality. Optimal management consists of a combination of the proper medical antifungal treatment based on susceptibility testing and surgical intervention. Although there have been reports of successful treatment of such cases with OSRA and debridement only, TSRA should be strongly recommended. The combination of TSRA separated by 3–6 mo and a prolonged period of antifungal therapy is suggested on the basis of limited data. Additional issues, such as the duration of antifungal therapy after prosthesis implantation (second stage of the TSRA), as well as the role of antifungal-loaded cement spacers, need to be addressed in order to determine the optimal treatment combinations.

ARTICLE HIGHLIGHTS

Research background

Prosthetic joint infection (PJI) represents a severe complication of joint reconstruction surgery, causing total arthroplasty failure. Many pathogens have been identified in PJIs, such as Gram-positive and negative bacteria, while fungal microorganisms are considered rare causes, occurring in 1-2% of cases. *Candida* spp represent the most common fungal pathogens in these infections, with *Candida albicans* being the most prevalent species. However, the incidence of non-*albicans Candida* PJIs has increased over the last years. Hence, regarding non-*albicans Candida* PJIs, only case reports or small series have been reported so far. Optimal treatment is considered the two stage revision surgery in combination with an antifungal agent. However, no clear guidelines have yet been developed regarding the agent and treatment duration. Hence, a broad range of antifungal and surgical treatments has been reported so far. The present review article represents the first effort of evaluating the reported non-*albicans Candida* PJIs, aiming to clarify the treatment options of these infections and, possibly, to improve the medical and surgical care of such cases.

Research motivation

The absence of clear guidelines regarding fungal PJIs represents a primary issue in managing these infections in clinical practice. A broad range of antifungal and surgical treatments have been reported, while treatment duration remains unclear. Furthermore, due to the limited data regarding these infections, information about patient demographics, responsible non- *albicans Candida* species, time between initial arthroplasty and symptom onset, time between symptom onset and definite diagnosis (culture), and outcome of the infection has not been reported in a systematic way. Hence, it is of utmost importance in the future to report such cases in order to obtain a better understanding about this devastating arthroplasty complication.

Research objectives

The main objective of this study was to clarify, by systematically reviewing current published cases in the literature, the treatment options of non-*albicans Candida* PJIs and, possibly, to improve the medical and surgical care of such cases. During the process of reviewing the literature, it became apparent that information about patient demographics, fungal species, time between initial arthroplasty and symptom onset, time between symptom onset and definite diagnosis (culture), as well as outcome of the infection should also be reported, due to the absence of a systematic review regarding this topic.

Research methods

A meticulous electronic search of PubMed and MEDLINE databases was performed to identify all articles reporting the management of non-*albicans Candida* PJIs cases through April 2018 by two independent investigators. The citations in each article were reviewed to locate additional references that were not retrieved during the initial search. The evaluated parameters were patient demographics and comorbidities, affected joints, responsible non- *albicans Candida* species, duration and type of antifungal treatment, type of surgical treatment, time between initial arthroplasty and symptom onset, time between symptom onset and definite diagnosis (culture), and outcome of the infection. Data were recorded and analyzed using Microsoft Excel 2010 (Microsoft Corporation, Redmond, Washington). Two-sided Fisher's exact tests were used to compare success rates between groups. Statistical analyses were carried out at the 5% level of significance.

Research results

A total of 83 non-*albicans Candida* PJIs were located, with a mean age of 66.3 years (SD = 10.2). The knee was the affected joint in 52 cases (62.6%), the hip in 29 (35%) and the shoulder in 2 (2.4%). The mean time from arthroplasty to symptoms onset was found to be 27.2 mo (SD = 43), while the mean time from symptoms onset to culture-confirmed diagnosis was 7.5 mo (SD = 12.5). The most commonly isolated non-*albicans Candida* species was *C. parapsilosis*, found in 45 cases (54.2%), followed by *C. glabrata* in 18 (21.7%), *C. tropicalis* in 10 (12%), *C pelliculosa* in 3 (3.6%) and *C. lusitanae* in 2 (2.4%), while *C. famata*, *C. lipolytica*, *C. utilis*, *C. guilliermondii* and *C. freyschussii* had caused one case each (1.2%). A two stage revision arthroplasty (TSRA) was performed in most cases (44 cases; 53%), followed by RA (18 cases; 22%), OSRA (8 cases; 9.6%),

arthrodesis (5 cases; 6%), debridement (3 cases; 3.6%) and amputation (2 cases; 2.4%), while 3 cases (3.6%) received no surgical treatment. TSRA when compared to OSRA had a higher success rate (96% *vs* 73%; *P*-value = 0.023). Fluconazole was used in most cases as antifungal treatment [59; (71%), in 31 of them (52.5%) as monotherapy], followed by amphotericin B [41; (49.4%), in 4 (9.8%) as monotherapy], flucytosine [13; (15.7%), in 1 (7.7%) as monotherapy], caspofungin [7; (8.4%), in 1 (14.3%) as monotherapy], voriconazole [7; (8.4%), in 2 (28.6%) as monotherapy], ketoconazole [5; (6%), none as monotherapy], itraconazole [3; (3.6%), none as monotherapy] and anidulafungin [l; (1.2%), none as monotherapy]. The final outcome was successful in 74 cases (89.2%). The mean antifungal treatment duration was 12.8 wk (SD = 10.9), while the mean follow-up of these cases was 33.3 mo (SD = 19.6). The present review has shown that the optimal management of non-*albicans Candida* consists of a combination of the proper medical antifungal treatment and surgical intervention. Although there have been reports of the successful treatment of such cases with OSRA and debridement only, TSRA should be strongly recommended. The combination of TSRA and a prolonged period of antifungal therapy based on susceptibility testing is suggested on the basis of limited data. Additional issues, such as the duration of antifungal therapy after prosthesis implantation (second stage of the TSRA) and the role of antifungal-loaded cement spacers need to be addressed in order to determine an optimal treatment combination.

Research conclusions

The present study is an effort to review, in a systematic way, the non-*albicans Candida* PJI cases described in the literature. The study focuses on the preferred antifungal agent, the optimal surgical treatment, and the duration of therapy. *C. parapsilosis* was found to be the predominant pathogen causing PJIs, as compared to other non-*albicans Candida* species. For successful management of non-*albicans Candida* PJI, susceptibility testing to obtain accurate MIC values should always be performed following the *Candida* isolation, considering that different *Candida* species are characterized by intrinsic resistance to certain antifungal compounds. The mean duration of antifungal treatment in the present review was 12.8 wk, while it ranged from 1 to 53 wk. Although, guidelines for the treatment of osteoarticular infections from *Candida* spp are available, no clear recommendations exist for the treatment of such PJIs. Therefore, the treatment duration is mostly based upon clinical and laboratory findings. In most cases (44 cases; 53%) a TSRA was performed, followed by RA (18 cases; 22%), OSRA (8 cases; 9.6%), arthrodesis (5 cases; 6%), debridement (3 cases; 3.6%) and amputation (2 cases; 2.4%). Three cases did not receive surgical treatment (3.6%). RA, arthrodesis, amputation and debridement are usually considered alternative options to arthroplasty exchange. TSRA when compared to OSRA had a statistically significant higher success rate (96% *vs* 73%; *P*-value= 0.023). Therefore, it seems more proper that TSRA should be considered as the optimal surgical intervention. The present review has shown that the optimal management of non-*albicans Candida* PJIs consists of a combination of the proper medical antifungal treatment based on susceptibility testing and a surgical intervention, while TSRA should be strongly recommended. The combination of TSRA separated by 3–6 mo, in addition to a prolonged period of antifungal therapy, is suggested.

Research perspectives

Non-*albicans Candida* PJIs represent a dangerous reality. The combination of TSRA separated by 3–6 mo and a prolonged period of antifungal therapy is suggested on the basis of limited data. It is of paramount importance to report the treatment of such cases, even the failed ones, in order to obtain a better understanding of these infections and to determine the optimum treatment combination.

REFERENCES

1 **Pulido L**, Ghanem E, Joshi A, Purtill JJ, Parvizi J. Periprosthetic joint infection: the incidence, timing, and predisposing factors. *Clin Orthop Relat Res* 2008; **466**: 1710-1715 [PMID: 18421542 DOI: 10.1007/s11999-008-0209-4]

2 **Schoof B**, Jakobs O, Schmidl S, Klatte TO, Frommelt L, Gehrke T, Gebauer M. Fungal periprosthetic joint infection of the hip: a systematic review. *Orthop Rev (Pavia)* 2015; **7**: 5748 [PMID: 25874063 DOI: 10.4081/or.2015.5748]

3 **Azzam K**, Parvizi J, Jungkind D, Hanssen A, Fehring T, Springer B, Bozic K, Della Valle C, Pulido L, Barrack R. Microbiological, clinical, and surgical features of fungal prosthetic joint infections: a multi-institutional experience. *J Bone Joint Surg Am* 2009; **91** Suppl 6: 142-149 [PMID: 19884422 DOI: 10.2106/JBJS.I.00574]

4 **Hwang BH**, Yoon JY, Nam CH, Jung KA, Lee SC, Han CD, Moon SH. Fungal peri-prosthetic joint infection after primary total knee replacement. *J Bone Joint Surg Br* 2012; **94**: 656-659 [PMID: 22529086 DOI: 10.1302/0301-620X.94B5.28125]

5 **Deorukhkar SC**, Saini S, Mathew S. Virulence Factors Contributing to Pathogenicity of Candida tropicalis and Its Antifungal Susceptibility Profile. *Int J Microbiol* 2014; **2014**: 456878 [PMID: 24803934 DOI: 10.1155/2014/456878]

6 **Koutserimpas C**, Samonis G, Velivassakis E, Iliopoulou-Kosmadaki S, Kontakis G, Kofteridis DP. Candida glabrata prosthetic joint infection, successfully treated with anidulafungin: A case report and review of the literature. *Mycoses* 2018; **61**: 266-269 [PMID: 29272049 DOI: 10.1111/myc.12736]

7 **Geng L**, Xu M, Yu L, Li J, Zhou Y, Wang Y, Chen J. Risk factors and the clinical and surgical features of fungal prosthetic joint infections: A retrospective analysis of eight cases. *Exp Ther Med* 2016; **12**: 991-999 [PMID: 27446310 DOI: 10.3892/etm.2016.3353]

8 **Klatte TO**, Kendoff D, Kamath AF, Jonen V, Rueger JM, Frommelt L, Gebauer M, Gehrke T. Single-stage revision for fungal peri-prosthetic joint infection: a single-centre experience. *Bone Joint J* 2014; **96-**

B: 492-496 [PMID: 24692616 DOI: 10.1302/0301-620X.96B4.32179]
9 **Zhu Y**, Yue C, Huang Z, Pei F. Candida glabrata infection following total hip arthroplasty: A case report. *Exp Ther Med* 2014; **7**: 352-354 [PMID: 24396403 DOI: 10.3892/etm.2013.1420]
10 **Anagnostakos K**, Kelm J, Schmitt E, Jung J. Fungal periprosthetic hip and knee joint infections clinical experience with a 2-stage treatment protocol. *J Arthroplasty* 2012; **27**: 293-298 [PMID: 21752583 DOI: 10.1016/j.arth.2011.04.044]
11 **Bartalesi F**, Fallani S, Salomoni E, Marcucci M, Meli M, Pecile P, Cassetta MI, Latella L, Bartoloni A, Novelli A. Candida glabrata prosthetic hip infection. *Am J Orthop (Belle Mead NJ)* 2012; **41**: 500-505 [PMID: 23431513]
12 **Hall RL**, Frost RM, Vasukutty NL, Minhas H. Candida glabrata: an unusual fungal infection following a total hip replacement. *BMJ Case Rep* 2012; **2012** [PMID: 23008369 DOI: 10.1136/bcr-2012-006491]
13 **Dumaine V**, Eyrolle L, Baixench MT, Paugam A, Larousserie F, Padoin C, Tod M, Salmon D. Successful treatment of prosthetic knee Candida glabrata infection with caspofungin combined with flucytosine. *Int J Antimicrob Agents* 2008; **31**: 398-399 [PMID: 18242959 DOI: 10.1016/j.ijantimicag.2007.12.001]
14 **Lejko-Zupanc T**, Mozina E, Vrevc F. Caspofungin as treatment for Candida glabrata hip infection. *Int J Antimicrob Agents* 2005; **25**: 273-274 [PMID: 15737527 DOI: 10.1016/j.ijantimicag.2005.01.005]
15 **Fabry K**, Verheyden F, Nelen G. Infection of a total knee prosthesis by Candida glabrata: a case report. *Acta Orthop Belg* 2005; **71**: 119-121 [PMID: 15792220]
16 **Gaston G**, Ogden J. Candida glabrata periprosthetic infection: a case report and literature review. *J Arthroplasty* 2004; **19**: 927-930 [PMID: 15483812 DOI: 10.1016/j.arth.2004.04.012]
17 **Açikgöz ZC**, Sayli U, Avci S, Doğruel H, Gamberzade S. An extremely uncommon infection: Candida glabrata arthritis after total knee arthroplasty. *Scand J Infect Dis* 2002; **34**: 394-396 [PMID: 12069030 DOI: 10.1080/00365540110080232]
18 **Ramamohan N**, Zeineh N, Grigoris P, Butcher I. Candida glabrata infection after total hip arthroplasty. *J Infect* 2001; **42**: 74-76 [PMID: 11243760 DOI: 10.1053/jinf.2000.0763]
19 **Selmon GP**, Slater RN, Shepperd JA, Wright EP. Successful 1-stage exchange total knee arthroplasty for fungal infection. *J Arthroplasty* 1998; **13**: 114-115 [PMID: 9493549 DOI: 10.1016/S0883-5403(98)90086-9]
20 **Nayeri F**, Cameron R, Chryssanthou E, Johansson L, Söderström C. Candida glabrata prosthesis infection following pyelonephritis and septicaemia. *Scand J Infect Dis* 1997; **29**: 635-638 [PMID: 9571751 DOI: 10.3109/00365549709035912]
21 **Darouiche RO**, Hamill RJ, Musher DM, Young EJ, Harris RL. Periprosthetic candidal infections following arthroplasty. *Rev Infect Dis* 1989; **11**: 89-96 [PMID: 2916098 DOI: 10.1093/clinids/11.1.89]
22 **Goodman JS**, Seibert DG, Reahl GE, Geckler RW. Fungal infection of prosthetic joints: a report of two cases. *J Rheumatol* 1983; **10**: 494-495 [PMID: 6684169]
23 **Wang QJ**, Shen H, Zhang XL, Jiang Y, Wang Q, Chen YS, Shao JJ. Staged reimplantation for the treatment of fungal peri-prosthetic joint infection following primary total knee arthroplasty. *Orthop Traumatol Surg Res* 2015; **101**: 151-156 [PMID: 25676891 DOI: 10.1016/j.otsr.2014.11.014]
24 **Ueng SW**, Lee CY, Hu CC, Hsieh PH, Chang Y. What is the success of treatment of hip and knee candidal periprosthetic joint infection? *Clin Orthop Relat Res* 2013; **471**: 3002-3009 [PMID: 23633184 DOI: 10.1007/s11999-013-3007-6]
25 **Kuiper JW**, van den Bekerom MP, van der Stappen J, Nolte PA, Colen S. 2-stage revision recommended for treatment of fungal hip and knee prosthetic joint infections. *Acta Orthop* 2013; **84**: 517-523 [PMID: 24171675 DOI: 10.3109/17453674.2013.859422]
26 **Chiu WK**, Chung KY, Cheung KW, Chiu KH. Candida parapsilosis total hip arthroplasty infection: case report and literature review. *J Orthop Trauma* 2013; **17**: 33-36 [DOI: 10.1016/j.jotr.2012.04.008]
27 **Dutronc H**, Dauchy FA, Cazanave C, Rougie C, Lafarie-Castet S, Couprie B, Fabre T, Dupon M. Candida prosthetic infections: case series and literature review. *Scand J Infect Dis* 2010; **42**: 890-895 [PMID: 20608769 DOI: 10.3109/00365548.2010.498023]
28 **Antony S**, Dominguez D C, Jackson J, Misenheimer G. *Evaluation and treatment of candida species in prosthetic joint infections. Infect Dis Clin Pract* 2008; 354-359 [DOI: 10.1097/IPC.0b013e31817cfdb7]
29 **Yang SH**, Pao JL, Hang YS. Staged reimplantation of total knee arthroplasty after Candida infection. *J Arthroplasty* 2001; **16**: 529-532 [PMID: 11402423 DOI: 10.1054/arth.2001.21458]
30 **Bruce AS**, Kerry RM, Norman P, Stockley I. Fluconazole-impregnated beads in the management of fungal infection of prosthetic joints. *J Bone Joint Surg Br* 2001; **83**: 183-184 [PMID: 11284561 DOI: 10.1302/0301-620X.83B2.0830183]
31 **Brooks DH**, Pupparo F. Successful salvage of a primary total knee arthroplasty infected with Candida parapsilosis. *J Arthroplasty* 1998; **13**: 707-712 [PMID: 9741450 DOI: 10.1016/S0883-5403(98)80017-X]
32 **Wada M**, Baba H, Imura S. Prosthetic knee Candida parapsilosis infection. *J Arthroplasty* 1998; **13**: 479-482 [PMID: 9645532 DOI: 10.1016/S0883-5403(98)90019-5]
33 **Cushing RD**, Fulgenzi WR. Synovial fluid levels of fluconazole in a patient with Candida parapsilosis prosthetic joint infection who had an excellent clinical response. *J Arthroplasty* 1997; **12**: 950 [PMID: 9458262 DOI: 10.1016/S0883-5403(97)90166-2]
34 **Fukasawa N**, Shirakura K. Candida arthritis after total knee arthroplasty--a case of successful treatment without prosthesis removal. *Acta Orthop Scand* 1997; **68**: 306-307 [PMID: 9247001 DOI: 10.3109/17453679708996709]
35 **White A**, Goetz MB. Candida parapsilosis prosthetic joint infection unresponsive to treatment with fluconazole. *Clin Infect Dis* 1995; **20**: 1068-1069 [PMID: 7795057 DOI: 10.1093/clinids/20.4.1068]
36 **Tunkel AR**, Thomas CY, Wispelwey B. Candida prosthetic arthritis: report of a case treated with fluconazole and review of the literature. *Am J Med* 1993; **94**: 100-103 [PMID: 8420285 DOI: 10.1016/0002-9343(93)90127-B]
37 **Paul J**, White SH, Nicholls KM, Crook DW. Prosthetic joint infection due to Candida parapsilosis in the UK: case report and literature review. *Eur J Clin Microbiol Infect Dis* 1992; **11**: 847-849 [PMID: 1468427 DOI: 10.1007/BF01960889]
38 **Lim EV**, Stern PJ. Candida infection after implant arthroplasty. A case report. *J Bone Joint Surg Am* 1986; **68**: 143-145 [PMID: 3510212 DOI: 10.2106/00004623-198668010-00020]
39 **Younkin S**, Evarts CM, Steigbigel RT. Candida parapsilosis infection of a total hip-joint replacement: successful reimplantation after treatment with amphotericin B and 5-fluorocytosine. A case report. *J Bone Joint Surg Am* 1984; **66**: 142-143 [PMID: 6690437 DOI: 10.2106/00004623-198466010-00023]
40 **Lichtman EA**. Candida infection of a prosthetic shoulder joint. *Skeletal Radiol* 1983; **10**: 176-177 [PMID: 6635692 DOI: 10.1007/BF00357775]

41 **MacGregor RR**, Schimmer BM, Steinberg ME. Results of combined amphotericin B-5-fluorcytosine therapy for prosthetic knee joint infected with Candida parapsilosis. *J Rheumatol* 1979; **6**: 451-455 [PMID: 392095]

42 **Sebastian S**, Malhotra R, Pande A, Gautam D, Xess I, Dhawan B. Staged Reimplantation of a Total Hip Prosthesis After Co-infection with Candida tropicalis and Staphylococcus haemolyticus: A Case Report. *Mycopathologia* 2018; **183**: 579-584 [PMID: 28735470 DOI: 10.1007/s11046-017-0177-x]

43 **Reddy KJ**, Shah JD, Kale RV, Reddy TJ. Fungal prosthetic joint infection after total knee arthroplasty. *Indian J Orthop* 2013; **47**: 526-529 [PMID: 24133317 DOI: 10.4103/0019-5413.118213]

44 **Lidder S**, Tasleem A, Masterson S, Carrington RW. Candida tropicalis: diagnostic dilemmas for an unusual prosthetic hip infection. *J R Army Med Corps* 2013; **159**: 123-125 [PMID: 23720596 DOI: 10.1136/jramc-2013-000053]

45 **Azam A**, Singh PK, Singh VK, Siddiqui A. A Rare Case of Candida Tropicalis Infection of a Total Hip Arthroplasty: A Case Report and Review of Literature. *MOJ* 2008; **2**: 43-46 [DOI: 10.5704/MOJ.0811.011]

46 **Wyman J**, McGough R, Limbird R. Fungal infection of a total knee prosthesis: successful treatment using articulating cement spacers and staged reimplantation. *Orthopedics* 2002; **25**: 1391-4; discussion 1394 [PMID: 12502204 DOI: 10.1007/s00132-002-0391-0]

47 **Lambertus M**, Thordarson D, Goetz MB. Fungal prosthetic arthritis: presentation of two cases and review of the literature. *Rev Infect Dis* 1988; **10**: 1038-1043 [PMID: 3055186 DOI: 10.1093/clinids/10.5.1038]

48 **Pappas PG**, Kauffman CA, Andes DR, Clancy CJ, Marr KA, Ostrosky-Zeichner L, Reboli AC, Schuster MG, Vazquez JA, Walsh TJ, Zaoutis TE, Sobel JD. Executive Summary: Clinical Practice Guideline for the Management of Candidiasis: 2016 Update by the Infectious Diseases Society of America. *Clin Infect Dis* 2016; **62**: 409-417 [PMID: 26810419 DOI: 10.1093/cid/civ1194]

49 **Trofa D**, Gácser A, Nosanchuk JD. Candida parapsilosis, an emerging fungal pathogen. *Clin Microbiol Rev* 2008; **21**: 606-625 [PMID: 18854483 DOI: 10.1128/CMR.00013-08]

50 **Sanguinetti M**, Posteraro B, Lass-Flörl C. Antifungal drug resistance among Candida species: mechanisms and clinical impact. *Mycoses* 2015; **58** Suppl 2: 2-13 [PMID: 26033251 DOI: 10.1111/myc.12330]

51 **Pasternak B**, Wintzell V, Furu K, Engeland A, Neovius M, Stephansson O. Oral Fluconazole in Pregnancy and Risk of Stillbirth and Neonatal Death. *JAMA* 2018; **319**: 2333-2335 [PMID: 29896619 DOI: 10.1001/jama.2018.6237]

52 **Dimopoulou D**, Hamilos G, Tzardi M, Lewis RE, Samonis G, Kontoyiannis DP. Anidulafungin versus caspofungin in a mouse model of candidiasis caused by anidulafungin-susceptible Candida parapsilosis isolates with different degrees of caspofungin susceptibility. *Antimicrob Agents Chemother* 2014; **58**: 229-236 [PMID: 24145540 DOI: 10.1128/AAC.01025-13]

World Journal of Clinical Cases

Submit a Manuscript: https://www.f6publishing.com

World J Clin Cases 2019 June 26; 7(12): 1444-1455

DOI: 10.12998/wjcc.v7.i12.1444

ISSN 2307-8960 (online)

META-ANALYSIS

Relationship between circulating irisin levels and overweight/obesity: A meta-analysis

Jue Jia, Fan Yu, Wei-Ping Wei, Ping Yang, Ren Zhang, Yue Sheng, Yong-Qin Shi

ORCID number: Jue Jia (0000-0003-1871-5015); Fan Yu (0000-0003-2009-3702); Wei-Ping Wei (0000-0002-2774-0354); Ping Yang (0000-0003-3555-847X); Ren Zhang (0000-0003-4783-5243); Yue Sheng (0000-0002-4001-6993); Yong-Qin Shi (0000-0002-7334-3130).

Author contributions: Jia J conceived and designed the study; Jia J, Yu F, and Zhang R searched the related articles; Yang P, Wei WP, Sheng Y, and Shi YQ analyzed the data; Jia J and Yu F wrote the manuscript; all authors read and approved the final manuscript.

Supported by the National Natural Science Foundation of China, No. 81500351; the Youth Medical Talent Project of Jiangsu Province, No. QNRC2016842; the Jiangsu University Affiliated Hospital "; 5123"; Talent Plan, No. 51232017305; and the 169 Talent Project of Zhenjiang.

Conflict-of-interest statement: The authors deny any conflict of interest.

PRISMA 2009 Checklist statement: The authors have read the PRISMA 2009 Checklist, and the manuscript was prepared and revised according to the PRISMA 2009 Checklist.

Jue Jia, Fan Yu, Wei-Ping Wei, Ping Yang, Yue Sheng, Yong-Qin Shi, Affiliated Hospital of Jiangsu University, Zhenjiang 212001, Jiangsu Province, China

Ren Zhang, Department of Library of Jiangsu University, Zhenjiang 212001, Jiangsu Province, China

Corresponding author: Jue Jia, MD, Lecturer, Associate Chief Physician, Affiliated Hospital of Jiangsu University, No. 438, Jiefang North Road, Jingkou District, Zhenjiang 212001, Jiangsu Province, China. 1000011436@ujs.edu.cn
Telephone: +86-511-85031120
Fax: +86-511-85019237

Abstract

BACKGROUND

Currently, the findings about irisin as a novel myokine related to obesity are inconsistent in overweight/obese people. To our knowledge, no systematic analysis has been conducted to evaluate the relationship between irisin levels and overweight/obesity.

AIM

To evaluate the association between circulating irisin levels and overweight/obesity.

METHODS

The Cochrane Library, MEDLINE, SCOPUS, and the ISI Web of Science were searched to retrieve all of the studies associated with circulating irisin levels and overweight/obesity. Standard mean difference values and 95% confidence intervals (CI) were estimated and pooled using meta-analysis methodology.

RESULTS

A total of 18 studies were included in our meta-analysis containing 1005 cases and 1242 controls. Our analysis showed that the circulating irisin level in overweight/obese people was higher than that in overall healthy controls (random effects MD = 0.63; 95%CI: 0.22-1.05; $P = 0.003$). In the subgroup analysis by ethnicity, the irisin level was higher in overweight/obesity people than that in controls in Africa (random effects MD = 3.41; 95%CI: 1.23-5.59; $P < 0.05$) but not in European, Asian, or American populations. In addition, in a subgroup analysis by age, the results showed that obese children exhibited a higher irisin level than controls (random effects MD = 0.86; 95%CI: 0.28-1.43; $P < 0.05$).

CONCLUSION

Manuscript source: Invited manuscript

Received: February 25, 2019
Peer-review started: February 26, 2019
First decision: April 18, 2019
Revised: April 27, 2019
Accepted: May 2, 2019
Article in press: May 2, 2019
Published online: June 26, 2019

P-Reviewer: Avtanski D, Hosseinpour-Niazi S
S-Editor: Ji FF
L-Editor: Wang TQ
E-Editor: Liu JH

This meta-analysis provides evidence that circulating irisin is higher in obese individuals compared to healthy controls and it is important to identify the relationship between circulating irisin levels and overweight/obesity in predicting overweight/obesity.

Key words: Irisin; Overweight/obesity; Myokines; Body mass index

Core tip: This study is the first meta-analysis that systematically assessed circulating irisin in overweight/obese people. This meta-analysis showed that circulating irisin levels were higher in obese individuals than in healthy controls. It also suggested that circulating irisin levels were higher in obese people in Africa than in controls. This meta-analysis further suggested that obese children exhibited a higher irisin level than controls.

Citation: Jia J, Yu F, Wei WP, Yang P, Zhang R, Sheng Y, Shi YQ. Relationship between circulating irisin levels and overweight/obesity: A meta-analysis. *World J Clin Cases* 2019; 7(12): 1444-1455
URL: https://www.wjgnet.com/2307-8960/full/v7/i12/1444.htm
DOI: https://dx.doi.org/10.12998/wjcc.v7.i12.1444

INTRODUCTION

The definition of obesity is the increase of fat mass which could cause serious health problems[1]. Guidelines of obesity treatment defined that body mass index (BMI) ≥ 25 is overweight and greater than 30 is obesity in adults. For children, age needs to be considered when defining overweight and obesity[2]. Over the past three decades, obesity has been a worldwide epidemic and a serious threat to human health for the steady rising of global obesity rate as well as no-declined prevalence rates[3]. Accumulating evidence suggests that overweight/obesity has been identified as an independent risk factor for chronic diseases, including metabolic syndrome, cardiovascular disease, and diabetes mellitus, leading to a negative effect on health-related quality of life and a heavy pressure on the health care system[4-6]. Hence, identification of overweight/obesity-oriented factors that are potential biomarkers that could be used to predict obesity and related complications is important.

It is well known that muscle tissues can secrete some cytokines and other peptides named myokines that are essential for maintaining metabolic homeostasis[7]. Irisin is a novel myokine produced by proteolytical cleavage of fibronectin type III domain-containing 5 (FNDC5) both in mice and humans, and it can also be secreted by adipose tissue and the liver in a small amounts[8]. Recent meta-analysis reported that circulating irisin levels were associated with polycystic ovary syndrome and coronary artery diseases[9,10], and it was considered a critical myokine related to body metabolism. Interestingly, irisin can promote white adipose tissue browning, which dissipates energy to produce heat and decreases the appearance of cellulite[11]. Recently, a growing number of studies suggested that circulating irisin levels in plasma or serum may be related to overweight/obesity in different groups of people[7]; however, this relationship remains controversial due to conflicting results that have been reported[12-18]. A clinical study involving 94 obese patients who participated in a weight loss program showed that obese subjects had a higher circulating irisin level than controls[12]. These findings are consistent with other studies[13-16]. Puzzlingly, although most studies support a role for irisin in forecasting obesity, several studies do not have a consistent trend and concluded that circulating irisin levels were lower in the obese group compared to the control group[17-19]. Moreover, in obese *vs* healthy children, boys, or girls, results regarding circulating irisin were also incompatible[20-22].

To our knowledge, no systematic analysis has been conducted to evaluate the relationship between irisin levels and overweight/obesity. As a result, the objective of this study was to analyze all of the available data to perform a quantitative assessment of the association and deepen our understanding of the role of circulating irisin levels in the development of obesity *via* a meta-analysis.

MATERIALS AND METHODS

Search strategies

Databases including the Cochrane Library, PUBMED, and the ISI Web of Science were searched in English to identify studies published up to April 1, 2018, which addressed both irisin and overweight/obesity. Our overall search terms were irisin OR frcp2 OR fibronectin type III domain containing protein 5 OR fndc5 AND fat OR MS OR metabolic syndrome OR overweight/obesity. The reference lists of identified articles were also reviewed for more studies.

Selection criteria

To be considered for the meta-analysis, the studies had to be case-control or cohort studies that reported irisin levels in overweight/obese patients compared with healthy controls regardless of age or gender. We incorporated overweight into the obese group. Conference abstracts were also included if they contained sufficient information to extract effect estimates. Literature reviews, articles of research on the drug, articles in which the mean and standard deviation (SD) could not be calculated, and studies with no healthy control group were excluded.

Data extraction

The titles and abstracts of all eligible studies were reviewed by two authors independently. To settle disagreements, a third author was consulted. The following information was collected from each study: The first author, publication year, study design, study location, numbers of cases and controls, age, BMI, types of blood sample, assays for irisin measurement, study quality, and circulating irisin levels (means and standard deviations).

Data synthesis and analysis

The primary variables, circulating irisin levels in patients with obesity, were reported as standard mean differences (SMD) and the corresponding 95% confidence intervals (CIs). The SMD for circulating irisin levels were calculated for all of the studies that were identified for the meta-analysis, and the results were combined using fixed- or random-effects modeling, as appropriate. Publication bias was assessed using Begg's funnel plot and Egger's test[22,23]. Heterogeneity in the results of the different studies was examined using χ^2 tests for significance (a P-value < 0.1 was considered statistically significant) and the I^2 test (I^2 > 50%: significant heterogeneity; I^2 < 25%: insignificant heterogeneity), which can be interpreted as the percentage of total variation across several studies owing to heterogeneity[24,25]. A sensitivity analysis was performed to assess whether the summary results had been significantly influenced by removing one study that investigated the association between circulating irisin levels and obesity. Subgroup analyses were conducted by geographic area and age. All statistical analyses were performed with Review Manager 5.2 and Stata version 11.0. P < 0.05 was considered statistically significant.

RESULTS

Description of the studies

The literature search identified 1295 possible relevant articles. From these, 507 were duplicates, 788 were excluded after reading the title or abstract for obvious irrelevance, and 51 were finally included for further full-text evaluation. Of the 51 articles, five were excluded because they were reviews. Fifteen articles were excluded because they did not include healthy controls. Eight articles were excluded because data were represented by the median. Five articles were excluded because they did not contain detailed data. Finally, a total of 18 studies (1005 cases and 1242 controls) were included in our meta-analysis.

Figure 1 displays the flow chart describing the process of study inclusion/exclusion. Among the 18 studies, six were conducted in Europe, six in Asia, four in America, and two in Africa. The main characteristics of the included studies are presented in Table 1. Serum samples were used in 11 studies for irisin measurement, while plasma samples were used in the others. The sample size for each study ranged from 10 to 618. All of the irisin levels were measured with ELISA kits.

There were nine studies utilizing irisin ELISA kits from Phoenix Pharmaceuticals (Burlingame, CA, United States), three from BioVendor (Brno, Czech Republic), two from Bio Vision (Milpitas, United States), and one each from CUSABIO Life Science (Wuhan, China), Bioscience (Santa Clara, California, United States), Mercodia AB (Uppsala, Sweden), and MyBioSource (San Diego, United States). The details of

Table 1 Characteristics of included studies

Ref.	Country	Blood sample	Participants' age, years (case-control)	Cases/controls, *n*	Irisin assay	BMI (kg/m²) (case-control)	ELISA kit
Moreno-Navarrete *et al*[7], 2013	Spain	Plasma	52.41 ± 10.99-47.28 ± 10.15	51/18	ELISA	28.98 ± 3.17-23.33 ± 1.2	SK00170-01; Aviscera Bioscience Inc, Santa Clara, California
Stengel *et al*[13], 2013	Germany	Plasma	47.17 ± 11.91-48.5 ± 12.16	24/8	ELISA	50.63 ± 15.27-22.6 ± 2.55	Phoenix Pharmaceuticals, Inc., Burlingame, CA, United States
Crujeiras *et al*[12], 2014	Spain	Plasma	49.4 ± 9.4-35.71 ± 8.8	94/48	ELISA	35.6 ± 4.5-22.9 ± 2.2	Mercodia, AB (Uppsala, Sweden)
Hou *et al*[18], 2015	China	Serum	33 ± 9-31 ± 7	41/40	ELISA	30.8 ± 3.8-21.3 ± 1.8	Phoenix Pharmaceuticals, Inc., Burlingame, CA, United States
Palacios-González *et al*[20], 2015	Mexico	Serum	9.07 ± 0.88-9.0 ± 0.86	60/25	ELISA	-0.25 ± 0.67-2.11 ± 0.77[1]	CUSA-BIO BIOTECH
Viitasalo *et al*[26], 2016[26]	Finland	Plasma	7.71 ± 0.4-7.6 ± 0.4	55/388	ELISA	20.21 ± 1.52-15.5 ± 1.3	Phoenix Pharmaceuticals, Inc., Burlingame, CA, United States
Belviranli *et al*[17], 2016	Turkey	Plasma	34.40 ± 10.60-28.70 ± 6.82	10/10	ELISA	32.65 ± 3.04-23.00 ± 2.23	BioVendor, Czech Republic
Chen *et al*[14], 2016	China	Serum	34.4 ± 7.6-32.8 ± 7.8	30/20	ELISA	33.3 ± 4.2-21.1 ± 2.0	PHOENIX PHARMACEUTICAL
Fagundo *et al*[15], 2016	Spain	Plasma	44.49 ± 11.50-29.04 ± 6.22	65/49	ELISA	42.83 ± 6.63-21.61 ± 1.54	EK-067-52; Phoenix Pharmaceuticals, INC, CA
Mehrabian *et al*[27], 2016	Iran	Serum	28.76 ± 4.67-29.23 ± 4.50	38/26	ELISA	22.26 ± 1.23-20.88 ± 1.28	Biovendor, Laboratory Medicine, Modrice Czech Republic
Rizk *et al*[28], 2016	Egypt	Serum	45.45 ± 8.30-44.25 ± 10.46	20/20	ELISA	32.54 ± 1.80-22.85 ± 1.68	BioVendor, Bmo, Czechrepublic (cat. No. RAG018R)
Shoukry *et al*[29], 2016	Egypt	Serum	47.06 ± 4.76-45.12 ± 4.72	119/31	ELISA	34.72 ± 5.68-23.27 ± 0.50	BioVision, Milpitas, CA
Elizondo-Montemayor *et al*[21], 2017	Mexico	Plasma	8.0 (6–11)-8.5 (6-12)	5/5	ELISA	98 (98-99)-66 (35-73)	Phoenix Pharmaceuticals, Inc., Burlingame, CA, United States
Jang *et al*[30], 2017	South Korea	Serum	13.7 ± 0.7-13.5 ± 0.5	248/370	ELISA	31.4 ± 3.8-19.4 ± 1.5	Cat#EK-067-52; Phoenix, Pharmaceuticals, Belmont, CA
Liu *et al*[19], 2017	China	Serum	35.20 ± 6.51-35.01 ± 7.09	51/75	ELISA	27.80 ± 3.04-22.62 ± 2.52-	Bio Vision, Milpitas, CA95035, United States
Nigro *et al*[22], 2017	Italy	Serum	9.7 ± 2.7-8 ± 2.4	27/13	ELISA	2.7 ± 0.5-—0.46 ± 1.2	Phoenix Pharmaceuticals, Belmont, CA, United States
Tibana *et al*[16], 2017	Brazil	Serum	66.5 ± 5.0-68.0 ± 6.2	26/23	ELISA	30.9 ± 3.1-24.3 ± 3.6	MyBioSource Inc., San Diego, CA, United States

Sahin-Efe *et al*[31], 2018	United States	Serum	69.4 ± 8.6-69.5 ± 9.2	41/73	ELISA	30.5 (29.6–31.5)-24.0 (23.3–24.7)	CAT#EK-067-52; Phoenix Pharmaceuticals, Burlingame, CA

[1]BMI z-score. Data are presented as the mean ± SD for continuous parametric variables or median (interquartile range) for continuous nonparametric variables. ELISA: Enzyme-linked immunosorbent assay.

characteristics related to the included studies are shown in Table 1.

Main analysis

A meta-analysis of 18 studies involving a total of 2247 subjects (1005 cases and 1242 controls) was performed. Among them, four studies showed that obese individuals expressed lower irisin levels than healthy controls[7,17-19], while nine articles observed the opposite outcome where significantly higher irisin levels were exhibited in obese individuals compared to healthy controls. The results of the remaining four studies had no significance. Data were all described as the means ± SD. The *P*-value of heterogeneity between studies was significant ($P < 0.05$, Figure 2), so we used the random effects model and found that the overall effect was significant (random effects MD = 0.63; 95%CI: 0.22-1.05; $P = 0.003$). The effect size revealed that the irisin level was higher in obese people compared to healthy people.

In the subgroup analysis by ethnicity, the irisin level was higher in obese people in Africa than in controls and the test for overall effect was significant ($I^2 = 91\%$; random effects MD = 3.41; 95%CI: 1.23-5.59; $P < 0.05$). While the irisin levels in European ($I^2 = 90\%$, random effects MD = 0.57; 95%CI: -0.02-1.15), Asian ($I^2 = 93\%$; random effects MD = -0.05; 95%CI: -0.67-0.58), and American populations ($I^2 = 91\%$; random effects MD = 0.61; 95%CI: -0.38-1.61) were not higher in obese individuals than in healthy controls, and the test for overall effect was not significant ($P = 0.06$, 0.89, and 0.31, respectively) (Figure 3).

Furthermore, we performed a subgroup analysis by age. Five studies included children. Three of these studies suggested that obese children exhibited a higher irisin level than controls, and another two studies showed different outcomes. The *P*-value of heterogeneity between studies was significant ($P < 0.05$, Figure 4), then we used the random effects model and found that the overall effect was significant (random effects MD = 0.86; 95%CI: 0.28-1.43; $P = 0.004$). The effect size revealed that the irisin levels were higher in obese children than in controls. Conversely, the irisin levels in adult patients were not significantly different from controls and the total effect was not significant ($I^2 = 95\%$; random effects MD = 0.57; 95%CI: -0.03-1.18; $P = 0.06$) (Figure 4).

We omitted one study at a time and calculated the pooled SMD for the remainder of the studies to conduct a sensitivity analysis. There was no considerable change in the direction of the effect when omitting each of the studies.

We also conducted analyses by the Begg's test and Egger's test. Begg's funnel plot had the expected funnel shape (Figure 5). Begg's test ($Z = 0.61$, $P = 0.544$) and Egger's test for publication bias ($t = 0.46$, $P = 0.65$) indicated that there was no publication bias in our analysis.

DISCUSSION

This meta-analysis showed that circulating irisin levels in obese individuals were higher than those in overall healthy controls. It also suggested that circulating irisin levels were higher in obese people than in healthy controls in Africa, while studies in other regions showed a negative result. This meta-analysis further suggested that obese children exhibited higher irisin levels than controls.

First, the overall result of this meta-analysis is positive that circulating irisin levels increased in obesity compared with health controls, although some studies did not draw the same conclusion. When it comes to underlying mechanisms, it is speculated that the rising circulating irisin level in obesity is an accommodative compensatory response to obesity-induced metabolic dysfunction, such as a decline of insulin levels or "irisin resistance"[32] as has already been established for leptin or insulin in obesity. Second, the results suggest that age may be a factor for the increasing circulating irisin levels in obese children compared to controls. It is deduced that diet habits and lifestyle are also related factors. Due to their growth and development needs, children differ from adults in the above-mentioned factors. In addition, there are other differences such as exercise and underlying diseases[33-37]. Recent studies explored that baseline irisin levels were lower in the old compared to the young participants for age-related decline in muscle function[38,39]. Third, in the subgroup analysis by

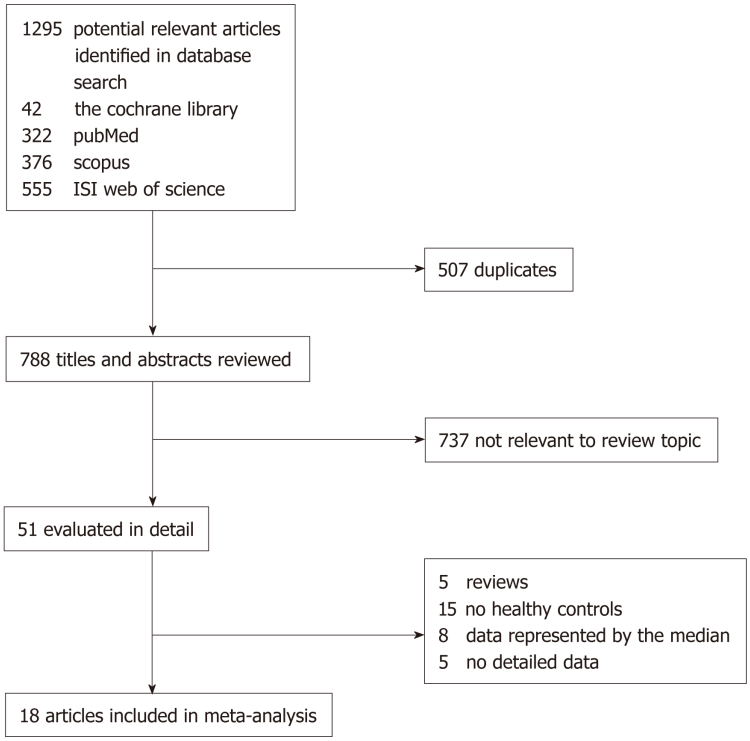

Figure 1 Flow chart of article selection for meta-analysis.

ethnicity, the irisin level was only higher in obese individuals than in controls in Africa, while there were no significant differences in European, Asian, or American populations. These results indicate that genetic differences can influence specific hormone levels such as those of irisin. Weight stratification in the Asian population based on different BMI criteria from other regions may also lead to no significance of the subgroup analysis. Besides the above, gender is another interesting aspect. Murawska-Cialowicz *et al*[38] found that the level of irisin at baseline was higher in men than in women and after a 3-mo CrossFit training program, the changes of irisin level between women and men did not have a uniform trend[38], while in obese children, there was no evidence for differences of irisin levels between genders[37].

To our knowledge, this study is the first meta-analysis that systematically assessed circulating irisin in obese people, yet some limitations should be noted. First, in the above articles, how to choose the criteria to judge obesity is still in question. Although most studies chose to use BMI as the criterion of obesity, Mehrabian *et al*[27] suggested that body fat percentage is a better indicator of total adiposity compared to BMI for some individuals with normal weight obesity. Second, due to different methods, we cannot analyze whether the quality of serum or plasma samples has a decisive impact on the test results. For human FNDC5 does not have a canonical ATA translation start and some reports questioned that many human irisin antibodies used in commercial ELISA kits may lack necessary specificity[40], it is hard to determine the reliability of the results detected with the kits of many brands, although mass spectrometry has clearly demonstrated the existence of human irisin. Third, there were differences in the number of research subjects in different regions or countries; the majority of those surveyed were in Asia and Europe, while relatively few were in Africa. A larger sample survey is needed in the future for a more reliable result. Additionally, influences of the intensity and time of exercise on circulating irisin levels are also of interest, since irisin is a myokine associated with exercise. Future studies are required to investigate whether circulating irisin could predict the risk of obesity. Moreover, studies on the effects of exercise, lifestyle, and weight loss on the irisin level and related prospective studies are also needed.

In conclusion, our meta-analysis provides evidence that circulating irisin is higher in obese individuals compared to healthy controls and that circulating irisin levels seem to be affected by ethnicity and age. More investigations are necessary to clarify the association between the circulating irisin levels and overweight/obesity.

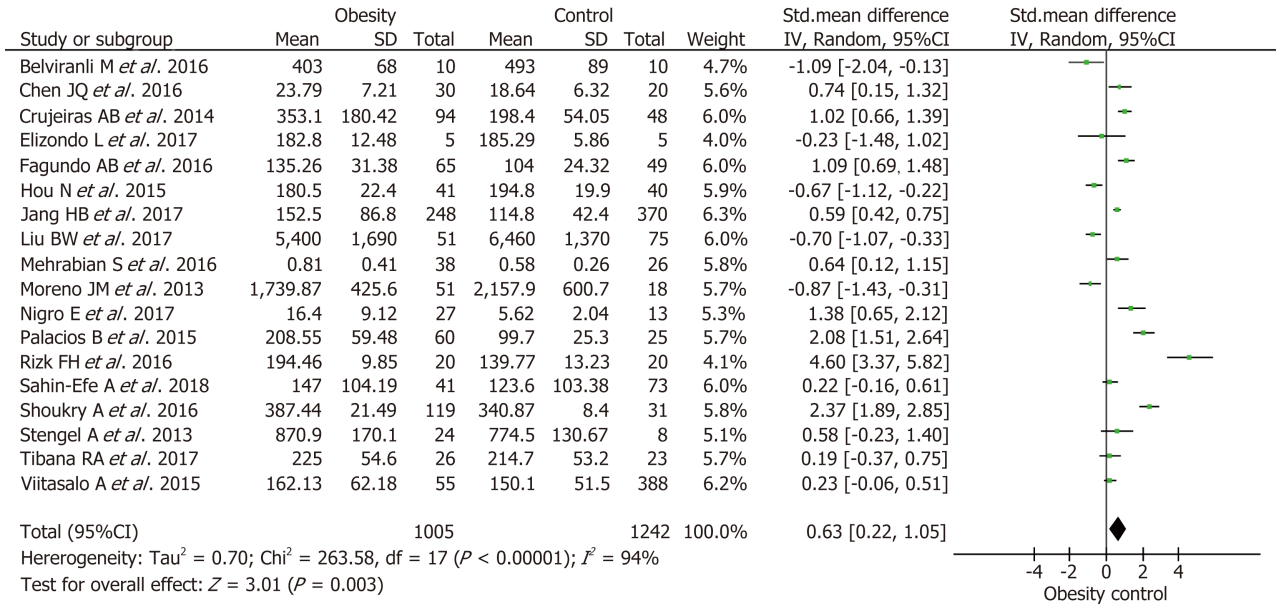

Figure 2 Forest plot of meta-analysis of the association between irisin and obesity.

A

Study or subgroup	Obesity Mean	Obesity SD	Obesity Total	Control Mean	Control SD	Control Total	Weight	Std.mean difference IV, Random, 95%CI
Belviranli M *et al*. 2016	403	68	10	493	89	10	13.2%	-1.09 [-2.04, -0.13]
Chen JQ *et al*. 2016	23.79	7.21	30	18.64	6.32	20	16.3%	0.74 [0.15, 1.32]
Hou N *et al*. 2015	180.5	22.4	41	194.8	19.9	40	17.3%	-0.67 [-1.12, -0.22]
Jang HB *et al*. 2017	152.5	86.8	248	114.8	42.4	370	18.7%	0.59 [0.42, 0.75]
Liu BW *et al*. 2017	5,400	1,690	51	6,460	1,370	75	17.8%	-0.70 [-1.07, -0.33]
Mehrabian S *et al*. 2016	0.81	0.41	38	0.58	0.26	26	16.8%	0.64 [0.12, 1.15]
Total (95%CI)			418			541	100.0%	-0.05 [-0.67, 0.58]

Hererogeneity: Tau^2 = 0.54; Chi^2 = 70.24, df = 5 (P < 0.00001); I^2 = 93%

Test for overall effect: Z = 0.14 (P = 0.89)

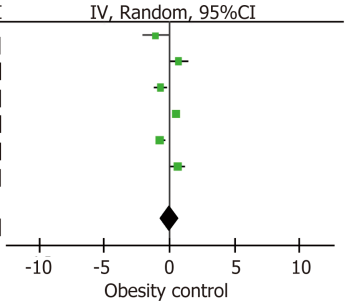

B

Study or subgroup	Obesity Mean	Obesity SD	Obesity Total	Control Mean	Control SD	Control Total	Weight	Std.mean difference IV, Random, 95%CI
Crujeiras AB *et al*. 2014	353.1	180.42	94	198.4	54.05	48	18.1%	1.02 [0.66, 1.39]
Fagundo AB *et al*. 2016	135.26	31.38	65	104	24.32	49	17.8%	1.09 [0.69, 1.48]
Moreno JM *et al*. 2013	1,739.87	425.6	51	2,157.9	600.7	18	16.5%	-0.87 [-1.43, -0.31]
Nigro E *et al*. 2017	16.4	9.12	27	5.62	2.04	13	14.9%	1.38 [0.65, 2.12]
Stengel A *et al*. 2013	870.9	170.1	24	774.5	130.67	8	14.1%	0.58 [-0.23, 1.40]
Viitasalo A *et al*. 2015	162.13	62.18	55	150.1	51.5	388	18.6%	0.23 [-0.06, 0.51]
Total (95%CI)			316			524	100.0%	0.57 [-0.02, 1.15]

Hererogeneity: Tau^2 = 0.46; Chi^2 = 48.17, df = 5 (P < 0.00001); I^2 = 90%

Test for overall effect: Z = 1.90 (P = 0.06)

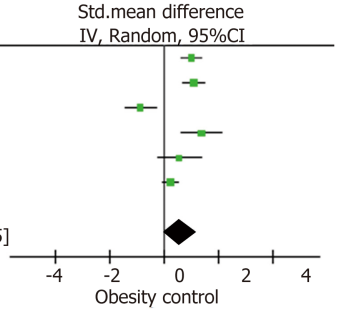

C

Study or subgroup	Obesity Mean	Obesity SD	Obesity Total	Control Mean	Control SD	Control Total	Weight	Std.mean difference IV, Random, 95%CI
Rizk FH *et al*. 2016	194.46	9.85	20	139.77	13.23	20	46.6%	4.60 [3.37, 5.82]
Shoukry A *et al*. 2016	387.44	21.49	119	340.87	8.4	31	53.4%	2.37 [1.89, 2.85]
Total (95%CI)			139			51	100.0%	3.41 [1.23, 5.59]

Hererogeneity: Tau^2 = 2.25; Chi^2 = 10.95, df = 1 (P < 0.00009); I^2 = 91%

Test for overall effect: Z = 3.07 (P = 0.002)

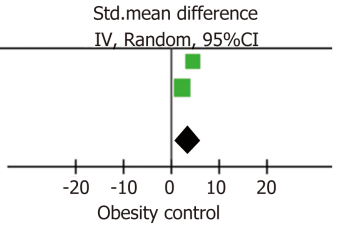

D

Study or subgroup	Obesity Mean	Obesity SD	Obesity Total	Control Mean	Control SD	Control Total	Weight	Std.mean difference IV, Random, 95%CI
Elizondo L *et al*. 2017	182.8	12.48	5	185.29	5.86	5	19.8%	-0.23 [-1.48, 1.02]
Palacios B *et al*. 2015	208.55	59.48	60	99.7	25.3	25	26.3%	2.08 [1.51, 2.64]
Sahin-Efe A *et al*. 2018	147	104.19	41	123.6	103.38	73	27.6%	0.22 [-0.16, 0.61]
Tibana RA *et al*. 2017	225	54.6	26	214.7	53.2	23	26.3%	0.19 [-0.37, 0.75]
Total (95%CI)			132			126	100.0%	0.61 [-0.38, 1.61]

Hererogeneity: Tau^2 = 0.90; Chi^2 = 33.61, df = 3 (P < 0.00001); I^2 = 91%

Test for overall effect: Z = 1.21 (P = 0.23)

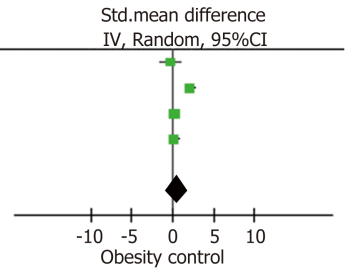

Figure 3 Forest plot of irisin in obese patients in different racial groups. A: Forest plot of irisin in obese patients in Asia; B: Forest plot of irisin in obese patients in Europe; C: Forest plot of irisin in obese patients in Africa; D: Forest plot of irisin in obese patients in America.

A

Study or subgroup	Obesity Mean	SD	Total	Control Mean	SD	Total	Weight	Std.mean difference IV, Random, 95%CI
Elizondo L *et al*. 2017	182.8	12.48	5	185.29	5.86	5	11.7%	-0.23 [-1.48, 1.02]
Jang HB *et al*. 2017	152.5	86.8	248	114.8	42.4	370	25.3%	0.59 [0.42, 0.75]
Nigro E *et al*. 2017	16.4	9.12	27	5.62	2.04	13	18.2%	1.38 [0.65, 2.12]
Palacios B *et al*. 2015	208.55	59.48	60	99.7	25.3	25	20.6%	2.08 [1.51, 2.64]
Viitasalo A *et al*. 2015	162.13	62.18	55	150.1	51.5	388	24.3%	0.23 [-0.06, 0.51]
Total (95%CI)			395			801	100.0%	0.89 [0.28, 1.43]

Hererogeneity: Tau^2 = 0.33; Chi^2 = 38.95, df = 4 (P < 0.00001); I^2 = 90%

Test for overall effect: Z = 2.92 (P = 0.004)

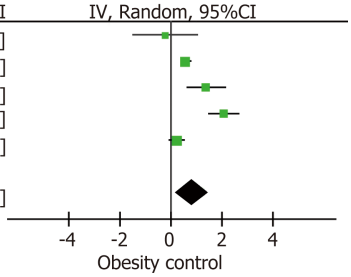

B

Study or subgroup	Obesity Mean	SD	Total	Control Mean	SD	Total	Weight	Std.mean difference IV, Random, 95%CI
Belviranli M *et al*. 2016	403	68	10	493	89	10	6.9%	-1.09 [-2.04, -0.13]
Chen JQ *et al*. 2016	23.79	7.21	30	18.64	6.32	20	7.8%	0.74 [0.15, 1.32]
Crujeiras AB *et al*. 2014	353.1	180.42	94	198.4	54.05	48	8.1%	1.02 [0.66, 1.39]
Fagundo AB *et al*. 2016	135.26	31.38	65	104	24.32	49	8.1%	1.09 [0.69, 1.48]
Hou N *et al*. 2015	180.5	22.4	41	194.8	19.9	40	8.0%	-0.67 [-1.12, -0.22]
Liu BW *et al*. 2017	5,400	1,690	51	6,460	1,370	75	8.1%	-0.70 [-1.07, -0.33]
Mehrabian S *et al*. 2016	0.81	0.41	38	0.58	0.26	26	7.9%	0.64 [0.12, 1.15]
Moreno JM *et al*. 2013	1,739.87	425.6	51	2,157.9	600.7	18	7.8%	-0.87 [-1.43, -0.31]
Rizk FH *et al*. 2016	194.46	9.85	20	139.77	13.23	20	6.2%	4.60 [3.37, 5.82]
Sahin-Efe A *et al*. 2018	147	104.19	41	123.6	103.38	73	8.1%	0.22 [-0.16, 0.61]
Shoukry A *et al*. 2016	387.44	21.49	119	340.87	8.4	31	7.9%	2.37 [1.89, 2.85]
Stengel A *et al*. 2013	870.9	170.1	24	774.5	130.67	8	7.3%	0.58 [-0.23, 1.40]
Tibana RA *et al*. 2017	225	54.6	26	214.7	53.2	23	7.8%	0.19 [-0.37, 0.75]
Total (95%CI)			610			441	100.0%	0.57 [-0.03, 1.18]

Hererogeneity: Tau^2 = 1.13; Chi^2 = 221.15, df = 12 (P < 0.00001); I^2 = 95%

Test for overall effect: Z = 1.87 (P = 0.06)

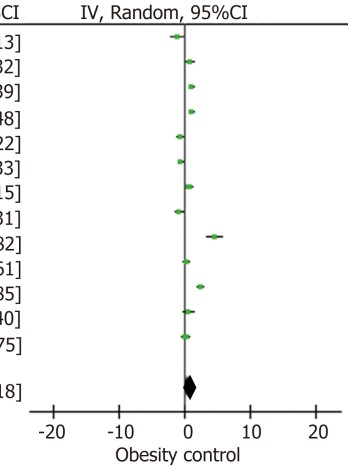

Figure 4 Forest plot of irisin in obese patients in children and adults. A: Forest plot of irisin in obese children *vs* nonobese children; B: Forest plot of irisin in obese adults *vs* nonobese adults.

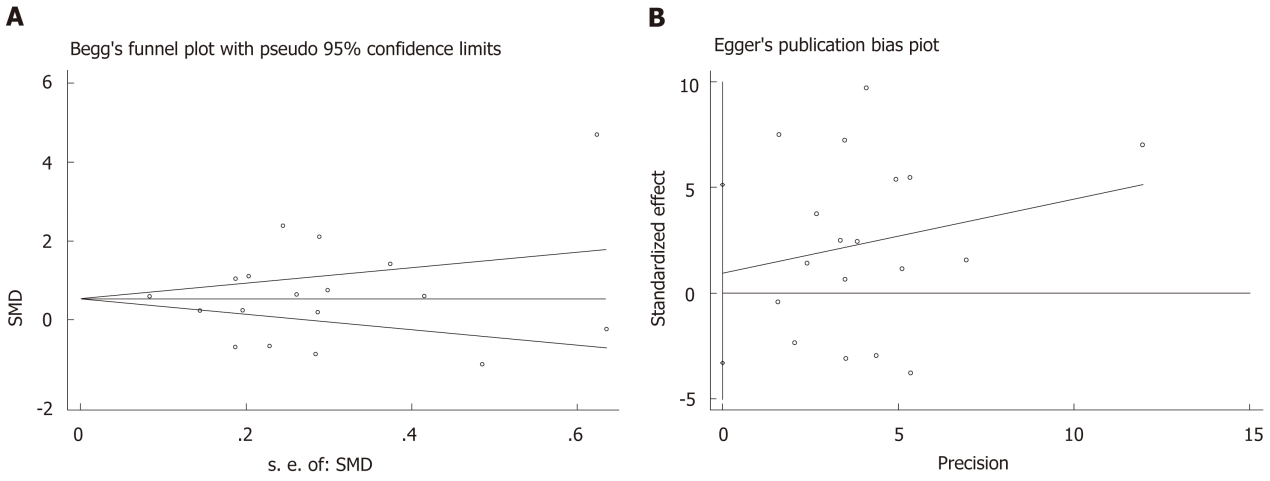

Figure 5 Analysis of publication bias. A: Begg's funnel plot had the expected funnel shape (Begg's test P = 0.544); B: Egger's publication bias plot (Egger's test P = 0.65).

ARTICLE HIGHLIGHTS

Research background

Overweight/obesity has been a global health challenge and irisin as a novel myokine is reported to play an important role in the development of metabolism dysfunction and obesity, however, the exact relationship between irisin and overweight/obesity remains unclear.

Research motivation

Many studies on the results of circulating irisin levels in overweight/obesity people are incon-

sistent, which has puzzled us in confirming the role of irisin in overweight/obesity, thus, it is necessary to do such an analysis to clarify the relationship between them.

Research objectives
The main objective was to extract available data from studies and clarify the relationship between irisin and overweight/obesity.

Research methods
We searched Cochrane Library, MEDLINE, SCOPUS, and the ISI Web of Science to retrieve all of the studies associated with circulating irisin levels and overweight/obesity. We estimated standard mean difference values and 95% confidence intervals and used meta-analysis methodology to get final results.

Research results
A total of 18 studies were included in this meta-analysis containing 1005 cases and 1242 controls. The overall analysis showed that the circulating irisin level in overweight/obese people was higher than that in overall healthy controls. In the subgroup analysis by ethnicity, the irisin level was higher in overweight/obese people than that in controls in Africa. In addition, in a subgroup analysis by age, the results showed that obese children exhibited a higher irisin level than controls. Studies of larger population samples are needed to better explore the relationship between irisin and overweight/obesity.

Research conclusions
This study integrated the existing data to show that the circulating irisin levels in overweight/obese people was higher than those in healthy controls overall, and explored the potential of irisin as a predictive factor for overweight/obesity.

Research perspectives
More studies on the effects of exercise, lifestyle, and weight loss on the irisin level and related prospective studies are needed.

REFERENCES

1 **van der Klaauw AA**, Farooqi IS. The hunger genes: pathways to obesity. *Cell* 2015; **161**: 119-132 [PMID: 25815990 DOI: 10.1016/j.cell.2015.03.008]
2 **Ryan DH**, Kahan S. Guideline Recommendations for Obesity Management. *Med Clin North Am* 2018; **102**: 49-63 [PMID: 29156187 DOI: 10.1016/j.mcna.2017.08.006]
3 **Kushner RF**, Kahan S. Introduction: The State of Obesity in 2017. *Med Clin North Am* 2018; **102**: 1-11 [PMID: 29156178 DOI: 10.1016/j.mcna.2017.08.003]
4 **El-Lebedy DH**, Ibrahim AA, Ashmawy IO. Novel adipokines vaspin and irisin as risk biomarkers for cardiovascular diseases in type 2 diabetes mellitus. *Diabetes Metab Syndr* 2018; **12**: 643-648 [PMID: 29673927 DOI: 10.1016/j.dsx.2018.04.025]
5 **Polyzos SA**, Anastasilakis AD, Efstathiadou ZA, Makras P, Perakakis N, Kountouras J, Mantzoros CS. Irisin in metabolic diseases. *Endocrine* 2018; **59**: 260-274 [PMID: 29170905 DOI: 10.1007/s12020-017-1476-1]
6 **Park KH**, Zaichenko L, Brinkoetter M, Thakkar B, Sahin-Efe A, Joung KE, Tsoukas MA, Geladari EV, Huh JY, Dincer F, Davis CR, Crowell JA, Mantzoros CS. Circulating irisin in relation to insulin resistance and the metabolic syndrome. *J Clin Endocrinol Metab* 2013; **98**: 4899-4907 [PMID: 24057291 DOI: 10.1210/jc.2013-2373]
7 **Moreno-Navarrete JM**, Ortega F, Serrano M, Guerra E, Pardo G, Tinahones F, Ricart W, Fernández-Real JM. Irisin is expressed and produced by human muscle and adipose tissue in association with obesity and insulin resistance. *J Clin Endocrinol Metab* 2013; **98**: E769-E778 [PMID: 23436919 DOI: 10.1210/jc.2012-2749]
8 **Polyzos SA**, Kountouras J, Anastasilakis AD, Geladari EV, Mantzoros CS. Irisin in patients with nonalcoholic fatty liver disease. *Metabolism* 2014; **63**: 207-217 [PMID: 24140091 DOI: 10.1016/j.metabol.2013.09.013]
9 **Cai X**, Qiu S, Li L, Zügel M, Steinacker JM, Schumann U. Circulating irisin in patients with polycystic ovary syndrome: a meta-analysis. *Reprod Biomed Online* 2018; **36**: 172-180 [PMID: 29217128 DOI: 10.1016/j.rbmo.2017.10.114]
10 **Guo W**, Zhang B, Wang X. Lower irisin levels in coronary artery disease: a meta-analysis. *Minerva Endocrinol* 2017 [PMID: 29160049 DOI: 10.23736/S0391-1977.17.02663-3]
11 **Boström P**, Wu J, Jedrychowski MP, Korde A, Ye L, Lo JC, Rasbach KA, Boström EA, Choi JH, Long JZ, Kajimura S, Zingaretti MC, Vind BF, Tu H, Cinti S, Højlund K, Gygi SP, Spiegelman BM. A PGC1-α-dependent myokine that drives brown-fat-like development of white fat and thermogenesis. *Nature* 2012; **481**: 463-468 [PMID: 22237023 DOI: 10.1038/nature10777]
12 **Crujeiras AB**, Pardo M, Arturo RR, Navas-Carretero S, Zulet MA, Martínez JA, Casanueva FF. Longitudinal variation of circulating irisin after an energy restriction-induced weight loss and following weight regain in obese men and women. *Am J Hum Biol* 2014; **26**: 198-207 [PMID: 24375850 DOI: 10.1002/ajhb.22493]
13 **Stengel A**, Hofmann T, Goebel-Stengel M, Elbelt U, Kobelt P, Klapp BF. Circulating levels of irisin in patients with anorexia nervosa and different stages of obesity--correlation with body mass index. *Peptides* 2013; **39**: 125-130 [PMID: 23219488 DOI: 10.1016/j.peptides.2012.11.014]
14 **Chen JQ**, Fang LJ, Song KX, Wang XC, Huang YY, Chai SY, Bu L, Qu S. Serum Irisin Level is Higher and Related with Insulin in Acanthosis Nigricans-related Obesity. *Exp Clin Endocrinol Diabetes* 2016; **124**: 203-207 [PMID: 26588491 DOI: 10.1055/s-0035-1565060]
15 **Fagundo AB**, Jiménez-Murcia S, Giner-Bartolomé C, Agüera Z, Sauchelli S, Pardo M, Crujeiras AB,

Granero R, Baños R, Botella C, de la Torre R, Fernández-Real JM, Fernández-García JC, Frühbeck G, Rodríguez A, Mallorquí-Bagué N, Tárrega S, Tinahones FJ, Rodriguez R, Ortega F, Menchón JM, Casanueva FF, Fernández-Aranda F. Modulation of Irisin and Physical Activity on Executive Functions in Obesity and Morbid obesity. *Sci Rep* 2016; **6**: 30820 [PMID: 27476477 DOI: 10.1038/srep30820]

16 **Tibana RA**, da Cunha Nascimento D, Frade de Souza NM, de Souza VC, de Sousa Neto IV, Voltarelli FA, Pereira GB, Navalta JW, Prestes J. Irisin Levels Are not Associated to Resistance Training-Induced Alterations in Body Mass Composition in Older Untrained Women with and without Obesity. *J Nutr Health Aging* 2017; **21**: 241-246 [PMID: 28244561 DOI: 10.1007/s12603-016-0748-4]

17 **Belviranli M**, Okudan N, Çelik F. Association of Circulating Irisin with Insulin Resistance and Oxidative Stress in Obese Women. *Horm Metab Res* 2016; **48**: 653-657 [PMID: 27632149 DOI: 10.1055/s-0042-116155]

18 **Hou N**, Han F, Sun X. The relationship between circulating irisin levels and endothelial function in lean and obese subjects. *Clin Endocrinol (Oxf)* 2015; **83**: 339-343 [PMID: 25382211 DOI: 10.1111/cen.12658]

19 **Liu BW**, Yin FZ, Qi XM, Fan DM, Zhang Y. The Levels of Serum Irisin as a Predictor of Insulin Resistance in Han Chinese Adults with Metabolically Healthy Obesity. *Clin Lab* 2017; **63**: 881-886 [PMID: 28627815 DOI: 10.7754/Clin.Lab.2016.160805]

20 **Palacios-González B**, Vadillo-Ortega F, Polo-Oteyza E, Sánchez T, Ancira-Moreno M, Romero-Hidalgo S, Meráz N, Antuna-Puente B. Irisin levels before and after physical activity among school-age children with different BMI: a direct relation with leptin. *Obesity (Silver Spring)* 2015; **23**: 729-732 [PMID: 25820255 DOI: 10.1002/oby.21029]

21 **Elizondo-Montemayor L**, Silva-Platas C, Torres-Quintanilla A, Rodríguez-López C, Ruiz-Esparza GU, Reyes-Mendoza E, Garcia-Rivas G. Association of Irisin Plasma Levels with Anthropometric Parameters in Children with Underweight, Normal Weight, Overweight, and Obesity. *Biomed Res Int* 2017; **2017**: 2628968 [PMID: 28553647 DOI: 10.1155/2017/2628968]

22 **Nigro E**, Scudiero O, Ludovica Monaco M, Polito R, Schettino P, Grandone A, Perrone L, Miraglia Del Giudice E, Daniele A. Adiponectin profile and Irisin expression in Italian obese children: Association with insulin-resistance. *Cytokine* 2017; **94**: 8-13 [PMID: 28385328 DOI: 10.1016/j.cyto.2016.12.018]

23 **Begg CB**, Mazumdar M. Operating characteristics of a rank correlation test for publication bias. *Biometrics* 1994; **50**: 1088-1101 [PMID: 7786990 DOI: 10.2307/2533446]

24 **Egger M**, Davey Smith G, Schneider M, Minder C. Bias in meta-analysis detected by a simple, graphical test. *BMJ* 1997; **315**: 629-634 [PMID: 9310563 DOI: 10.1136/bmj.315.7109.629]

25 **Higgins JP**, Thompson SG, Deeks JJ, Altman DG. Measuring inconsistency in meta-analyses. *BMJ* 2003; **327**: 557-560 [PMID: 12958120 DOI: 10.1136/bmj.327.7414.557]

26 **Viitasalo A**, Ågren J, Venäläinen T, Pihlajamäki J, Jääskeläinen J, Korkmaz A, Atalay M, Lakka TA. Association of plasma fatty acid composition with plasma irisin levels in normal weight and overweight/obese children. *Pediatr Obes* 2016; **11**: 299-305 [PMID: 26305484 DOI: 10.1111/ijpo.12062]

27 **Mehrabian S**, Taheri E, Karkhaneh M, Qorbani M, Hosseini S. Association of circulating irisin levels with normal weight obesity, glycemic and lipid profile. *J Diabetes Metab Disord* 2016; **15**: 17 [PMID: 27354972 DOI: 10.1186/s40200-016-0239-5]

28 **Rizk FH**, Elshweikh SA, Abd El-Naby AY. Irisin levels in relation to metabolic and liver functions in Egyptian patients with metabolic syndrome. *Can J Physiol Pharmacol* 2016; **94**: 359-362 [PMID: 26695389 DOI: 10.1139/cjpp-2015-0371]

29 **Shoukry A**, Shalaby SM, El-Arabi Bdeer S, Mahmoud AA, Mousa MM, Khalifa A. Circulating serum irisin levels in obesity and type 2 diabetes mellitus. *IUBMB Life* 2016; **68**: 544-556 [PMID: 27220658 DOI: 10.1002/iub.1511]

30 **Jang HB**, Kim HJ, Kang JH, Park SI, Park KH, Lee HJ. Association of circulating irisin levels with metabolic and metabolite profiles of Korean adolescents. *Metabolism* 2017; **73**: 100-108 [PMID: 28732566 DOI: 10.1016/j.metabol.2017.05.007]

31 **Sahin-Efe A**, Upadhyay J, Ko BJ, Dincer F, Park KH, Migdal A, Vokonas P, Mantzoros C. Irisin and leptin concentrations in relation to obesity, and developing type 2 diabetes: A cross sectional and a prospective case-control study nested in the Normative Aging Study. *Metabolism* 2018; **79**: 24-32 [PMID: 29108900 DOI: 10.1016/j.metabol.2017.10.011]

32 **Perakakis N**, Triantafyllou GA, Fernández-Real JM, Huh JY, Park KH, Seufert J, Mantzoros CS. Physiology and role of irisin in glucose homeostasis. *Nat Rev Endocrinol* 2017; **13**: 324-337 [PMID: 28211512 DOI: 10.1038/nrendo.2016.221]

33 **Kim HJ**, Lee HJ, So B, Son JS, Yoon D, Song W. Effect of aerobic training and resistance training on circulating irisin level and their association with change of body composition in overweight/obese adults: a pilot study. *Physiol Res* 2016; **65**: 271-279 [PMID: 26447516]

34 **Pathak K**, Woodman RJ, James AP, Soares MJ. Fasting and glucose induced thermogenesis in response to three ambient temperatures: a randomized crossover trial in the metabolic syndrome. *Eur J Clin Nutr* 2018; **72**: 1421-1430 [PMID: 29326420 DOI: 10.1038/s41430-017-0058-x]

35 **Daneshi-Maskooni M**, Keshavarz SA, Mansouri S, Qorbani M, Alavian SM, Badri-Fariman M, Jazayeri-Tehrani SA, Sotoudeh G. The effects of green cardamom on blood glucose indices, lipids, inflammatory factors, paraxonase-1, sirtuin-1, and irisin in patients with nonalcoholic fatty liver disease and obesity: study protocol for a randomized controlled trial. *Trials* 2017; **18**: 260 [PMID: 28592311 DOI: 10.1186/s13063-017-1979-3]

36 **Hron BM**, Ebbeling CB, Feldman HA, Ludwig DS. Hepatic, adipocyte, enteric and pancreatic hormones: response to dietary macronutrient composition and relationship with metabolism. *Nutr Metab (Lond)* 2017; **14**: 44 [PMID: 28694840 DOI: 10.1186/s12986-017-0198-y]

37 **Blüher S**, Panagiotou G, Petroff D, Markert J, Wagner A, Klemm T, Filippaios A, Keller A, Mantzoros CS. Effects of a 1-year exercise and lifestyle intervention on irisin, adipokines, and inflammatory markers in obese children. *Obesity (Silver Spring)* 2014; **22**: 1701-1708 [PMID: 24644099 DOI: 10.1002/oby.20739]

38 **Murawska-Cialowicz E**, Wojna J, Zuwala-Jagiello J. Crossfit training changes brain-derived neurotrophic factor and irisin levels at rest, after wingate and progressive tests, and improves aerobic capacity and body composition of young physically active men and women. *J Physiol Pharmacol* 2015; **66**: 811-821 [PMID: 26769830]

39 **Kim HJ**, So B, Choi M, Kang D, Song W. Resistance exercise training increases the expression of irisin concomitant with improvement of muscle function in aging mice and humans. *Exp Gerontol* 2015; **70**: 11-17 [PMID: 26183690 DOI: 10.1016/j.exger.2015.07.006]

40 **Jedrychowski MP**, Wrann CD, Paulo JA, Gerber KK, Szpyt J, Robinson MM, Nair KS, Gygi SP,

Spiegelman BM. Detection and Quantitation of Circulating Human Irisin by Tandem Mass Spectrometry. *Cell Metab* 2015; **22**: 734-740 [PMID: 26278051 DOI: 10.1016/j.cmet.2015.08.001]

World Journal of Clinical Cases

Submit a Manuscript: https://www.f6publishing.com

World J Clin Cases 2019 June 26; 7(12): 1456-1460

DOI: 10.12998/wjcc.v7.i12.1456

ISSN 2307-8960 (online)

CASE REPORT

Cirrhosis complicating Shwachman-Diamond syndrome: A case report

Sandra M Camacho, Lucille McLoughlin, Michael J Nowicki

ORCID number: Sandra Mabel Camacho (0000-0001-8392-0897); Lucille McLoughlin (0000-0003-3602-7451); Michael J Nowicki (0000-0001-9395-3027).

Author contributions: Camacho SM wrote the case report portion and edited the final manuscript; McLoughlin L reviewed and edited the final manuscript; Nowicki MJ wrote the discussion portion and reviewed and edited the final manuscript.

Informed consent statement: Informed consent was given by the parents.

Conflict-of-interest statement: None of the authors have any conflict of interest to report.

Manuscript source: Invited manuscript

Received: January 25, 2019
Peer-review started: January 25, 2019
First decision: March 14, 2019

Sandra M Camacho, Michael J Nowicki, Division of Pediatric Gastroenterology, University of Mississippi Medical Center, Jackson, MS 39216, United States

Sandra M Camacho, Lucille McLoughlin, Division of Pediatric Gastroenterology, Children's Hospital of San Antonio, San Antonio, TX 78207, United States

Corresponding author: Michael J Nowicki, MD, Professor, Division of Pediatric Gastroenterology, University of Mississippi Medical Center, 2500 North State Street, Jackson, MS 39216, United States. mnowicki@umc.edu
Telephone: +1-601-9845294
Fax: +1-601-8151053

Abstract

BACKGROUND

The features of Shwachman-Diamond syndrome (SDS) include exocrine pancreatic insufficiency, skeletal abnormalities and bone marrow dysfunction; an often overlooked feature is hepatic involvement.

CASE SUMMARY

We report a child who initially presented with failure to thrive and mildly elevated transaminase levels and was determined to have pancreatic insufficiency due to SDS. During follow-up he had persistently elevated transaminase levels and developed hepatosplenomegaly. An investigation was performed to determine the etiology of ongoing liver injury, including a liver biopsy which revealed hepatic cirrhosis.

CONCLUSION

Cirrhosis has rarely been reported with SDS. While many of the hepatic disorders associated with SDS improve with age, there are rare exceptions with serious implications for long-term outcome.

Key words: Shwachman-Diamond syndrome; Cirrhosis; Liver dysfunction; Case report

Core tip: Shwachman-Diamond syndrome (SDS) is an uncommon disorder characterized by skeletal abnormalities, bone marrow dysfunction and exocrine pancreatic insufficiency (EPI); a rarely reported complication is hepatic cirrhosis. Similar to the natural history of EPI, most of the hepatic abnormalities associated with SDS improve or resolve with age. We report this patient to highlight the importance of close follow-up of

Revised: April 11, 2019
Accepted: May 2, 2019
Article in press: May 3, 2019
Published online: June 26, 2019

P-Reviewer: Borzio M, Rong G
S-Editor: Gong ZM
L-Editor: A
E-Editor: Xing YX

patients with SDS and hepatic dysfunction as some will progress to cirrhosis, which portends a less favorable prognosis.

Citation: Camacho SM, McLoughlin L, Nowicki MJ. Cirrhosis complicating Shwachman-Diamond syndrome: A case report. *World J Clin Cases* 2019; 7(12): 1456-1460
URL: https://www.wjgnet.com/2307-8960/full/v7/i12/1456.htm
DOI: https://dx.doi.org/10.12998/wjcc.v7.i12.1456

INTRODUCTION

Shwachman-Diamond syndrome (SDS) is a multi-organ, autosomal recessive disorder caused by compound heterozygous or homozygous mutations in SBDS gene located on chromosome 7q11[1]. Common features of SDS include exocrine pancreatic insufficiency (EPI), diarrhea, failure to thrive during infancy, normal sweat electrolytes, neutropenia associated with bone marrow hypoplasia, anemia, and elevation in fetal hemoglobin[2,3]. Hepatic involvement is also seen, most commonly presenting as mild elevation in transaminase levels and/or hepatomegaly. Rarely, more severe hepatic involvement has been reported. We describe a child with failure to thrive due to SDS who developed cirrhosis.

CASE PRESENTATION

Clinical observations

A 16-month-old white male presented with a chief complaint of long-standing failure to thrive first noted around 2-mo of age. The parents reported that initially he had poor weight gain but after several months he also developed poor linear growth. He maintained excellent oral intake without vomiting. Bowel movements were described as large, foul-smelling, non-watery and without blood, occurring 3 to 5 times per day. Past medical history revealed the he was delivered via spontaneous vaginal birth following a benign pregnancy and labor. Intrauterine growth restriction was not present. He had no history of recurrent gastrointestinal or sino-pulmonary infections. At presentation he weighed 6.99-kg (50% for a 4-month old infant). There were no cardiac murmurs, the lung examination revealed good air exchange without adventitious sounds. Abdominal examination revealed hepatomegaly without splenomegaly. He had markedly thin extremities with muscle wasting but no edema or clubbing. Laboratory evaluation included a complete blood count, complete metabolic panel, creatinine kinase, thyroid stimulating hormone, free-T4, serum IgA, tissue transglutaminase, and urinalysis, which were all normal except for very mild elevation of the transaminase levels (ALT = 52 U/L, ULN = 41 U/L; AST = 124 U/L, ULN = 40 U/L). Fecal qualitative fat was increased. Sweat chloride testing was normal on two occasions. Due to concern for SDS a skeletal survey was performed revealing abnormal tubulation of the long bones and narrowing of the sacral sciatic notches, suggestive for SDS. Esophagastroduodenoscopy (EGD) with biopsies and pancreatic stimulation test was performed. Biopsies of the antrum and duodenum were normal. Pancreatic stimulation test showed a generalized deficiency in pancreatic enzyme activities (trypsin, amylase, lipase, and chymotrypsinogen). Pancreatic enzyme replacement was started. Subsequent gene sequencing confirmed two heterozygous mutations in the SBDS gene confirming the diagnosis.

The patient maintained mildly elevated transaminases (Figure 1). Due to worsening hepatomegaly, and development of splenomegaly, a liver biopsy was performed at 32 mo of age. The biopsy showed hepatocytes with moderate to severe macrovesicular steatosis without necrosis and hepatocyte nodules surrounded by fibrous septa with moderate lymphocytic inflammation consistent with cirrhosis. Further testing for an etiology of cirrhosis was non-diagnostic, including ceruloplasmin, alpha-1-antitrypsin phenotype, autoimmune markers (anti-smooth muscle antibody, anti-liver-kidney-microsomal antibody, and anti-nuclear antibody), carbohydrate deficient transferrin, and the EGL Genetic Cholestasis Panel (a proprietary test that screens for 66 genetic disorders associated with liver disease).

At 5-years of age he was noted to have pancytopenia (hemoglobin = 10.3 g/dL, white blood cell count = 1.5K/cmm, platelet count = 29 K/cmm). Examination revealed mild hepatomegaly and massively enlarged spleen. Bone marrow biopsy

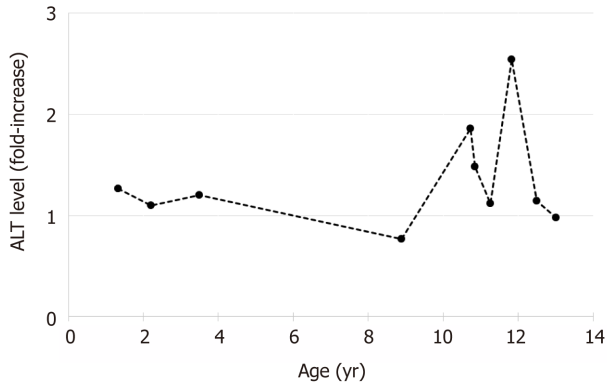

Figure 1 Changes in alanine aminotransferase levels with age. Alanine aminotransferase levels over time (expressed as fold-increase above upper limit of normal).

showed marrow hypercellularity and erythroid hyperplasia consistent with hypersplenism. He underwent an open splenectomy with normalization of his blood indices.

At 8-years of age, he presented with acute onset of hematemesis and hematochezia. Laboratory studies showed severe acute blood loss anemia (hemoglobin = 4.6 gm/dL); coagulation studies (prothrombin time and partial thromboplastin time) were normal. An EGD was performed revealing four large tortuous esophageal varices with wale signs and two varices in the gastric cardia; the esophageal varices were ablated with banding. The gastric mucosa showed changes consistent with hypertensive gastropathy.

At 13-years of age he remains asymptomatic, without abdominal pain, diarrhea, jaundice, pruritus, easy bruising, or gastrointestinal bleeding. Despite compliance with pancreatic enzyme replacement, his growth remains poor, with a height at the first percentile and a BMI at the second percentile for age and gender. He has no hepatomegaly or cutaneous stigmata of chronic liver disease, to include spider angiomata, palmar erythema, and xanthomas.

FINAL DIAGNOSES

The final diagnosis of the patient was Shwachman-Diamond syndrome complicated by cirrhosis, portal hypertension and resulting esophageal varices.

TREATMENT

The patient was treated with pancreatic enzyme replacement for pancreatic insufficiency due to Shwachman-Diamond syndrome. The esophageal varices were treated with band ligation without further bleeding.

OUTCOME AND FOLLOW-UP

The patient continues to have need for pancreatic enzyme replacement. He has been referred for evaluation for liver transplantation due to cirrhosis.

DISCUSSION

Typical clinical features of SDS include EPI, neutropenia associated with bone marrow hypoplasia, anemia, skeletal abnormalities, diarrhea, and poor growth; hepatic involvement is less commonly reported[1,3]. The spectrum of liver involvement associated with SDS includes asymptomatic elevation of serum transaminase levels, hepatomegaly, fatty-infiltration, and varying degrees of hepatic fibrosis, including cirrhosis.

Biochemical hepatic abnormalities are a common finding in SDS patients, but are limited to elevation in aminotransferase levels; serum bilirubin, alkaline phosphatase,

and gamma glutamyltransferase levels are typically normal[2,4-11]. There are five studies that have assessed liver involvement in nearly 140 SDS patients, the overall incidence of elevated aminotransferase levels in these studies ranged from 57% to 100%[2,7,9-11]. Mild aminotransferase elevation (< 5X the upper limit of normal) was reported in 38% to 84% of patients[2,9,10]. In patients followed longitudinally, normalization of transaminase levels was seen in 56% to 67%, improvement in 33%, and no significant change in 11%[2,9]. Three studies reported improvement in aminotransferase levels with increasing age[7,10,11]. Mack, *et al*[7], reported that transaminase levels were highest before 2 years of age and normalized over time[10]. Similarly, Toivianen-Salo, *et al*[11], reported that transaminase levels were highest in early childhood and normalized by 5-years of age[11]. A pattern the mirrors the gradual improvement in pancreatic function seen in patients with SDS.

Hepatomegaly is also a well described finding in SDS, reported in 4% to 62% of affected patients[2,7,8,10,11]. The liver tends to be mildly enlarged, although massive hepatomegaly can be seen[7]. Hepatomegaly is a more common finding in younger children and tends to normalize in most by 3-years of age (85%-86%), similar to the pattern seen for aminotransferase levels[2,11]. Histologic abnormalities on liver biopsy include varying degrees and combinations of steatosis, cellular inflammation, and fibrosis. Patients with hepatomegaly show the same spectrum of histologic findings as those without hepatomegaly[8,10]. Steatosis has been reported as microvesicular, macrovesicular, and mixed micro- and macrovesicular. Hepatic steatosis is thought to arise secondary to malnutrition or infection[2]. Inflammatory cell infiltrate tends to be mild and localized to the portal and periportal areas. Scarring is frequently reported as portal or periportal fibrosis, and less commonly bridging fibrosis. Cirrhosis has rarely been reported in association SDS, with no reports in over 50 years[4,5]. In a review by Bodian *et al*[4], five children were described with SDS and cirrhosis, which was discovered at autopsy in all cases[4]. Four of the children were between the ages of 12 years and 14 years, the other child was only 2 years old, and was described as having "early cirrhosis".

The pancreas and liver share a common embryonic origin and precursor cells of these organs may share many phenotypical and functional traits, which may help explain why pancreatic and hepatic function both improve over time in patients with SDS[11]. However, the mechanism of improvement remains unclear.

CONCLUSION

We report a child with SDS discovered to have cirrhosis at an extremely early age; extensive investigation failed to reveal an etiology other than SDS. It is important for Pediatric health care providers to recognize that children with SDS may have hepatic involvement which tends to be mild and improves or resolves with age. Rarely, more severe hepatic disease can occur that will require evaluation by a Pediatric Gastroenterologist. This information may be beneficial to the primary care provider in the care of children with SDS.

REFERENCES

1 **Kusick VA**. Shwachman-Diamond Syndrome; SDS. Omim, 4 June 1986. web. 3 May 2017.
2 **Aggett PJ**, Cavanagh NP, Matthew DJ, Pincott JR, Sutcliffe J, Harries JT. Shwachman's syndrome. A review of 21 cases. *Arch Dis Child* 1980; **55**: 331-347 [PMID: 7436469 DOI: 10.1136/adc.55.5.331]
3 **Shwachman H**, Diamond LK, Oski FA, Khaw KT. The syndrome of pancreatic insufficiency and bone marrow dysfunction. *J Pediatr* 1964; **65**: 645-663 [PMID: 14221166 DOI: 10.1016/S0022-3476(64)80150-5]
4 **Bodian M**, Sheldon W, Lightwood R. Congenital hypoplasia of the exocrine pancreas. *Acta Paediatr* 1964; **53**: 282-293 [PMID: 14158482 DOI: 10.1111/j.1651-2227.1964.tb07237.x]
5 **Liebman WM**, Rosental E, Hirshberger M, Thaler MM. Shwachman-Diamond sydnrome and chronic liver disease. *Clin Pediatr (Phila)* 1979; **18**: 695-696, 698 [PMID: 498691 DOI: 10.1177/000992287901801106]
6 **Mäki M**, Sorto A, Hällström O, Visakorpi JK. Hepatic dysfunction and dysgammaglobulinaemia in Shwachman-Diamond syndrome. *Arch Dis Child* 1978; **53**: 693-694 [PMID: 708113 DOI: 10.1136/adc.53.8.693-b]
7 **Mack DR**, Forstner GG, Wilschanski M, Freedman MH, Durie PR. Shwachman syndrome: exocrine pancreatic dysfunction and variable phenotypic expression. *Gastroenterology* 1996; **111**: 1593-1602 [PMID: 8942739 DOI: 10.1016/S0016-5085(96)70022-7]
8 **Wilschanski M**, van der Hoeven E, Phillips J, Shuckett B, Durie P. Shwachman-Diamond syndrome presenting as hepatosplenomegaly. *J Pediatr Gastroenterol Nutr* 1994; **19**: 111-113 [PMID: 7965460 DOI: 10.1097/00005176-199407000-00019]
9 **Cipolli M**, D'Orazio C, Delmarco A, Marchesini C, Miano A, Mastella G. Shwachman's syndrome: pathomorphosis and long-term outcome. *J Pediatr Gastroenterol Nutr* 1999; **29**: 265-272 [PMID: 10467990 DOI: 10.1097/00005176-199909000-00006]

10 **Ginzberg H**, Shin J, Ellis L, Morrison J, Ip W, Dror Y, Freedman M, Heitlinger LA, Belt MA, Corey M, Rommens JM, Durie PR. Shwachman syndrome: phenotypic manifestations of sibling sets and isolated cases in a large patient cohort are similar. *J Pediatr* 1999; **135**: 81-88 [PMID: 10393609 DOI: 10.1016/S0022-3476(99)70332-X]

11 **Toiviainen-Salo S**, Durie PR, Numminen K, Heikkilä P, Marttinen E, Savilahti E, Mäkitie O. The natural history of Shwachman-Diamond syndrome-associated liver disease from childhood to adulthood. *J Pediatr* 2009; **155**: 807-811.e2 [PMID: 19683257 DOI: 10.1016/j.jpeds.2009.06.047]

World Journal of Clinical Cases

Submit a Manuscript: https://www.f6publishing.com

World J Clin Cases 2019 June 26; 7(12): 1461-1466

DOI: 10.12998/wjcc.v7.i12.1461

ISSN 2307-8960 (online)

CASE REPORT

Robot-assisted trans-gastric drainage and debridement of walled-off pancreatic necrosis using the EndoWrist stapler for the da Vinci Xi: A case report

Luca Morelli, Niccolò Furbetta, Desirée Gianardi, Matteo Palmeri, Gregorio Di Franco, Matteo Bianchini, Gianni Stefanini, Simone Guadagni, Giulio Di Candio

ORCID number: Luca Morelli (0000-0002-7742-9556); Niccolò Furbetta (0000-0002-7135-2666); Desirée Gianardi (0000-0002-6238-9176); Matteo Palmeri (0000-0002-9343-278X); Gregorio Di Franco (0000-0003-2156-369X); Matteo Bianchini (0000-0002-2403-0621); Gianni Stefanini (0000-0003-3936-5691); Simone Guadagni (0000-0001-9072-8166); Giulio Di Candio (0000-0002-5221-2756).

Author contributions: Morelli L, Furbetta N, Gianardi D, Palmeri M, Di Franco G, Bianchini M, Stefanini G, Guadagni S and Di Candio G conceived and design the study; Furbetta N, Gianardi D, Palmeri M, Di Franco G, Stefanini G, Bianchini M and Guadagni S acquired data; Morelli L and Di Candio G analyzed and interpreted the data; Morelli L, Furbetta N, Gianardi D, Palmeri M, Di Franco G, Bianchini M, Stefanini G and Guadagni S drafted the manuscript; Morelli L and Di Candio G critically revised the manuscript; all authors have read and approved the final version to be published.

Informed consent statement: The patient and his family provided informed written consent.

Conflict-of-interest statement: The authors declare that they have no conflict of interest.

CARE Checklist (2016) statement: The authors have read the CARE

Luca Morelli, Niccolò Furbetta, Desirée Gianardi, Matteo Palmeri, Gregorio Di Franco, Matteo Bianchini, Gianni Stefanini, Simone Guadagni, Giulio Di Candio, General Surgery Unit, Department of Translational Research and New Technologies in Medicine and Surgery, University of Pisa, Pisa 56124, Italy

Luca Morelli, EndoCAS (Center for Computer Assisted Surgery), University of Pisa, Pisa 56124, Italy

Corresponding author: Luca Morelli, FACS, MD, Associate Professor, General Surgery Unit, Department of Translational Research and New Technologies in Medicine and Surgery, University of Pisa, Via Paradisa 2, Pisa 56124, Italy. luca.morelli@unipi.it
Telephone: +39-50-995470
Fax: +39-50-996985

Abstract

BACKGROUND

Walled-off pancreatic necrosis (WOPN) is a late complication of acute pancreatitis. The management of a WOPN depends on its location and on patient's symptoms. Trans-gastric drainage and debridement of WOPN represents an important surgical treatment option for selected patients. The da Vinci surgical System has been developed to allow an easy, minimally invasive and fast surgery, also in challenging abdominal procedures. We present here a case of a WOPN treated with a robotic trans-gastric drainage using the da Vinci Xi.

CASE SUMMARY

A 63-year-old man with an episode of acute necrotizing pancreatitis was referred to our center. Six wk after the acute episode the patient developed a walled massive fluid collection, with an extensive pancreatic necrosis, causing obstruction of the gastrointestinal tract. The patient underwent a robotic trans-gastric drainage and debridement of the WOPN performed with the da Vinci Xi platform. Firstly, an anterior ideal gastrotomy was carried out, guided by intraoperative ultrasound (US)-scan using the TilePro™ function. Then, through the gastrotomy, the best location for drainage on the posterior gastric wall was again US-guided identified. The anastomosis between the posterior gastric wall and the walled-off necrosis wall was carried out with the new EndoWrist stapler with vascular cartridge. Debridement and washing of the cavity through the

Checklist (2016), and the manuscript was prepared and revised according to the CARE Checklist (2016).

Manuscript source: Invited manuscript

Received: January 26, 2019
Peer-review started: January 28, 2019
First decision: April 18, 2019
Revised: April 24, 2019
Accepted: May 2, 2019
Article in press: May 3, 2019
Published online: June 26, 2019

P-Reviewer: Isik A, Paydas S, Sun S
S-Editor: Ji FF
L-Editor: A
E-Editor: Xing YX

anastomosis were performed. Finally, the anterior gastrotomy was closed and the cholecystectomy was performed. The postoperative course was uneventful and a post-operative computed tomography-scan showed the collapse of the fluid collection.

CONCLUSION
In selected cases of WOPN the da Vinci Surgical System can be safely used as a valid surgical treatment option.

Key words: Case report; da Vinci Xi; EndoWrist stapler; Walled-off pancreatic necrosis; TilePro; Minimally-invasive surgery

Core tip: Trans-gastric drainage and debridement of the walled-off pancreatic necrosis is a valid surgical treatment in selected cases. The da Vinci Xi robotic platform with its increased flexibility, together with its new technologies, gives advantages in performing this surgical procedure. In particular, the new EndoWrist robotic stapler, noting the suitable thickness of the tissues between the branches, should reduce the risk of bleeding related to the cystogastrostomy. Moreover, it can be articulated with a range of 108° allowing the operator to directly control all the steps of the suture. Finally, the TilePro™ function can superimpose ultrasound imaging on the console screen, alongside the operatory field, giving high degree of precision in defining the best location for the gastrostomy.

Citation: Morelli L, Furbetta N, Gianardi D, Palmeri M, Di Franco G, Bianchini M, Stefanini G, Guadagni S, Di Candio G. Robot-assisted trans-gastric drainage and debridement of walled-off pancreatic necrosis using the EndoWrist stapler for the da Vinci Xi: A case report. *World J Clin Cases* 2019; 7(12): 1461-1466
URL: https://www.wjgnet.com/2307-8960/full/v7/i12/1461.htm
DOI: https://dx.doi.org/10.12998/wjcc.v7.i12.1461

INTRODUCTION

Walled-off pancreatic necrosis (WOPN), first described by Connor *et al*[1], is a late complication of acute pancreatitis that generally needs some interventions[2]. WOPN represents a challenging critical problem and it is still burdened by a high rate of mortality and morbidity[3]. The management of a WOPN depends on its location and on patient's symptoms. Trans-gastric drainage and debridement of WOPN represents an important surgical treatment option for selected patients[4].

While laparoscopic trans-gastric drainage of WOPN is well-described in the literature, only few cases of robotic approach have been published[5-7]. Furthermore, these described cases were all performed with the da Vinci Si platform and without the use of the TilePro™ function and the robotic EndoWrist staplers. Herein we report the case of a WOPN treated with a trans-gastric drainage and debridement using the da Vinci Xi surgical system with its tools such as the EndoWrist stapler and the TilePro™ function.

CASE PRESENTATION

Chief complaints

A 63-year-old man presented an acute episode of postprandial epigastric pain and vomiting.

History of present illness

An acute necrotizing pancreatitis was found at computed tomography (CT) scan at the time of admission. The patient was subsequently admitted to the Intensive Care Unit and underwent medical conservative treatment (nihil *per os* and total parenteral nutrition), with progressive normalization of pancreatic enzymes. After 6 wk the patient developed a walled massive fluid collection, with an extensive pancreatic

necrosis, causing obstruction of the gastrointestinal tract.

History of past illness

Hypertension, dyslipidemia, chronic alcohol consumption and smoking.

Physical examination upon admission

During the physical examination the patient presented diffusive abdominal pain. Vital signs on admission were as follows: temperature was 37.2 °C, heart rate was 94 beats per minute (bpm), initial blood pressure was 115/70 mmHg. In addition, his lungs and heart were found to be normal by auscultation. He always remained cardiovascularly stable.

Laboratory examinations

Abnormal laboratory data at time of admission of complete blood count were as follows: RBC 3.76 × 10^6/μL, Hb 11.7 g/dL, HCT 34.7%, MCHC 256 g/L, WBC 18.15 × 10^3/μL, PLT 580 × 10^3/μL, lipase 3165 U/L, amylase 2765 U/L and the latter progressively decreased in the days after admission.

Imaging examinations

The CT-scan performed at the time of admission showed an extensive pancreatic necrosis with multiple perivisceral fluid collections. CT-scans performed 1 and 3 wk after the admission revealed the development of a walled massive fluid collection (7 cm × 20 cm × 18 cm). The CT-scan performed 6 wk after the acute episode confirmed the presence of a WOPN with increased dimensions that compressed the stomach and the first duodenal portion.

FINAL DIAGNOSIS

WOPN.

TREATMENT

A trans-gastric drainage and debridement was successfully performed using the da Vinci Xi robotic platform. The procedure was completed in 130 min. Firstly, guided by intraoperative ultrasound (US)-scan, an anterior ideal gastrotomy was carried out (Figure 1). The intra-operative US scan was performed with a dedicated robotic probe using the TilePro™ function. This technology consents the surgeon to view 3D video of the operative field along with ultrasound exam. Then, through the gastrotomy, the best location for drainage on the posterior gastric wall was again US-guided identified. The anastomosis between the posterior gastric wall and the walled-off necrosis wall was carried out with the new EndoWrist stapler with vascular cartridge (Figure 2). Debridement and washing of the cavity through the anastomosis were performed (Figure 3). Finally, the anterior gastrotomy was closed with three layers of 3-0 V-Lock running sutures and the cholecystectomy was performed.

OUTCOME AND FOLLOW-UP

No intra-operative complications were recorded. The postoperative course was uneventful and a post-operative CT-scan showed the collapse of the fluid collection. Six months after discharge, the patient underwent abdominal ultrasound that confirmed the complete collapse of the abdominal fluid collections and the good mid-term result of the operation. The scheduled follow-up consists in blood tests and ultrasound examination every 6 months. CT-scan or MRI will be reserved for any variations in clinical evaluation.

DISCUSSION

The advantages of a minimally-invasive approach for the treatment of pancreatic pseudocysts and WOPN are well known[8,9]. In the last decades different minimally invasive approaches have been described in literature, including endoscopic[10], laparoscopic[11,12], SILS[13] and robotic approach[5-7]. Several cases of laparoscopic drainage of pancreatic pseudocysts by cystogastrostomy have been described since the late 90s by Smadja *et al*[14]. Recently, Dua *et al*[12] analyzed the outcomes of 46

Figure 1 TilePro™ function, used to identify the best location for anterior gastrotomy, consenting the surgeon to view 3D video of the operative field along with ultrasound exam.

patients underwent open and laparoscopic trans-gastric pancreatic necrosectomy, in terms of postoperative complications and mortality. Thirty-seven of these patients were treated with a laparoscopic approach and 9 with an open one. In this case series, with a median post-operative hospital stay of 6 d, 4 patients have required a percutaneous drainage for residual fluid collection and only 6 patients (13%) had postoperative bleeding. Series of robotic approaches are lacking in literature, only some isolated case reports are present[5-7], demonstrating all the feasibility of robotic cystogastrostomy and the possibility to easier perform the debridement of the cavity.

The endoscopic approach remains a valid option for WOPN, as reported in several papers, but, in our experience, it results more indicated for the treatment of pancreatic pseudocysts, where there is not a solid component. Indeed, in the WOPN which requires extended debridement, the endoscopic approach can be very laborious and often it does not lead to the desired result. In fact, it allows to perform a small communication between the stomach and the cavity, draining predominantly the fluid component. On the other hand, in case of WOPN with significant solid component and characterized by irregular shape, the endoscopic instruments may not allow the extensive debridement that we have obtained with the described technique.

Thus, we proposed a robotic technique that presents three main key points: (1)The increased dexterity guaranteed by the robotic technology which allows to perform a safer and more radical debridement of the WOPN cavity; (2) The use of the new EndoWrist robotic stapler with the smart clamp technology, which could reduce the risk of bleeding related to the cystogastrostomy; (3) The Tile-pro™ function which gives high degree of precision in defining the best location for the gastrostomy and in detecting the presence of blood vessels.

As described in the "2012 revision of the Atlanta Classification of acute pancreatitis"[2] the WOPN ("a mature, encapsulated acute necrotic collection with a well defined inflammatory wall") differs from the pancreatic pseudocyst ("an encapsulated, well defined collection of fluid but no or minimal solid component") based on the presence of a solid component and the onset timing, with a direct implication on the necessity and on the difficulty in the performing the debridement. Indeed, usually in the treatment of a pancreatic pseudocyst the only need is to let the cyst communicate with the stomach or the bowel in order to drain the liquid, thus reducing the pressure inside the pseudocyst. Instead, the necrotic material contained within the WOPN is usually denser and requires a substantial debridement. In this context, in dealing with the WOPN, the dexterity of the robotic platform can give advantages compared to laparoscopy in the execution of a more extensive and safer debridement. Indeed, the debridement of the large, irregular cavity could be compromised because of the kinematics limitations of laparoscopy, mainly due to the less degrees of freedom which limit the accessibility to the cavity in all directions and angles. The only limitation of this robotic procedure can be the lack of tactile feedback, but it could be overcome with the surgeon's experience.

The issue of bleeding after the pseudocystogastrostomy is well known and described in literature[15-17] and it is due to the state of inflammation resulting from the pancreatitis and to the exposure of the suture to gastric acidity. Furthermore, the gastric wall is highly vascularized and the suture performed is not always completely hemostatic. The robotic stapler used in this case report thanks to the smart clamp technology, is able to note the suitable thickness of the tissues between the branches, guaranteeing to perform the suture only if the chosen charge is compatible. In this way, the controlled use of the stapler with a vascular charge, when allowed by the

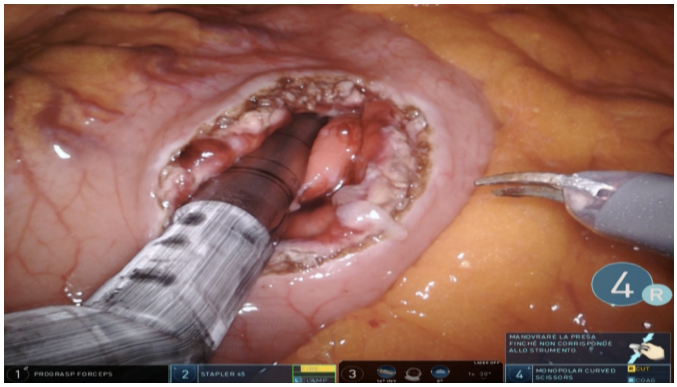

Figure 2 Anastomosis between the posterior gastric wall and the walled-off necrosis wall carried out with the new EndoWrist stapler with vascular cartridge.

system, reduces the risk of post-operative bleeding, the main feared problem of this procedure. Moreover, the robotic stapler with its new EndoWrist technology can be articulated with a range of 108° and allows the operator to directly control all the steps of the suture ("positioning, grip, clamp and fire"). Finally, the new Tilepro™ function and the Xi platform, used in this case report, brought further benefits in the execution of the surgical procedure.

We used a dedicated intraoperative US probe (12-5 MHz, linear curved array, BK Medical APS, Peabody MA, United States) to identify the best location for the gastrostomy. This probe can be introduced through the assistant port and it is designed to perfectly fit the robotic instruments in order to join the maximum direct control. The TilePro™ function can superimpose ultrasound imaging on the console screen, alongside the 3D vision of the operatory field, eliminating several problems related to hand-eye coordination[18]. This specific robotic ultrasound probe, thanks to the flexible cable and the small surface, can give more flexibility than those used in pure laparoscopy, because the surgeon sitting at the console is able to manipulate the probe tip directly with the dominant hand, maintaining the perpendicular contact to the target with a high degree of precision in defining the best location for the gastrostomy and in detecting the presence of blood vessels.

The use of the Xi robotic platform is the latest addition to this clinical case. Indeed, the few previously described cases had all been performed with the Si platform[5-7]. The WOPN cavity can be anfractuous, irregular and long, increasing the risk of conflicts between the instruments. Therefore, the new da Vinci Xi, having more flexibility and reducing the risk of collision between the arms, could allow a better accessibility in the cavity during the debridement.

CONCLUSION

In selected cases of WOPN the da Vinci Surgical System can be safely used as a valid surgical treatment option in alternative to the endoscopic and to the laparoscopic approach. The enhanced surgical dexterity and the EndoWrist stapler together with the Tile-Pro multi-input display and the new Xi platform, could give some advantages in the treatment of this challenging disease.

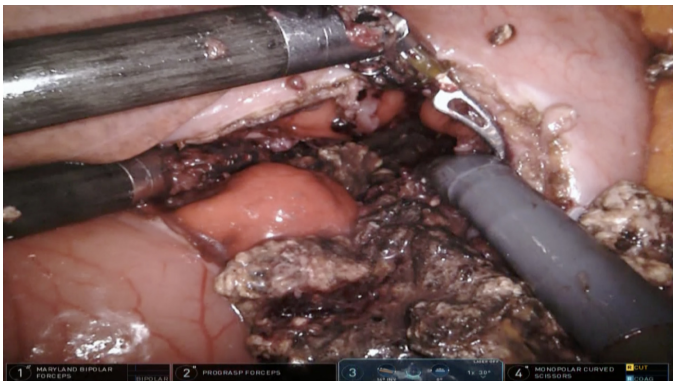

Figure 3 Debridement and washing of the cavity performed through the anastomosis.

REFERENCES

1 **Connor S**, Raraty MG, Howes N, Evans J, Ghaneh P, Sutton R, Neoptolemos JP. Surgery in the treatment of acute pancreatitis--minimal access pancreatic necrosectomy. *Scand J Surg* 2005; **94**: 135-142 [PMID: 16111096 DOI: 10.1177/145749690509400210]

2 **Sarr MG**. 2012 revision of the Atlanta classification of acute pancreatitis. *Pol Arch Med Wewn* 2013; **123**: 118-124 [PMID: 23396317 DOI: 10.1136/gutjnl-2012-304051]

3 **Boškoski I**, Costamagna G. Walled-off pancreatic necrosis: where are we? *Ann Gastroenterol* 2014; **27**: 93-94 [PMID: 24733647]

4 **Kulkarni S**, Bogart A, Buxbaum J, Matsuoka L, Selby R, Parekh D. Surgical transgastric debridement of walled off pancreatic necrosis: an option for patients with necrotizing pancreatitis. *Surg Endosc* 2015; **29**: 575-582 [PMID: 25055889 DOI: 10.1007/s00464-014-3700-x]

5 **Nassour I**, Ramzan Z, Kukreja S. Robotic cystogastrostomy and debridement of walled-off pancreatic necrosis. *J Robot Surg* 2016; **10**: 279-282 [PMID: 27039191 DOI: 10.1007/s11701-016-0581-0]

6 **Kirks RC**, Sola R, Iannitti DA, Martinie JB, Vrochides D. Robotic transgastric cystgastrostomy and pancreatic debridement in the management of pancreatic fluid collections following acute pancreatitis. *J Vis Surg* 2016; **2**: 127 [PMID: 29078515 DOI: 10.21037/jovs.2016.07.04]

7 **Cardenas A**, Abrams A, Ong E, Jie T. Robotic-assisted cystogastrostomy for a patient with a pancreatic pseudocyst. *J Robot Surg* 2014; **8**: 181-184 [PMID: 27637530 DOI: 10.1007/s11701-013-0428-x]

8 **Redwan AA**, Hamad MA, Omar MA. Pancreatic Pseudocyst Dilemma: Cumulative Multicenter Experience in Management Using Endoscopy, Laparoscopy, and Open Surgery. *J Laparoendosc Adv Surg Tech A* 2017; **27**: 1022-1030 [PMID: 28459653 DOI: 10.1089/lap.2017.0006]

9 **Worhunsky DJ**, Qadan M, Dua MM, Park WG, Poultsides GA, Norton JA, Visser BC. Laparoscopic transgastric necrosectomy for the management of pancreatic necrosis. *J Am Coll Surg* 2014; **219**: 735-743 [PMID: 25158913 DOI: 10.1016/j.jamcollsurg.2014.04.012]

10 **ASGE Standards of Practice Committee**. Muthusamy VR, Chandrasekhara V, Acosta RD, Bruining DH, Chathadi KV, Eloubeidi MA, Faulx AL, Fonkalsrud L, Gurudu SR, Khashab MA, Kothari S, Lightdale JR, Pasha SF, Saltzman JR, Shaukat A, Wang A, Yang J, Cash BD, DeWitt JM. The role of endoscopy in the diagnosis and treatment of inflammatory pancreatic fluid collections. *Gastrointest Endosc* 2016; 481-488 [PMID: 26796695 DOI: 10.1016/j.gie.2015.11.027]

11 **Gerin O**, Prevot F, Dhahri A, Hakim S, Delcenserie R, Rebibo L, Regimbeau JM. Laparoscopy-assisted open cystogastrostomy and pancreatic debridement for necrotizing pancreatitis (with video). *Surg Endosc* 2016; **30**: 1235-1241 [PMID: 26275532 DOI: 10.1007/s00464-015-4331-6]

12 **Dua MM**, Worhunsky DJ, Malhotra L, Park WG, Poultsides GA, Norton JA, Visser BC. Transgastric pancreatic necrosectomy-expedited return to prepancreatitis health. *J Surg Res* 2017; **219**: 11-17 [PMID: 29078869 DOI: 10.1016/j.jss.2017.05.089]

13 **Singh Y**, Cawich SO, Olivier L, Kuruvilla T, Mohammed F, Naraysingh V. Pancreatic pseudocyst: combined single incision laparoscopic cystogastrostomy and cholecystectomy in a resource poor setting. *J Surg Case Rep* 2016; **2016**: pii: rjw176 [PMID: 27803243 DOI: 10.1093/jscr/rjw176]

14 **Smadja C**, Badawy A, Vons C, Giraud V, Franco D. Laparoscopic cystogastrostomy for pancreatic pseudocyst is safe and effective. *J Laparoendosc Adv Surg Tech A* 1999; **9**: 401-403 [PMID: 10522534 DOI: 10.1089/lap.1999.9.401]

15 **George A**, Panwar R, Pal S. Surgical Management of Life Threatening Bleeding after Endoscopic Cystogastrostomy. *J Invest Surg* 2017; 1-6 [PMID: 28945487 DOI: 10.1080/08941939.2017.1362081]

16 **Nielsen OS**. Bleeding after pancreatic cystogastrostomy. *Acta Chir Scand* 1979; **145**: 247-249 [PMID: 494972]

17 **Ikoma A**, Tanaka K, Ishibe R, Ishizaki N, Taira A. Late massive hemorrhage following cystogastrostomy for pancreatic pseudocyst: report of a case. *Surg Today* 1995; **25**: 79-82 [PMID: 7749296 DOI: 10.1007/BF00309393]

18 **Guerra F**, Amore Bonapasta S, Annecchiarico M, Bongiolatti S, Coratti A. Robot-integrated intraoperative ultrasound: Initial experience with hepatic malignancies. *Minim Invasive Ther Allied Technol* 2015; **24**: 345-349 [PMID: 25835093 DOI: 10.3109/13645706.2015.1022558]

World Journal of Clinical Cases

Submit a Manuscript: https://www.f6publishing.com

World J Clin Cases 2019 June 26; 7(12): 1467-1474

DOI: 10.12998/wjcc.v7.i12.1467

ISSN 2307-8960 (online)

CASE REPORT

Fulminant liver failure following a marathon: Five case reports and review of literature

Wojciech Figiel, Marcin Morawski, Michał Grąt, Oskar Kornasiewicz, Grzegorz Niewiński, Joanna Raszeja-Wyszomirska, Maciej Krasnodębski, Arkadiusz Kowalczyk, Wacław Hołówko, Waldemar Patkowski, Krzysztof Zieniewicz

ORCID number: Wojciech Figiel (0000-0001-9716-7824); Marcin Morawski (0000-0002-7056-8668); Michał Grąt (0000-0003-3372-3072); Oskar Kornasiewicz (0000-0003-4027-0059); Grzegorz Niewiński (0000-0002-3185-5250); Joanna Raszeja-Wyszomirska (0000-0001-7204-9784); Maciej Krasnodębski (0000-0002-6234-615X); Arkadiusz Kowalczyk (0000-0002-2765-1271); Wacław Hołówko (0000-0003-1419-2704); Waldemar Patkowski (0000-0002-6238-1967); Krzysztof Zieniewicz (0000-0003-4481-1289).

Author contributions: Figiel W, Morawski M designed the study concept; Figiel W, Morawski M, Grąt M, Kornasiewicz O, Niewiński G, Raszeja-Wyszomirska J, Krasnodębski M, Kowalczyk A, Hołówko W, Patkowski W collected the data; Figiel W, Morawski M, Zieniewicz K analyzed the data; Figiel W, Morawski M wrote the draft of the article; all authors critically revised the manuscript; Zieniewicz K supervised the study.

Supported by the Foundation for Polish Science (FNP) with START stipend, No. START 032.2018.

Informed consent statement: Informed consent statement was obtained from the reported patients.

Conflict-of-interest statement: The authors deny any conflict of interest.

Wojciech Figiel, Marcin Morawski, Michał Grąt, Oskar Kornasiewicz, Maciej Krasnodębski, Arkadiusz Kowalczyk, Wacław Hołówko, Waldemar Patkowski, Krzysztof Zieniewicz, Department of General, Transplant, and Liver Surgery, Medical University of Warsaw, Warsaw 02097, Poland

Grzegorz Niewiński, Department of Anaesthesiology and Intensive Care, Medical University of Warsaw, Warsaw 02097, Poland

Joanna Raszeja-Wyszomirska, Liver and Internal Medicine Unit, Department of General, Transplant, and Liver Surgery, Medical University of Warsaw, Warsaw 02097, Poland

Corresponding author: Marcin Morawski, MD, Doctor, PhD student, Department of General, Transplant, and Liver Surgery, Medical University of Warsaw, ul. Banacha 1A, Warsaw 02097, Poland. marcin.morawski@wum.edu.pl
Telephone: +48-22-5992545
Fax: +48-22-5991545

Abstract

BACKGROUND

The growing popularity of marathon and half-marathon runs has led to an increased number of patients presenting with exertion-induced heat stroke. Mild hepatic involvement is often observed in these patients; however, fulminant liver failure may occur in approximately 5% of all cases. Liver transplantation is a potentially curative approach for exertion-induced liver failure, although there is a lack of consensus regarding the criteria and optimal timing of this intervention.

CASE SUMMARY

This paper describes 5 patients (4 men and 1 woman) who were referred to the department where this study was performed with the diagnosis of exertion-induced acute liver failure. Three patients underwent liver transplantation, 1 recovered spontaneously, and 1 patient died on day 11 following the exertion.

CONCLUSION

Exertion-induced heat stroke may present as fulminant liver failure. These patients may recover with conservative treatment, may require liver transplantation, or may die. No definitive criteria are available to determine patient suitability for a conservative *vs* surgical approach.

CARE Checklist (2016) statement: The authors have read the CARE Checklist (2016), and the manuscript was prepared and revised according to the CARE Checklist (2016).

Manuscript source: Unsolicited manuscript

Received: March 3, 2019
Peer-review started: March 4, 2019
First decision: April 18, 2019
Revised: April 29, 2019
Accepted: May 1, 2019
Article in press: May 2, 2019
Published online: June 26, 2019

P-Reviewer: Nag DS
S-Editor: Dou Y
L-Editor: A
E-Editor: Xing YX

Key words: Heat Stroke; Hepatic insufficiency; Liver transplantation; Case report

Core tip: Patients with exertion-induced heat stroke may develop fulminant liver failure and may recover with conservative treatment alone or require liver transplantation. To date, there is a lack of definitive criteria to identify patients who could potentially benefit from a surgical vs. a conservative approach. This study discusses a series of 5 cases in which the following 3 distinct clinical outcomes were observed in patients: spontaneous recovery, the need for liver transplantation, and death following exertion-induced liver failure.

Citation: Figiel W, Morawski M, Grąt M, Kornasiewicz O, Niewiński G, Raszeja-Wyszomirska J, Krasnodębski M, Kowalczyk A, Hołówko W, Patkowski W, Zieniewicz K. Fulminant liver failure following a marathon: Five case reports and review of literature. *World J Clin Cases* 2019; 7(12): 1467-1474
URL: https://www.wjgnet.com/2307-8960/full/v7/i12/1467.htm
DOI: https://dx.doi.org/10.12998/wjcc.v7.i12.1467

INTRODUCTION

In recent years, marathons have gained widespread popularity and attract both, professional and homegrown runners. More than 800 races are held every year[1], usually during the spring and summer, when high external temperature and humidity can create unfavorable conditions for exercise.

Heat produced by the human body at rest is a by-product of baseline metabolism. Homeostatic mechanisms tend to maintain the core body temperature within a range of 37 ± 0.5 °C[2]. The liver, the heart, and the brain are organs with high metabolic rates and the main heat generators in the body. This heat is spread *via* the circulation to other body parts. Additional heat generated by the muscles during exercise can be dissipated by radiation or conduction to prevent hyperthermic injury to organs only when the core temperature exceeds the external temperature. However, when the conditions are reversed, sweating and evaporation occur to achieve heat loss. Under unfavorable conditions (*e.g.*, high external temperature and humidity and/or strenuous exercise) sweating and evaporation may be inadequate with a consequent elevation in core body temperature and multi-organ failure, which is defined as exertional heat stroke (EHS).

Individuals with EHS show core temperature > 40 °C with consequent loss of consciousness and multi-organ damage[3]. Hepatic injury is common under such conditions; however, owing to the remarkable hepatic functional reserve, those affected might typically remain asymptomatic. However, acute liver failure has been reported in approximately 5% of patients with EHS[4]. Orthotopic liver transplantation (OLTx) is indicated in these individuals[5], although a few reports have described spontaneous recovery in such patients[4].

CASE PRESENTATION

Between 2005 and 2017, 4 patients (3 men and 1 woman) were referred to the Department of General, Transplant, and Liver Surgery at the Medical University of Warsaw, and 1 man was referred to the Department of General and Transplant Surgery in Szczecin following a marathon run with clinical and biochemical findings suggesting EHS-induced fulminant liver failure (FLF).

Case 1

A previously healthy 24-year-old man collapsed after a 10-km run and was admitted to a local hospital. On initial examination, he was conscious with body temperature of 39.9 °C and right upper quadrant abdominal tenderness, but no neurological symptoms. The patient reported slight upper abdominal discomfort lasting a few weeks before the marathon and also the use of protein and amino acid supplements as part of his preparations for the marathon. Blood tests performed on days 2 and 3 of

hospitalization revealed sudden elevation of serum alanine aminotransferase (ALT) and aspartate aminotransferase (AST) (ALT from 430 U/L to 8166 U/L and AST from 1397 U/L to 7550 U/L) (Figure 1A), lactate dehydrogenase (LDH) activity elevation from 4349 U/L to 10096 U/L, creatine kinase (CK) of 135400 U/L (indicating rhabdomyolysis), as well as deterioration of the synthetic function of the liver represented by an increased international normalized ratio (INR) of 7.12 (Figure 1B). Rhabdomyolysis caused acute kidney injury and elevation of serum creatinine levels (2.08 mg/dL, 4.70 mg/dL, and 6.28 mg/dL on days 1, 2, and 3, respectively) and a reduced estimated glomerular filtration rate (from 41.7 mL/min/1.73 m^2 to 11.7 mL/min/1.73 m^2). Owing to the progressive worsening of his clinical status and biochemical parameters, the patient was referred to the department where this study was performed on day 3. On admission to our department, the patient was completely conscious [Glasgow Coma Scale (GCS) = 15] and cooperative. He was anuric (serum creatinine = 5.29 mg/dL) with anasarca. His abdomen was soft with normal peristalsis with slight epigastric tenderness. Additionally, subconjunctival and subcutaneous right cubital fossa hemorrhage was observed. Triple-phase abdominal computed tomography (CT) showed mild pleural and pelvic effusions, and faint contrast enhancement of the liver parenchyma [without contrast: 15 Hounsfield Units (HU), arterial phase: 20 HU, portal phase: 33 HU].

Case 2

A previously healthy 26-year-old woman collapsed after a marathon run at the seaside (ambient temperature of 25°C) and was admitted to a local hospital. On initial examination, she was unconscious, with body temperature of 42°C, and upper body muscle rigidity. She regained consciousness within a few hours after admission; however, she demonstrated psychomotor irritability and reported upper abdominal discomfort. Head CT was performed to evaluate her prolonged upper body muscle rigidity, and the study was unremarkable. Blood tests performed on day 3 revealed markedly elevated serum ALT and AST levels of 6161 U/L and 7322 U/L, respectively (Figure 1C), LDH of 38910 U/L, serum CK levels > 40000 U/L (indicating rhabdomyolysis), as well as severe deterioration of the synthetic function of the liver represented by an increased INR of 18.1 on day 3 (Figure 1D). Owing to the severe hepatic impairment and rhabdomyolysis, the patient was referred to the department where this study was performed on day 3 to assess her suitability to undergo urgent liver transplantation. On admission to our department, the patient was stuporous. Her laboratory test results showed signs of acute renal failure (serum creatinine = 4.2 mg/dL) and disseminated intravascular coagulation (DIC, INR = 18.1, D-dimer = 13310 μg/mL, 28000 platelets/mm^3, fibrinogen = 79 mg/dL) with no signs of hemorrhage or active bleeding.

Case 3

A previously healthy 27-year-old man collapsed after an 11-km marathon run and was admitted to a local hospital. On initial examination, he was unconscious, and his initial medical records did not show details of his temperature, neurological status, or the efforts made to reduce his body temperature. He regained consciousness within a few hours after admission and was asymptomatic except for upper abdominal discomfort. Owing to rapid elevation of liver function tests on day 2 (Figures 1E, 1F), he was transferred to the department where this study was performed on day 2 for further evaluation. On admission to our department, the patient was fully conscious (GCS = 15) and only reported mild upper abdominal tenderness. His serum AST and ALT levels were high at 2916 U/L and 4085 U/L, respectively, LDH elevation to 3557 U/L, thrombocytopenia of 74000 platelets/mm^3, and INR = 1.74.

Case 4

A previously healthy 33-year-old man collapsed after running several kilometers during a marathon (ambient temperature = 30 °C) and was admitted to a local hospital. On admission, he was comatose (GCS = 6) with blood pressure of 90/60 mmHg, as well as nuchal and upper body muscle rigidity. CT upon admission did not show any abnormalities of the central nervous system. His early medical records did not show any information regarding body temperature or endeavors to reduce hyperthermia. He regained consciousness within a few hours after admission and was treated conservatively with crystalloid infusion. Assessment performed on consecutive days showed laboratory tests indicating DIC (INR = 8.81, 23000 platelets/mm^3) accompanied by anterior chest wall hemorrhages without any signs of major bleeding. He was treated with fresh frozen plasma and intramuscular vitamin K1 injections. Blood tests performed on days 3 and 4 showed marked elevation of serum AST, ALT, and bilirubin levels (Figures 1G, 1H). Owing to the development of anuria and deterioration of his condition, he was transferred to the intensive care unit

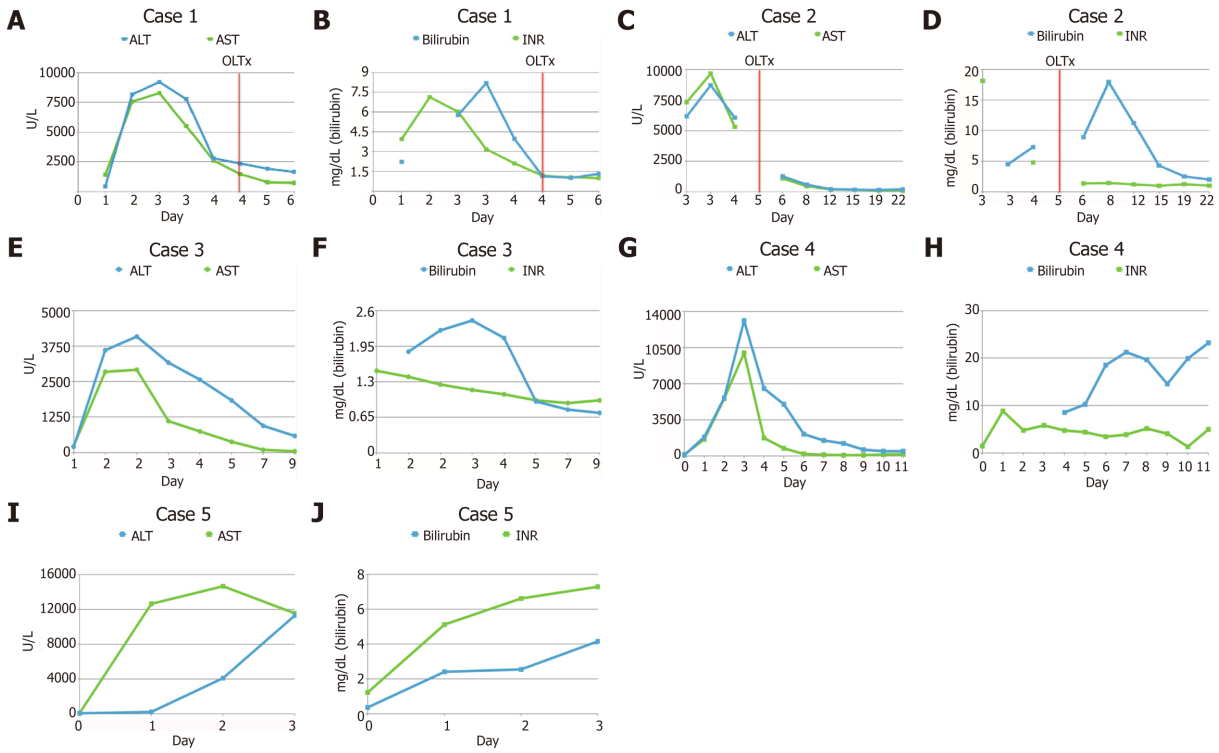

Figure 1 Laboratory findings following the exertion and liver transplantation. A, B: Case 1; C, D: Case 2; E, F: Case 3; G, H: Case 4; I, J: Case 5.

where he was intubated and continuous veno-venous hemodialysis was initiated. He was transferred to the department where this study was performed on day 7 following the exertion. On admission to our department, he was unconscious (GCS = 3) and was intubated.

Case 5

A previously healthy 39-year-old man fainted after running several kilometers during a marathon and was admitted to a local hospital. On admission, the patient was stuporous and presented with generalized seizures. However, clinical examination did not show any significant abnormalities, and body cooling efforts were not deemed necessary. His medical history revealed several-year treatment for bipolar disorder (carbamazepine, clomipramine, and piracetam). Owing to rapidly progressing liver failure (Figure 1I, 1J) and rhabdomyolysis (CK = 15755 U/L, myoglobin > 1000 μg/L), the patient was referred to the department where this study was performed on day 3 to assess his suitability to undergo liver transplantation. On admission to our department, he was conscious and cooperative but slightly drowsy.

FINAL DIAGNOSIS

In all five cases that were treated at our department, an exertion induced fulminant liver failure was confirmed the diagnostic follow up including other causes of fulminant liver failure. The diagnosis of heat stroke was established in accordance with criteria of Japanese Association of Acute Medicine Heat Stroke Committee Working Group[6].

TREATMENT

Case 1

Immediately after admission, the patient's case was reviewed by the transplant team, and he was shortlisted for OLTx as an urgent recipient. Continuous renal replacement therapy was initiated to treat persistent rhabdomyolysis. The patient received cryoprecipitate and prothrombin complex concentrate transfusions, as well as parenteral vitamin K1 owing to severe coagulopathy (INR = 6.02) and thrombocytopenia (50000 platelets/mm^3). OLTx was performed on day 4 following the

exertion. The liver was procured from a deceased donor and a piggy-back technique with end-to-end biliary anastomosis was used.

Case 2
Body cooling was performed in the emergency department. The patient was examined by the transplant team and considered an appropriate candidate to receive urgent OLTx, which was performed (using the liver from a deceased donor) on day 5 following her initial admission to the previous hospital. A standard piggy-back technique and end-to-end biliary anastomosis were performed.

Case 3
The case was reviewed by the transplant team, and the patient was listed for urgent OLTx.

Case 4
Immediately after arrival to our department, his case was reviewed by our transplant team, and he was listed as an urgent candidate for OLTx. On day 9 following exertion, progression of liver failure necessitated the institution of the Prometheus liver support therapy system.

Case 5
The case was reviewed by the transplant team, and he was listed as a candidate for OLTx. The OLTx was performed on day 4 following the exertion. The liver was procured from a deceased donor, and a piggy-back technique with end-to-end biliary anastomosis was used. A burst abdomen necessitated a reoperation on days 11 and 22 after the OLTx. His perioperative period was complicated by renal insufficiency treated with continuous veno-venous hemofiltration on the 1st and 2nd postoperative days.

OUTCOME AND FOLLOW-UP

Case 1
Liver and renal function recovered immediately after OLTx (day 5 onwards). Serum AST, ALT, bilirubin, and INR levels were normalized over a 30-d period following the OLTx (ALT = 63 U/L, AST = 31 U/L, bilirubin = 0.5 mg/dL, and INR = 0.98), and his serum creatinine level was sustained at 2.19 mg/dL. He was transferred from the surgical unit to the inpatient liver ward on post-transplantation day 10 and was discharged on postoperative day 30. He is presently 44 wk post-transplantation without any complaints.

Case 2
A rapid decrease in serum aminotransferases (ALT = 580 U/L and AST = 440 U/L on post-transplantation day 3 and restoration of hepatic synthetic function (INR = 1.37 on post-transplantation day 1) occurred following the OLTx. Persistent features of kidney failure (serum creatinine = 7.42 mg/dL on post-transplantation day 3) necessitated the initiation of hemodialysis over 2 d. Intra-abdominal hemorrhage necessitated 2 reoperations (on post-transplantation days 7 and 14). She was discharged on postoperative day 40 without any signs of liver or renal impairment. She is now 13 years post-transplantation.

Case 3
While awaiting a suitable graft, his biochemical parameters started improving, and his serum AST and ALT levels were 44 U/L and 584 U/L, respectively on day 9. He was discharged on day 9 following the exertion with no clinical and biochemical signs of liver or renal damage.

Case 4
On the following day after admission, the patient developed hypertensive urgency (blood pressure 320/220 mmHg) followed by a rapid decline in blood pressure requiring noradrenaline infusion. The incident was accompanied by bilaterally dilated pupils that soon became unreactive. CT showed intracerebral hemorrhage in the left parietal area. A second episode of severe elevation of blood pressure was observed, and the patient died on day 11 following the exertion.

Case 5
The patient was discharged on day 37 following OLTx after his laboratory test results showed normalization, with no signs of liver or renal function impairment. He is now

10 years post-transplantation.

DISCUSSION

This report discusses a case series comprising 5 previously healthy individuals who developed signs of EHS-induced FLF. All patients were screened for other causes of FLF including hepatitis B and C infection, Wilson's disease, autoimmune hepatitis, and hemochromatosis. Owing to a lack of admission records in a few patients, it was not possible to determine whether all patients met Bouchama's criteria for heat stroke[7], although all patients fulfilled the Japanese Association of Acute Medicine Heat Stroke Committee Working Group (JAAM-HS-WG) criteria[6]: The JAAM-HS-WG definition includes patients exposed to high environmental temperature meeting at least 1 of the following criteria: **(**1) GCS of ≤ 14; **(**2) Serum creatinine or total bilirubin levels of ≥ 1.2 mg/dL; and (3) JAAM DIC score of ≥ 4[8].

All patients in this case series showed the classical evolution of the clinical course observed in such cases, comprising the following: (1) Hyperthermic phase (neurological disturbances associated with hyperthermia); (2) Hematological and enzymatic phase (leukocytosis and hypocoagulability); and (3) Renal and hepatic phase (acute liver and renal failure)[9]. The mechanisms for heat-induced liver failure remain unclear; however, it has previously been suggested that heat-triggered systemic inflammation can cause multi-organ failure with consequent activation of multiple pathways promoting cell death including interleukin 1b and high mobility group box protein 1 downstream signaling[10,11]. It is also known that the pathophysiology of EHS-induced liver failure is associated with ischemia-induced hypoxic hepatitis[12], which may be attributed to systemic hypoperfusion caused by shunting of blood to the skin, thrombosis of inflow vessels, or congestive heart failure[12]. This hypothesis is supported in this study by the radiological finding of poor contrast enhancement in Case 1 suggesting flow disturbances in the liver parenchyma observed on day 3 [4,5,12,16-32] (Figure 1I) and significant hypotension (blood pressure 60/40 mmHg) upon admission in Case 4.

This study highlights 3 distinct clinical outcomes in these patients: (1) Death while awaiting a suitable graft; (2) OLTx; and (3) Spontaneous recovery with supportive treatment alone. These observations highlight the need for criteria to determine the necessity and urgency of OLTx. Currently, the King's College Criteria (KCC) and the Clichy criteria are widely accepted prognostic indicators to select patients with FLF who require OLTx. Based on the KCC, OLTx should be performed in patients presenting with non-acetaminophen-induced acute liver injury when the prothrombin time is longer than 100 s (INR > 6.5), or if any 3 of the following criteria are observed: (1) Prothrombin time > 50 s (INR > 3.5); (2) Age < 10 years or > 40 years; (3) Duration of jaundice before onset of encephalopathy > 7 d; (4) Total serum bilirubin level > 17.5 mg/dL; and (5) Etiology attributable to non-A and non-B hepatitis, halothane hepatitis, or idiosyncratic drug reactions[13]. In this study, 4 of 5 patients met the KCC within 3 d following exertion. Interestingly, the only patient who did not meet the KCC was Case 4 who recovered spontaneously. This observation suggests that KCC could potentially predict patient suitability for OLTx; however, further studies are warranted to verify this hypothesis. Patients with FLF are not routinely screened for Factor V levels at the hospital where this study was performed; therefore, identifying which patients met the Clichy criteria was not possible[14]. Furthermore, the Clichy criteria were designed to predict outcomes in patients with acute viral hepatitis, which would limit their value/applicability in patients with EHS-induced FLF[15].

A PubMed database search (keywords: Liver transplantation, heatstroke) yielded 20 cases of EHS-induced FLF (Figure 2). Of these 20 patients, 14 (70%) were treated conservatively and 6 (30%) received OLTx. Among the patients treated conservatively, 6 patients (43%) died and 8 (57%) recovered spontaneously.

CONCLUSION

This case series and a review of the literature show that EHS constitute a heterogeneous group of patients observed at emergency departments with varying clinical presentations. Thus, it is difficult to conclusively predict patient outcomes and the urgency of OLTx. Multicenter analysis of existing cases would help to establish more accurate guidelines to manage patients presenting with EHS-induced FLF.

Figure 2 Poor contrast enhancement of liver parenchyma in arterial phase in Case 1.

REFERENCES

1 **Day SM**, Thompson PD. Cardiac risks associated with marathon running. *Sports Health* 2010; **2**: 301-306 [PMID: 23015951 DOI: 10.1177/1941738110373066]
2 **Hutchison JS**, Ward RE, Lacroix J, Hébert PC, Barnes MA, Bohn DJ, Dirks PB, Doucette S, Fergusson D, Gottesman R, Joffe AR, Kirpalani HM, Meyer PG, Morris KP, Moher D, Singh RN, Skippen PW; Hypothermia Pediatric Head Injury Trial Investigators and the Canadian Critical Care Trials Group. Hypothermia therapy after traumatic brain injury in children. *N Engl J Med* 2008; **358**: 2447-2456 [PMID: 18525042 DOI: 10.1056/NEJMoa0706930]
3 **Adams T**, Stacey E, Stacey S, Martin D. Exertional heat stroke. *Br J Hosp Med (Lond)* 2012; **73**: 72-78 [PMID: 22504748 DOI: 10.12968/hmed.2012.73.2.72]
4 **Hadad E**, Ben-Ari Z, Heled Y, Moran DS, Shani Y, Epstein Y. Liver transplantation in exertional heat stroke: a medical dilemma. *Intensive Care Med* 2004; **30**: 1474-1478 [PMID: 15105986 DOI: 10.1007/s00134-004-2312-7]
5 **Hassanein T**, Perper JA, Tepperman L, Starzl TE, Van Thiel DH. Liver failure occurring as a component of exertional heatstroke. *Gastroenterology* 1991; **100**: 1442-1447 [PMID: 2013389 DOI: 10.1016/0016-5085(91)70036-W]
6 **Hifumi T**, Kondo Y, Shimizu K, Miyake Y. Heat stroke. *J Intensive Care* 2018; **6**: 30 [PMID: 29850022 DOI: 10.1186/s40560-018-0298-4]
7 **Bouchama A**, Knochel JP. Heat stroke. *N Engl J Med* 2002; **346**: 1978-1988 [PMID: 12075060 DOI: 10.1056/NEJMra011089]
8 **Gando S**, Saitoh D, Ogura H, Mayumi T, Koseki K, Ikeda T, Ishikura H, Iba T, Ueyama M, Eguchi Y, Otomo Y, Okamoto K, Kushimoto S, Endo S, Shimazaki S; Japanese Association for Acute Medicine Disseminated Intravascular Coagulation (JAAM DIC) Study Group. Disseminated intravascular coagulation (DIC) diagnosed based on the Japanese Association for Acute Medicine criteria is a dependent continuum to overt DIC in patients with sepsis. *Thromb Res* 2009; **123**: 715-718 [PMID: 18774163 DOI: 10.1016/j.thromres.2008.07.006]
9 **Epstein Y**. Exertional heatstroke: lessons we tend to forget. *Am J Med Sports* 2000; **2**: 143-152
10 **Leon LR**, Helwig BG. Heat stroke: role of the systemic inflammatory response. *J Appl Physiol (1985)* 2010; **109**: 1980-1988 [PMID: 20522730 DOI: 10.1152/japplphysiol.00301.2010]
11 **Geng Y**, Ma Q, Liu YN, Peng N, Yuan FF, Li XG, Li M, Wu YS, Li BL, Song WB, Zhu W, Xu WW, Fan J, Su L. Heatstroke induces liver injury via IL-1β and HMGB1-induced pyroptosis. *J Hepatol* 2015; **63**: 622-633 [PMID: 25931416 DOI: 10.1016/j.jhep.2015.04.010]
12 **Heneghan HM**, Nazirawan F, Dorcaratto D, Fiore B, Boylan JF, Maguire D, Hoti E. Extreme heatstroke causing fulminant hepatic failure requiring liver transplantation: a case report. *Transplant Proc* 2014; **46**: 2430-2432 [PMID: 24998305 DOI: 10.1016/j.transproceed.2013.12.055]
13 **O'Grady JG**, Alexander GJ, Hayllar KM, Williams R. Early indicators of prognosis in fulminant hepatic failure. *Gastroenterology* 1989; **97**: 439-445 [PMID: 2490426 DOI: 10.1016/0016-5085(89)90081-4]
14 **Pauwels A**, Mostefa-Kara N, Florent C, Lévy VG. Emergency liver transplantation for acute liver failure. Evaluation of London and Clichy criteria. *J Hepatol* 1993; **17**: 124-127 [PMID: 8445211 DOI: 10.1016/S0168-8278(05)80532-X]
15 **Bernuau J**, Samuel D, Durand F. Criteria for emergency liver transplantation in patients with acute viral hepatitis and factor V below 50% of normal: a prospective study. *Hepatology* 1991; **14**: 49A
16 **Berger J**, Hart J, Millis M, Baker AL. Fulminant hepatic failure from heat stroke requiring liver transplantation. *J Clin Gastroenterol* 2000; **30**: 429-431 [PMID: 10875474 DOI: 10.1097/00004836-200006000-00015]
17 **Chavoutier-Uzzan F**, Bernuau J, Degott C, Rueff B, Benhamou JP. [Heatstroke: a rare cause of massive hepatic necrosis due to hypoxia]. *Gastroenterol Clin Biol* 1988; **12**: 668-669 [PMID: 3063579]
18 **Dunker M**, Rehm M, Briegel J, Thiel M, Schelling G. [Exertion-related heat stroke. Lethal multiorgan failure from accidental hyperthermia in a 23 year old athlete]. *Anaesthesist* 2001; **50**: 500-505 [PMID: 11496687 DOI: 10.1007/s001010100169]
19 **Feller RB**, Wilson JS. Hepatic failure in fatal exertional heatstroke. *Aust N Z J Med* 1994; **24**: 69 [PMID: 8002866 DOI: 10.1111/j.1445-5994.1994.tb04433.x]
20 **Fidler S**, Fagan E, Williams R, Dewhurst I, Cory CE. Heatstroke and rhabdomyolysis presenting as fulminant hepatic failure. *Postgrad Med J* 1988; **64**: 157-159 [PMID: 3174530 DOI: 10.1136/pgmj.64.748.157]
21 **Giercksky T**, Boberg KM, Farstad IN, Halvorsen S, Schrumpf E. Severe liver failure in exertional heat stroke. *Scand J Gastroenterol* 1999; **34**: 824-827 [PMID: 10499485 DOI: 10.1080/003655299750025778]

22 **Heyman SN**, Marmor S, Ben-Abraham R, Shani Y, Heled Y, Shapira I, Lifschitz-Mercer B, Amital H. [Multi-organ failure in a young soldier: a clinical-pathological meeting]. *Harefuah* 2002; **141**: 204-209, 220 [PMID: 11905096]

23 **Ichai C**, Ciais JF, Hyvernat H, Labib Y, Fabiani P, Grimaud D. [Fatal acute liver failure: a rare complication of exertion-induced heat stroke]. *Ann Fr Anesth Reanim* 1997; **16**: 64-67 [PMID: 9686100 DOI: 10.1016/S0750-7658(97)84282-7]

24 **Inayat F**, Virk HU. Liver Transplantation after Exertional Heatstroke-Induced Acute Liver Failure. *Cureus* 2016; **8**: e768 [PMID: 27738568 DOI: 10.7759/cureus.768]

25 **Jin Q**, Chen E, Jiang J, Lu Y. Acute hepatic failure as a leading manifestation in exertional heat stroke. *Case Rep Crit Care* 2012; **2012**: 295867 [PMID: 24826335 DOI: 10.1155/2012/295867]

26 Extreme physical effort in summer heat followed by collapse, stupor, purpura, jaundice and azotemia. *Am J Med* 1955; **18**: 659-670 [PMID: 14361451 DOI: 10.1016/0002-9343(55)90466-6]

27 **Pastor MA**, Pérez-Aguilar F, Ortiz V, Nicolás D, Berenguer J. [Acute hepatitis due to heatstroke]. *Gastroenterol Hepatol* 1999; **22**: 398-399 [PMID: 10592672]

28 **Saissy JM**. Liver transplantation in a case of fulminant liver failure after exertion. *Intensive Care Med* 1996; **22**: 831 [PMID: 8880256 DOI: 10.1007/BF01709530]

29 **Sørensen JB**, Ranek L. Exertional heatstroke: survival in spite of severe hypoglycemia, liver and kidney damage. *J Sports Med Phys Fitness* 1988; **28**: 108-110 [PMID: 3398504]

30 **Sukenik S**, Livnat S, Hausmann MJ, Sikuler E. [Heat stroke associated with massive hepatic necrosis]. *Harefuah* 1991; **121**: 425-429 [PMID: 1786888]

31 **Takahashi K**, Chin K, Ogawa K, Kasahara M, Sakaguchi T, Hasegawa S, Sumi K, Nakamura T, Tamaki A, Mishima M, Nakamura T, Tanaka K. Living donor liver transplantation with noninvasive ventilation for exertional heat stroke and severe rhabdomyolysis. *Liver Transpl* 2005; **11**: 570-572 [PMID: 15838872 DOI: 10.1002/lt.20400]

32 **Vescia FG**, Peck OC. Liver disease from heat stroke. *Gastroenterology* 1962; **43**: 340-343 [PMID: 13925606 DOI: 10.1016/S0016-5085(19)35014-0]

33 **Davis BC**, Tillman H, Chung RT, Stravitz RT, Reddy R, Fontana RJ, McGuire B, Davern T, Lee WM; Acute Liver Failure Study Group. Heat stroke leading to acute liver injury & failure: A case series from the Acute Liver Failure Study Group. *Liver Int* 2017; **37**: 509-513 [PMID: 28128878 DOI: 10.1111/liv.13373]

World Journal of Clinical Cases

Submit a Manuscript: https://www.f6publishing.com

World J Clin Cases 2019 June 26; 7(12): 1475-1482

DOI: 10.12998/wjcc.v7.i12.1475

ISSN 2307-8960 (online)

CASE REPORT

Gaucher disease in Montenegro - genotype/phenotype correlations: Five cases report

Snezana Vujosevic, Sanja Medenica, Vesko Vujicic, Milena Dapcevic, Nikola Bakic, Ruhua Yang, Jun Liu, Pramod K Mistry

ORCID number: Snezana Vujosevic (0000-0002-6939-0612); Sanja Medenica (0000-0002-6241-3033); Vesko Vujicic (0000-0003-3708-4204); Milena Dapcevic (0000-0002-1287-7788); Nikola Bakic (0000-0002-8198-1642); Ruhua Yang (0000-0001-6051-145X); Jun Liu (0000-0001-5206-3028); Pramod K Mistry (0000-0003-3447-6421).

Author contributions: Vujosevic S, Vujicic V and Mistry PK made the study design, execution, analysis, critical discussion and final approval; Medenica S made the study design, execution, analysis, manuscript drafting, final approval; Dapcevic M, Bakic N, Yang R and Liu J made the execution, analysis, final approval.

Informed consent statement: All study participants provided informed written consent for publication of this report.

Conflict-of-interest statement: The authors declare no conflicts of interest.

CARE Checklist (2016) statement: The authors have read the CARE Checklist (2016), and the manuscript was prepared and revised according to the CARE Checklist (2016).

Snezana Vujosevic, Sanja Medenica, Department of Endocrinology, Internal Medicine Clinic, Clinical Center of Montenegro, Faculty of Medicine, University of Montenegro, Podgorica 81000, Montenegro

Vesko Vujicic, Milena Dapcevic, Nikola Bakic, Hematology Department, Internal Medicine Clinic, Clinical Center of Montenegro, Faculty of Medicine, University of Montenegro, Podgorica 81000, Montenegro

Ruhua Yang, Jun Liu, Pramod K Mistry, Yale Lysosomal Disease Center and Inherited Metabolic Liver Disease Clinic, Yale University School of Medicine, New Haven, CT 06510, United States

Corresponding author: Sanja Medenica, MD, MSc, Doctor, Department of Endocrinology, Internal Medicine Clinic, Clinical Center of Montenegro, Ljubljanska bb, 81000 Podgorica, Montenegro. medenicasanja@gmail.com
Telephone: +38-26-9157843

Abstract

BACKGROUND

The most common lysosomal storage disorder is Gaucher disease (GD). It is a deficiency of lysosomal glucocerebrosidase (GBA) due to biallelic mutations in the *GBA* gene, characterized by the deposition of glucocerebroside in macrophage-monocyte system cells. The report targets clinical phenotypes of GD in order to correlate them with *GBA* gene mutations, as well as to identify *GBA* gene mutation in patients in Montenegro that are diagnosed with GD.

CASES SUMMARY

Five patients (4 male, 1 female) of type 1 GD (GD1) are reported. The age at diagnosis ranged from 7 to 40. Patients experienced delays of 1-12 years in diagnosis after the original onset of symptoms. The most common mode of presentation was a variable degree of splenomegaly and thrombocytopenia, while other symptoms included bone pain, hepatomegaly, abdominal pain and fatigue. Osteopenia was present in a majority of the patients: 4/5. All patients were found to have an asymptomatic Erlenmeyer flask deformity of the distal femur. On enzyme replacement therapy (ERT), the hematological and visceral parameters showed significant improvement, but no significant progression in bone mineral density was noticed. *GBA* gene sequencing revealed homozygosity for the *N370S* mutation in one patient. The genotypes of the other patients were N370S/55bp deletion, N370S/D409H (2 patients), and H255Q/N370S (1 patient).

Manuscript source: Unsolicited manuscript

Received: November 21, 2018
Peer-review started: November 21, 2018
First decision: March 10, 2019
Revised: May 1, 2019
Accepted: May 11, 2019
Article in press: May 11, 2019
Published online: June 26, 2019

P-Reviewer: Ma K, Piccaluga PP, Ali I, Gheita TA, Tanabe S
S-Editor: Dou Y
L-Editor: A
E-Editor: Wang J

CONCLUSION
The phenotypes of the GD1 encountered in Montenegro were severe but all responded well to ERT.

Key words: Gaucher disease; Lysosomal storage disorder; Glucocerebrosidase; *GBA* gene sequencing; Genotype; Case report

Core tip: This is the first report on Gaucher disease (GD) originating from Montenegro that presents clinical phenotypes of GD and glucocerebrosidase (*GBA*) gene mutations in patients in Montenegro that are diagnosed with GD and genotype/phenotype correlations. While *GBA* gene sequencing revealed a homozygosity for the *N370S* mutation in 1 patient, the genotypes of the other patients were N370S/55bp deletion, N370S/D409H (in 2 patients), and H255Q/N370S (1 patient). The phenotypes of the GD type 1 encountered were severe but all responded well to enzyme replacement therapy. Genetic testing for their progeny was also planned.

Citation: Vujosevic S, Medenica S, Vujicic V, Dapcevic M, Bakic N, Yang R, Liu J, Mistry PK. Gaucher disease in Montenegro - genotype/phenotype correlations: Five cases report. *World J Clin Cases* 2019; 7(12): 1475-1482
URL: https://www.wjgnet.com/2307-8960/full/v7/i12/1475.htm
DOI: https://dx.doi.org/10.12998/wjcc.v7.i12.1475

INTRODUCTION

The most common lysosomal storage is Gaucher disease (GD), occurring in 1 in every 850 live births for Ashkenazi Jews[1] and approximately from 1 in every 57000 to 1 in 75000 worldwide[2]. The most prominent characteristic of the disease is the accumulation of glucosphingolipids glucosylceramide and glucosylsphingosine within the lysosomes of mononuclear phagocytes[3]. The defect itself is a deficiency of glucocerebrosidase (GBA) due to biallelic mutations in the *GBA* gene[4], where significant clinical heterogeneity differentiates into three clinical subtypes that give rise to the appearance of the characteristic Gaucher cells[5]: Type 1 (GD1)-nonneuronopathic GD, type 2-acute neuronopathic GD, and type 3-chronic neuronopathic GD. Type 1 disease is commonly presented in patients by splenomegaly, anemia, and thrombocytopenia accompanied by potential subsequent bleeding; in addition, patients may also present hepatomegaly, bone pain or pathologic fractures[6]. Type 2 GD is rare, but may be present at birth or during infancy. It is characterized by a rapid neurodegenerative course with extensive visceral involvement, resulting in death within the first 2 years of life[7,8]. Type 3 GD is characterized by the slower progression of neurologic symptoms when compared to the acute type 2 GD, presenting with splenomegaly and/or hepatomegaly, seizures, skeletal malformations, as well as eye movement disorders, anemia, and respiratory problems. Patients suffering from type 3 GD often live into their early teens and adulthood[9]. Diagnosis can be confirmed by measuring GBA activity in peripheral blood leukocytes, whereby less than 15% of mean normal activity tests positive. Confirming the *GBA* gene mutation is also another means of diagnosis.

The aim of this study is to report clinical phenotypes of GD to correlate them with *GBA* gene mutations as well as to identify the *GBA* gene mutation in 5 patients (4 males and 1 female) in Montenegro that were diagnosed with GD. While an additional female patient was also diagnosed in Montenegro, the patient was lost to further follow-ups and is therefore not presented here.

CASE PRESENTATION

Chief complaints

Patient 1: Fatigue, left hip joint pain, poor quality of life.

Patient 2: Abdominal and lumbosacral pain, as well as loss of appetite.

Patient 3: Nasal bleeding, pain under the right costal arch.

Patient 4: Abdominal pain.

Patient 5: Abdominal pain, massive genital bleeding.

History of present illness

Patient 1: Patients symptoms were recognized 6 mo before admission with gradual worsening.

Patient 2: Patients symptoms were recognized 2 mo before admission with gradual worsening.

Patient 3: Patients symptoms were recognized 4 d before admission with gradual worsening.

Patient 4: Patients symptoms were recognized in early childhood; therapy was administrated at the age of 17.

Patient 5: Patients symptoms were recognized 3 mo before admission with gradual worsening.

History of past illness

Patient 1: Splenectomy was done at the age of 17 due to hypersplenism, previous chronic gastritis, gastroesophageal reflux disease, chronic hepatitis B.

Patient 2: Hypertension, pneumothorax in two occasions 1996 and 2003.

Patient 3: The patient experienced a spontaneous hemothorax on his right side at the age of 41 and 48. His pulmonary diffusion capacity for carbon monoxide was also low. Echocardiography showed a dilated left chamber. The patient was diagnosed with Parkinson's disease at the age of 55.

Patient 4: No past illness of disease.

Patient 5: Hepatosplenomegaly was detected in childhood at the age of 11, further diagnostics were not carried out in the interim.

Personal and family history

Patient 1: No family history of disease.

Patient 2: No family history of disease.

Patient 3: His brother had been previously diagnosed with GD.

Patient 4: No family history of disease.

Patient 5: Suture of a perineal rupture had been done following excessive bleeding after delivery. Two months subsequent to this incident, while undergoing a reconstructive operation of the cloaca, massive bleeding also occurred. No family history of disease.

Physical examination upon admission

Patient 1: Normal vital signs, abdomen slightly soar to touch, hepatomegaly.

Patient 2: By physical examination a systolic murmur at apex was found, abdominal pain, hepatosplenomegaly.

Patient 3: Abdominal pain, hepatosplenomegaly.

Patient 4: Under routine examination, abdominal pain and splenomegaly.

Patient 5: Normal vital sings, abdominal pain on examination.

Laboratory examination

Patient 1: Thrombocytopenia (84 × 109/L), Gaucher cells findings in the sternal bone marrow aspirate. Low beta-glucosidase activity (0.74 U/mL) in the leucocytes, accompanied by markedly elevated plasma-chitotriosidase activity (8685 nmol/h/mL) and a confirmation of the mutation N370S/55bp deletion.

Patient 2: Elevated serum transaminases (AST 135, ALT 154, GGT 261) and thrombocytopenia were noted (96 × 10^9/L). A cholecystectomy was conducted, normalizing the transaminase level, but the thrombocytopenia remained. Finding of

Gaucher cells from a bone marrow biopsy. Further low beta- glucosidase activity (0.58 U/mL) in the leucocytes and markedly elevated plasma-chitotriosidase activity (7752 nmol/h/mL). *GBA* gene sequencing revealed the genotype N370S/D409H.

Patient 3: Thrombocytopenia (79 × 10^9/L), Gaucher cells were found in bone marrow and liver biopsy. Low leucocyte-beta glucosidase activity (1.43 nmol/mg prot/h) and markedly elevated plasma-chitotriosidase activity (5397.5 nmol/h/mL). Subsequent *GBA* gene sequencing revealed the genotype N370S/D409H.

Patient 4: Slightly reduced platelet count (136 × 109/L), Gaucher cell in bone marrow biopsy, low leucocyte-beta glucosidase activity (0.32 U/mL) and markedly elevated plasma-chitotriosidase activity (28657 nmol/h/mL). The diagnosis was further confirmed by *GBA* gene sequencing for the genotype H255Q/N370S.

Patient 5: The laboratory analysis indicated a low platelet count (102 × 109/L), low leucocyte (3.1 × 109/L) beta-glucosidase (0.63 U/mL) activity and markedly elevated plasma-chitotriosidase activity (25578 nmol/h/mL), HBs, HCV, HIV negative. Gaucher cells in bone marrow biopsy. The *GBA* gene sequencing established homozygosity for the N370S mutation.

Imaging examination

Patient 1: Abdominal ultrasound liver (15 cm × 13 cm × 19 cm), magnetic resonance imaging (MRI) of the femurs and lumbosacral spine visualized an Erlenmeye flask deformity of both the distal femurs, bone marrow infiltration of both the femurs and diffuse bone marrow infiltration of the lumbal spine.

Patient 2: Abdominal-multislice computed tomography (MSCT) showed an enlarged liver (18 cm × 16 cm × 21cm) and spleen (23.5 cm × 8.5 cm × 8cm). Nuclear magnetic resonance (NMR) of LS spine and pelvis showed no pathological finding. An endocranial MR showed no pathological finding.

Patient 3: Hepatosplenomegaly (spleen 167 mm), MRI of the lumbosacral spine showed a hypodense zone as a sign of infiltration in the trochanter region on both sides. NMR of head normal finding.

Patient 4: Splenomegaly (ultrasound 19 cm), an MRI of the patient's bones indicated osteolytic leasions of both the femurs and the tibiae. No reduction in bone mineral density has since been found present by osteodensitometry.

Patient 5: Abdominal ultrasound liver 20 cm, spleen > 22 cm, pelvic CT scan no abnormalities.

FINAL DIAGNOSIS

GD 1.

TREATMENT

Patient 1

Enzyme replacement therapy (ERT) by imiglucerase initiating when the patient was 19 years old (30 IU/kg once, bi-weekly).

Patient 2

ERT by imiglucerase was recommended, but was only initiated after three years due to financial difficulties.

Patient 3

Eliglustat treatment was started at 55 years of age. However, owing to financial difficulties, was discontinued. At the age of 57, ERT by imiglucerase was initiated.

Patient 4

ERT with imiglucerase was started at the age of 17. The current dose is 40 IU/kg (once, bi-weekly).

Patient 5

ERT with imiglucerase was initiated four months after the diagnosis. The current dose is 40 IU/kg (once, bi-weekly).

OUTCOME AND FOLLOW-UP

Patient 1

Treatment was noncompliant. Owing to financial difficulties, ERT was discontinued at the age of 38.

Patient 2

The current dose administered is 40 IU/kg (once, bi-weekly).

Patient 3

The current dose is 40 IU/kg (once, bi-weekly).

Patient 4

His spleen diameter and hepatogram have since normalized in the treatment.

Patient 5

Spleen and liver diameters as well as her hepatogram have since normalized.

DISCUSSION

Concerning the cases covered in this report, whereas type 2 and 3 affect only 5% of patients, GD1 is the most common GD type[10]. It has been estimated that 66% of GD1 patients are diagnosed before the age of 20[11], but the age at diagnosis for these Montenegrin patients ranges from 7 to 40. Diagnosis thereof has been confirmed based on low leucocyte-acid beta-glucosidase activity and *GBA* gene mutation. The *GBA* gene is located on chromosome 1q21. Containing 11 exons and 10 introns and covering 7.6 kilobases of sequence, a highly homologous pseudogene is located 16 kb downstream where nearly 300 mutations and polymorphisms in GBA have been identified[12]. Mutations in saposin C, the β-GBA activator gene, have been reported in cases of GD[13] (Table 1.) The most distinct hallmark is the presence of Gaucher cells (Figure 1) in the macrophage monocyte system[14], in bone marrow or in liver biopsy samples. Patients generally experience delays of one to twelve years in diagnosis after the first onset of symptoms. The most common mode of presentation here is the variable degree of splenomegaly and thrombocytopenia, thought her symptoms include bone pain, hepatomegaly, abdominal pain and fatigue. Hematologic manifestations of GD include anemia, thrombocytopenia and less frequent leucopenia[15]. One patient suffered from profuse bleeding due to thrombocytopenia. Hypersplenism, accompanied by an increased risk of infection, rupture and infracts are some of the possible splenomegaly complications[7]. Osteopenia is present in a majority of the patients under review here: 4/5. All patients show an asymptomatic Erlenmeyer-flask deformity of the distal femur. Unusual manifestations in GD1 noted are malignancy, Parkinsonism and pulmonary hypertension[7,16]. Parkinsonism in GD1 is believed to arise from synuclein aggregation within dopaminergic neurons that are induced either by the gain of function mutations in GBA1 that lead to protein misfolding (N370S is such a mutation) or the accumulation of lipids[16]. Recent publications have established a link between GD and impaired host- defense against microbial infections, up-regulation of T-helper (Th)1 and Th2 cytokines, the dysfunction of monocytes, as well as an increased risk for lymphoid malignancies (most strikingly, for multiplemyeloma)[17].

In addition to the reduced acid beta-glucosidase activity and genotyping at the *GBA* gene locus that may yield additional prognostic information, elevated plasma-chitotriosidase activity can be found in GD[18]. Several markers are used in therapeutic monitoring: chitotriosidase, ferritin, ACE and acid phosphatase, but no prognostic marker can predict long-term complications of GD. All these markers also increase with disease progression as well as decrease under ERT[19]. The prognosis for type 1 or type3 GD patients receiving ERT is good, where in normal life expectancy is common. One study has estimated life expectancy at birth type 1 GD individuals to be 68 years, compared to 77 years in the general population[20]. Type-2 GD patients usually die within the first years of life. Patients who have a splenectomy are at a higher mortality risk[21], which may worsen skeletal and lung manifestations[20]. In a clinical sense, GBA1 mutations might not prove to be a reliable prognostic indicator in Parkinson's disease[22]. ERT is indicated for type 1 GD patients who also have anemia, thrombocytopenia, skeletal disease or visceromegaly[12,23]. An alternative oral approach is substrate synthesis inhibition therapy, based on inhibiting glucosylceramide synthesis[12]. When undergoing ERT, the hematological and visceral parameters indicate marked improvement; no significant progression in bone mineral density was found in these cases. The delay in initiating treatment for these cases under

Table 1 Genotype/phenotype correlations

Patient	Age at diagnosis	Symptoms and signs	Lab findings	Organomegaly; Bone disorder	Genetics	Children
Patient 1 Gender: M	8	Stunted growth; distended stomch; bone pain	Thrombocytopenia; Gaucher cells in BM; plasma: Chitotriosidase ↑; β-glucosidase ↓	Splenomegaly; Erlenmeyer flask deformity of both femurs	N370S/55bp	No
Patient 2 Gender: M	40	Loss of appetite; Abdominal and lumbosacral pain	Thrombocytopenia; Gaucher cells in BM; plasma: Chitotriosidase ↑; β-glucosidase ↓	Splenomegaly, hepatomegaly; No bone disorder	N370S/D409H	2
Patient 3 Gender: M	36	Nasal bleeding; pain under right costal arch	Thrombocytopenia; Gaucher cells in BM; plasma: Chitotriosidase ↑; β-glucosidase ↓	Splenomegaly, hepatomegaly; Infiltration in the trochanter region on both sides and LS spine	N370S/D409H	2
Patient 4 Gender: M	7	None	Thrombocytopenia; Gaucher cells in BM; plasma: Chitotriosidase ↑; β-glucosidase ↓	Splenomegaly; Both femurs and tibias were affected	H255Q/N370S	No
Patient 5 Gender: F	23	Massive bleeding after childbirth	Thrombocytopenia; Gaucher cells in BM; plasma: Chitotriosidase ↑; β-glucosidase ↓	Splenomegaly, hepatomegaly; No bone disorder	Homozygosity N370S	1

review stemmed from financial reasons not in the treatment itself.

In patients who are Ashkenazi Jews, the mutations N370S, 84GG, L444P and IVS2+1G account for over 90% of disease alleles[24]. The two mutations of N370S and L444P are common in Jewish and non-Jewish patients alike, but the latter exhibits a much wider range of genotype, in which homozygosis for L444P results in neuronopathic disease. The presence of a single mutant N370S allele, however, usually prevents neurological involvement[12]. The most prevalent disease genotype worldwide across many ethnicities is L444P. In those of European descent, it is the N370S/L444P mutation[16], which is often characterized by mild cytopenia and splenomegaly. Non-Jewish GD individuals are mostly compound heterozygotes. Patients who are homozygous for the N370S variant suffer from a milder disease than those who are compound heterozygous. *GBA* gene sequencing revealed homozygosity for the N370S mutation in 1 patient, while the genotypes of other patients were N370S/55bp deletion, N370S/D409H (in 2 patients) and H255Q/N370S (1 patient). Genetic testing for their progeny has also been planned.

CONCLUSION

This is the first report of GD from Montenegro. N370S was the most common mutation, occurring in all five patients. One patient was found to be homozygous while others were heterozygous. The phenotypes of GD type 1 encountered in Montenegro were severe; notwithstanding, they all responded well to ERT.

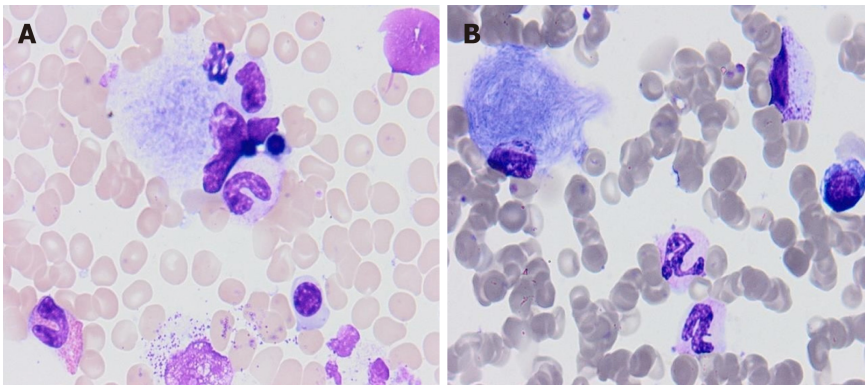

Figure 1 One marrow aspirate. A, B: Bone marrow aspirate showing Gaucher cells.

REFERENCES

1 **Mistry PK**, Liu J, Sun L, Chuang WL, Yuen T, Yang R, Lu P, Zhang K, Li J, Keutzer J, Stachnik A, Mennone A, Boyer JL, Jain D, Brady RO, New MI, Zaidi M. Glucocerebrosidase 2 gene deletion rescues type 1 Gaucher disease. *Proc Natl Acad Sci U S A* 2014; **111**: 4934-4939 [PMID: 24639522 DOI: 10.1073/pnas.1400768111]

2 **Meikle PJ**, Hopwood JJ, Clague AE, Carey WF. Prevalence of lysosomal storage disorders. *JAMA* 1999; **281**: 249-254 [PMID: 9918480 DOI: 10.1001/jama.281.3.249]

3 **Mistry PK**, Liu J, Yang M, Nottoli T, McGrath J, Jain D, Zhang K, Keutzer J, Chuang WL, Mehal WZ, Zhao H, Lin A, Mane S, Liu X, Peng YZ, Li JH, Agrawal M, Zhu LL, Blair HC, Robinson LJ, Iqbal J, Sun L, Zaidi M. Glucocerebrosidase gene-deficient mouse recapitulates Gaucher disease displaying cellular and molecular dysregulation beyond the macrophage. *Proc Natl Acad Sci U S A* 2010; **107**: 19473-19478 [PMID: 20962279 DOI: 10.1073/pnas.1003308107]

4 **Grabowski GA**. Gaucher disease and other storage disorders. *Hematology Am Soc Hematol Educ Program* 2012; **2012**: 13-18 [PMID: 23233555 DOI: 10.1182/asheducation-2012.1.13]

5 **Sidransky E**. Gaucher disease: insights from a rare Mendelian disorder. *Discov Med* 2012; **14**: 273-281 [PMID: 23114583]

6 **Andersson HC**, Charrow J, Kaplan P, Mistry P, Pastores GM, Prakash-Cheng A, Rosenbloom BE, Scott CR, Wappner RS, Weinreb NJ, International Collaborative Gaucher Group U. S. Regional Coordinators. Individualization of long-term enzyme replacement therapy for Gaucher disease. *Genet Med* 2005; **7**: 105-110 [PMID: 15714077 DOI: 10.109701.GIM.0000153660.88672.3C]

7 **Essabar L**, Meskini T, Lamalmi N, Ettair S, Erreimi N, Mouane N. Gaucher's disease: report of 11 cases with review of literature. *Pan Afr Med J* 2015; **20**: 18 [PMID: 25995815 DOI: 10.11604/pamj.2015.20.18.4112]

8 **Laks Y**, Passwell J. The varied clinical and laboratory manifestations of type II Gaucher's disease. *Acta Paediatr Scand* 1987; **76**: 378-380 [PMID: 3035864]

9 **Dreborg S**, Erikson A, Hagberg B. Gaucher disease--Norrbottnian type. I. General clinical description. *Eur J Pediatr* 1980; **133**: 107-118 [PMID: 7363908 DOI: 10.1007/BF00441578]

10 **Grabowski GA**. Gaucher disease: lessons from a decade of therapy. *J Pediatr* 2004; **144**: S15-S19 [PMID: 15126979 DOI: 10.1016/j.jpeds.2004.01.050]

11 **Grabowski GA**, Andria G, Baldellou A, Campbell PE, Charrow J, Cohen IJ, Harris CM, Kaplan P, Mengel E, Pocovi M, Vellodi A. Pediatric non-neuronopathic Gaucher disease: presentation, diagnosis and assessment. Consensus statements. *Eur J Pediatr* 2004; **163**: 58-66 [PMID: 14677061 DOI: 10.1007/s00431-003-1362-0]

12 **Linari S**, Castaman G. Clinical manifestations and management of Gaucher disease. *Clin Cases Miner Bone Metab* 2015; **12**: 157-164 [PMID: 26604942 DOI: 10.11138/ccmbm/2015.12.2.157]

13 **Tamargo RJ**, Velayati A, Goldin E, Sidransky E. The role of saposin C in Gaucher disease. *Mol Genet Metab* 2012; **106**: 257-263 [PMID: 22652185 DOI: 10.1016/j.ymgme.2012.04.024]

14 **Sgambato JA**, Park TS, Miller D, Panicker LM, Sidransky E, Lun Y, Awad O, Bentzen SM, Zambidis ET, Feldman RA. Gaucher Disease-Induced Pluripotent Stem Cells Display Decreased Erythroid Potential and Aberrant Myelopoiesis. *Stem Cells Transl Med* 2015; **4**: 878-886 [PMID: 26062980 DOI: 10.5966/sctm.2014-0213]

15 **Chaabouni M**, Aoulou H, Tebib N, Hachicha M, Ben Becher S, Monastiri K, Yacoub M, Sfar T, Elloumi M, Chakroun N, Miled M, Ben Dridi MF. [Gaucher's disease in Tunisia (multicenter study)]. *Rev Med Interne* 2004; **25**: 104-110 [PMID: 14744639 DOI: 10.1016/S0248-8663(03)00267-4]

16 **Mistry PK**, Cappellini MD, Lukina E, Ozsan H, Mach Pascual S, Rosenbaum H, Helena Solano M, Spigelman Z, Villarrubia J, Watman NP, Massenkeil G. A reappraisal of Gaucher disease-diagnosis and disease management algorithms. *Am J Hematol* 2011; **86**: 110-115 [PMID: 21080341 DOI: 10.1002/ajh.21888]

17 **Liu J**, Halene S, Yang M, Iqbal J, Yang R, Mehal WZ, Chuang WL, Jain D, Yuen T, Sun L, Zaidi M, Mistry PK. Gaucher disease gene GBA functions in immune regulation. *Proc Natl Acad Sci U S A* 2012; **109**: 10018-10023 [PMID: 22665763 DOI: 10.1073/pnas.1200941109]

18 **Mistry PK**, Abrahamov A. A practical approach to diagnosis and management of Gaucher's disease. *Baillieres Clin Haematol* 1997; **10**: 817-838 [PMID: 9497866 DOI: 10.1016/S0950-3536(97)80042-X]

19 **Stirnemann J**, Boutten A, Vincent C, Mekinian A, Heraoui D, Fantin B, Fain O, Mentré F, Belmatoug N. Impact of imiglucerase on the serum glycosylated-ferritin level in Gaucher disease. *Blood Cells Mol Dis* 2011; **46**: 34-38 [PMID: 21084203 DOI: 10.1016/j.bcmd.2010.10.014]

20 **Nagral A**. Gaucher disease. *J Clin Exp Hepatol* 2014; **4**: 37-50 [PMID: 25755533 DOI:

10.1016/j.jceh.2014.02.005]
21 **Weinreb NJ**, Deegan P, Kacena KA, Mistry P, Pastores GM, Velentgas P, vom Dahl S. Life expectancy in Gaucher disease type 1. *Am J Hematol* 2008; **83**: 896-900 [PMID: 18980271 DOI: 10.1002/ajh.21305]
22 **Lopez G**, Kim J, Wiggs E, Cintron D, Groden C, Tayebi N, Mistry PK, Pastores GM, Zimran A, Goker-Alpan O, Sidransky E. Clinical course and prognosis in patients with Gaucher disease and parkinsonism. *Neurol Genet* 2016; **2**: e57 [PMID: 27123476 DOI: 10.1212/NXG.0000000000000057]
23 **Elstein D**, Zimran A. Review of the safety and efficacy of imiglucerase treatment of Gaucher disease. *Biologics* 2009; **3**: 407-417 [PMID: 19774208 DOI: 10.2147/BTT.S3769]
24 **Koprivica V**, Stone DL, Park JK, Callahan M, Frisch A, Cohen IJ, Tayebi N, Sidransky E. Analysis and classification of 304 mutant alleles in patients with type 1 and type 3 Gaucher disease. *Am J Hum Genet* 2000; **66**: 1777-1786 [PMID: 10796875 DOI: 10.1086/302925]

World Journal of Clinical Cases

Submit a Manuscript: https://www.f6publishing.com

World J Clin Cases 2019 June 26; 7(12): 1483-1491

DOI: 10.12998/wjcc.v7.i12.1483

ISSN 2307-8960 (online)

CASE REPORT

Longitudinal observation of ten family members with idiopathic basal ganglia calcification: A case report

Seiju Kobayashi, Kumiko Utsumi, Masaru Tateno, Tomo Iwamoto, Tomonori Murayama, Hitoshi Sohma, Wataru Ukai, Eri Hashimoto, Chiaki Kawanishi

ORCID number: Seiju Kobayashi (0000-0002-1557-1426); Kumiko Utsumi (0000-0003-2781-3303); Masaru Tateno (0000-0002-5084-0193); Tomo Iwamoto (0000-0001-6178-402X); Tomonori Murayama (0000-0003-2371-8421); Hitoshi Sohma (0000-0003-2861-3186); Wataru Ukai (0000-0002-3614-8141); Eri Hashimoto (0000-0003-0558-8002); Chiaki Kawanishi (0000-0003-3464-3787).

Author contributions: Kobayashi S was the principal investigator, he made manuscript draft preparation, design or conceptualization; Utsumi K made the study supervision, acquisition and collection of data, design or conceptualization; Tateno M made the manuscript draft preparation, design or conceptualization; Iwamoto T and Murayama T made manuscript draft preparation; Sohma H made acquisition and collection of data, analysis and interpretation; Ukai W, Hashimoto E, and Kawanishi C made study supervision.

Supported by the grant-in-Aid for Scientific Research (C) from the Japan Society for the Promotion of Science (JSPS), No. 17K103112.

Informed consent statement: Consent was obtained from relatives of the patient for publication of this report and any accompanying images.

Conflict-of-interest statement: The authors declare that they have no conflicts of interest.

Seiju Kobayashi, Shinyukai Nakae Hospital, Sapporo 0010022, Japan

Seiju Kobayashi, Tomo Iwamoto, Tomonori Murayama, Wataru Ukai, Eri Hashimoto, Chiaki Kawanishi, Department of Neuropsychiatry, Sapporo Medical University Graduate School of Medicine, Sapporo 0608543, Japan

Kumiko Utsumi, Department of Psychiatry, Sunagawa City Medical Center, Sunagawa 0730196, Japan

Masaru Tateno, Tokiwa Child Development Center, Tokiwa Hospital, Sapporo, Japan, Department of Neuropsychiatry, Sapporo Medical University Graduate School of Medicine, Sapporo 0050853, Japan

Hitoshi Sohma, Wataru Ukai, Department of Educational Development, Sapporo Medical University Center for Medical Education, Sapporo 0608543, Japan

Hitoshi Sohma, Department of Biomedical Engineering, Sapporo Medical University, School of Medicine, Sapporo 0608543, Japan

Corresponding author: Seiju Kobayashi, MD, PhD, Director, Doctor, Department of Neuropsychiatry, Shinyukai Nakae Hospital, North-22, West-7-2-1, Kita-ku, Sapporo 0010022, Japan. seij@pastel.ocn.ne.jp
Telephone: +81-11-7167181
Fax: +81-11-7581451

Abstract

BACKGROUND

Familial idiopathic basal ganglia calcification (FIBGC) is a rare autosomal dominant disorder that causes bilateral calcification of the basal ganglia and/or cerebellar dentate nucleus, among other locations.

CASE SUMMARY

The aim of this study is to report 10 cases of FIBGC observed in a single family. Seven patients showed calcification on their computed tomography scan, and all of these patients carried the *SLC20A2* mutation. However, individuals without the mutation did not show calcification. Three patients among the 7 with calcification were symptomatic, while the remaining 4 patients were asymptomatic. Additionally, we longitudinally observed 10 subjects for ten years. In this paper, we mainly focus on the clinical course and neuroradiological findings in the proband and her son.

CARE Checklist (2016) statement: The authors have read the CARE Checklist (2016), and the manuscript was prepared and revised according to the CARE Checklist (2016).

Manuscript source: Unsolicited manuscript

Received: January 17, 2019
Peer-review started: January 17, 2019
First decision: March 10, 2019
Revised: April 18, 2019
Accepted: May 2, 2019
Article in press: May 2, 2019
Published online: June 26, 2019

P-Reviewer: Kvolik S
S-Editor: Dou Y
L-Editor: A
E-Editor: Wang J

CONCLUSION
The accumulation of more case reports and further studies related to the manifestation of FIBGC are needed.

Key words: Idiopathic basal ganglia calcification; Fahr's disease; *SLC20A2*; Diffuse neurofibrillary tangles with calcification; Single-photon emission computed tomography; Case report

Core tip: The aim of this study is to report a rare case of familial idiopathic basal ganglia calcification (FIBGC) solely presenting cognitive and behavioural impairments. Since patients with FIBGC show variability in clinical manifestations, even among the families, we should accumulate and report as many cases as possible. Additionally, there are no previous reports that include as many as 10 family members (spanning 3 generations) with genetic information and computed tomography findings that have been observed longitudinally for over ten years. For these reasons, we think that this report is valuable.

Citation: Kobayashi S, Utsumi K, Tateno M, Iwamoto T, Murayama T, Sohma H, Ukai W, Hashimoto E, Kawanishi C. Longitudinal observation of ten family members with idiopathic basal ganglia calcification: A case report. *World J Clin Cases* 2019; 7(12): 1483-1491
URL: https://www.wjgnet.com/2307-8960/full/v7/i12/1483.htm
DOI: https://dx.doi.org/10.12998/wjcc.v7.i12.1483

INTRODUCTION

Idiopathic basal ganglia calcification (IBGC), which is also known as Fahr's disease, is a relatively rare neurological disease characterized by symmetrical calcification in the basal ganglia, cerebellar dentate nucleus, and subcortical brain white matter. Clinical manifestations range widely from asymptomatic to variable symptoms including movement disorders, dementia, and behavioural abnormalities[1]. The diagnosis of IBGC relies mainly on the visualization of bilateral calcification in the basal ganglia through neuroimaging and the absence of metabolic, infectious, toxic, or traumatic causes[2]. The prevalence of IBGC is unknown, but an incidence of basal ganglia calcification ranging from 0.3% to 1.9% has been reported in routine radiological examinations[3-4]. Primary familial brain calcification is usually inherited in an autosomal dominant manner; thus far, mutations in three genes have been found to cause the disease: *SLC20A2*, *PDGFB*, and *PDGFRB*. These mutations are implicated in phosphate homeostasis in IBGC[5].

The aim of this study is to report a rare case of familial idiopathic basal ganglia calcification (FIBGC) with cognitive and behavioural impairments presenting at onset only. Since patients with FIBGC show variability in clinical manifestations, even among the families, we should accumulate and report as many cases as possible. There are few clinical reports that precisely evaluate patients not only neuropsychologically but also neuroradiologically with computed tomography (CT), magnetic resonance imaging (MRI), and brain perfusion Single-Photon Emission Computed Tomography (SPECT). Additionally, there are no previous reports of FIBGC with as many as 10 related patients (spanning 3 generations), with DNA information and CT findings that have been observed longitudinally for over ten years. After we briefly reported on the female proband and her relatives with FIBGC in Neurology[6], additional symmetrical calcification in the basal ganglia and the same gene mutation (*SLC20A2*: c.344C>T) were found in her son (III-1 in the pedigree in Figure 1). Furthermore, we describe manifestations in the proband and her son, who we recently had contact with, in more detail.

CASE PRESENTATION

Chief complaints

Forgetfulness.

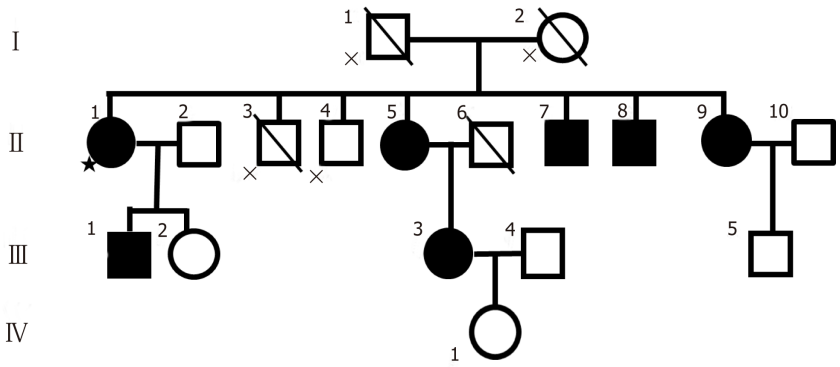

Figure 1 Pedigree of the Sunagawa family. Legend The star sign indicates the index subject. Filled symbols represent patients affected with brain calcification. The cross marks indicate persons from whom samples and symptom were not available.

History of present illness

The proband was a 76-year-old woman (II-1 in the pedigree in Figure 1). She was admitted to a hospital at the age of 65 because of forgetfulness that had been present since she was 60 years old. She could make only a simple meal, repeated the same conversations, and bought the same things many times. Her MMSE (mini mental state examination) score and HDS-R (Revised Hasegawa Dementia Scale) scores were 19 and 20, respectively, which indicated a possibility of dementia (MMSE score below 24, HDS-R score below 21). The coefficient of correlation of the HDS-R to the MMSE was as high as 0.94, which suggested the HDS-R was valid in terms of compatibility with the established dementia screening test[7]. Her Wechsler adult intelligence scale-revised (WIAS-R) total intelligence quotient (IQ) was 87, verbal IQ was 83 and performance IQ was 92.

History of past illness

42 year: Uterine myoma.

58 year: Cerebral aneurysm clipping surgery.

Personal and family history

The proband graduated from a junior high school, married at the age of 21, and had been employed in farming, for a construction, and food service, *etc.*

She had a positive family history of brain calcification, as shown in Figure 1. Her brother had calcification in the brain (Figure 1-II-7, Figure 6-C) as well as mental retardation, and another brother (Figure 1-II-8, Figure 6-D) presented with alcoholism. Her parents had no clinical symptoms and lived a normal life as far as we know, and they had no dementia. Although we do not know the details, her father died of heart disease and her mother died of stroke.

Physical examination upon admission

No pyramidal or extrapyramidal signs were observed. The Albright sign was negative.

Laboratory examinations

Biochemical examination showed that the levels of thyroid hormones, parathyroid hormone (PT), serum calcium, serum phosphate and cerebrospinal fluid (CSF) were all in the range of normal values. Additionally, the *Treponema pallidum* haemagglutination assay test was negative.

Imaging examinations

Symmetrical calcifications in the globus pallidus, pulvinar thalami, subcortical area in the right frontal lobe, and border area of the cortex and white matter in the occipital lobe were found in CT scanning (Figure 2). A T1-weighted MRI revealed small patchy hypersignals in the globus pallidus and pulvinar thalami (Figure 2). A T2-weighted MRI revealed small patchy hyposignals in the globus pallidus (Figure 2). However, it is obscure in MRI scans compared to CT scans. Her brain perfusion SPECT images showed decreased perfusion in the bilateral basal ganglia and thalamus as well as the right frontal lobe (Figure 3).

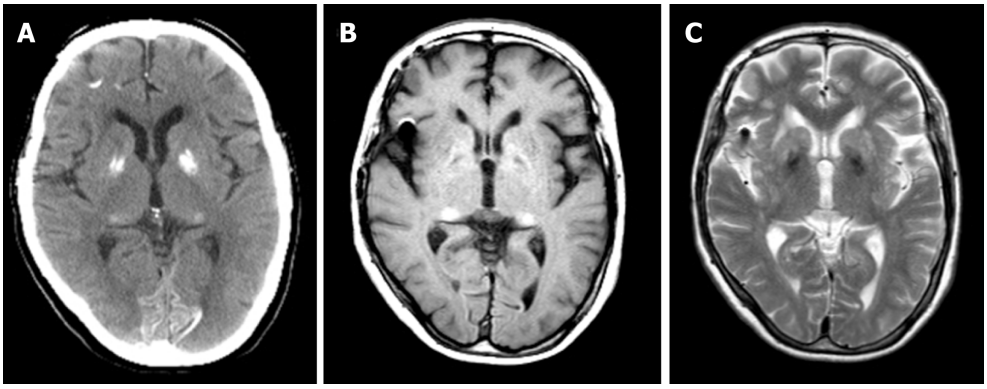

Figure 2 Computed tomography, magnetic resonance imaging-T1, and magnetic resonance imaging-T2 images of the proband (65 yr).

FINAL DIAGNOSIS

The initial clinical diagnosis had been diffuse neurofibrillary tangles with calcification (DNTC)[8]; to the best of our knowledge, familial cases of DNTC have not been reported. Therefore, the patients were diagnosed as FIBGC.

TREATMENT

There is no causal treatment for FIBGC, so we only have the options of symptomatic treatment or observation.

OUTCOME AND FOLLOW-UP

The change in the MMSE and HDS-R scores of the proband is summarized in Table 1. At the one-year follow-up (66 years old), although she could not communicate very well and recognize the expiration date of food, however, there weren't substantial changes in her overall cognitive function (MMSE: 21/30, HDS-R: 20).

At the two-year follow-up (67 years old), the patient presented with further decreased short-term memory and disorientation. She performed misplaced acts of kindness such as delivering the same things to neighbours many times. Her daughter recognized that her memory impairment was gradually progressing, which was confirmed by her HDS-R score. The MMSE and HDS-R scores were 23/30 and 16/30, respectively. At the four-year follow-up (69 years old), she started losing memory daily and presented aggressive and restless behaviours that required antipsychotic medication. The MMSE and HDS-R scores were 21/30 and 13/30, respectively. The decreased score of HDS-R indicated deteriorated memory disturbance. She entered a nursing home at the age of 70 due to personality changes, such as increased irritability and displaying aggression to her family. Brain atrophy of frontotemporal lobe was slightly seen compared to her results at 65 years old (Figure 4, 5). At the six-year follow-up (71 years old), a gradual progression of cognitive dysfunction was found. The MMSE and HDS-R scores were 19/30 and 12/30, respectively. At the nine-year follow-up (74 years old), though she showed signs of excessive meddling with other patients, only a slight progression in dementia was found. The MMSE and HDS-R scores were 19/30 and 12/30, respectively. When she was 75 years old, she suffered from acute Stanford an aortic dissection and multiple cerebral infarction as a result. Further brain atrophy of frontotemporal lobe was seen compared to her results at 65 and 69 years old (Figure 4, 5). Although she received an operation that saved her life, her disordered consciousness remained. Therefore, she moved to a recuperation hospital away from our advanced treatment hospital at the age of 76.

She had a positive family history of brain calcification, as shown in Figure 1. Demographic information, clinical features, and instrumental data of all the patients are summarized in Table 2. Among the two children of the patient, her son (III-1) showed evidence of brain calcification; however, brain CT scans of her daughter (III-2) did not reveal the same finding. Her son, a 49-year-old male, had no remarkable history of illness until 47 years of age. He worked at a machine production manufacturing company for ten years. When he moved to another department of the company, he started to be confounded by unfamiliar tasks and would sometimes

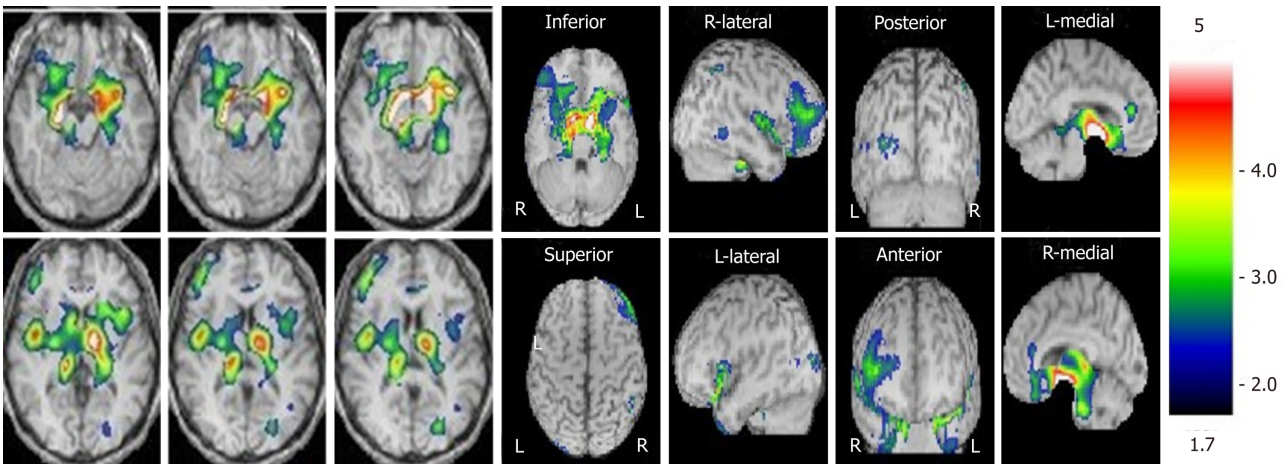

Figure 3 Brain perfusion single photon emission computed tomography (easy Z-score imaging system) of the proband (65 yr).

make some mistakes. Although he had managed to continue working, he became depressed and anxious. Finally, he decided to visit our hospital and requested treatment. He was diagnosed with an adjustment disorder based on his history. Neither parkinsonism nor cerebellar ataxia were recognized. A biochemical examination revealed that levels of PTH, serum calcium, serum phosphate and CSF were all within normal ranges. The Albright sign was negative. There was no evidence of hypoparathyroidism and pseudohypoparathyroidism. A cranial CT revealed distinct, symmetrical calcification of the basal ganglia, primarily in the caudate nucleus, globus pallidus, putamen, and pulvinar thalami (Figure 6-F). Since we recognized by chance that he was the proband's son, informed consent for genic analysis of FIBGC was obtained from him. The *SLC20A2* mutation was found in his blood sample.

The proband's brother had calcification in the brain (Figure 1-II-7, Figure 6-C) as well as mental retardation, and another brother (Figure 1-II-8, Figure 6-D) presented with alcoholism. He died of descending colon cancer and frequent cerebral infarctions at the age of 62, four years after we checked his brain CT and blood sample. The three other relatives with calcification (Figure 1-II-5, II-9, and III-3) were basically asymptomatic, although the proband's sister (Figure 1-II-5) only had headaches. The degree of calcification in these families was relatively mild compared to the calcification observed in other families we examined.

The symptomatic patients (Figure 6A, C, and D) showed more apparent brain atrophy than the others (Figure 6B, E, F, and G). The individuals with calcification on the CT images (II-1, II-5, II-7, II-8, II-9, III-1, and III-3) had the same mutation in exon 3 in *SLC20A2* (c.344C>T). However, the individuals with no calcification (III-2, III-5, and IV-1) revealed no mutation in *SLC20A2*. In summary, 7 patients had calcification among the 10 individuals who were examined by CT scan in the family, and all of the patients carrying the *SLC20A2* mutation exhibited similar calcification in their CT images. However, individuals without the mutation did not show calcification.

For other family members outside of the 10 included in this study, mutational analysis and CT scan were not performed due to death (II-3) and lack of consent (II-4).

DISCUSSION

This is a rare case of FIBGC solely presenting cognitive and behavioural impairments. Indeed, to the best of our knowledge, only a few cases with the same clinical features have been described so far[9]. In the "Fahr's Disease Registry," the most common manifestation was movement disorders (55%), in particular parkinsonism, while hyperkinetic movement disorders accounted for the rest[9]. Other manifestations are described, including memory disturbance, hallucination, delusions and personality change, depression[10-13], and stereotypical behaviours[12], which may be accompanied by extrapyramidal signs, such as parkinsonism and paroxysmal non-kinesigenic dyskinesia[14,15]. Thus, patients who met the criteria for IBGC[2] have diverse manifestations. Patients with FIBGC show variability in clinical manifestations, even among families. Therefore, we should accumulate and report as many cases as possible. In our familial cases, the proband has dementia followed by personality changes, such as irritability and aggression. Her cognitive function gradually worsened according to her history and HDS-R. Compared with MMSE, the relative weight of

Table 1 The changes in mini mental state examination and revised hasegawa dementia scale scores of the proband

Age	MMSE	HDS-R
65 yr	19	20
66 yr	21	20
67 yr	23	16
69 yr	21	13
71 yr	19	12
74 yr	19	12
75 yr	Disordered consciousness	Disordered consciousness
76 yr	Disordered consciousness	Disordered consciousness

MMSE: Mini mental state examination; HDS-R: Revised hasegawa dementia scale.

HDS-R for memory was strengthened, and a measure for language was added[16]. The study by Kim[16] indicated that the HDS-R did better than MMSE because of the larger AUC (area under the curve) as well as the higher sensitivity and specificity for dementia regardless of severity and the educational level of the subjects. One of the proband's brothers (Figure 1-II-7) has mental retardation and another one (Figure 1-II-8) had alcoholism. Although the association between these symptoms and calcification is unclear, 3 symptomatic patients had signs of brain atrophy, especially in the frontal lobe in CT images.

Considering the gradual progressive frontotemporal atrophy of the proband (II-1) as well, the differential diagnosis of DNTC is needed[8]; however, to the best of our knowledge, familial cases of DNTC have not been reported. We hope to perform a pathological diagnosis in the future.

The proband's son (Figure 1-III-1) has adjustment disorder instead of depression. Although it is difficult to judge whether this disorder is related to calcification or not, it is possible that depression is one of the symptoms of IBGC. At least vulnerability to stress may be associated with IBGC. Interestingly, none of our patients with calcification showed neurological deficits. The non-existence of calcification in the cerebellum may be able to explain why there was no ataxia. On the other hand, the association between parkinsonism and calcification in portions of the brain is unclear. Though the proband's son (III-1) has calcification in the bilateral striatum, but there is no sign of a movement disorder such as parkinsonism. Additionally, we did not find a correlation between clinical severity and the extent of brain calcification.

With vague criteria and an unknown aetiology, Fahr's disease presents a blind spot in medical care. The discovery of the mutations in the gene *SLC20A2* that cause IBGC3 was a turning point in understanding the disease's pathophysiology. In our familial cases, all of the individuals carrying the *SLC20A2* mutation exhibited similar calcification in their CT images. However, individuals without the mutation did not show calcification.

In the proband, the bilateral basal ganglia and thalamus as well as the right dominant frontal lobe hypoperfusion were observed (Figure 3). The hypoperfusion presumably results from a disruption of pathways interconnecting the basal ganglia to frontal areas as well as calcification.

We acknowledge some limitations to our report. We have not confirmed the diagnosis through neuropathological means. However, we strongly believe that a detailed history combined with careful physical, neuro-psychological cognitive tests, neuroimaging tools (CT, MRI and brain perfusion SPECT), and genetic tests can significantly increase the precision of clinical diagnosis. Since the members of our memory clinic include psychiatrists, a neurologist, a neurosurgeon, a clinical psychologist and radiological technicians, team collaboration also contributed to providing accurate diagnoses.

CONCLUSION

In summary, the patients in this study showed heterogeneity in terms of their manifestations and different severity in their symptoms, even within the same family. More case reports and further studies related to the manifestations of FIBGC are needed. The elucidation of the molecular basis underlying IBGC will contribute to the development of therapeutic measures for patients with calcification in their brains.

Table 2 Demographic information, clinical features, and instrumental data for all patient

Patient	Age at examination	Sex	Clinical features	Localization of brain calcification			Mutation
				Striatum	Pallidum	Cerebellar dentate nuclei	
II-1	69	F	Dementia, Irritability and agression	-	+	-	SLC20A2 (c.344C>T)
II-5	61	F	Asymptomatic (only headache)	-	+	-	SLC20A2 (c.344C>T)
II-7	59	M	Mental retardation	-	+	-	SLC20A2 (c.344C>T)
II-8	58	M	Alcoholism	+	-	-	SLC20A2 (c.344C>T)
II-9	56	F	Asymptomatic	-	+	-	SLC20A2 (c.344C>T)
III-1	49	M	Adjustment disorder	+	+	-	SLC20A2 (c.344C>T)
III-2	44	F	Asymptomatic	-	-	-	-
III-3	36	F	Panic disorder	+	+	-	SLC20A2 (c.344C>T)
III-5	18	M	Asymptomatic	-	-	-	-
IV-1	8	F	Asymptomatic	-	-	-	-

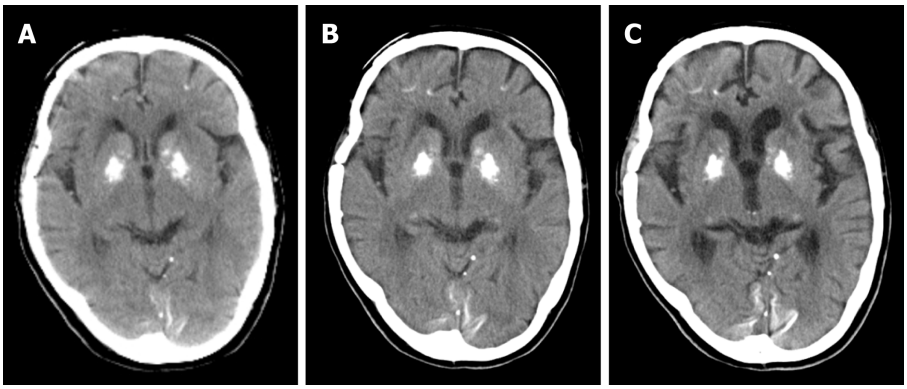

Figure 4 Computed tomography images of the proband. A: 65 yr; B: 69 yr; C: 75 yr.

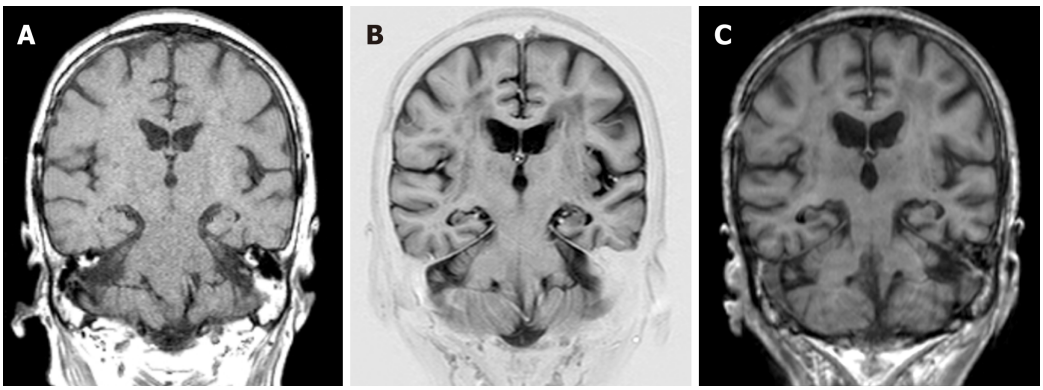

Figure 5 Magnetic resonance imaging-coronal images of the proband. A: 65 yr; B: 69 yr; C: 75 yr.

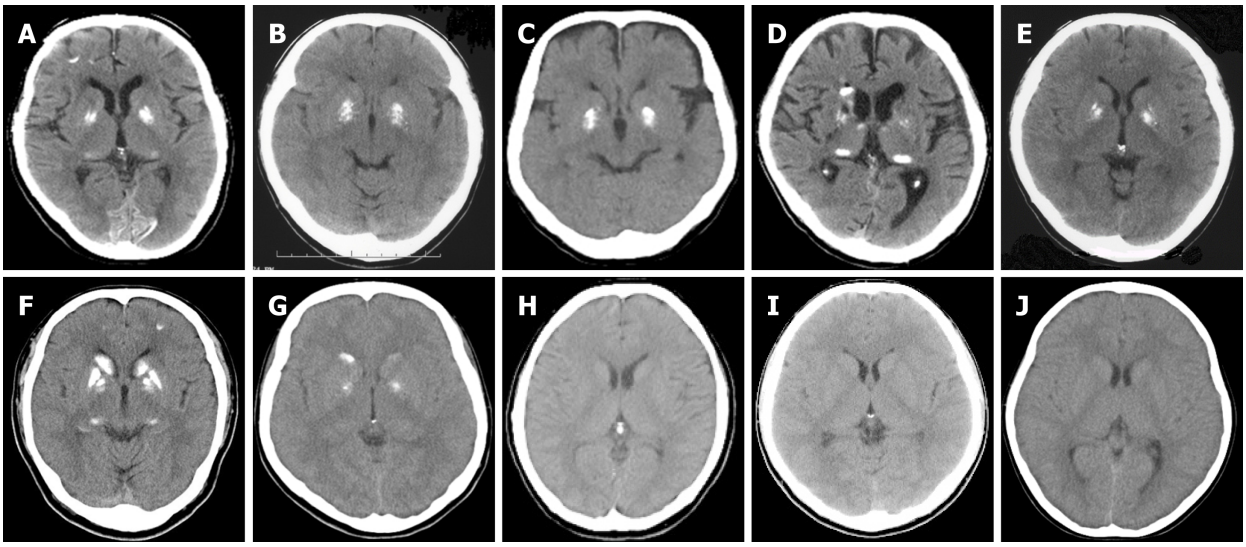

Figure 6 Computed tomography images of the family members. A: Computed tomography (CT) image of the proband (II-1 in pedigree of the family); B: CT image of asymptomatic II-5; C: CT image of symptomatic II-7; D: CT image of symptomatic II-8; E: CT image of asymptomatic II-9; F: CT image of asymptomatic III-1; G: CT image of asymptomatic III-3; H: CT image of asymptomatic III-2; I: CT image of asymptomatic III-5; J: CT image of asymptomatic IV-1.

ACKNOWLEDGEMENTS

The authors thank the patients and their families who supported this research.

We also thank the involved doctors (Dr. Kenjirou Kamiguchi, Sunagawa Jikeikai Hospital, Dr. Megumi Yamada and Dr. Isao Hozumi, Laboratory of Medical Therapeutics and Molecular Therapeutics, Gifu Pharmaceutical University).

REFERENCES

1 **Manyam BV**. What is and what is not 'Fahr's disease'. *Parkinsonism Relat Disord* 2005; **11**: 73-80 [PMID: 15734663 DOI: 10.1016/j.parkreldis.2004.12.001]

2 **Bonazza S**, La Morgia C, Martinelli P, Capellari S. Strio-pallido-dentate calcinosis: a diagnostic approach in adult patients. *Neurol Sci* 2011; **32**: 537-545 [PMID: 21479613 DOI: 10.1007/s10072-011-0514-7]

3 **Kazis AD**. Contribution of CT scan to the diagnosis of Fahr's syndrome. *Acta Neurol Scand* 1985; **71**: 206-211 [PMID: 3993326 DOI: 10.1111/j.1600-0404.1985.tb03190.x]

4 **Yamada M**, Asano T, Okamoto K, Hayashi Y, Kanematsu M, Hoshi H, Akaiwa Y, Shimohata T, Nishizawa M, Inuzuka T, Hozumi I. High frequency of calcification in basal ganglia on brain computed tomography images in Japanese older adults. *Geriatr Gerontol Int* 2013; **13**: 706-710 [PMID: 23279700 DOI: 10.1111/ggi.12004]

5 **Legati A**, Giovannini D, Nicolas G, López-Sánchez U, Quintáns B, Oliveira JR, Sears RL, Ramos EM, Spiteri E, Sobrido MJ, Carracedo Á, Castro-Fernández C, Cubizolle S, Fogel BL, Goizet C, Jen JC, Kirdlarp S, Lang AE, Miedzybrodzka Z, Mitarnun W, Paucar M, Paulson H, Pariente J, Richard AC, Salins NS, Simpson SA, Striano P, Svenningsson P, Tison F, Unni VK, Vanakker O, Wessels MW, Wetchaphanphesat S, Yang M, Boller F, Campion D, Hannequin D, Sitbon M, Geschwind DH, Battini JL, Coppola G. Mutations in XPR1 cause primary familial brain calcification associated with altered phosphate export. *Nat Genet* 2015; **47**: 579-581 [PMID: 25938945 DOI: 10.1038/ng.3289]

6 **Yamada M**, Tanaka M, Takagi M, Kobayashi S, Taguchi Y, Takashima S, Tanaka K, Touge T, Hatsuta H, Murayama S, Hayashi Y, Kaneko M, Ishiura H, Mitsui J, Atsuta N, Sobue G, Shimozawa N, Inuzuka T, Tsuji S, Hozumi I. Evaluation of SLC20A2 mutations that cause idiopathic basal ganglia calcification in Japan. *Neurology* 2014; **82**: 705-712 [PMID: 24463626 DOI: 10.1212/WNL.0000000000000143]

7 **Imai Y**, Hasegawa K. The Revised Hasegawa's Dementia Scale (HDS-R) – Evaluation of its usefulness as a screening test for dementia. *J Hong Kong Coll Psychiatr* 1994; **4**: 20-24

8 **Kosaka K**. Diffuse neurofibrillary tangles with calcification: a new presenile dementia. *J Neurol Neurosurg Psychiatry* 1994; **57**: 594-596 [PMID: 8201331 DOI: 10.1136/jnnp.57.5.594]

9 **Calabrò RS**, Spadaro L, Marra A, Bramanti P. Fahr's disease presenting with dementia at onset: a case report and literature review. *Behav Neurol* 2014; **2014**: 750975 [PMID: 24803731 DOI: 10.1155/2014/750975]

10 **Modrego PJ**, Mojonero J, Serrano M, Fayed N. Fahr's syndrome presenting with pure and progressive presenile dementia. *Neurol Sci* 2005; **26**: 367-369 [PMID: 16388376 DOI: 10.1007/s10072-005-0493-7]

11 **Shakibai SV**, Johnson JP, Bourgeois JA. Paranoid delusions and cognitive impairment suggesting Fahr's disease. *Psychosomatics* 2005; **46**: 569-572 [PMID: 16288137 DOI: 10.1176/appi.psy.46.6.569]

12 **Kümmer A**, de Castro M, Caramelli P, Cardoso F, Teixeira AL. [Severe behavioral changes in a patient with Fahr's disease]. *Arq Neuropsiquiatr* 2006; **64**: 645-649 [PMID: 17119811 DOI: 10.1590/S0004-282X2006000400024]

13 **Glück-Vanlaer N**, Fallet A, Plas J, Chevalier JF. [Depression and calcinosis of the basal ganglia: apropos of a case]. *Encephale* 1996; **22**: 127-131 [PMID: 8706622]

14 **Alemdar M**, Selek A, Işeri P, Efendi H, Komsuoğlu SS. Fahr's disease presenting with paroxysmal non-kinesigenic dyskinesia: a case report. *Parkinsonism Relat Disord* 2008; **14**: 69-71 [PMID: 17240186 DOI: 10.1016/j.parkreldis.2006.11.008]

15 **Oliveira JR**, Spiteri E, Sobrido MJ, Hopfer S, Klepper J, Voit T, Gilbert J, Wszolek ZK, Calne DB, Stoessl AJ, Hutton M, Manyam BV, Boller F, Baquero M, Geschwind DH. Genetic heterogeneity in familial idiopathic basal ganglia calcification (Fahr disease). *Neurology* 2004; **63**: 2165-2167 [PMID: 15596772 DOI: 10.1212/01.WNL.0000145601.88274.88]

16 **Kim KW**, Lee DY, Jhoo JH, Youn JC, Suh YJ, Jun YH, Seo EH, Woo JI. Diagnostic accuracy of mini-mental status examination and revised hasegawa dementia scale for Alzheimer's disease. *Dement Geriatr Cogn Disord* 2005; **19**: 324-330 [PMID: 15785033 DOI: 10.1159/000084558]

World Journal of Clinical Cases

Submit a Manuscript: https://www.f6publishing.com

World J Clin Cases 2019 June 26; 7(12): 1492-1498

DOI: 10.12998/wjcc.v7.i12.1492

ISSN 2307-8960 (online)

CASE REPORT

Secondary lymphoma develops in the setting of heart failure when treating breast cancer: A case report

Sen Han, Tao An, Wei-Ping Liu, Yu-Qin Song, Jun Zhu

ORCID number: Sen Han (0000-0001-8231-9207); Tao An (0000-0003-0836-9251); Wei-Ping Liu (0000-0002-2770-7626); Yu-Qin Song (0000-0001-9442-0871); Jun Zhu (0000-0003-0179-3623).

Author contributions: Zhu J and Han S designed and wrote the report; An T reviewed the manuscript for its intellectual content; Liu WP and Song YQ performed the analysis and evaluations; all authors have read and approved the final manuscript.

Informed consent statement: The patient involved in this study gave written informed consent authorizing the use and disclosure of her protected health information.

Conflict-of-interest statement: The authors of this manuscript have no conflicts of interest to disclose.

CARE Checklist (2016) statement: The authors have read the CARE Checklist (2016), and the manuscript was prepared and revised according to the CARE Checklist (2016).

Sen Han, Wei-Ping Liu, Yu-Qin Song, Jun Zhu, Key Laboratory of Carcinogenesis and Translational Research (Ministry of Education), Department of Lymphoma, Peking University Cancer Hospital and Institute, Beijing 100142, China

Tao An, Fuwai Hospital, National Center for Cardiovascular Diseases, Chinese Academy of Medical Science and Peking Union Medical College, Heart Failure Center, Beijing 100142, China

Corresponding author: Jun Zhu, MD, Professor, Key Laboratory of Carcinogenesis and Translational Research (Ministry of Education), Department of Lymphoma, Peking University Cancer Hospital and Institute, No. 52, Fucheng Road, Haidian District, Beijing 100142, China.
zhujun_med@126.com
Telephone: +86-10-88196109
Fax: +86-10-88196115

Abstract

BACKGROUND

Cardiovascular side effects occur frequently during anti-cancer treatment, and there is a growing concern that they may lead to premature morbidity and death.

CASE SUMMARY

A 32-year-old woman was diagnosed with breast cancer. After comprehensive treatment with neoadjuvant chemotherapy, surgery, postoperative adjuvant chemotherapy, postoperative adjuvant radiotherapy, and endocrine therapy, her breast cancer was cured. However, heart failure associated with anti-cancer treatment presented, most probably related to chemotherapy containing anthracycline. After active treatment, her cardiac function returned to normal. Unfortunately, follow-up visits revealed a second primary malignancy, lymphoma. After multiple courses of chemotherapy combined with targeted therapy, her lymphoma acquired complete remission and no cardiotoxicity was observed again. Heart failure related to breast treatment may be reversible.

CONCLUSION

Using alternatives to anthracycline in patients with lymphoma who are at risk of cardiac failure may preserve cardiac function.

Key words: Breast cancer; Chemotherapy; Cardiac toxicity; Heart failure; Anthracycline; Cardio-oncology; Case report

Manuscript source: Unsolicited manuscript

Received: February 2, 2019
Peer-review started: February 11, 2019
First decision: March 9, 2019
Revised: April 24, 2019
Accepted: May 2, 2019
Article in press: May 2, 2019
Published online: June 26, 2019

P-Reviewer: Altarabsheh SE, Barik R, Petix NR, Teragawa H
S-Editor: Ji FF
L-Editor: Wang TQ
E-Editor: Wang J

Core tip: Anti-cancer treatment is frequently associated with the development of cardiovascular side effects. A 32-year-old woman diagnosed and treated for breast cancer was cured after comprehensive treatment. Unfortunately, the patient later presented with heart failure associated with anti-cancer treatment involving the use of anthracycline. Her cardiac function returned to normal after active treatment but a second primary malignancy, lymphoma, was detected in subsequent visits. Following multiple courses of chemotherapy combined with targeted therapy, there was complete remission of the acquired lymphoma with no re-occurrence of cardiotoxicity. Thus, heart failure related to breast cancer treatment may be reversible. Furthermore, anthracycline should be avoided in patients at risk of cardiac failure having lymphoma to preserve cardiac function.

Citation: Han S, An T, Liu WP, Song YQ, Zhu J. Secondary lymphoma develops in the setting of heart failure when treating breast cancer: A case report. *World J Clin Cases* 2019; 7(12): 1492-1498
URL: https://www.wjgnet.com/2307-8960/full/v7/i12/1492.htm
DOI: https://dx.doi.org/10.12998/wjcc.v7.i12.1492

INTRODUCTION

Advances in anti-cancer treatment have greatly improved the survival rate of breast cancer patients, but morbidity and mortality due to side effects remain a concern[1]. Cardiovascular diseases (CVDs) are the most frequent side effects that may lead to premature morbidity and death among cancer survivors[2]. Among anticancer agents, anthracyclines are probably the most well-known class of cardiotoxic drugs capable of causing myocardial dysfunction and heart failure[3].

Besides unpleasant effects from chemotherapy, another challenge affecting the growing population of cancer survivors is the development of a second primary malignancy[4]. The development of a second primary malignancy is under multifactorial influence not least the late effects of chemotherapy and radiotherapy[5].

CASE PRESENTATION

Chief complaints

A 34-year-old Chinese woman presented with chest tightness and shortness of breath.

History of present illness

A right breast tumor was found during a routine physical examination 2 years prior to presentation. The diagnosis made was stage IIIA (T3N1M0) breast invasive ductal carcinoma, with ipsilateral axillary lymph node metastasis, ER (+), PR (+), and Her-2 (-). Thereafter, the patient first underwent four cycles of neoadjuvant chemotherapy using the following regimen: cyclophosphamide 600 mg/m^2 1.0 g D1, epirubicin 100 mg/m^2 160 mg D1, and fluorouracil 600 mg/m^2 1.0 g D1, q21d. After this course of therapy, the patient was assessed as having partial remission (PR). Subsequently, a modified radical mastectomy was performed. Based on her postoperative pathological stage ypT1cN3, the patient further received another four cycles of adjuvant chemotherapy comprising paclitaxel 90 mg/m^2 150 mg D1, 120 mg D8 and D15, q21d. Postoperative adjuvant radiotherapy (50 Gy/30f) was also introduced. The irradiation field included the right chest wall and supraclavicular region. Since the patient tested positive for hormone receptor, the patient accepted being given adjuvant endocrine therapy consisting of goserelin acetate 3.6 mg once a month and anastrozole 1 mg qd. At the one-year follow-up visit, no recurrence or metastasis of breast cancer was observed.

History of past illness

The patient had good health.

Personal and family history

The patient had no relevant personal or family history.

Physical examination upon admission

She was unable to lie down. Blood pressure was 119/86 mmHg. Heart rate was 78 beats per minute. Dry and wet rales could be heard in both lungs.

Laboratory examinations

Laboratory results indicated negative myocardial enzymes and a brain natriuretic peptide level exceeding 2000 pg/mL. Her electrocardiogram showed T-wave inversion in chest leads V1-V6 (Figures 1 and 2).

Imaging examinations

Echocardiography reported a left ventricular ejection fraction (LVEF) of 30%-38%. Cardiac contrast-enhanced magnetic resonance imaging showed that the left ventricle was markedly dilated (left ventricular end diastolic diameter was 60 mm), the left ventricular systolic function was diffused, and the left ventricular myocardial wall thickening rate was reduced. Moreover, the LVEF was 33%.

FINAL DIAGNOSIS

The patient was diagnosed as having acute left heart failure, which was considered as a morbidity of previous anti-cancer therapy.

TREATMENT

After treatment with diuretics, nitrates, angiotensin converting enzyme inhibitor, and digoxin, the patient's symptoms and signs gradually improved. Finally, the patient reported complete resolution of symptoms. She adhered to a treatment protocol consisting of digoxin, trimetazidine, and spironolactone for 3 years. Echocardiography was reviewed at 12 mo after the diagnosis of heart failure, which indicated that the anteroposterior diameter of the left atrium was 30 mm, left ventricular end diastolic diameter was 45 mm, and LVEF had returned to normal (76%).

One year later, a left supraclavicular lymph node enlargement was found in the patient (Figure 3A). Lymph node biopsy indicated diffuse large B cell lymphoma (DLBCL) leading to a diagnosis of stage IIA involving the neck, left clavicle area, posterior left lobe of thyroid, and superior mediastinal lymph nodes. After fully assessing her cardiac function and the cardiac toxicity risk of chemotherapy, the patient was placed on a treatment regimen of rituximab combined with chemoregimen. Considering her heart condition, the CHOP regimen was adjusted to CEOP (cyclophosphamide, vincristine, prednisone, and etoposide instead of doxorubicin). Thus, anthracycline was avoided. The patient received eight cycles of chemotherapy plus targeted therapy.

OUTCOME AND FOLLOW-UP

After four cycles of R-CEOP, complete remission (CR) was achieved and maintained continuously (Figure 3B). The major adverse effect was myelosuppression (leukocyte reduction). There was no obvious cardiotoxicity.

Follow-up visits continued for another 3 years. No recurrence of breast cancer or lymphoma was observed and cardiac function remained normal. The patient discontinued use of cardiac drugs but maintained endocrine therapy for breast cancer. The whole course of the patient's treatment is shown in Figure 4.

DISCUSSION

The application of anthracyclines is a landmark in the development of medical oncology. Even today, this class of drugs are still widely used in the treatment of many solid tumors and hematological malignancies. However, the main dose limitation of these drugs is cardiac toxicities, which restrict their clinical use. The cardiotoxicity of anthracyclines may be acute, delayed, or chronic. Acute toxicities, predominantly appearing as supraventricular arrhythmia, transient LV dysfunction, and ECG changes, develop immediately after infusion and are usually reversible. The changes in the electrophysiologic properties of the heart may lead to QT prolongation. Though rare, this condition is dangerous because QT prolongation can lead to life-threatening arrhythmias such as torsades de pointes[6]. Direct activation of the delayed

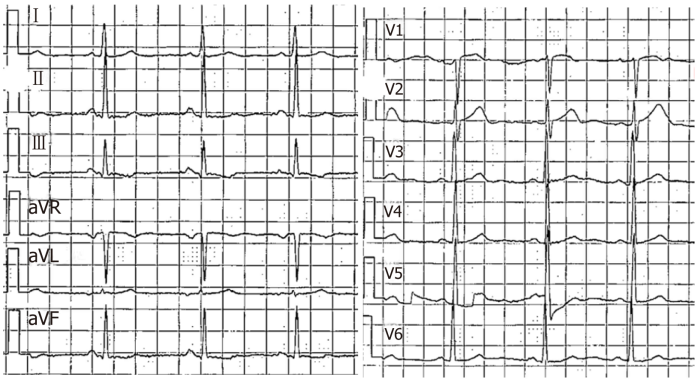

Figure 1 Electrocardiogram at the initial diagnosis of breast cancer showing an almost normal profile.

rectifier potassium current and inhibition of the expression of potassium current channels may be potential mechanisms for the observed cardiac toxicity[7]. Besides arrhythmia, anthracyclines are well known for their potential to cause cardiac insufficiency and heart failure. A higher cumulative dose of anthracycline poses a higher risk of cardiac toxicity[8]. For example, when the cumulative dose of doxorubicin reaches 400 mg/m^2, the incidence of congestive heart failure is 5%, which increases to 48% when the cumulative amount reaches 700 mg/m^2[3]. Therefore, in clinical practice, the cumulative dose of doxorubicin is generally kept below 450 mg/m^2. Nonetheless, there is no absolute safe dose. As we have reported in this case, the patient received an epirubicin total dose of only 400 mg/m^2. After comprehensive anti-cancer treatment, including chemotherapy, surgery, radiotherapy, and endocrine therapy, the patient presented with serious heart failure. This condition was directly associated with anti-cancer therapy and anthracycline was undoubtedly the most important contributor. The risk factors of anthracycline-induced cardiotoxicity include cumulative doses, gender (female), age (older than 65 years or less than 18 years), renal insufficiency, mediastinal radiotherapy history, and other associated drugs with cardiac toxicity (including cyclophosphamide, trastuzumab, and paclitaxel), and potential CVDs[9-11]. As mentioned earlier, the main cardiac toxicities of anthracycline are myocardial dysfunction and heart failure. The left ventricular dysfunction caused by anthracycline is partly due to the production of oxygen free radicals and the increased oxidative stress. As a result, myocardial damage occurs, partly due to the inhibition of topoisomerase II beta by the oxidation-reduction cycle of the quinone group, which indirectly leads to mitochondrial abnormalities. Anthracyclines also inhibit iron metabolism and lead to iron accumulation in cardiac myocytes; therefore, iron balance may also play a role in myocardial injury[12]. A consequence of exposure to anthracyclines is cardiomyocyte apoptosis or necrosis. This patient's cardiotoxicity occurred more than one year after the treatment for breast cancer and, hence, is a delayed cardiotoxicity. It is generally believed that anthracycline-induced cardiac toxicity is irreversible[13]. However, some studies have shown that it is reversible in the first 3-6 mo after the decrease in ejection fraction[14,15]. In this case, the patient's heart function gradually returned to normal after active treatment.

The complexity of this case is that the patient developed a second primary malignancy, lymphoma. Developing a secondary malignancy is not rare but, a comorbidity of heart failure presents a great challenge in the treatment of lymphoma. For DLBCL, the classic regimen is CHOP, which contains cardiotoxic drugs. So, it is important to fully assess the cardiac function and the cardiac toxicity risk before initiating chemotherapy. In this case, anthracycline was replaced by etoposide, which may have lower efficacy but no significant cardiac toxicity. Fortunately, this patient acquired persistent CR without experiencing further cardiac toxicity. There is no standard treatment for DLBCL in elderly patients or patients with underlying diseases, such as cardiac dysfunction, which restricts the use of anthracycline. If there are contraindications in the use of anthracycline, other drugs such as gemcitabine, etoposide, and bendamustine can be explored as alternatives. Although most published large-scale clinical data show that chemotherapy without anthracycline had a negative effect on the long-term survival of aggressive non-Hodgkin lymphoma, if anthracycline use poses potentially life-threatening cardiac toxicity, it may well be in the patient's best interest to discontinue its use[16].

The adjuvant treatment for early breast cancer is associated with improved survival but at the expense of increased cardiotoxicity risk and cardiac dysfunction. It seems

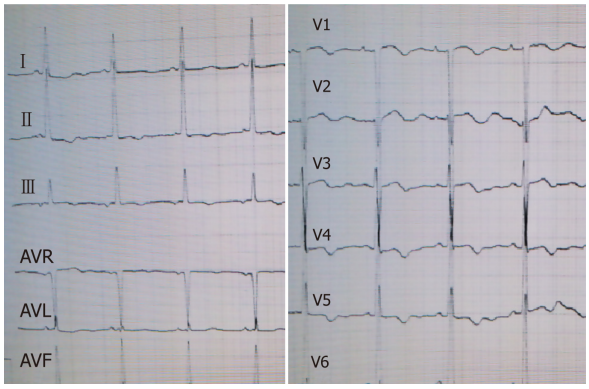

Figure 2 Electrocardiogram when the patient presented with dyspnea. T-wave inversion can be seen in the leads II, III, AVF, and V1-V6.

that concomitant therapy with angiotensin receptor blocker and/or beta-blocker can alleviate the decline in LVEF associated with adjuvant anthracycline-containing regimens with or without trastuzumab and radiation[17]. For a long time, the clinical use of doxorubicin is limited by its cardiotoxic effects that can lead to heart failure. However, earlier work focused on the direct impact of doxorubicin on cardiomyocytes. Recent studies have evaluated the effects on the endothelium, because doxorubicin-induced endothelial damage can trigger the development and progression of cardiomyopathy by decreasing the release and activity of key endothelial factors and inducing endothelial cell death. Thus, the endothelium represents a novel target for improving the detection, management, and prevention of doxorubicin-induced cardiomyopathy[18].

The process of anti-cancer treatment should be adjusted according to the risks of cardiac toxicities, medical history, and previous treatment[19]. So, similar to the reported case, if we diligently weigh the pros and cons, choose regimens carefully, monitor cardiac toxicity closely, and even take some preventive measures, patients would benefit more without encountering high risks.

CONCLUSION

Comprehensive treatment of breast cancer may induce cardiac toxicity such as heart failure. However, heart failure related to anti-cancer treatment may be reversible. A second primary tumor is not rare for breast cancer survivors. When a secondary lymphoma develops in the setting of heart failure when treating breast cancer, anthracycline should be avoided to preserve cardiac function. Etoposide may be chosen instead of anthracycline, with equal effects.

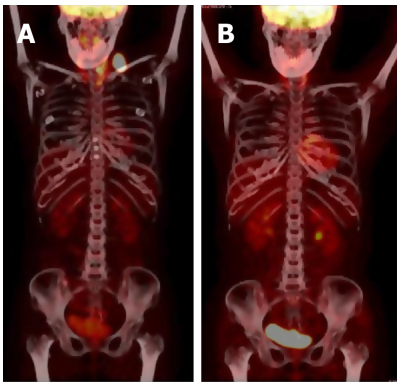

Figure 3 [^{18}F]-fluorodeoxyglucose positron emission tomography findings. A: Left supraclavicular lymph node enlargement with high uptake of fluorodeoxyglucose at the time of lymphoma diagnosis; B: Disease remission after eight cycles of chemotherapy.

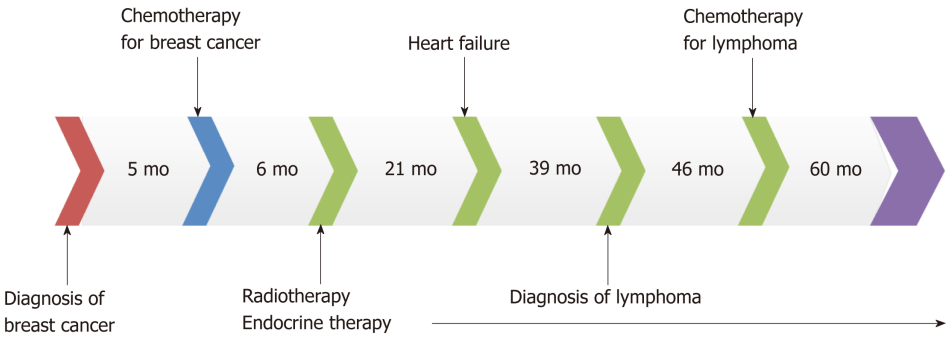

Figure 4 Patient's anti-cancer treatment schedule from the initial diagnosis of breast cancer to the treatment of lymphoma and accompanying follow-up.

REFERENCES

1 **Siegel R**, DeSantis C, Virgo K, Stein K, Mariotto A, Smith T, Cooper D, Gansler T, Lerro C, Fedewa S, Lin C, Leach C, Cannady RS, Cho H, Scoppa S, Hachey M, Kirch R, Jemal A, Ward E. Cancer treatment and survivorship statistics, 2012. *CA Cancer J Clin* 2012; **62**: 220-241 [PMID: 22700443 DOI: 10.3322/caac.21149]

2 **Ewer MS**, Ewer SM. Cardiotoxicity of anticancer treatments. *Nat Rev Cardiol* 2015; **12**: 620 [PMID: 26292190 DOI: 10.1038/nrcardio.2015.133]

3 **Swain SM**, Whaley FS, Ewer MS. Congestive heart failure in patients treated with doxorubicin: a retrospective analysis of three trials. *Cancer* 2003; **97**: 2869-2879 [PMID: 12767102 DOI: 10.1002/cncr.11407]

4 **Donin N**, Filson C, Drakaki A, Tan HJ, Castillo A, Kwan L, Litwin M, Chamie K. Risk of second primary malignancies among cancer survivors in the United States, 1992 through 2008. *Cancer* 2016; **122**: 3075-3086 [PMID: 27377470 DOI: 10.1002/cncr.30164]

5 **Berrington de Gonzalez A**, Curtis RE, Kry SF, Gilbert E, Lamart S, Berg CD, Stovall M, Ron E. Proportion of second cancers attributable to radiotherapy treatment in adults: a cohort study in the US SEER cancer registries. *Lancet Oncol* 2011; **12**: 353-360 [PMID: 21454129 DOI: 10.1016/S1470-2045(11)70061-4]

6 **Arbel Y**, Swartzon M, Justo D. QT prolongation and Torsades de Pointes in patients previously treated with anthracyclines. *Anticancer Drugs* 2007; **18**: 493-498 [PMID: 17351403 DOI: 10.1097/CAD.0b013e328012d023]

7 **Milberg P**, Fleischer D, Stypmann J, Osada N, Mönnig G, Engelen MA, Bruch C, Breithardt G, Haverkamp W, Eckardt L. Reduced repolarization reserve due to anthracycline therapy facilitates torsade de pointes induced by IKr blockers. *Basic Res Cardiol* 2007; **102**: 42-51 [PMID: 16817026 DOI: 10.1007/s00395-006-0609-0]

8 **Yeh ET**, Bickford CL. Cardiovascular complications of cancer therapy: incidence, pathogenesis, diagnosis, and management. *J Am Coll Cardiol* 2009; **53**: 2231-2247 [PMID: 19520246 DOI: 10.1016/j.jacc.2009.02.050]

9 **Cardinale D**, Colombo A, Bacchiani G, Tedeschi I, Meroni CA, Veglia F, Civelli M, Lamantia G, Colombo N, Curigliano G, Fiorentini C, Cipolla CM. Early detection of anthracycline cardiotoxicity and improvement with heart failure therapy. *Circulation* 2015; **131**: 1981-1988 [PMID: 25948538 DOI: 10.1161/CIRCULATIONAHA.114.013777]

10 **Chow EJ**, Chen Y, Kremer LC, Breslow NE, Hudson MM, Armstrong GT, Border WL, Feijen EA, Green DM, Meacham LR, Meeske KA, Mulrooney DA, Ness KK, Oeffinger KC, Sklar CA, Stovall M, van der Pal HJ, Weathers RE, Robison LL, Yasui Y. Individual prediction of heart failure among childhood cancer survivors. *J Clin Oncol* 2015; **33**: 394-402 [PMID: 25287823 DOI: 10.1200/JCO.2014.56.1373]

11 **Mackey JR**, Martin M, Pienkowski T, Rolski J, Guastalla JP, Sami A, Glaspy J, Juhos E, Wardley A,

Fornander T, Hainsworth J, Coleman R, Modiano MR, Vinholes J, Pinter T, Rodríguez-Lescure A, Colwell B, Whitlock P, Provencher L, Laing K, Walde D, Price C, Hugh JC, Childs BH, Bassi K, Lindsay MA, Wilson V, Rupin M, Houé V, Vogel C; TRIO/BCIRG 001 investigators. Adjuvant docetaxel, doxorubicin, and cyclophosphamide in node-positive breast cancer: 10-year follow-up of the phase 3 randomised BCIRG 001 trial. *Lancet Oncol* 2013; **14**: 72-80 [PMID: 23246022 DOI: 10.1016/S1470-2045(12)70525-9]

12 **Kwok JC**, Richardson DR. Anthracyclines induce accumulation of iron in ferritin in myocardial and neoplastic cells: inhibition of the ferritin iron mobilization pathway. *Mol Pharmacol* 2003; **63**: 849-861 [PMID: 12644586 DOI: 10.1124/mol.63.4.849]

13 **Cardinale D**, Colombo A, Lamantia G, Colombo N, Civelli M, De Giacomi G, Rubino M, Veglia F, Fiorentini C, Cipolla CM. Anthracycline-induced cardiomyopathy: clinical relevance and response to pharmacologic therapy. *J Am Coll Cardiol* 2010; **55**: 213-220 [PMID: 20117401 DOI: 10.1016/j.jacc.2009.03.095]

14 **Felker GM**, Thompson RE, Hare JM, Hruban RH, Clemetson DE, Howard DL, Baughman KL, Kasper EK. Underlying causes and long-term survival in patients with initially unexplained cardiomyopathy. *N Engl J Med* 2000; **342**: 1077-1084 [PMID: 10760308 DOI: 10.1056/NEJM200004133421502]

15 **Cardinale D**, Colombo A, Sandri MT, Lamantia G, Colombo N, Civelli M, Martinelli G, Veglia F, Fiorentini C, Cipolla CM. Prevention of high-dose chemotherapy-induced cardiotoxicity in high-risk patients by angiotensin-converting enzyme inhibition. *Circulation* 2006; **114**: 2474-2481 [PMID: 17101852 DOI: 10.1161/CIRCULATIONAHA.106.635144]

16 **Lin RJ**, Behera M, Diefenbach CS, Flowers CR. Role of anthracycline and comprehensive geriatric assessment for elderly patients with diffuse large B-cell lymphoma. *Blood* 2017; **130**: 2180-2185 [PMID: 28814386 DOI: 10.1182/blood-2017-05-736975]

17 **Gulati G**, Heck SL, Ree AH, Hoffmann P, Schulz-Menger J, Fagerland MW, Gravdehaug B, von Knobelsdorff-Brenkenhoff F, Bratland Å, Storås TH, Hagve TA, Røsjø H, Steine K, Geisler J, Omland T. Prevention of cardiac dysfunction during adjuvant breast cancer therapy (PRADA): a 2 × 2 factorial, randomized, placebo-controlled, double-blind clinical trial of candesartan and metoprolol. *Eur Heart J* 2016; **37**: 1671-1680 [PMID: 26903532 DOI: 10.1093/eurheartj/ehw022]

18 **Luu AZ**, Chowdhury B, Al-Omran M, Teoh H, Hess DA, Verma S. Role of Endothelium in Doxorubicin-Induced Cardiomyopathy. *JACC Basic Transl Sci* 2018; **3**: 861-870 [PMID: 30623145 DOI: 10.1016/j.jacbts.2018.06.005]

19 **Zamorano JL**, Lancellotti P, Rodriguez Muñoz D, Aboyans V, Asteggiano R, Galderisi M, Habib G, Lenihan DJ, Lip GYH, Lyon AR, Lopez Fernandez T, Mohty D, Piepoli MF, Tamargo J, Torbicki A, Suter TM; ESC Scientific Document Group. 2016 ESC Position Paper on cancer treatments and cardiovascular toxicity developed under the auspices of the ESC Committee for Practice Guidelines: The Task Force for cancer treatments and cardiovascular toxicity of the European Society of Cardiology (ESC). *Eur Heart J* 2016; **37**: 2768-2801 [PMID: 27567406 DOI: 10.1093/eurheartj/ehw211]

World Journal of Clinical Cases

Submit a Manuscript: https://www.f6publishing.com

World J Clin Cases 2019 June 26; 7(12): 1499-1507

DOI: 10.12998/wjcc.v7.i12.1499

ISSN 2307-8960 (online)

CASE REPORT

Removal of pediatric stage IV neuroblastoma by robot-assisted laparoscopy: A case report and literature review

Di-Xiang Chen, Yi-Han Hou, Ya-Nan Jiang, Li-Wei Shao, Shan-Jie Wang, Xian-Qiang Wang

ORCID number: Di-Xiang Chen (0000-0003-1083-9902); Yi-Han Hou (0000-0003-1873-788X); Ya-Nan Jiang (0000-0001-8082-9473); Li-Wei Shao (0000-0001-7763-2506); Shan-Jie Wang (0000-0002-5741-1762); Xian-Qiang Wang (0000-0002-8914-6545).

Author contributions: Chen DX and Hou YH contributed equally to this article and should be considered as co-first authors. Chen DX, Hou YH, Wang SJ, and Wang XQ designed this case report; Hou YH, Jiang YN, Shao LW, and Wang XQ wrote the manuscript.

Supported by the PLA General Hospital Clinical Support Grant, No. 2017FC-TSYS-3031 and No. 2017FC-TSYS-3010.

Informed consent statement: The patient provided informed written consent.

Conflict-of-interest statement: The authors declare that they have no conflicts of interest.

CARE Checklist (2016) statement: The authors have read the CARE Checklist (2016), and the manuscript was prepared and revised according to the CARE Checklist (2016).

Di-Xiang Chen, Xian-Qiang Wang, Department of Pediatrics, PLA General Hospital, Beijing 100853, China

Yi-Han Hou, Ya-Nan Jiang, Beijing University of Chinese Medicine, Beijing 100029, China

Li-Wei Shao, Department of Pathology, PLA General Hospital, Beijing 100853, China

Shan-Jie Wang, Department of Hepatobiliary Disease, Sixth People's Hospital of Jinan Affiliated to Jining Medical School, Jinan 250200, Shandong Province, China

Corresponding author: Xian-Qiang Wang, MD, PhD, Assistant Professor, Department of Pediatrics, PLA General Hospital, No. 28, Fuxing Road, Haidian District, Beijing 100853, China. wxq301@gmail.com
Telephone: +86-13522891848
Fax: +86-10-66938418

Abstract

BACKGROUND

Neuroblastoma (NB) is the most common extracranial solid tumor in children, with an incidence of approximately 1/10000. Surgical resection is an effective treatment for children with NB. Robot-assisted laparoscopic surgery is a new method and is superior to conventional laparoscopic surgery, since it has been preliminarily applied in clinical practice with a significant curative effect. This paper discusses significance and feasibility of complete resection of stage IV NB using robot-assisted laparoscopic surgery, while comparing its safety and effectiveness with conventional laparoscopic surgery.

CASE SUMMARY

In June 2018, a girl with stage IV retroperitoneal NB, aged 3 years and 5 mo, was admitted. Her weight was 15 kg, and her height was 100 cm. Robot-assisted, five-port laparoscopic resection of NB was performed. Starting from the middle point between the navel and the anterior superior iliac spine to the left lower abdomen, the pneumoperitoneum and observation hole (10 mm) were established using the Hasson technique. Operation arm #1 was located between the left anterior axillary line, the navel, and the costal margin (8 mm); operation arm #2 was located at the intersection of the right anterior axillary line and Pfannenstiel line (8 mm); one auxiliary hole was located between arm #2 (on the Pfannenstiel line) and the observation hole (12 mm); and another auxiliary hole (5 mm) was located slightly below the left side of the xiphoid. Along the right line of Toldt and the hepatic flexure of the transverse colon, the colon was turned to the left and below with a hook electrode. Through Kocher's incision, the duodenum and the

Manuscript source: Unsolicited manuscript

Received: February 16, 2019
Peer-review started: February 18, 2019
First decision: April 18, 2019
Revised: April 29, 2019
Accepted: May 11, 2019
Article in press: May 11, 2019
Published online: June 26, 2019

P-Reviewer: Hayes MJ, Higgins PD
S-Editor: Wang JL
L-Editor: Wang TQ
E-Editor: Wang J

pancreatic head were turned to the left to expose the inferior vena cava and the abdominal aorta. The vein was separated along the right external iliac, and the inferior vena cava was then lifted to expose the right renal vein from the bottom to the top. The tumor was transected horizontally below the renal vein, and it was first cut into pieces and then resected. The right renal artery and the left renal vein were also exposed, and the retrohepatic inferior vena cava was isolated. The tumor was resected along the surface of the psoas muscle, the back of the inferior vena cava, and the right side of the abdominal aorta. Finally, the lymph node metas-tases in front of the abdominal aorta and left renal vein were completely removed. The specimens were loaded into a disposable specimen retrieval bag and removed from the enlarged auxiliary hole. T-tube drainage was placed and brought out through a hole in the right lower quadrant of the abdomen. The operative time was 389 min, the time of pneumoperitoneum was 360 min, the intraoperative blood loss was approximately 200 mL, and the postoperative recovery was smooth. There were no complications, such as lymphatic fistula, diarrhea, bleeding, and paralytic ileus. Two months after discharge, there were no other complications. The literature on the application of robot-assisted laparoscopic surgery in the treatment of NB in children was reviewed

CONCLUSION
The robot has the advantages of a three-dimensional view and flexible operation, and it can operate finely along blood vessels. The successful experience of this case confirmed that robot-assisted laparoscopic surgery can skeletonize the abdominal blood vessels in the tumor and cut the tumor into pieces, indicating that robot-assisted laparoscopic surgery is feasible.

Key words: Robot-assisted surgery; Retroperitoneal neuroblastoma; Children; Case report

Core tip: Our paper describes the key surgical points in pediatric stage IV neuroblastoma that was completely resected using the Da Vinci robotic system. An adrenalectomy was carried out for a girl aged 3 years and 5 months by robot-assisted laparoscopic surgery at our hospital, and then systematic literature review was done to discuss the significance and feasibility of complete resection of stage IV neuroblastoma, the surgical safety and advantages, and the safety and effectiveness of robot-assisted surgery compared with traditional laparoscopic surgery.

Citation: Chen DX, Hou YH, Jiang YN, Shao LW, Wang SJ, Wang XQ. Removal of pediatric stage IV neuroblastoma by robot-assisted laparoscopy: A case report and literature review. *World J Clin Cases* 2019; 7(12): 1499-1507
URL: https://www.wjgnet.com/2307-8960/full/v7/i12/1499.htm
DOI: https://dx.doi.org/10.12998/wjcc.v7.i12.1499

INTRODUCTION

Neuroblastoma (NB) is a highly heterogeneous tumor. Some tumors can spontaneously subside without treatment. However, most tumors are occult and rapidly metastasize throughout the body, ultimately becoming life-threatening. Surgical resection is an effective treatment for children with NB. Minimally invasive surgery has unique advantages in NB resection, and case reports of laparoscopic NB resection confirm its safety and feasibility[1]. Robot-assisted laparoscopic surgery is a new method and is superior to conventional laparoscopic surgery, which has been preliminarily applied in clinical practice, yielding significant curative effects[2]. This method can further promote the resection of pediatric tumors in a minimally invasive manner.

Robot-assisted surgery has been widely used in adult surgery, including general surgery[3-5], urinary surgery[6-8], and cardiac surgery[9-11]. Currently, robot-assisted systems, either alone or in combination with laparoscopic surgery, have been relatively mature in adult surgery, especially in the field of urology[12]. There are many retrospective clinical case reports comparing the safety and efficacy of robotic surgery

in adult surgery through randomized controlled studies[13-15], which have confirmed its safety and feasibility.

Compared with adults, the age, physio-pathological conditions, and lesion location of children are unique and complex, rendering the advantages of robot-assisted surgery more prominent in the field of pediatric surgery. Pediatric surgeries involving the abdominal cavity, pelvic cavity, and thoracic cavity have been reported in China and abroad[16-18]. It is confirmed that with robot-assisted systems, pediatric surgery is safe and feasible.

In the field of pediatric NB, Yu *et al*[1] from the University of Oklahoma reported the first robot-assisted resection of pediatric NB in the *Journal of Robotic Surgery* in 2014. In that study, the prenatal ultrasound already suggested bilateral hydronephrosis in the patient, and a left adrenal gland mass with a size of 2.5 cm × 1.5 cm was found in the subsequent examinations. Therefore, when the patient was 15 mo old, robotic-assisted left adrenal gland mass resection and ipsilateral retroperitoneal lymph node dissection were performed. The transumbilical approach was used to perform the surgery. The robotic cannula was placed and the surgery was successfully performed using the Da Vinci robotic system. Pathological examination confirmed that the tumor was an NB (stage 2b). The patient did not have intraoperative or postoperative complications and was discharged 24 h after surgery. The patient resumed all activities within one week after the surgery, and no signs of recurrence were found during the regular postoperative follow-ups. This case shows that, compared with open surgery, robot-assisted surgery can not only successfully yield the same oncological results but also help reduce the disease recurrence rate and shorten the durations of surgery, hospitalization stay, and postoperative recovery.

Zhu *et al*[19] from Tongji Hospital of Huazhong University of Science and Technology reported the application of a robotic surgical system in the surgical treatment of pediatric NB in 2017 in China. The outcomes of three cases of pediatric adrenal pheochromocytoma treated using the Da Vinci robot system were reported. Among the patients, one was male and the other two were female, with an average age of 5.2 years. The tumors were all on the right side, with a size of (2.0-3.6) cm × (1.0-3.6) cm. The Da Vinci robotic system was used to successfully complete the surgery, and the robotic surgery advantages of minimal trauma and quick recovery were confirmed. The study by Zhu *et al*[19] provided practical experience in applying robot-assisted surgery in the field of pediatric NB resection.

We successfully completed a stage IV pediatric NB resection using the Da Vinci Si robot system. The purpose of this study was to explore the feasibility and effectiveness of robotic surgery in the treatment of complicated NB in children and to summarize the preliminary experience in applying this technique.

CASE PRESENTATION

Chief complaints

The patient was a girl aged 3 years and 5 mo. At the end of 2017, the patient was admitted due to abdominal discomfort, and a mass in the right upper quadrant of the abdomen was found. After supraclavicular lymph node biopsy, the patient was diagnosed with stage IV retroperitoneal NB. After chemotherapy (four cycles), the tumor shrank significantly, but the primary tumor behind the inferior vena cava remained.

Physical examination

The abdomen was soft, without tenderness, rebound pain, or an obvious mass. The liver and spleen were impalpable, Murphy's sign was negative, and the bowel sounds were normal.

Laboratory examinations

The laboratory values were the following: Serum ferratin, 1957.00 ng/mL; alanine transaminase, 31.2 U/L; aspartate transaminase, 38.9 U/L; alkaline phosphatase, 165.2 U/L; urea, 3.06 mmol/L; SCr, 33.4 μmol/L; hemoglobin, 87 g/L; red blood cell count, 2.78×10^{12}/L; and white blood cell count, 9.24×10^{9}/L.

Imaging examination

Before chemotherapy, abdominal enhanced computed tomography showed a middle line retroperitoneal neoplasm with the inferior vena cava, right renal vessels, and abdominal aorta traversing in it. After chemotherapy, the tumor shrank considerably and the above-mentioned vessels were still encased by the tumor. After surgery, the clearance of the tumor around the vessels was achieved (Figure 1).

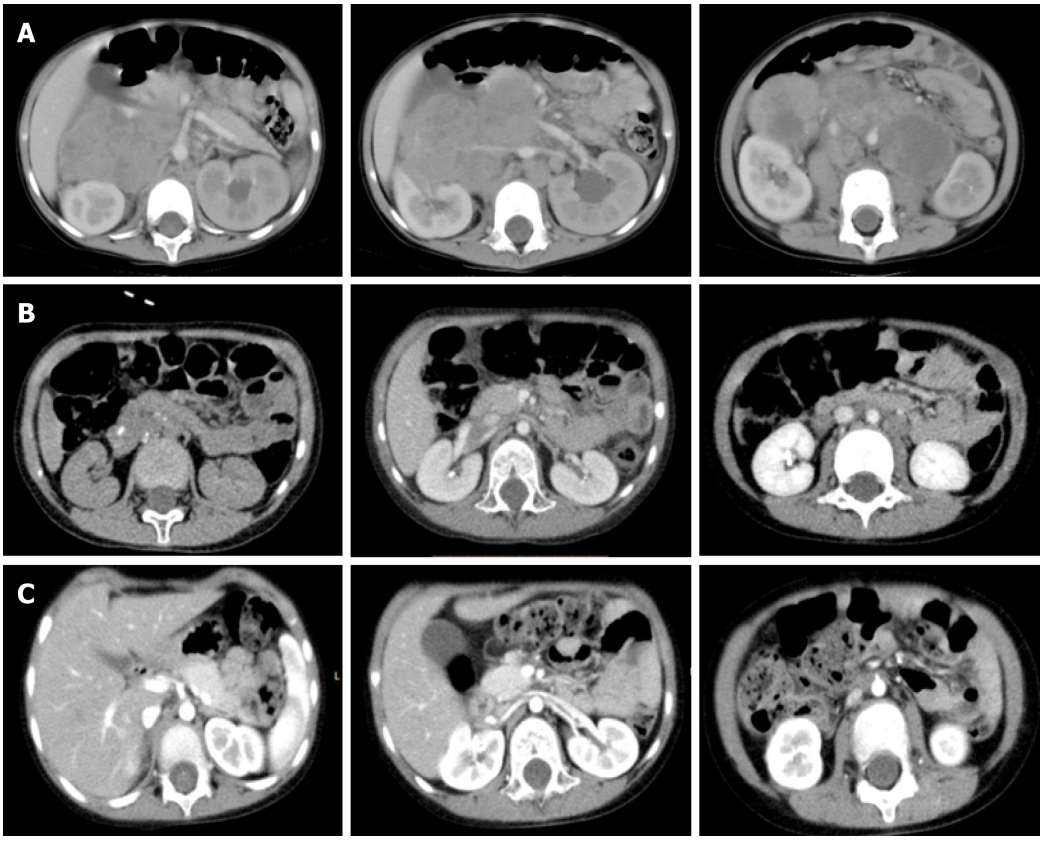

Figure 1 Abdominal enhanced computed tomography images. A: A middle line retroperitoneal neoplasm with the inferior vena cava, right renal vessels, and abdominal aorta traversing in it (before chemotherapy); B: The tumor shrank considerably, but the above-mentioned vessels were still encased by the tumor (preoperatively after chemotherapy); C: Clearance of the tumor around the vessels (postoperative changes).

Preoperative biopsy pathological diagnosis

The preoperative biopsy pathological diagnosis from the left cervical lymph nodes, combined with the pathological morphology and immune phenotype, was consistent with an undifferentiated NB metastasis. The immunohistochemical results were CD-56 (+), CD-ROM9 (+, spotty), nuclear CgA (+), CKpan (-), HMB-45 (-), Ki-67 (+, >95%), LCA (-), NSE (+, focal and weak), S-100 (-), and Syn (+).

FINAL DIAGNOSIS

The preoperative diagnosis was NB.

TREATMENT

Anesthesia and position

Tracheal intubation was performed under general anesthesia, followed by urinary catheterization. The catheterization of the right internal jugular vein and blood pressure monitoring of the right radial artery were performed routinely. The left lateral position at an angle of 45° was used. Stretch socks were worn on the lower extremities to prevent thrombosis. The robot was put on the patient's back, the first assistant was located on the ventral side of the patient, and the instrument nurse was close to the patient's feet.

Trocar location

The five-port technique was used (Figure 2). Starting from the middle point between the navel and the anterior superior iliac spine to the left lower abdomen, the pneumoperitoneum and observation hole (10 mm) were established using the Hasson technique. Operation arm #1 was located between the left anterior axillary line, the navel, and the costal margin (8 mm); operation arm #2 was located at the intersection of the right anterior axillary line and Pfannenstiel line (8 mm); one auxiliary hole was located between arm #2 (on the Pfannenstiel line) and the observation hole (12 mm);

and another auxiliary hole (5 mm) (initially taken as arm 3, changing into auxiliary hole because of the narrow space leading to collision of the robotic arms) was located slightly below the left side of the xiphoid.

Surgical procedure

Along the right line of Toldt and the hepatic flexure of the transverse colon, the colon was turned to the left and below with a hook electrode. Through Kocher's incision, the duodenum and the pancreatic head were turned to the left to expose the inferior vena cava and the abdominal aorta. The vein was separated along the right external iliac, and the inferior vena cava was then lifted to expose the right renal vein from the bottom to the top. The tumor was transected horizontally below the renal vein and was first cut into pieces and then resected. The right renal artery and the left renal vein were also exposed, and the retrohepatic inferior vena cava was isolated. The tumor was resected along the surface of the psoas muscle, the back of the inferior vena cava, and the right side of the abdominal aorta. Finally, the lymph node metastases in front of the abdominal aorta and left renal vein were completely removed. The specimens were loaded into a disposable specimen retrieval bag and removed from the enlarged auxiliary hole. T-tube drainage was placed and brought out through a hole in the right lower quadrant of the abdomen. Each puncture hole was sutured using a 3-0 absorbable suture.

Postoperative management

Conventional administrations of anti-inflammatory medications, fluid replacement, gastrointestinal decompression, acid suppression, and enzymatic inhibition were performed. The abdominal drainage volume and amylase level were monitored. The gastric tube was extracted on the third day after surgery, and the patient was placed on a liquid diet. After eating a normal diet, the abdominal drainage tube was removed when no lymphatic leakage or exudate was observed, and the patient was discharged (Figure 3).

OUTCOME AND FOLLOW-UP

Intraoperative status

The operative time was 389 min, the time of pneumoperitoneum was 360 min, and the intraoperative blood loss was approximately 200 mL.

Postoperative status

Immediately after surgery, the blood amylase level was 1426.3 U/L (normal range, 0-150), the blood lipase level was 54.6 U/L (normal range, 23-300), the blood alanine aminotransferase level was 197.6 U/L (normal range, 0-40), and the blood aspartate aminotransferase level was 302.7 U/L (normal range, 0-40). The gastric tube was extracted on the third day after surgery, and no abdominal discomfort was found after drinking water. A liquid diet was administered to the patient on the fourth day. The blood amylase level was 64.3 U/L (normal range, 0-150), the blood lipase level was 240.6 U/L (normal range, 23-300), the blood alanine aminotransferase level was 73.7 U/L (normal range, 0-40), and the blood aspartate aminotransferase level was 49.1 U/L (normal range, 0-40) on the fourth day. The patient was given pediatric food on the seventh day. The fluid in the retroperitoneal drainage tube gradually decreased; therefore, on the tenth day, the retroperitoneal drainage tube was removed, and the patient was discharged. The patient continued to receive chemotherapy after discharge. A follow-up visit was performed 2 months later. Contrast-enhanced computed tomography showed that no tumor recurrence was observed, and no effusion was found in the surgical area.

Postoperative pathological examination

On June 29, 2018, the pathological (conventional) examination results for the right adrenal gland and retroperitoneum were obtained. Degenerated small-round cells, ganglion cells with foam cell aggregation, and hemosiderosis were scattered in the adrenal tissue and hyperplastic fibrous tissue. Locally degenerated and necrotic nodules with a large amount of foam cell aggregation and scattered calcification were found, which is consistent with postoperative changes in NB. Immunohistochemistry results were: CD56 (+), CD99 (-), NSE (+), Ki-67 (+, 2%), Syn (+), CgA (-), NF (+), S-100 (+) (Tumor metastasis in the left abdominal aorta). Necrosis and calcification of small lesions in fibrous connective tissues were present, but no tumor cells were found (Figure 4).

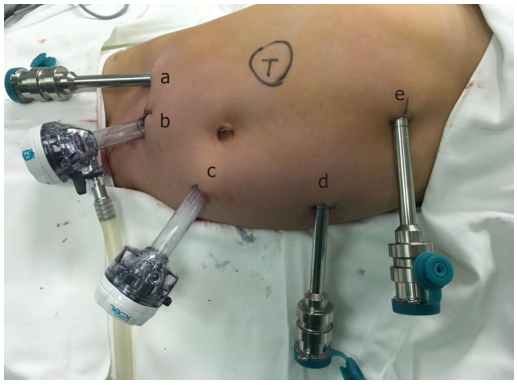

Figure 2 Trocar locations. A is the hole for the second arm of the robot, b is the auxiliary hole, c is the lens hole, d is the hole for the first arm of the robot, and e is the second auxiliary hole.

DISCUSSION

NB is the most common extracranial solid tumor in children, with an incidence of approximately 1/10000. It is also one of the most challenging operations in pediatric surgery. Traditional open surgery has disadvantages, such as the creation of a large incision, difficulty achieving deep exposure, severe trauma, and a long recovery period. Since the first report of laparoscopic adrenalectomy[20], laparoscopic adrenalectomy has been frequently reported[21-23]. The application of laparoscopy in NB resection is very extensively reported in the literature; however, if the NB is closely associated with important blood vessels, the use of a laparoscope in NB resection is still challenging and has limitations. Robotic surgery is a minimally invasive surgery with greater convenience and effectiveness[24]. Robot-assisted laparoscopic resection of retroperitoneal NB is rarely reported[1].

The resection of the primary foci of stage IV NB is still a controversial issue, with some studies suggesting that it is only superior to a simple biopsy, and the prognosis is more dependent on biological characteristics rather than the number of resected primary foci[25,26] . However, most researchers still suggest the resection of over 95% of the tumor foci[27,28]. The primary foci of stage IV NB are often large and envelope important blood vessels, and different five-year survival rates after complete primary tumor resection (26%, 30%, 52%, and 65%) have been reported[29-31]. To achieve a good prognosis, the resection of 95% of the tumor tissue is the goal of tumor surgeons. However, Kiely and Sultan reported that this goal can only be achieved in 89% and 58% of patients, respectively.

La Quaglia *et al*[32] reported the effect of aggressive surgical resection of the tumor on the prognosis. For children with a diagnosis of stage IV NB, complete removal of the tumor is unachievable. Delayed surgery or a second surgery can improve local tumor shrinkage and the metastasis disappearance rate after preoperative chemotherapy and prolong survival. However, the study by Castel *et al*[26] denied the therapeutic effect of surgical resection of stage IV NB and suggested that age, N-myc gene amplification, and distant metastasis have a much greater influence on the prognosis of stage IV NB than complete resection. Therefore, the treatment of stage IV NB should be a combination of surgery, radiotherapy, chemotherapy, and other treatments. Preoperative chemotherapy is necessary to remove the NB that envelopes important peritoneal blood vessels. Through chemotherapy, tumors can shrink significantly and harden, and the blood supply and other risk factors can decrease, making the resection of unresectable tumors possible[33,34].

Separation is one of the techniques used to protect important blood vessels. We started from the relatively normal right common iliac vein, separated the inferior vena cava from bottom to top, ligated the right gonadal vein, and separated the right renal vein and left renal vein. Horizontal tumor transection was performed below the right renal vein to facilitate the exposure of the right renal artery and the right superior mesenteric artery. The inferior vena cava was lifted again, and the tumor above the right renal vein and on the right side of the abdominal aorta was resected. During the resection, the right adrenal gland covered the top of the tumor in the form of a sheet, and there was no significant thickened right middle adrenal vein. It is considered that the tumor originated from the retroperitoneal sympathetic nerve chain instead of the right adrenal gland. Finally, metastatic tumors in front of the left kidney were excised. During the separation process, we found that the stability of the hook electrode was better than that of electric scissors, and the hemostatic effect of the bipolar

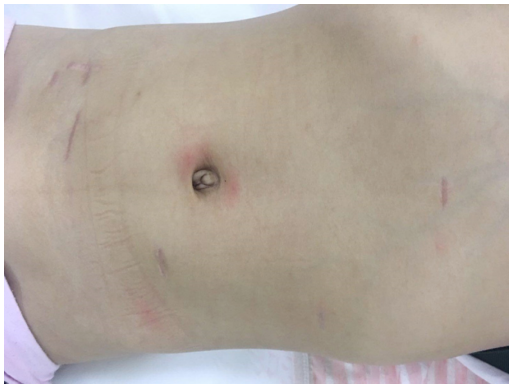

Figure 3 Incision healing at 2 mo after five-port laparoscopic surgery.

electrosurgical knife was good.

Piecemeal resection is a necessary technique[35]. Because the tumor envelopes the blood vessels, the vessels cannot be preserved without opening the tumor; thus, the tumor cannot be removed wholly. During NB resection in the advanced stages, *en bloc* resection cannot be achieved; therefore, piecemeal resection is necessary to improve the prognosis.

Maximization of the operating space should be considered. Children are typically short, and the abdominal space is small. The appropriate Trocar positions are below and to the left of the umbilicus. After placing the Trocar and the lens under the umbilicus, two auxiliary holes (left lower abdomen and left lateral xiphoid) should be arranged, since the operation is mainly performed in the right upper abdomen and behind the inferior vena cava. Arms #1 and #2 were arranged on the left side of the abdomen and the right lower abdomen, respectively, which can operate on the lesions on the right side and upper abdomen. During the operation, a cold lens was placed in the left lower abdomen, expanding the operating space. The operation was completed using the five-port approach, and no instruments collided with each other.

Robot assistance is the key to the skeletonization of blood vessels. Conventional laparoscopic surgery is difficult and cannot achieve the resection of complex tumors. During the operation, the inferior vena cava, the bilateral renal veins, and the right renal artery are skeletonized; therefore, surgery is difficult, and the risk is high. Robots can provide a three-dimensional view with 10 × magnification. Shaking can be eliminated, and hand actions can be simulated. The robots can complete clamping, suturing, knotting, and other operations and achieve results similar to those of open surgery. Robotic surgery can preserve the aesthetic characteristics of the laparoscopic surgical incision. We placed arm #2 and auxiliary hole #1 on the Pfannenstiel line, and the tumor specimens were obtained from this line, which improves the postoperative appearance. No common complications, such as postoperative diarrhea[36], lymphatic fistula, or intestinal obstruction, were found. However, due to the long operative time, redness and swelling of the left waist skin occurred but completely disappeared after one week. Because of the isolation of the pancreas and liver, the amylase and transaminase levels also showed a transient increase but soon returned to normal. Robotic-assisted surgery not only maintains the advantages of minimally invasive surgery, such as small wounds, good aesthetics, and short operative time, hospitalization stay, and postoperative recovery time, but also addresses the limitations of open surgery and laparoscopic technology.

This case is the first pediatric robot-assisted laparoscopic resection of stage IV NB (according to the International Neuroblastoma Staging System criteria) at our hospital, and no serious complications during or after surgery were found. The surgical experience of this case showed that robot-assisted resection of retroperitoneal NB is feasible and can be a new approach for the treatment of advanced NB.

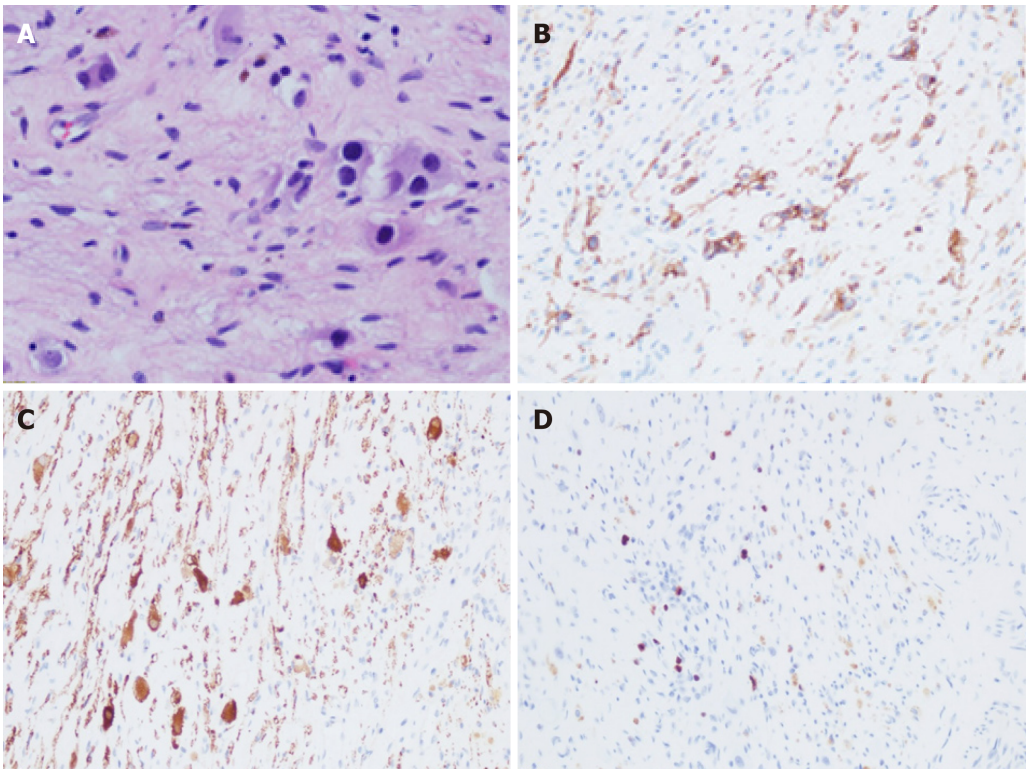

Figure 4 Pathological images. A: Hematoxylin and eosin staining (40×); B-D: Immunohistochemical staining for CD56 (B), NSE (C), and Ki-67 (D) (20×).

REFERENCES

1 **Uwaydah NI**, Jones A, Elkaissi M, Yu Z, Palmer BW. Pediatric robot-assisted laparoscopic radical adrenalectomy and lymph-node dissection for neuroblastoma in a 15-month-old. *J Robot Surg* 2014; **8**: 289-293 [PMID: 27637693 DOI: 10.1007/s11701-013-0441-0]

2 **Guan R**, Chen Y, Yang K, Ma D, Gong X, Shen B, Peng C. Clinical efficacy of robot-assisted versus laparoscopic liver resection: a meta analysis. *Asian J Surg* 2019; **42**: 19-31 [PMID: 30170946 DOI: 10.1016/j.asjsur.2018.05.008]

3 **van der Sluis PC**, van Hillegersberg R. Robot assisted minimally invasive esophagectomy (RAMIE) for esophageal cancer. *Best Pract Res Clin Gastroenterol* 2018; **36-37**: 81-83 [PMID: 30551860 DOI: 10.1016/j.bpg.2018.11.004]

4 **Niu X**, Yu B, Yao L, Tian J, Guo T, Ma S, Cai H. Comparison of surgical outcomes of robot-assisted laparoscopic distal pancreatectomy versus laparoscopic and open resections: A systematic review and meta-analysis. *Asian J Surg* 2019; **42**: 32-45 [PMID: 30337121 DOI: 10.1016/j.asjsur.2018.08.011]

5 **Zhao W**, Liu C, Li S, Geng D, Feng Y, Sun M. Safety and efficacy for robot-assisted versus open pancreaticoduodenectomy and distal pancreatectomy: A systematic review and meta-analysis. *Surg Oncol* 2018; **27**: 468-478 [PMID: 30217304 DOI: 10.1016/j.suronc.2018.06.001]

6 **Perez-Ardavin J**, Sanchez-Gonzalez JV, Martinez-Sarmiento M, Monserrat-Monfort JJ, García-Olaverri J, Boronat-Tormo F, Vera-Donoso CD. Surgical Treatment of Completely Endophytic Renal Tumor: a Systematic Review. *Curr Urol Rep* 2019; **20**: 3 [PMID: 30649644 DOI: 10.1007/s11934-019-0864-x]

7 **Skolarikos A**. Re: Robot-assisted Laparoscopic Prostatectomy Versus Open Radical Retropubic Prostatectomy: 24-month Outcomes from a Randomised Controlled Study. *Eur Urol* 2019; **75**: 200 [PMID: 30391081 DOI: 10.1016/j.eururo.2018.10.039]

8 **Ranasinghe W**, de Silva D, Bandaragoda T, Adikari A, Alahakoon D, Persad R, Lawrentschuk N, Bolton D. Robotic-assisted vs. open radical prostatectomy: A machine learning framework for intelligent analysis of patient-reported outcomes from online cancer support groups. *Urol Oncol* 2018; **36**: 529.e1-529.e9 [PMID: 30236854 DOI: 10.1016/j.urolonc.2018.08.012]

9 **Canale LS**, Mick S, Mihaljevic T, Nair R, Bonatti J. Robotically assisted totally endoscopic coronary artery bypass surgery. *J Thorac Dis* 2013; **5** Suppl 6: S641-S649 [PMID: 24251021 DOI: 10.3978/j.issn.2072-1439.2013.10.19]

10 **Lehr EJ**. Blazing the trail for robot-assisted cardiac surgery. *J Thorac Cardiovasc Surg* 2016; **152**: 14-17 [PMID: 27343905 DOI: 10.1016/j.jtcvs.2016.05.001]

11 **Buehler AM**, Ferri C, Flato UA, Fernandes JG. Robotically assisted coronary artery bypass grafting: a systematic review and meta-analysis. *Int J Med Robot* 2015; **11**: 150-158 [PMID: 25219464 DOI: 10.1002/rcs.1611]

12 **Navaratnam A**, Abdul-Muhsin H, Humphreys M. Updates in Urologic Robot Assisted Surgery. *F1000Res* 2018; 7 [PMID: 30613380 DOI: 10.12688/f1000research.15480.1]

13 **Yu HY**, Hevelone ND, Lipsitz SR, Kowalczyk KJ, Nguyen PL, Choueiri TK, Kibel AS, Hu JC. Comparative analysis of outcomes and costs following open radical cystectomy versus robot-assisted laparoscopic radical cystectomy: results from the US Nationwide Inpatient Sample. *Eur Urol* 2012; **61**: 1239-1244 [PMID: 22482778 DOI: 10.1016/j.eururo.2012.03.032]

14 **Pelletier JS**, Gill RS, Shi X, Birch DW, Karmali S. Robotic-assisted hepatic resection: a systematic

review. *Int J Med Robot* 2013; **9**: 262-267 [PMID: 23749316 DOI: 10.1002/rcs.1500]
15 **Robertson C**, Close A, Fraser C, Gurung T, Jia X, Sharma P, Vale L, Ramsay C, Pickard R. Relative effectiveness of robot-assisted and standard laparoscopic prostatectomy as alternatives to open radical prostatectomy for treatment of localised prostate cancer: a systematic review and mixed treatment comparison meta-analysis. *BJU Int* 2013; **112**: 798-812 [PMID: 23890416 DOI: 10.1111/bju.12247]
16 **Mizuno K**, Kojima Y, Nishio H, Hoshi S, Sato Y, Hayashi Y. Robotic surgery in pediatric urology: Current status. *Asian J Endosc Surg* 2018; **11**: 308-317 [PMID: 30264441 DOI: 10.1111/ases.12653]
17 **Binet A**, Fourcade L, Amar S, Alzahrani K, Cook AR, Braïk K, Cros J, Longis B, Villemagne T, Lardy H, Ballouhey Q. Robot-Assisted Laparoscopic Fundoplications in Pediatric Surgery: Experience Review. *Eur J Pediatr Surg* 2019; **29**: 173-178 [PMID: 29258148 DOI: 10.1055/s-0037-1615279]
18 **Tomaszewski JJ**, Casella DP, Turner RM 2nd, Casale P, Ost MC. Pediatric laparoscopic and robot-assisted laparoscopic surgery: technical considerations. *J Endourol* 2012; **26**: 602-613 [PMID: 22050504 DOI: 10.1089/end.2011.0252]
19 **Zhu TQ**, Liu SB, Zhang W, Yuan JY. Preliminary experience of robotic-assisted laparoscopic adrenalectomy in children. *Zhonghua Xiaoer Waike Zazhi* 2017; **38**: 775-777 [DOI: 10.3760/cma.j.issn.0253-3006.2017.10.01]
20 **Gagner M**, Lacroix A, Bolté E. Laparoscopic adrenalectomy in Cushing's syndrome and pheochromocytoma. *N Engl J Med* 1992; **327**: 1033 [PMID: 1387700 DOI: 10.1056/NEJM199210013271417]
21 **Carvalho JA**, Nunes PT, Antunes H, Parada B, Retroz E, Tavares-da-Silva E, Paiva I, Figueiredo AJ. Transumbilical laparoendoscopic single-site adrenalectomy: A feasible and safe alternative to standard laparoscopy. *Arch Ital Urol Androl* 2019; **91**: 1-4 [PMID: 30932420 DOI: 10.4081/aiua.2019.1.1]
22 **Mohammed A**, Amine H, Atiq SE, Mohammed B, Ouadii M, Khalid M, Khalid AT, Abdelmalek O. Applicability and outcome of laparoscopic adrenalectomy for large tumours. *Pan Afr Med J* 2018; **31**: 23 [PMID: 30918550 DOI: 10.11604/pamj.2018.31.23.15153]
23 **Wind P**, Genser L, Zarzavadjian Le Bian A. The Modified Semi-lateral Transmesocolic Approach for Laparoscopic Left Adrenalectomy. *World J Surg* 2019 [PMID: 30820736 DOI: 10.1007/s00268-019-04954-8]
24 **Zhou X**, Zhang H, Feng M, Zhao J, Fu Y. New remote centre of motion mechanism for robot-assisted minimally invasive surgery. *Biomed Eng Online* 2018; **17**: 170 [PMID: 30453983 DOI: 10.1186/s12938-018-0601-6]
25 **Luo YB**, Cui XC, Yang L, Zhang D, Wang JX. Advances in the Surgical Treatment of Neuroblastoma. *Chin Med J (Engl)* 2018; **131**: 2332-2337 [PMID: 30246719 DOI: 10.4103/0366-6999.241803]
26 **Castel V**, Tovar JA, Costa E, Cuadros J, Ruiz A, Rollan V, Ruiz-Jimenez JI, Perez-Hernández R, Cañete A. The role of surgery in stage IV neuroblastoma. *J Pediatr Surg* 2002; **37**: 1574-1578 [PMID: 12407542]
27 **Yeung F**, Chung PH, Tam PK, Wong KK. Is complete resection of high-risk stage IV neuroblastoma associated with better survival? *J Pediatr Surg* 2015; **50**: 2107-2111 [PMID: 26377869 DOI: 10.1016/j.jpedsurg.2015.08.038]
28 **Zwaveling S**, Tytgat GA, van der Zee DC, Wijnen MH, Heij HA. Is complete surgical resection of stage 4 neuroblastoma a prerequisite for optimal survival or may >95 % tumour resection suffice? *Pediatr Surg Int* 2012; **28**: 953-959 [PMID: 22722825 DOI: 10.1007/s00383-012-3109-3]
29 **Adkins ES**, Sawin R, Gerbing RB, London WB, Matthay KK, Haase GM. Efficacy of complete resection for high-risk neuroblastoma: a Children's Cancer Group study. *J Pediatr Surg* 2004; **39**: 931-936 [PMID: 15185228]
30 **Sultan I**, Ghandour K, Al-Jumaily U, Hashem S, Rodriguez-Galindo C. Local control of the primary tumour in metastatic neuroblastoma. *Eur J Cancer* 2009; **45**: 1728-1732 [PMID: 19447607 DOI: 10.1016/j.ejca.2009.04.021]
31 **Koh CC**, Sheu JC, Liang DC, Chen SH, Liu HC. Complete surgical resection plus chemotherapy prolongs survival in children with stage 4 neuroblastoma. *Pediatr Surg Int* 2005; **21**: 69-72 [PMID: 15647910 DOI: 10.1007/s00383-004-1353-x]
32 **La Quaglia MP**, Kushner BH, Su W, Heller G, Kramer K, Abramson S, Rosen N, Wolden S, Cheung NK. The impact of gross total resection on local control and survival in high-risk neuroblastoma. *J Pediatr Surg* 2004; **39**: 412-7; discussion 412-7 [PMID: 15017562]
33 **Irtan S**, Brisse HJ, Minard-Colin V, Schleiermacher G, Galmiche-Rolland L, Le Cossec C, Elie C, Canale S, Michon J, Valteau-Couanet D, Sarnacki S. Image-defined risk factor assessment of neurogenic tumors after neoadjuvant chemotherapy is useful for predicting intra-operative risk factors and the completeness of resection. *Pediatr Blood Cancer* 2015; **62**: 1543-1549 [PMID: 25820608 DOI: 10.1002/pbc.25511]
34 **Avanzini S**, Pio L, Erminio G, Granata C, Holmes K, Gambart M, Buffa P, Castel V, Valteau Couanet D, Garaventa A, Pistorio A, Cecchetto G, Martucciello G, Mattioli G, Sarnacki S. Image-defined risk factors in unresectable neuroblastoma: SIOPEN study on incidence, chemotherapy-induced variation, and impact on surgical outcomes. *Pediatr Blood Cancer* 2017; **64**: e26605 [PMID: 28440012 DOI: 10.1002/pbc.26605]
35 **Kiely E**. A technique for excision of abdominal and pelvic neuroblastomas. *Ann R Coll Surg Engl* 2007; **89**: 342-348 [PMID: 17535608 DOI: 10.1308/003588407X179071]
36 **Han W**, Wang HM. Refractory diarrhea: A paraneoplastic syndrome of neuroblastoma. *World J Gastroenterol* 2015; **21**: 7929-7932 [PMID: 26167095 DOI: 10.3748/wjg.v21.i25.7929]

World Journal of Clinical Cases

Submit a Manuscript: https://www.f6publishing.com

World J Clin Cases 2019 June 26; 7(12): 1508-1514

DOI: 10.12998/wjcc.v7.i12.1508

ISSN 2307-8960 (online)

CASE REPORT

Premonitory urges located in the tongue for tic disorder: Two case reports and review of literature

Ying Li, Ji-Shui Zhang, Fang Wen, Xiao-Yan Lu, Chun-Mei Yan, Fang Wang, Yong-Hua Cui

ORCID number: Ying Li (0000-0002-7595-2212); Ji-Shui Zhang (0000-0002-9259-4824); Xiao-Yan Lu (0000-0002-5759-0393); Wen Fang (0000-0003-0362-3409); Chun-Mei Yan (0000-0002-8737-6507); Fang Wang (0000-0002-2819-739X); Yong-Hua Cui (0000-0002-8244-5884).

Author contributions: Cui YH supervised the inpatient treatment and hospitalization; Li Y wrote the case presentation; Zhang JS, Lu XY, Yan CM and Wen F took in charge the patient and contribute to describe the case presentation; Wang F and Cui YH reviewed the literature.

Informed consent statement: Written informed consent was provided by the two patients prior to study inclusion. All details of these two cases that might disclose the identity of the subject were omitted or anonymized.

Conflict-of-interest statement: All the authors declare that they have no conflicts of interest to disclose.

CARE Checklist (2016) statement: The authors have read the CARE Checklist (2016), and the manuscript was prepared and revised according to the CARE Checklist (2016).

Ying Li, Ji-Shui Zhang, Fang Wen, Xiao-Yan Lu, Chun-Mei Yan, Fang Wang, Yong-Hua Cui, National Center for Children's Health, Beijing Children's Hospital, Capital Medical University, Beijing 100045, China

Corresponding author: Yong-Hua Cui, MD, Associate Professor, National Center for Children's Health, Beijing Children's Hospital, Capital Medical University, Nanlishi Road 56, Beijing 100045, China. cuiyonghuapsy@126.com
Telephone: +86-10-59616161
Fax: +86-10-59616161

Abstract

BACKGROUND

Premonitory urges (PUs) was defined as the uncomfortable physical sensations of inner tension that can be relieved by producing movement responses. Nearly 70%-90% patients with Tourette syndrome reported experiences of PUs.

CASE SUMMARY

In this paper, we present two cases of young patients with PUs located in their tongue, which is very rare and easily misdiagnosed in clinical work. Both two young patients complained of an itchy tongue and cannot help biting their tongue. These two cases were worth reporting because it was rare that PUs was the initial symptom and located in the tongue. The results indicated that PUs seem to play an important role in the generation of tics.

CONCLUSION

Thus, PUs may be the first process, and an essential part, of the formation of tics.

Key words: Premonitory urges; Sensory tics; Tic disorders; Tourette syndrome; Case report

Core tip: These two cases were worth reporting because it was rare that premonitory urges (PUs) was the initial symptom and located in the tongue. The results indicated that PUs seem to play an important role in the generation of tics.

Citation: Li Y, Zhang JS, Wen F, Lu XY, Yan CM, Wang F, Cui YH. Premonitory urges located in the tongue for tic disorder: Two case reports and review of literature. *World J Clin*

Manuscript source: Unsolicited manuscript

Received: February 2, 2019
Peer-review started: February 11, 2019
First decision: March 9, 2019
Revised: March 28, 2019
Accepted: April 9, 2019
Article in press: April 9, 2019
Published online: June 26, 2019

P-Reviewer: Abundo R, Chen YK, Gorseta K, Munhoz EA, Rattan V
S-Editor: Ji FF
L-Editor: A
E-Editor: Wu YXJ

Cases 2019; 7(12): 1508-1514
URL: https://www.wjgnet.com/2307-8960/full/v7/i12/1508.htm
DOI: https://dx.doi.org/10.12998/wjcc.v7.i12.1508

INTRODUCTION

Sensory tics, which were first described by Bliss[1] in 1980, have mainly been described as uncomfortable physical sensations of inner tension that can be relieved by producing movement responses. Over subsequent years, many researchers have used different terminologies to define this symptom[2-4]. For instance, Cohen and Leckman called it the "Sensory phenomena" including descriptors such as "Urge", "Somatic Sensation" and "Heightened sensational Impulsivity"[3]. Some studies have demonstrated that sensory phenomena mainly include bodily sensations, mental urges and feelings of incompleteness, the need for things to be "just right", and motor or vocal responses to the sensations are required[5,6]. However, most recent studies have used the term "premonitory urges (PUs)" to describe this sensory symptom[7-9].

Nearly 70%-90% patients with Tourette syndrome (TS) report experiences of PUs[10,11]. It has been proposed that there are three parts to PUs, including sensory urges (focal visceral-sensations or muscular-skeletal), autonomic urges (symptoms such as nausea, sweating, and palpitations) and cognitive urges (feelings of incompleteness)[5]. Although PUs were not included in the diagnostic criteria of TS, some published studies have regarded it as the core symptom of TS[12,13].

In this paper, we present two cases of young patients with PUs located in their tongue, which is very rare and easily misdiagnosed in clinical work. Both young patients complained of an itchy tongue and cannot help biting their tongue. These two cases were worth reporting because it was rare that PUs were the initial symptom and were located in the tongue. We also provide a literature review on PUs.

CASE PRESENTATION

Chief complaints

Case 1: A 9-year-old girl, started to eat less and less for half a year prior to examination. Her main complaint was "Why is my tongue itchy?" The girl described her feeling as "My tongue was so itchy that I cannot help biting my tongue!". Her weight went from 70 pounds to 36.

Case 2: A 5-year-old boy, also complained of an itchy tongue and could not stop biting the tip of his tongue (Figure 1).

Personal and family history

Case 1: Her medical and family history did not reveal any relevant information.

Case 2: His medical and family history did not reveal any relevant information.

Physical examination

Case 1: Her temperature was 36.1, heart rate was 95 bpm, respiratory rate was 16 breaths per minute, blood pressure was 120/85 mmHg with oxygen saturation in room air was 98%. A clinical intraoral examination was conducted but no significant signal was found.

Case 2: His temperature was 36.4, heart rate was 98 bpm, respiratory rate was 18 breaths per minute, blood pressure was 120/80 mmHg with oxygen saturation in room air was 95%. We also performed a clinical intraoral examination but no significant indicator was found.

Laboratory examinations

Case 1: During the hospitalization, the girl received a series of blood testing, but no significant clinical indicators were found (Table 1).

Case 2: There was no significant clinical indicators were found (Table 2).

Imaging examinations

Case 1: An Magnetic resonance imaging scan of her brain was also obtained but no

Figure 1 The tip of tongue for case 2. The boy can't help biting his tongue, the tip of the tongue has been bitten through.

significant findings were found (Figure 2).

FINAL DIAGNOSIS

Case 1

Provisional Tic Disorder (the Diagnostic Criteria of Provisional Tic Disorder see Supplementary Materials). The symptom of an "itchy tongue" was recognized as a PU, and "biting the tongue" was regarded as a symptom of the tic.

Case 2

The boy was finally diagnosed as having a Provisional Tic Disorder (the Diagnostic Criteria of Provisional Tic Disorder see Supplementary Materials). The symptom "itchy tongue" belonged to one kind of PU.

TREATMENT

Case 1

For medical treatment, Aripiprazole (2.5 mg per day) was used. Psychological interventions were also performed to relieve the PUs (*e.g.*, habit reversal training). The therapeutic effects and safety of this comprehensive treatment program were assessed during those treatments.

Case 2

Clonidine transdermal patch on his back for 4 wk (1 pin).

OUTCOME AND FOLLOW-UP

Case 1

The PUs was mostly relieved, "biting the tongue" has resolved, and her diet returned normal, as well, after four weeks. Finally, by following this treatment program, the girl recovered and was sent back to school after eight weeks.

Case 2

After 6 wk treatment mentioned above, the boy recovered, and the "itchy tongue" was gone.

DISCUSSION

Although most children with TS report PUs[10], few cases have shown the onset of PUs at such a young age (*i.e.*, Case 2). It should be noted that the reporting of PUs relies on an age-related ability to describe sensory phenomena[14]. Rozenman *et al*[15] reported that the severity of PUs increased with age. Woods *et al*[16] found that there were no correlations between the PUs and the severity of tics in young patients before the age of ten. Based on general clinical observations, Leckman *et al*[17,18] reported that young

Table 1 Blood tests of case 1

Items	Abbreviation	Results	Items	Abbreviation	Results
Potassium	K	4.86 mmol/L	White blood cell count	WBC	5.45×10^9
Sodium	Na	141.4 mmol/L	Red blood cell count	RBC	4.26×10^{12}
Chlorine	Cl	105.7 mmol/L	Hemoglobin	HGB	130 g/L
Bicarbonate	CO_2	25.3 mmol/L	Hematocrit	HCT	39.80%
Total protein	TP	76.2 g/L	Mean corpuscular volume	MCV	93.4 fl
blood urea nitrogen	Urea	6.41 mmol/L	Mean corpuscular hemoglobin	MCH	30.5 pg
Creatinine	Cre	43.0 μmol/L	Mean corpuscular hemoglobin concentration	MCHC	327 g/L
Cholesterol	Chol	4.23 mmol/L	Platelet	PLT	238×10^9
Uric acid	UA	352.8 μmol/L	Platelet distribution width	PDW	12.0 fl
Glucose	GLU	4.85 mmol/L	Mean platelet volume	MPV	10.8 fl
Calcium	Ca	2.52 mmol/L	Platelet larger cell ratio	PLCR	30.10%
Phosphorus	P	1.60 mmol/L	Plateletcrit	PCT	0.26
Alkaline phosphatase	ALP	298 U/L	Neutrophil ratio	NEUT	2.50×10^9
Aspartate aminotransferase	AST	33.3 U/L	Lymphocyte ratio	LYMPH	2.31×10^9
Alanine aminotransferase	ALT	26.6 U/L	Monocyte ratio	MONO	0.30×10^9
Gamma-GT	GGT	11.6 U/L	Eosinophil ratio	EO	0.32×10^9
Total bilirubin	TBIL	9.96 μmol/L	Basophil ratio	EASO	0.02×10^9
Triglyceride	TG	0.49 mmol/L	Neutrophil count	NEUT%	45.80%
Creatine kinase	CK	134 U/L	Lymphocyte count	LYMPH%	42.40%
Creatine kinase-MB	CK-MB	22 U/L	Monocyte count	MONO%	5.50%
Lactate dehydrogenase	LDH	235 U/L	Eosinophil count	EO%	5.90%
α-hydroxybutyric dehydrogenase	HBDH	195 U/L	Basophil count	BASO%	0.40%
High-density lipoprotein cholesterol	HDL-C	1.54 mmol/L	Antistreptolysin	ASO	75.30%
Low-density lipoprotein cholesterol	LDL-C	2.09 mmol/L	C-reactive protein	CRP	3.37 mg/L
Very low-density lipoprotein	VLDL-C	0.10 mmol/L	Ceruloplasmin	CER	296.0 mg/L

No significant clinical indicators were found in blood tests of case 1.

children with simple tics (*e.g.*, a quick head jerk or blinking) did not always show sensory phenomena or were unaware of these symptoms until they were ten years old. The first case report for the present study supported that being 10 years old may play an important role in tic awareness. However, a low level of PUs has also been reported in younger patients (such as Case 2). For example, Gulisano found a low level of PUs in young patients with TS (mean age, 7.3 years ± 1.5)[11]. We should pay more attention to the "uncomfortable feelings" in young children and take PUs into consideration in clinical work. Developmentally, PUs often appeared three years after the first onset of tics[12,19]. However, in the two abovementioned cases, PUs was regarded as the initial symptom, which is rarely reported in clinical work. These cases indicate that PUs might be the first process in tic disorders for some clinical cases. Indeed, in many studies on PUs, patients always report that tics were executed to alleviate distress-related PUs[13,20]. Some researchers have proposed that there are two processes related to tics: The PUs (negative reinforcement) and the relief after tic expression (positive reinforcement)[16,21]. In the two case reports discussed here, the PUs (itchy tongue) may be an early indicator for tic generation. With the development of PUs, tics (biting the tongue) emerged later.

Moreover, it should be noted that the feelings of PUs might be vague and poorly localized in a certain area, such as the face, neck, shoulder or arms, but rarely in the tongue[8,22]. For the assessment of PUs, two validated scales, the University of São Paulo Sensory Phenomena Scale (USP-SPS) and the Premonitory Urge for Tic Scale, have been developed, and both have shown good psychometric properties[16,23]. While these two scales have been widely used in clinical research related to tics, they report the feelings before tics and the corresponding severity, but they do not include the locations of PUs. Kwak *et al*[6] also designed a questionnaire to identify PUs in patients with TS, which included the locations of PUs. He found that the anatomical locations, including the face/head, neck, shoulders, arms, hands, throats, feet, and stomach/abdomen, were more often reported in TS with PUs. From the two abovementioned cases, we found that PUs could be easily misdiagnosed in clinical works. It seems that

Table 2 Blood tests of case 2

Items	Abbreviation	Results	Items	Abbreviation	Results
Potassium	K	4.15 mmol/L	White blood cell count	WBC	5.43×10^9
Sodium	Na	139.7 mmol/L	Red blood cell count	RBC	5.26×10^{12}
Chlorine	Cl	107.7 mmol/L	Hemoglobin	HGB	128 g/L
Bicarbonate	CO2	26.8 mmol/L	Hematocrit	HCT	37.80%
Total protein	TP	61.8 g/L	Mean corpuscular volume	MCV	92.4 fl
blood urea nitrogen	Urea	4.12 mmol/L	Mean corpuscular hemoglobin	MCH	31.6 pg
Creatinine	Cre	48.1 μmol/L	Mean corpuscular hemoglobin concentration	MCHC	318 g/L
Cholesterol	Chol	2.66 mmol/L	Platelet	PLT	227×10^9
Uric acid	UA	268.0 μmol/L	Platelet distribution width	PDW	11.7 fl
Glucose	GLU	4.93 mmol/L	Mean platelet volume	MPV	11.1 fl
Calcium	Ca	2.41 mmol/L	Platelet larger cell ratio	PLCR	32.10%
Phosphorus	P	1.74 mmol/L	Plateletcrit	PCT	0.29
Alkaline phosphatase	ALP	336 U/L	Neutrophil ratio	NEUT	2.34×10^9
Aspartate aminotransferase	AST	19.3 U/L	Lymphocyte ratio	LYMPH	2.35×10^9
Alanine aminotransferase	ALT	9.5 U/L	Monocyte ratio	MONO	0.28×10^9
Gamma-GT	GGT	12.5 U/L	Eosinophil ratio	EO	0.31×10^9
Total bilirubin	TBIL	13.33 μmol/L	Basophil ratio	EASO	0.02×10^9
Triglyceride	TG	0.51 mmol/L	Neutrophil count	NEUT%	45.60%
Creatine kinase	CK	79 U/L	Lymphocyte count	LYMPH%	41.40%
Creatine kinase-MB	CK-MB	17 U/L	Monocyte count	MONO%	5.45%
Lactate dehydrogenase	LDH	134 U/L	Eosinophil count	EO%	5.85%
α-hydroxybutyric dehydrogenase	HBDH	123 U/L	Basophil count	BASO%	0.42%
High-density lipoprotein cholesterol	HDL-C	1.53 mmol/L	Antistreptolysin	ASO	74.45%
Low-density lipoprotein cholesterol	LDL-C	0.73 mmol/L	C-reactive protein	CRP	3.21 mg/L
Very low-density lipoprotein	VLDL-C	0.10 mmol/L	Ceruloplasmin	CER	287.0 mg/L

No significant clinical indicators were found in blood tests of case 2.

the clinical information about the locations of PUs was an indispensable piece of information for the assessment of PUs.

Several recent studies on children with TS have reported that the severity of PUs increases with the severity of the tics[8,24]. It has been indicated that increased insight into PUs could help patients recognize alleviating factors for tic symptoms and improve their ability to suppress them. For example, higher awareness of PUs could benefit tic suppression[20]. Furthermore, as a potential focus for behavioral or psychological therapy, PUs has received increasingly more attention in recent years[25-27]. The structured behavioral therapy called Comprehensive Behavioral Intervention for Tics has mainly focused on improving the awareness of tics such as PUs[28]. Although the exact role of PUs is unknown, it has been postulated that they could reflect subjective experiences below the tic-production threshold[12]. PUs might be a useful predictor for treatment response due to their relationship with tic severity[29]. It is believed that the hyperactivity of the insula, as well as the anterior cingulate cortex and the supplementary motor area was involved in the neural mechanism of PUs[30-32]. A recent structural neuroimaging study suggested that tic generation was mediated by the insula, which is responsible for the subjective perception of PUs[33]. The study indicated that the insula might play an important role in the translation of urges to tics[34,35].

CONCLUSION

These two case reports are the first to describe PUs as the initial symptoms of TS in clinical work in China. The results indicated that PUs seem to play an important role in the generation of tics. Thus, PUs may be the first process, and an essential part, of the formation of tics. The study of PUs, especially neural mechanisms underlying PUs, would facilitate the understanding of the pathophysiology and pathogenesis of tics.

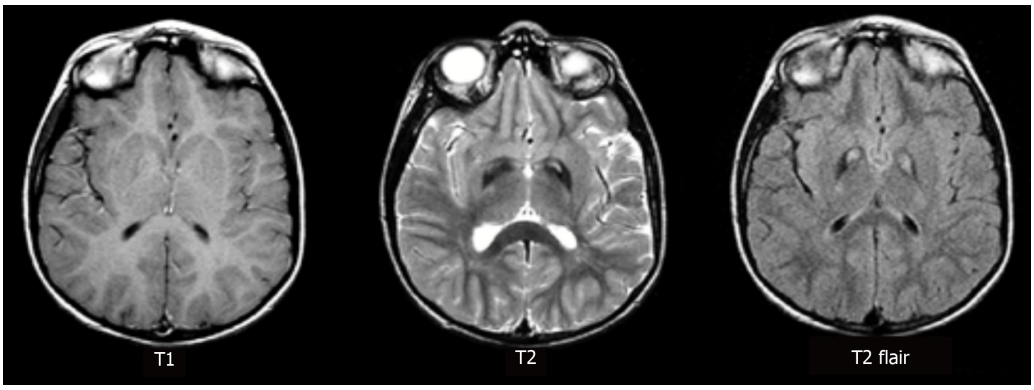

Figure 2 Magnetic resonance imaging scan for case 1. There was no abnormal signal found on T1, T2 and T2 FLAIR of brain scan for case 1.

REFERENCES

1 **Bliss J**. Sensory experiences of Gilles de la Tourette syndrome. *Arch Gen Psychiatry* 1980; **37**: 1343-1347 [PMID: 6934713 DOI: 10.1001/archpsyc.1980.01780250029002]
2 **Kurlan R**, Lichter D, Hewitt D. Sensory tics in Tourette's syndrome. *Neurology* 1989; **39**: 731-734 [PMID: 2710364 DOI: 10.1212/WNL.39.5.731]
3 **Cohen DJ**, Riddle MA, Leckman JF. Pharmacotherapy of Tourette's syndrome and associated disorders. *Psychiatr Clin North Am* 1992; **15**: 109-129 [PMID: 1549543 DOI: 10.1016/S0193-953X(18)30260-0]
4 **Chee KY**, Sachdev P. A controlled study of sensory tics in Gilles de 1a Tourette syndrome and obsessive-compulsive disorder using a structured interview. *J Neurol Neurosurg Psychiatry* 1997; **62**: 188-192 [PMID: 9048721 DOI: 10.1136/jnnp.62.2.188]
5 **Miguel EC**, do Rosário-Campos MC, Prado HS, do Valle R, Rauch SL, Coffey BJ, Baer L, Savage CR, O'Sullivan RL, Jenike MA, Leckman JF. Sensory phenomena in obsessive-compulsive disorder and Tourette's disorder. *J Clin Psychiatry* 2000; **61**: 150-156; quiz 157 [PMID: 10732667 DOI: 10.4088/JCP.v61n0213]
6 **Kwak C**, Dat Vuong K, Jankovic J. Premonitory sensory phenomenon in Tourette's syndrome. *Mov Disord* 2003; **18**: 1530-1533 [PMID: 14673893 DOI: 10.1002/mds.10618]
7 **Rajagopal S**, Seri And S, Cavanna AE. Premonitory urges and sensorimotor processing in Tourette syndrome. *Behav Neurol* 2013; **27**: 65-73 [PMID: 23187151 DOI: 10.3233/BEN-120308]
8 **Ganos C**, Garrido A, Navalpotro-Gómez I, Ricciardi L, Martino D, Edwards MJ, Tsakiris M, Haggard P, Bhatia KP. Premonitory urge to tic in Tourette's is associated with interoceptive awareness. *Mov Disord* 2015; **30**: 1198-1202 [PMID: 25879819 DOI: 10.1002/mds.26228]
9 **Draper A**, Jackson GM, Morgan PS, Jackson SR. Premonitory urges are associated with decreased grey matter thickness within the insula and sensorimotor cortex in young people with Tourette syndrome. *J Neuropsychol* 2016; **10**: 143-153 [PMID: 26538289 DOI: 10.1111/jnp.12089]
10 **Sambrani T**, Jakubovski E, Müller-Vahl KR. New Insights into Clinical Characteristics of Gilles de la Tourette Syndrome: Findings in 1032 Patients from a Single German Center. *Front Neurosci* 2016; **10**: 415 [PMID: 27672357 DOI: 10.3389/fnins.2016.00415]
11 **Gulisano M**, Calì P, Palermo F, Robertson M, Rizzo R. Premonitory Urges in Patients with Gilles de la Tourette Syndrome: An Italian Translation and a 7-Year Follow-up. *J Child Adolesc Psychopharmacol* 2015; **25**: 810-816 [PMID: 26288345 DOI: 10.1089/cap.2014.0154]
12 **Cox JH**, Seri S, Cavanna AE. Sensory aspects of Tourette syndrome. *Neurosci Biobehav Rev* 2018; **88**: 170-176 [PMID: 29559228 DOI: 10.1016/j.neubiorev.2018.03.016]
13 **Houghton DC**, Capriotti MR, Conelea CA, Woods DW. Sensory Phenomena in Tourette Syndrome: Their Role in Symptom Formation and Treatment. *Curr Dev Disord Rep* 2014; **1**: 245-251 [PMID: 25844305 DOI: 10.1007/s40474-014-0026-2]
14 **Banaschewski T**, Woerner W, Rothenberger A. Premonitory sensory phenomena and suppressibility of tics in Tourette syndrome: developmental aspects in children and adolescents. *Dev Med Child Neurol* 2003; **45**: 700-703 [PMID: 14515942 DOI: 10.1017/S0012162203001294]
15 **Rozenman M**, Johnson OE, Chang SW, Woods DW, Walkup JT, Wilhelm S, Peterson A, Scahill L, Piacentini J. Relationships between Premonitory Urge and Anxiety in Youth with Chronic Tic Disorders. *Child Health Care* 2015; **44**: 235-248 [PMID: 27110050 DOI: 10.1080/02739615.2014.986328]
16 **Woods DW**, Piacentini J, Himle MB, Chang S. Premonitory Urge for Tics Scale (PUTS): initial psychometric results and examination of the premonitory urge phenomenon in youths with Tic disorders. *J Dev Behav Pediatr* 2005; **26**: 397-403 [PMID: 16344654 DOI: 10.1097/00004703-200512000-00001]
17 **Leckman JF**, Walker DE, Cohen DJ. Premonitory urges in Tourette's syndrome. *Am J Psychiatry* 1993; **150**: 98-102 [PMID: 8417589 DOI: 10.1176/ajp.150.1.98]
18 **Leckman JF**, Peterson BS, King RA, Scahill L, Cohen DJ. Phenomenology of tics and natural history of tic disorders. *Adv Neurol* 2001; **85**: 1-14 [PMID: 11530419 DOI: 10.1016/s0387-7604(03)90004-0]
19 **Steinberg T**, Shmuel Baruch S, Harush A, Dar R, Woods D, Piacentini J, Apter A. Tic disorders and the premonitory urge. *J Neural Transm (Vienna)* 2010; **117**: 277-284 [PMID: 20033236 DOI: 10.1007/s00702-009-0353-3]
20 **Himle MB**, Woods DW, Conelea CA, Bauer CC, Rice KA. Investigating the effects of tic suppression on premonitory urge ratings in children and adolescents with Tourette's syndrome. *Behav Res Ther* 2007; **45**: 2964-2976 [PMID: 17854764 DOI: 10.1016/j.brat.2007.08.007]
21 **Evers RA**, van de Wetering BJ. A treatment model for motor tics based on a specific tension-reduction technique. *J Behav Ther Exp Psychiatry* 1994; **25**: 255-260 [PMID: 7852608 DOI: 10.1016/0005-7916(94)90026-4]

22 **Jeter CB**, Patel SS, Morris JS, Chuang AZ, Butler IJ, Sereno AB. Oculomotor executive function abnormalities with increased tic severity in Tourette syndrome. *J Child Psychol Psychiatry* 2015; **56**: 193-202 [PMID: 25040172 DOI: 10.1111/jcpp.12298]

23 **Rosario MC**, Prado HS, Borcato S, Diniz JB, Shavitt RG, Hounie AG, Mathis ME, Mastrorosa RS, Velloso P, Perin EA, Fossaluza V, Pereira CA, Geller D, Leckman J, Miguel E. Validation of the University of São Paulo Sensory Phenomena Scale: initial psychometric properties. *CNS Spectr* 2009; **14**: 315-323 [PMID: 19668122 DOI: 10.1017/S1092852900020319]

24 **Kano Y**, Matsuda N, Nonaka M, Fujio M, Kuwabara H, Kono T. Sensory phenomena related to tics, obsessive-compulsive symptoms, and global functioning in Tourette syndrome. *Compr Psychiatry* 2015; **62**: 141-146 [PMID: 26343478 DOI: 10.1016/j.comppsych.2015.07.006]

25 **Hollis C**, Pennant M, Cuenca J, Glazebrook C, Kendall T, Whittington C, Stockton S, Larsson L, Bunton P, Dobson S, Groom M, Hedderly T, Heyman I, Jackson GM, Jackson S, Murphy T, Rickards H, Robertson M, Stern J. Clinical effectiveness and patient perspectives of different treatment strategies for tics in children and adolescents with Tourette syndrome: a systematic review and qualitative analysis. *Health Technol Assess* 2016; **20**: 1-450, vii-viii [PMID: 26786936 DOI: 10.3310/hta20040]

26 **Burd L**. Ten-week comprehensive behavioural intervention for tics decreases tic severity compared to supportive therapy and education. *Evid Based Ment Health* 2010; **13**: 123 [PMID: 21036985 DOI: 10.1136/ebmh.13.4.123]

27 **Whittington C**, Pennant M, Kendall T, Glazebrook C, Trayner P, Groom M, Hedderly T, Heyman I, Jackson G, Jackson S, Murphy T, Rickards H, Robertson M, Stern J, Hollis C. Practitioner Review: Treatments for Tourette syndrome in children and young people - a systematic review. *J Child Psychol Psychiatry* 2016; **57**: 988-1004 [PMID: 27132945 DOI: 10.1111/jcpp.12556]

28 **Woods DW**, Walther MR, Bauer CC, Kemp JJ, Conelea CA. The development of stimulus control over tics: a potential explanation for contextually-based variability in the symptoms of Tourette syndrome. *Behav Res Ther* 2009; **47**: 41-47 [PMID: 19026406 DOI: 10.1016/j.brat.2008.10.013]

29 **Jankovic J**, Jimenez-Shahed J, Brown LW. A randomised, double-blind, placebo-controlled study of topiramate in the treatment of Tourette syndrome. *J Neurol Neurosurg Psychiatry* 2010; **81**: 70-73 [PMID: 19726418 DOI: 10.1136/jnnp.2009.185348]

30 **Jackson SR**, Parkinson A, Jung J, Ryan SE, Morgan PS, Hollis C, Jackson GM. Compensatory neural reorganization in Tourette syndrome. *Curr Biol* 2011; **21**: 580-585 [PMID: 21439830 DOI: 10.1016/j.cub.2011.02.047]

31 **Neuner I**, Werner CJ, Arrubla J, Stöcker T, Ehlen C, Wegener HP, Schneider F, Shah NJ. Imaging the where and when of tic generation and resting state networks in adult Tourette patients. *Front Hum Neurosci* 2014; **8**: 362 [PMID: 24904391 DOI: 10.3389/fnhum.2014.00362]

32 **Worbe Y**, Lehericy S, Hartmann A. Neuroimaging of tic genesis: Present status and future perspectives. *Mov Disord* 2015; **30**: 1179-1183 [PMID: 26377151 DOI: 10.1002/mds.26333]

33 **Cavanna AE**, Black KJ, Hallett M, Voon V. Neurobiology of the Premonitory Urge in Tourette's Syndrome: Pathophysiology and Treatment Implications. *J Neuropsychiatry Clin Neurosci* 2017; **29**: 95-104 [PMID: 28121259 DOI: 10.1176/appi.neuropsych.16070141]

34 **Tinaz S**, Malone P, Hallett M, Horovitz SG. Role of the right dorsal anterior insula in the urge to tic in Tourette syndrome. *Mov Disord* 2015; **30**: 1190-1197 [PMID: 25855089 DOI: 10.1002/mds.26230]

35 **Conceição VA**, Dias Â, Farinha AC, Maia TV. Premonitory urges and tics in Tourette syndrome: computational mechanisms and neural correlates. *Curr Opin Neurobiol* 2017; **46**: 187-199 [PMID: 29017141 DOI: 10.1016/j.conb.2017.08.009]

World Journal of Clinical Cases

Submit a Manuscript: https://www.f6publishing.com

World J Clin Cases 2019 June 26; 7(12): 1515-1521

DOI: 10.12998/wjcc.v7.i12.1515

ISSN 2307-8960 (online)

CASE REPORT

Female genital tract metastasis of lung adenocarcinoma with EGFR mutations: Report of two cases

Run-Lan Yan, Jie Wang, Jian-Ya Zhou, Zhen Chen, Jian-Ying Zhou

ORCID number: Run-Lan Yan (0000-0003-3200-7066); Jie Wang (0000-0003-4142-2675); Jian-Ya Zhou (0000-0001-8196-0166); Zhen Chen (0000-0001-6789-6188); Jian-Ying Zhou (0000-0002-8924-935X).

Author contributions: Zhou JY and Zhou JY designed the report; Wang J and Chen Z collected the patient's clinical data; Yan RL analyzed the data and wrote the paper.

Supported by the National Natural Science Foundation of China, No. 81670017.

Informed consent statement: Consent was obtained from the patient for publication of this report and any accompanying images and is available upon request.

Conflict-of-interest statement: The authors declare that they have no conflicts of interest.

CARE Checklist (2016) statement: The authors have read the CARE Checklist (2016), and the manuscript was prepared and revised according to the CARE Checklist (2016).

Run-Lan Yan, Jie Wang, Jian-Ya Zhou, Jian-Ying Zhou, Department of Respiratory Diseases, First Affiliated Hospital of Zhejiang University School of Medicine, Zhejiang University, Hangzhou 310003, Zhejiang Province, China

Zhen Chen, Department of Pathology, First Affiliated Hospital of Zhejiang University School of Medicine, Zhejiang University, Hangzhou 310003, Zhejiang Province, China

Corresponding author: Jian-Ying Zhou, MD, Chief Doctor, Professor, Department of Respiratory Diseases, First Affiliated Hospital of Zhejiang University School of Medicine, Zhejiang University, 79 Qingchun Road, Hangzhou 310003, Zhejiang Province, China.
zjyhz@zju.edu.cn
Telephone: +86-571-87236876
Fax: +86-571-87236877

Abstract

BACKGROUND

The female genital tract is an uncommon site of involvement for extra-genital malignancies. Ovarian metastases have been described as disseminations of lung adenocarcinoma; rare cases of secondary localizations in the cervix, adnexa, and vagina have also been reported in the literature. Here, we report two cases of advanced lung adenocarcinoma with female genital tract metastasis.

CASE SUMMARY

The first case was a 41-year-old woman with stage IV lung adenocarcinoma metastasizing to the cervix. Immunohistochemistry of the cervical biopsy specimen revealed thyroid transcription factor (TTF)-1(+), cytokeratin (CK)-7(+), and (CK)-20(-). Gene mutational analysis showed epidermal growth factor receptor (EGFR) L858R mutation in exon 21. She had a positive response to gefitinib, for both the pulmonary mass and cervical neoplasm. The second case was a 29-year-old woman who was diagnosed with stage IV lung adenocarcinoma with EGFR mutation. After 12 mo of treatment with icotinib, ovarian biopsy showed adenocarcinoma with CDX2(-), TTF-1(+++), PAX8(-), CK-7(+++), CK-20(++), and Ki67(15%+), accompanied with EGFR 19-del mutation and T790M mutation.

CONCLUSION

Immunohistochemistry and gene mutational testing have greatly helped in locating the initial tumor site when both pulmonary and female genital tract neoplasms exist.

Manuscript source: Unsolicited manuscript

Received: January 29, 2019
Peer-review started: January 29, 2019
First decision: March 9, 2019
Revised: March 24, 2019
Accepted: April 18, 2019
Article in press: April 19, 2019
Published online: June 26, 2019

P-Reviewer: Sipahi EY
S-Editor: Ji FF
L-Editor: Wang TQ
E-Editor: Liu JH

Key words: Lung adenocarcinoma; Epidermal growth factor receptor; Metastasis; Ovary; Cervix; Case report

Core tip: The female genital tract is an uncommon site of involvement for extra-genital malignancies. Ovarian metastases have been described as disseminations of lung adenocarcinoma; rare cases of secondary localizations in the cervix, adnexa, and vagina have also been reported in the literature. Here, we report two cases of advanced lung adenocarcinoma with female genital tract metastasis. The initial tumor site should be considered when both pulmonary and female genital tract neoplasms exist. Immunohistochemistry and gene mutational testing have greatly helped in locating the initial tumor site.

Citation: Yan RL, Wang J, Zhou JY, Chen Z, Zhou JY. Female genital tract metastasis of lung adenocarcinoma with EGFR mutations: Report of two cases. *World J Clin Cases* 2019; 7(12): 1515-1521
URL: https://www.wjgnet.com/2307-8960/full/v7/i12/1515.htm
DOI: https://dx.doi.org/10.12998/wjcc.v7.i12.1515

INTRODUCTION

Although metastases of lung adenocarcinoma may appear in any organ, they are more commonly observed in the bone, liver, adrenal gland, brain, and skin and seldom seen in the female genital tract, as metastasis in the female genital tract usually corresponds to small cell lung carcinomas[1]. Ovarian metastases have been described as disseminations of lung adenocarcinoma; rare cases of secondary localizations in the cervix, adnexa, and vagina have also been reported in the literature[2]. In these cases, immunohistochemistry and gene mutational analysis play an important role in determining the initial origin of tumor. In this article, we present two cases of advanced lung adenocarcinoma – the first case had cervical metastasis, and the other had metastasis to the ovary. The first case seemed to have cervical metastasis before targeted treatment; the other case developed ovarian metastasis accompanied by the newly presented T790M mutation in exon 20 during treatment with tyrosine kinase inhibitors (TKIs).

CASE PRESENTATION

Chief complaints

Case 1: A 41-year-old never-smoking woman came to our practice because of recurrent cough for 4 mo.

Case 2: A 29-year-old never-smoking woman was accepted because of complaints of cough and chest tightness.

History of present illness

There was no history of fever, weight loss, or sweating.

History of past illness

The patient's past medical history was a right lung nodule, which was observed 4 years ago. The history of past illness is a description of case1. We have marked it in highlight.

Personal and family history

Case 1: She was a non-smoker and there was no history of drug abuse or recent travel. The family history was unremarkable.

Case 2: She was a non-smoker and there was no history of drug abuse or recent travel. The family history was unremarkable.

Physical examination upon admission

Case 1: The patient had no palpable lymph node.

Case 2: The patient had a low auscultation of breath and had no palpable lymph node.

Laboratory examinations

Case 1: The initial laboratory investigations including complete blood count and blood chemistry tests were normal. Carcinoembryonic antigen level was 1.5 ng/mL (0-5 ng/mL), which was negative.

Case 2: The initial laboratory investigations including complete blood count and blood chemistry tests were normal. Carcinoembryonic antigen level was 4.4 ng/mL (0-5 ng/mL) and tumor-associated carbohydrate antigen 125 level was 42.9 U/mL (0-35 U/mL).

Imaging examinations

Case 1: Computed tomography (CT) showed a right pulmonary mass characterized by a solid region with contiguous ground-glass areas, stellate borders, and pleural puckering (Figure 1C). The result of endotracheal biopsy was unsatisfactory, although cytology revealed adenocarcinoma cells; however, there was insufficient sample for pathological examination and epidermal growth factor receptor (*EGFR*) gene testing. A positron emission tomography-CT (PET-CT) scan was performed before lung biopsy and showed hyper-metabolic activity in pulmonary lesions and the cervix uteri (Figure 1A and B).

Lung biopsy was performed with CT guidance, after exclusion of relevant contraindications. Pathological examination showed adenocarcinoma with necrosis. Immunohistochemistry revealed thyroid transcription factor TTF-1(+) (Figure 2B), cytokeratin CK-7(+), and CK-20(-). EGFR mutational analysis could not be performed because we did not have sufficient biopsy specimen. Cervical biopsy was performed based on the hypermetabolic activity in the cervix uteri, and it showed poorly differentiated adenocarcinoma (Figure 2A). Immunohistochemistry showed TTF-1(+), CK-7(+), and CK-20(-). EFGR mutational analysis of the cervical biopsy specimen showed EGFR *L858R* mutation in exon 21. The patient displayed clinical symptoms including frequent micturition and hypogastralgia, and thus, pelvic magnetic resonance imaging (MRI) was performed, and it showed thickened cervical canal, without lymphadenectasis or pelvic effusion. Cervical cell cytology indicated negative results.

Case 2: Her initial CT scan showed lung lesions with cavity, as well as pleural effusion (Figure 3A). Ultrasound examination also showed pelvic effusion, although no ovarian masses were found. Pleural fluid cytology revealed adenocarcinoma, and immunohistochemistry revealed TTF-1(+) (Figure 4). EGFR mutational analysis of cell block showed EGFR 19-del mutation.

FINAL DIAGNOSIS

Case 1

Lung adenocarcinoma with cervical metastasis, stage IV (cT4N3M1b), with EGFR *21 L858R* mutation.

Case 2

Lung adenocarcinoma with ovary metastasis, stage IV (cT2NxM1b), EGFR 19 deletion.

TREATMENT

Case 1

The patient received targeted therapy of gefitinib.

Case 2

The patient was started on icotinib, which is an EGFR TKI, with a plan of sequential antiangiogenic therapy.

OUTCOME AND FOLLOW-UP

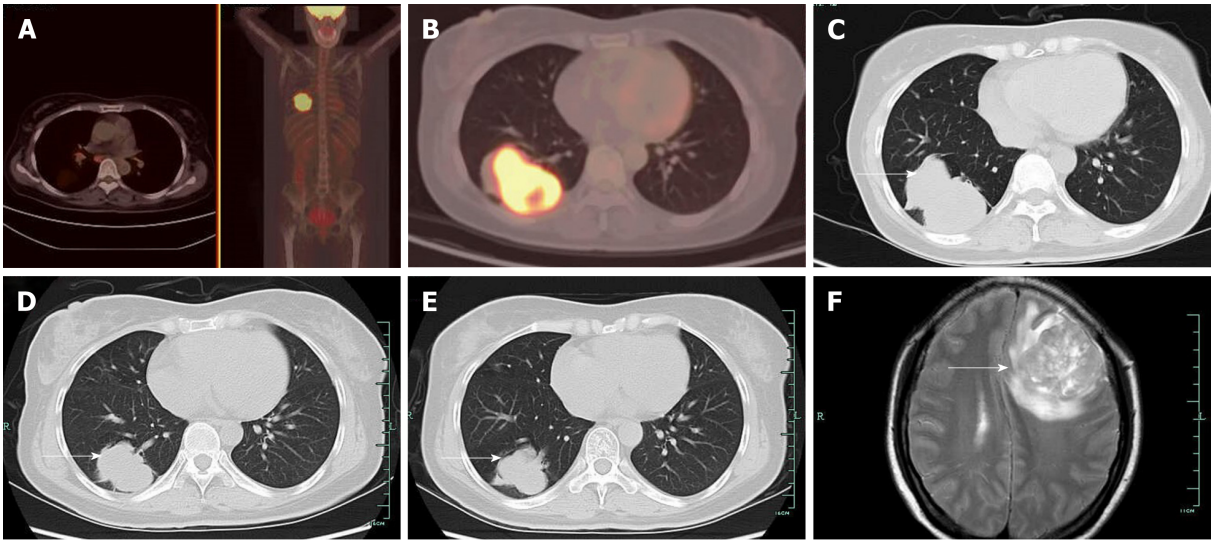

Figure 1 Case 1. A: Positron emission tomography-computed tomography (PET-CT) was performed before lung biopsy and showed hyper-metabolic activity in pulmonary lesions and the cervix uteri; B: PET-CT image showed hyper-metabolic activity in the inferior lobe of the right lung, where lung biopsy was performed; C: CT showed a right pulmonary mass characterized by a solid region with contiguous ground-glass areas, stellate borders, and pleural puckering before tyrosine kinase inhibitor treatment; D: CT showed a right pulmonary mass after 2 mo of gefitinib therapy, which indicated partial remission of tumor; E: CT image showed a right pulmonary mass after 4 mo of gefitinib therapy; F: Magnetic resonance imaging performed on April 12, 201 indicated brain metastasis.

Case 1

The patient had a positive response to gefitinib (Figure 1D and E), for both the pulmonary mass and cervical neoplasm. Routine examinations included chest CT scan and ultrasonography of the pelvic cavity and lymph nodes. Unfortunately, the patient was observed to have intracranial metastasis after 8 mo of gefitinib therapy (Figure 1F).

Case 2

Targeted therapy resulted in a partial response after 3 mo (Figure 3B). Since the patient complained of repeated pleural effusion, close drainage had to be done every two months. Since March 1, 2017, the patient has been treated with bevacizumab (Avastin) and icotinib to reduce pleural effusion. Routine CT scan examination showed pleural effusion without enlargement of the tumor (Figure 3C and D). Ultrasound examination of the pelvis showed ovarian mass, as well as pelvic effusion. Ovarian biopsy was performed on September 15, 2017, which revealed adenocarcinoma. Immunohistochemistry revealed CDX2(-), TTF-1(+++), PAX8(-), CK-7(+++), CK-20(++), and Ki67(15%+) (Figure 4B). EFGR mutational analysis of the ovarian biopsy specimen showed EGFR 19-del mutation and T790M mutation in exon 20. Lung biopsy could not be performed because of obstructive pneumonia and pleural effusion. Since the EGFR TKI resistance mutation (T790M) appeared in the ovarian biopsy sample, osimertinib (Tagrisso) therapy was started (September 26, 2017).

DISCUSSION

Although metastases of lung adenocarcinoma may appear in any organ, they are more frequently observed in the bone, liver, adrenal gland, brain, and skin and seldom seen in the female genital tract, as metastasis in the female genital tract usually corresponds to small cell carcinomas[3,4]. We review the relevant studies both at home and abroad in recent years corresponding to patients with lung cancer metastasis to the female genital tract; ovarian metastases have been described in several articles[1-3,5-8], while rare cases have been reported for cervical metastasis.

Metastases to the female genital tract of lung neoplasm have not received enough attention. According to the principles of precision medicine, the initial tumor site should be considered when both pulmonary and female genital tract neoplasms exist. Immunohistochemistry and gene mutational analysis have greatly helped in locating the initial tumor site. Between 74% and 92% of lung adenocarcinoma cases exhibit TTF-1 nuclear expression, and almost 90% of patients with lung adenocarcinoma are positive for CK-7 and negative for CK-20[9]. Thus, a combination of TTF-1(+), CK-7(+),

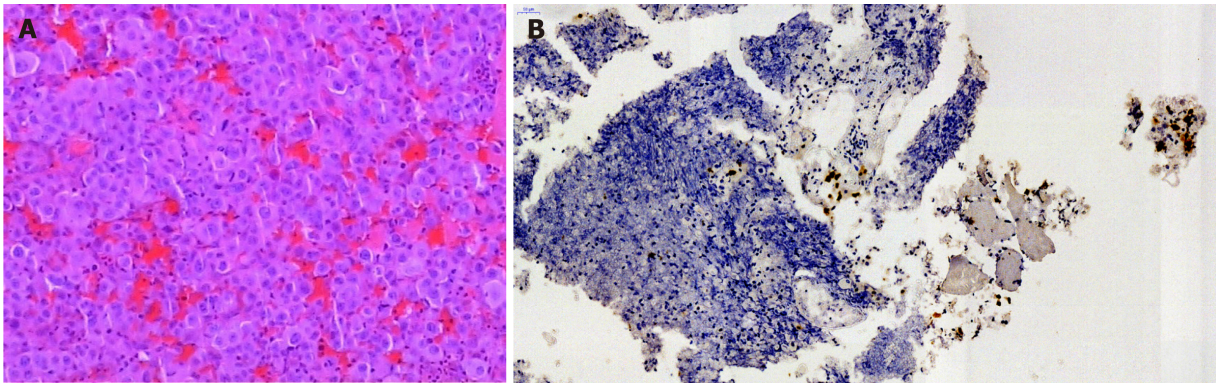

Figure 2 Case 1. A: Cervical biopsy showed poorly differentiated adenocarcinoma; B: Pathological examination of specimens obtained from lung biopsy showed adenocarcinoma with necrosis, and immunohistochemical staining for thyroid transcription factor-1 was positive.

and CK-20(-) immunophenotypes is highly suggestive of primary adenocarcinoma of the lung (specificity, 100%)[5,10]. The immunohistochemical profiles of the two cases described here are indicative of metastatic lung adenocarcinoma.

In the first case, the patient did not have enough tissue sample in percutaneous lung puncture biopsy for gene mutational analysis; fortunately, cervical biopsy produced adequate tissue specimen on which we confirmed cervical metastasis by immunohistochemistry. PET-CT showed hypermetabolic activity in pulmonary lesions and the cervix uteri. According to clinical pathologists, the cervical neoplasm was a metastasis from lung cancer, which also confirmed by immunohistochemistry. Subsequent EGFR gene mutational analysis (using the Amplification Refractory Mutation System, ARMS) of the cervical tissue sample revealed EGFR L858R mutation in exon 21. The patient was then started on gefitinib and achieved partial remission after 4 mo of treatment.

In case 2, lung biopsy could not be performed because of obstructive pneumonia and pleural effusion. Pleural fluid cytology was performed on a cell block; thus, EGFR mutational analysis could be optimized. Although tissue biopsy still represents the gold standard for the diagnosis of lung cancer[11,12], it is not always possible to obtain high-quality specimens from all patients. In certain situations, liquid biopsy could be an essential tool for clinicians, especially for patients who cannot undergo invasive diagnostic procedures[11]. The patient's disease progressed during treatment with TKI, accompanied by ovarian metastasis and bone metastasis. Since repeated biopsy of the lung mass is not recommended, analysis of the ovarian biopsy showed EGFR 19-del mutation and T790M mutation in exon 20, which represents one of the two confirmed mechanisms of drug resistance. Approximately half of the cancers that acquire resistance to EGFR TKIs develop a secondary mutation in EGFR (T790M), which abrogates the inhibitory activity of the TKI[13]. The patient was then started with osimertinib. As recently reported, osimertinib displays significantly greater efficacy than platinum therapy plus pemetrexed in patients with T790M-positive advanced non-small cell lung cancer (including cases with CNS metastases) in whom the disease has progressed during first-line EGFR TKI therapy[12,14]. Timely biopsy of the ovarian metastasis provided reference for the patient's treatment, which greatly contributed to the patient's prognosis.

CONCLUSION

According to the principles of precision medicine, the initial tumor site should be considered when both pulmonary and female genital tract neoplasms exist. Immunohistochemistry and gene mutational testing have greatly helped in locating the initial tumor site.

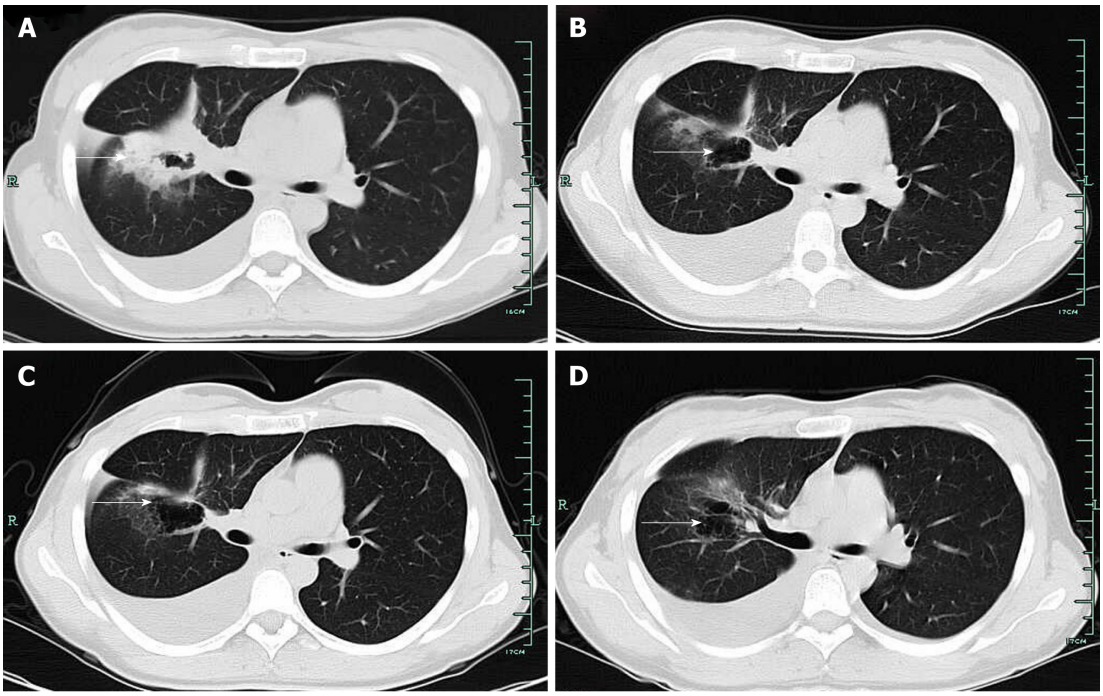

Figure 3 Case 2. A: Computed tomography (CT) scan showed lung lesions with cavity, as well as pleural effusion before tyrosine kinase inhibitor treatment; B: CT showed a right pulmonary mass after 3 mo of ecotinib therapy, which resulted in a partial response after 3 mo; C: CT scan showed pleural effusion after 1 mo of bevacizumab (Avastin) and icotinib therapy; D: CT scan showed pleural effusion after 4 mo of bevacizumab (Avastin) and icotinib therapy, without progression of initial tumor.

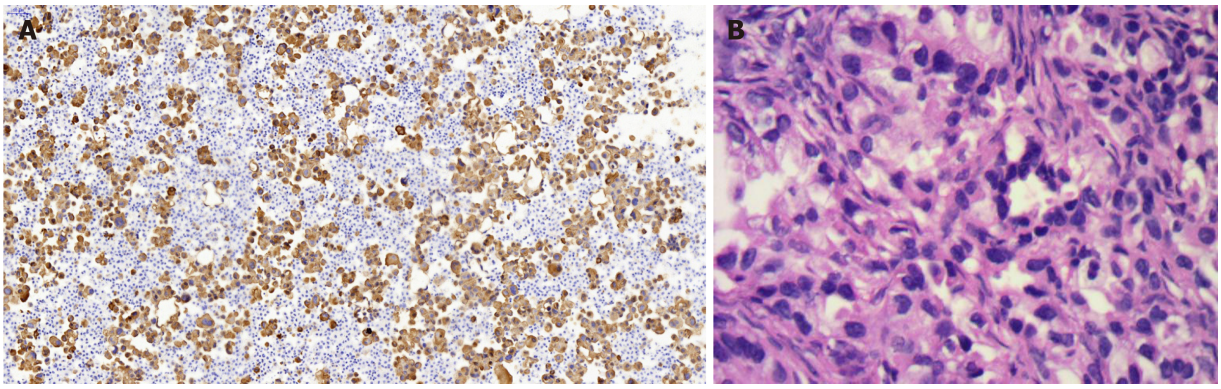

Figure 4 Case 2. A: Pathological examination of specimens obtained from lung biopsy showed adenocarcinoma, and immunohistochemical staining for thyroid transcription factor-1 (TTF-1) was positive; B: Ovarian biopsy revealed TTF-1 positive adenocarcinoma.

REFERENCES

1 **Mazur MT**, Hsueh S, Gersell DJ. Metastases to the female genital tract. Analysis of 325 cases. *Cancer* 1984; **53**: 1978-1984 [PMID: 6322966 DOI: 10.1002/1097-0142(19840501)53:9<1978::AID-CNCR2820530929>3.0.CO;2-1]

2 **Irving JA**, Young RH. Lung carcinoma metastatic to the ovary: a clinicopathologic study of 32 cases emphasizing their morphologic spectrum and problems in differential diagnosis. *Am J Surg Pathol* 2005; **29**: 997-1006 [PMID: 16006793]

3 **Fujiwara A**, Higashiyama M, Kanou T, Tokunaga T, Okami J, Kodama K, Nishino K, Tomita Y, Okamoto I. Bilateral ovarian metastasis of non-small cell lung cancer with ALK rearrangement. *Lung Cancer* 2014; **83**: 302-304 [PMID: 24360322 DOI: 10.1016/j.lungcan.2013.11.022]

4 **Howell NR**, Zheng W, Cheng L, Tornos C, Kane P, Pearl M, Chalas E, Liang SX. Carcinomas of ovary and lung with clear cell features: can immunohistochemistry help in differential diagnosis? *Int J Gynecol Pathol* 2007; **26**: 134-140 [PMID: 17413979 DOI: 10.1097/01.pgp.0000233166.56385.d0]

5 **Lee KA**, Lee JS, Min JK, Kim HJ, Kim WS, Lee KY. Bilateral Ovarian Metastases from ALK Rearranged Non-Small Cell Lung Cancer. *Tuberc Respir Dis (Seoul)* 2014; **77**: 258-261 [PMID: 25580142 DOI: 10.4046/trd.2014.77.6.258]

6 **Min KW**, Paik SS, Han H, Kim WS, Jang K. Tumour-to-tumour metastasis of lung adenocarcinoma to ovarian serous cystadenoma. *J Obstet Gynaecol* 2014; **34**: 650-651 [PMID: 24724546 DOI:

10.3109/01443615.2014.902431]
7 **Mushi RT**, Yang Y, Cai Q, Zhang R, Wu G, Dong X. Ovarian metastasis from non-small cell lung cancer with ALK and EGFR mutations: A report of two cases. *Oncol Lett* 2016; **12**: 4361-4366 [PMID: 28105150 DOI: 10.3892/ol.2016.5292]
8 **Giordano G**, Cruz Viruel N, Silini EM, Nogales FF. Adenocarcinoma of the Lung Metastatic to the Ovary With a Signet Ring Cell Component. *Int J Surg Pathol* 2017; **25**: 365-367 [PMID: 28178894 DOI: 10.1177/1066896917691613]
9 **Rossi G**, Cavazza A, Righi L, Sartori G, Bisagni A, Longo L, Pelosi G, Papotti M. Napsin-A, TTF-1, EGFR, and ALK Status Determination in Lung Primary and Metastatic Mucin-Producing Adenocarcinomas. *Int J Surg Pathol* 2014; **22**: 401-407 [PMID: 24651909 DOI: 10.1177/1066896914527609]
10 **Losito NS**, Scaffa C, Cantile M, Botti G, Costanzo R, Manna A, Franco R, Greggi S. Lung cancer diagnosis on ovary mass: a case report. *J Ovarian Res* 2013; **6**: 34 [PMID: 23663245 DOI: 10.1186/1757-2215-6-34]
11 **Hiley CT**, Le Quesne J, Santis G, Sharpe R, de Castro DG, Middleton G, Swanton C. Challenges in molecular testing in non-small-cell lung cancer patients with advanced disease. *Lancet* 2016; **388**: 1002-1011 [PMID: 27598680 DOI: 10.1016/S0140-6736(16)31340-X]
12 **Lam DC**, Tam TC, Lau KM, Wong WM, Hui CK, Lam JC, Wang JK, Lui MM, Ho JC, Ip MS. Plasma EGFR Mutation Detection Associated With Survival Outcomes in Advanced-Stage Lung Cancer. *Clin Lung Cancer* 2015; **16**: 507-513 [PMID: 26239567 DOI: 10.1016/j.cllc.2015.06.003]
13 **Xu Y**, Liu H, Chen J, Zhou Q. Acquired resistance of lung adenocarcinoma to EGFR-tyrosine kinase inhibitors gefitinib and erlotinib. *Cancer Biol Ther* 2010; **9**: 572-582 [PMID: 20404520 DOI: 10.4161/cbt.9.8.11881]
14 **Goss G**, Tsai CM, Shepherd FA, Bazhenova L, Lee JS, Chang GC, Crino L, Satouchi M, Chu Q, Hida T, Han JY, Juan O, Dunphy F, Nishio M, Kang JH, Majem M, Mann H, Cantarini M, Ghiorghiu S, Mitsudomi T. Osimertinib for pretreated EGFR Thr790Met-positive advanced non-small-cell lung cancer (AURA2): a multicentre, open-label, single-arm, phase 2 study. *Lancet Oncol* 2016; **17**: 1643-1652 [PMID: 27751847 DOI: 10.1016/S1470-2045(16)30508-3]

World Journal of Clinical Cases

Submit a Manuscript: https://www.f6publishing.com

World J Clin Cases 2019 June 26; 7(12): 1522-1528

DOI: 10.12998/wjcc.v7.i12.1522

ISSN 2307-8960 (online)

CASE REPORT

Novel heterozygous missense mutation of *SLC12A3* gene in Gitelman syndrome: A case report

Cheng-Lin Wang

ORCID number: Cheng-Lin Wang (0000-0002-6346-7252).

Author contributions: Wang CL designed the research, performed the research, analyzed the data, and wrote the paper.

Informed consent statement: Consent was obtained from the patient for publication of this report and any accompanying images.

Conflict-of-interest statement: I declare that I have no conflicts of interest to this work. I declare that I do not have any commercial or associative interest that represents a conflict of interest in connection with the work submitted.

CARE Checklist (2016) statement: I have read the CARE Checklist (2016), and the manuscript was prepared and revised according to the CARE Checklist (2016).

Manuscript source: Unsolicited manuscript

Cheng-Lin Wang, Department of Endocrinology, Shanxi Provincial People's Hospital Affiliated to Shanxi Medical University, Taiyuan 030012, Shanxi Province, China

Corresponding author: Cheng-Lin Wang, MBChB, Attending Doctor, Department of Endocrinology, Shanxi Provincial People's Hospital Affiliated to Shanxi Medical University, Shuangta Street No. 29, Taiyuan 030012, Shanxi Province, China. w15834147610@sina.com
Telephone: +86-351-4960140
Fax: +86-351-4960140

Abstract

BACKGROUND

To screen for possible pathogenic loci in a patient with Gitelman syndrome by high-throughput exome sequencing and to explore the relationship between genotype and phenotype.

CASE SUMMARY

The clinical data of the patient were collected. Peripheral blood samples were obtained to isolate white blood cells and extract genomic DNA. High-throughput whole exome sequencing for candidate pathogenic genes in the proband was completed by the Huada Gene Technology Co. Ltd (Shenzhen, China). Sequencing showed a novel heterozygous missense mutation (a G to A transition at nucleotide 2582) in exon 22 of the *SLC12A3* gene, which resulted in a substitution of histidine for arginine at position 816 of the LRP1B protein and caused the occurrence of disease.

CONCLUSION

This is the first report of a new pathogenic mutation in *SLC12A3*. Further functional studies are particularly necessary to explore potential molecular mechanisms.

Key words: Gitelman syndrome; *SLC12A3*; High-throughput sequencing; Bioinformatics analysis; Case report

Core tip: To screen for possible pathogenic loci in a patient with Gitelman syndrome by high-throughput exome sequencing and to explore the relationship between the genotype and phenotype. Sequencing showed a novel heterozygous missense mutation (a G to A transition at nucleotide 2582) in exon 22 of *SLC12A3* gene, which resulted in a

Received: January 26, 2019
Peer-review started: January 28, 2019
First decision: March 9, 2019
Revised: March 20, 2019
Accepted: April 18, 2019
Article in press: May 2, 2019
Published online: June 26, 2019

P-Reviewer: Cheungpasitporn W, Stavroulopoulos A
S-Editor: Ji FF
L-Editor: Filipodia
E-Editor: Liu JH

substitution of histidine for arginine at position 816 of the LRP1B protein and caused the occurrence of disease.

Citation: Wang CL. Novel heterozygous missense mutation of *SLC12A3* gene in Gitelman syndrome: A case report. *World J Clin Cases* 2019; 7(12): 1522-1528
URL: https://www.wjgnet.com/2307-8960/full/v7/i12/1522.htm
DOI: https://dx.doi.org/10.12998/wjcc.v7.i12.1522

INTRODUCTION

Gitelman syndrome (GS) is an inherited autosomal recessive renal tubular disorder that was first described by Gitelman in 1966. The main clinical manifestations include hypokalemia, hypomagnesia, hypocalciuria, and hypochloremic metabolic alkalosis[1-3]. GS is often found in infants and young children with growth retardation and convulsions. Patients usually have normal blood pressure. The prevalence of GS ranges from 1/1000 to 9/10000. It is easily neglected due to their mild clinical manifestations and good prognosis. Several studies have shown that GS may be associated with chondrocalcinosis and dysglycemia; in severe cases, the patients may also develop ventricular arrhythmia and progressive renal insufficiency, which can be highly dangerous.

The main pathogenic gene in GS is *SLC12A3*, which encodes for thiazide-sensitive NaCl cotransporter. The rapid development of gene sequencing technology in recent years has facilitated the gene diagnosis[4-6]. According to expert consensus, the sequencing gene panels for GS should include the *SLC12A3*, *CLCNKB*, and *HNF1B* genes[7]. Whole exome sequencing (WES) can detect exon regions of over 20000 genes at a time. With the decrease in its price, WES has been increasingly used in clinical diagnosis[8]. Therefore, we applied WES for the genetic analysis in a clinically confirmed GS patient. In addition to *SLC12A3*, the most common gene associated with GS, we also detected *CLCNKB* and *HNF1B*[9-11]. We report a patient with clinically confirmed GS and determined the relevant gene mutation loci in an attempt to further improve our understanding of this disease.

CASE PRESENTATION

Chief complaints

A sudden onset of limb weakness without obvious cause, followed by limb numbness/stiffness, which was accompanied by palpitation.

History of present illness

The patient was a 16-year-old male. He was admitted in January 2018 due to limb weakness and stiffness for two years. Two years ago, the patient had a sudden onset of limb weakness without obvious cause, followed by limb numbness/stiffness, which was accompanied by palpitation. Examination in a local hospital revealed hypokalemia, which was improved after potassium supplementation. However, the above symptoms recurred 2 mo ago due to cold, and the patient was admitted to our hospital for further treatment.

History of past illness

He denied any other medical conditions.

Personal and family history

There was no history of consanguineous marriage in the pedigree of three generations. The study was approved by the Ethics Committee of Shanxi Provincial People's Hospital, Taiyuan, China. The proband and his family members signed the informed consent.

Physical examination upon admission

The thyroid gland was not large. There was no obvious abnormality in the heart and lungs.

Laboratory examinations

Blood analysis: potassium, 2.64 mmol/L; sodium, 133.10 mmol/L; chlorine, 96.20 mmol/L; magnesium, 0.510 mmol/L; triglycerides, 1.64 mmol/L; blood pH, 7.35; standard bicarbonate, 25.60 mmol/L; and total carbon dioxide, 20.00 mmol/L. Urine analysis showed: calcium, 0.12 mmol/24 h; magnesium 2.200 mmol/24 h, phosphorus, 2.19 mmol/24 h; during the same period the blood potassium was 3.05 mmol/L and magnesium was 0.562 mmol/L. Circadian and pulsatile secretion of adrenocorticotropic hormone and cortisol were normal. Baseline renin-angiotensin-aldosterone system test: Angiotensin I (37 °C), 49.94 μg/L; angiotensin I (4 °C), 6.87 μg/L; aldosterone, 149.05 ng/L; renin activity, 31.87 UG/L per hour, and aldosterone/renin activity 0.47. The average 24-h ambulatory blood pressure was 105/71 mmHg.

Imaging examinations

No abnormality was seen on X-ray chest film, abdominal ultrasound, thyroid ultrasound, bilateral kidney and renal vascular ultrasound, adrenal ultrasound, and adrenal thin-slice computed tomography. Electrocardiogram showed sinus tachycardia at 105 beats/min.

WES and bioinformatics analysis

DNA extraction: Peripheral venous blood (2 mL) was collected with heparin as anticoagulant. Genomic DNA was isolated from peripheral blood lymphocytes using OMEGA SE Blood DNA Kit and then sent to the Shenzhen Huada Gene Technology Co. Ltd for WES.

Bioinformatics analysis: Quality control of the raw reads was managed *via* FastQC[12]. Sequences were aligned to human reference genome hg19 using the Burrows-Wheeler Aligner[13]. The duplicate reads were removed by the Samblaster[14]. The INDEL was re-aligned using GATK realignment and base quality score recalibration was performed. We used five kinds of software to analyze variation, including GATK, Samtools, Freebayes, Platypus, and Varscan2, to ensure the accuracy of identification. Marginal variants were annotated in databases including dbSNP, 1000 Genomes Project, dbNSFP, and ClinVar[15-17]. The possible pathogenic mutations on *SLC12A3*, *CLCNKB*, and *HNF1B* genes were analyzed, and the relevant literature was searched according to these loci.

Gene detection

The quality control results of the raw reads (Fastq) are shown in Figures 1 and 2. The average value of base qualities was larger than 30 (accuracy: 99.9%).

WES identified a total of 214137288 reads, among which 99.83% could be mapped to the human reference genome, and the duplicate reads accounted for 11.81%. The mean depth was 282X, which exceeded the general exome sequencing depth (Table 1).

A total of 67537 mutations were identified by bioinformatics analysis, including 55184 SNPs and 12353 INDELs (Figure 3). After dbSNP annotation, 94% of the SNPs were annotated in dbSNP, while only 35% of the INDELs could be annotated in dbSNP.

Mutations in *SLC12A3*, *CLCNKB*, and *HNF1B3* genes were filtered based on the following conditions: (1) The variant is located on an exon; (2) The variation does not belong to synonymous mutation; and (3) Population frequency is greater than 0.001.

After filtering, only one missense heterozygous mutation in the *SLC12A3* gene was left. Its population frequency was unknown. Most mutation prediction software such as Polyphen2 HDIV, SIFT, and FATHMM predicted it as a harmful mutation. The mutation information is shown in Table 2, and the mutation of exon 22 reported by another paper is shown in Table 3.

FINAL DIAGNOSIS

According to the typical symptoms, laboratory tests, and gene analysis, the patient was diagnosed with GS.

TREATMENT

The patient was given potassium therapy with antisterone.

OUTCOME AND FOLLOW-UP

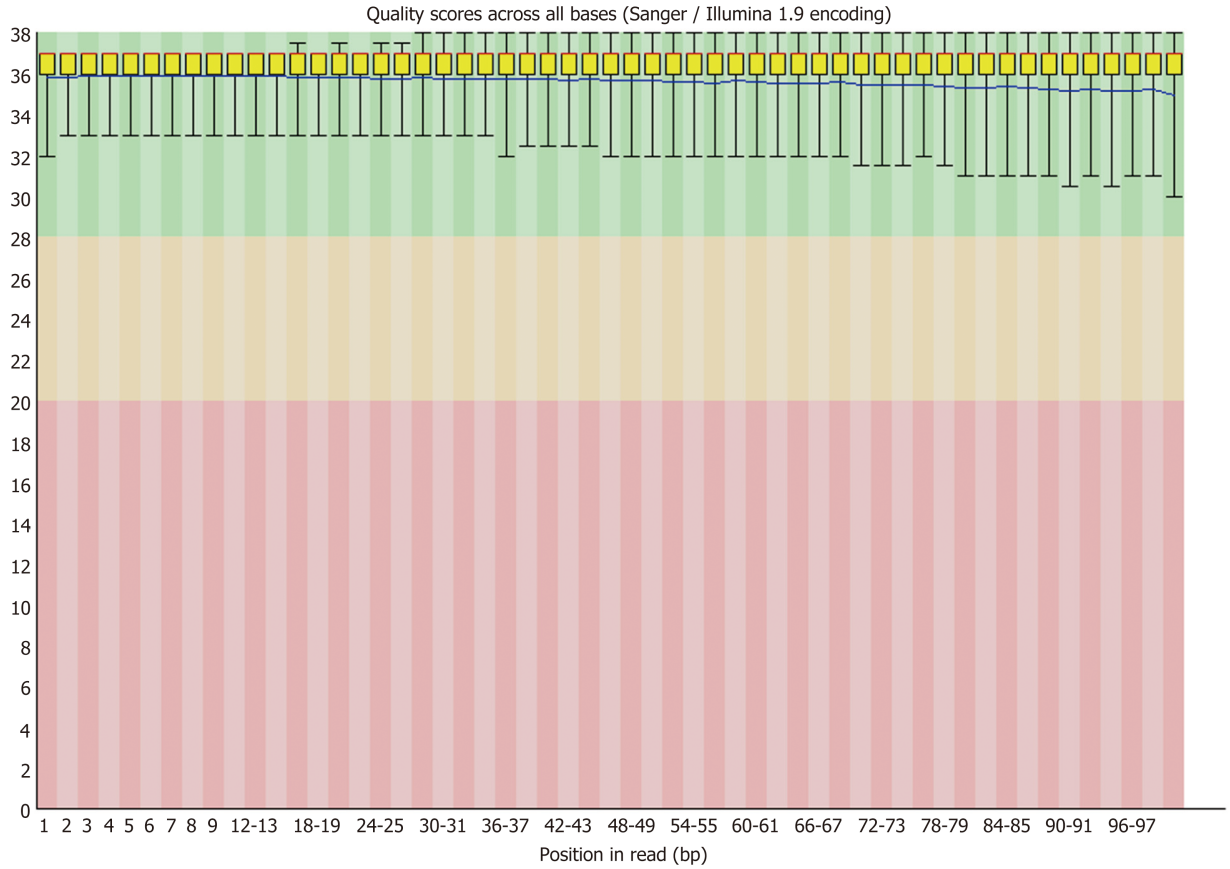

Figure 1 Raw reads of exome sequencing.

The patient recovered well and was discharged 7 d later. Regular detection of potassium is necessary.

DISCUSSION

WES can detect the exon information of all genes at one time. With the decreased cost of high-throughput next-generation sequencing, WES has been increasingly applied in clinical diagnoses. In the present study, we used WES to further clarify the gene mutations in our patient. After bioinformatics analysis and population frequency filtering, we found a non-synonymous mutation in *SLC12A3* gene. A G2582A heterozygous mutation has also been reported in this site in the literature[18].

Mutation analysis of the *SLC12A3* gene in our patient and his family members revealed a heterozygous missense mutation of G-to-A transition at nucleotide position 2582 within exon 22. An autosomal recessive disease does not present its traits in the heterozygous state. It occurs only when a pair of alleles is homozygous or compound heterozygotes of a recessive pathogenic gene. However, Balavoine *et al*[19] detected two mutation sites in the *SLC12A3* gene in most GS patients and only one mutation site in a small number of GS patients. In addition, patients with two mutation sites have more severe clinical symptoms than those with only one mutation site. GS is an autosomal recessive hereditary disease, and it does not occur in carriers. Current clinical studies have not found a significant correlation between GS genotype and phenotype.

With the decreased cost of sequencing and better understanding of diseases, the concept of precision medicine has been widely recognized over the past two years. Precision medicine represents the future direction of medical development. The core of precision medicine is to precisely identify pathogenic gene sites or pathogenic loci by gene sequencing and carry out targeted therapy according to pathogenic genes or pathogenic sites.

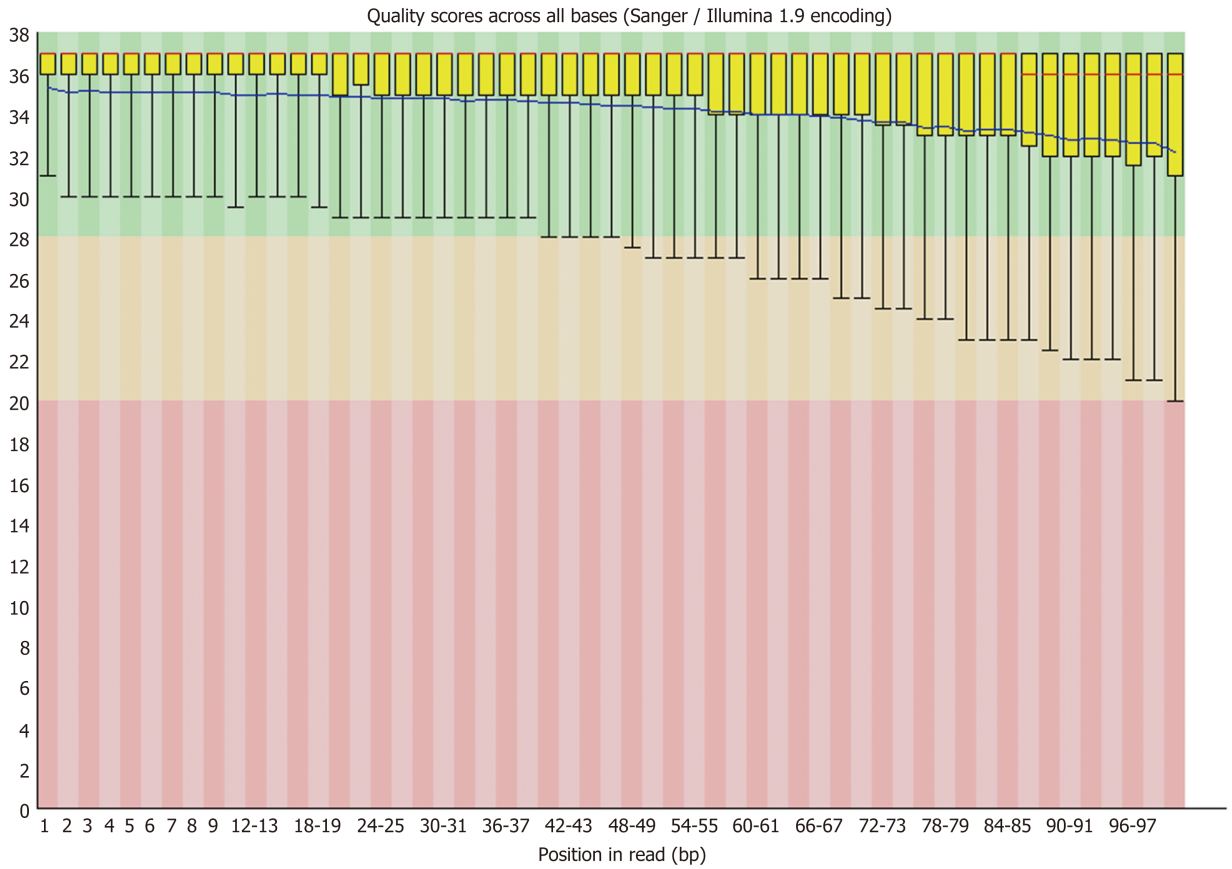

Figure 2 Quality control results of exome sequencing.

CONCLUSION

A novel heterozygous missense mutation (a G to A transition at nucleotide 2582) in exon 22 of the *SLC12A3* gene is the first report of a new pathogenic mutation in *SLC12A3*. Further functional studies are particularly necessary to explore potential molecular mechanisms.

Table 1 Reads alignment and sequencing depth

Total reads	Mapped reads	Duplicate reads	Mean depth
214137288	99.83%	11.81%	282X

Table 2 Candidate genes

Type	Information
Gene	*SLC12A3*
RNA	NM_000339
Exon	exon22
DNA mutation	G2582A
AA mutation	R861H
Mutation frequency	50%
Population frequency	Unknown
Polyphen2_HDIV	D, D, D
FATHMM	D
MutationTaster	D
MutationAssessor	L
LRT	D
SIFT	T

Table 3 Mutation in exon 22 of *SLC12A3* gene

Exon	Mutation	Pmid
exon22	Glv876Ser	17654016
exon22	Leu849His	17873326, 20229814
exon22	Arg852His	17873326, 20229814
exon22	Arg861Cys	27872838
exon22	Arg871His	21051746
exon22	Leu859Pro	21753071
exon22	Arg861Cys	21753071
exon22	Arg861His	Present study

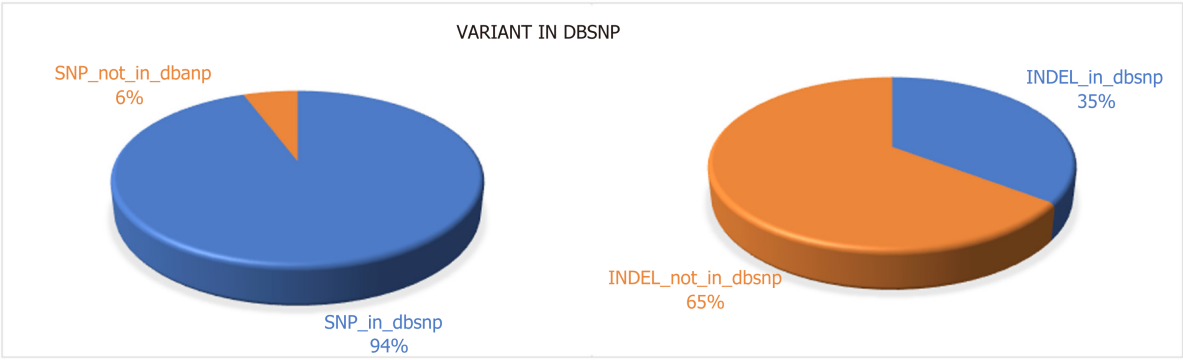

Figure 3 Number of variants.

REFERENCES

1 **van der Merwe PD**, Rensburg MA, Haylett WL, Bardien S, Davids MR. Gitelman syndrome in a South African family presenting with hypokalaemia and unusual food cravings. *BMC Nephrol* 2017; **18**: 38 [PMID: 28125972 DOI: 10.1186/s12882-017-0455-3]

2 **Chen Q**, Wu Y, Zhao J, Jia Y, Wang W. A case of hypokalemia and proteinuria with a new mutation in the SLC12A3 Gene. *BMC Nephrol* 2018; **19**: 275 [PMID: 30340552 DOI: 10.1186/s12882-018-1083-2]

3 **Gu X**, Su Z, Chen M, Xu Y, Wang Y. Acquired Gitelman syndrome in a primary Sjögren syndrome patient with a SLC12A3 heterozygous mutation: A case report and literature review. *Nephrology (Carlton)* 2017; **22**: 652-655 [PMID: 28685938 DOI: 10.1111/nep.13045]

4 **Chen Y**, Zhang Z, Lin X, Pan Q, Zheng F, Li H. A novel compound heterozygous variant of the SLC12A3 gene in Gitelman syndrome pedigree. *BMC Med Genet* 2018; **19**: 17 [PMID: 29378538 DOI: 10.1186/s12881-018-0527-7]

5 **Xia MF**, Bian H, Liu H, Wu HJ, Zhang ZG, Lu ZQ, Gao X. Hypokalemia, hypomagnesemia, hypocalciuria, and recurrent tetany: Gitelman syndrome in a Chinese pedigree and literature review. *Clin Case Rep* 2017; **5**: 578-586 [PMID: 28469853 DOI: 10.1002/ccr3.874]

6 **Takeuchi Y**, Mishima E, Shima H, Akiyama Y, Suzuki C, Suzuki T, Kobayashi T, Suzuki Y, Nakayama T, Takeshima Y, Vazquez N, Ito S, Gamba G, Abe T. Exonic mutations in the SLC12A3 gene cause exon skipping and premature termination in Gitelman syndrome. *J Am Soc Nephrol* 2015; **26**: 271-279 [PMID: 25060058 DOI: 10.1681/ASN.2013091013]

7 **Zhou H**, Liang X, Qing Y, Meng B, Zhou J, Huang S, Lu S, Huang Z, Yang H, Ma Y, Luo Z. Complicated Gitelman syndrome and autoimmune thyroid disease: a case report with a new homozygous mutation in the SLC12A3 gene and literature review. *BMC Endocr Disord* 2018; **18**: 82 [PMID: 30409157 DOI: 10.1186/s12902-018-0298-3]

8 **Lee JW**, Lee J, Heo NJ, Cheong HI, Han JS. Mutations in SLC12A3 and CLCNKB and Their Correlation with Clinical Phenotype in Patients with Gitelman and Gitelman-like Syndrome. *J Korean Med Sci* 2016; **31**: 47-54 [PMID: 26770037 DOI: 10.3346/jkms.2016.31.1.47]

9 **Subasinghe CJ**, Sirisena ND, Herath C, Berge KE, Leren TP, Bulugahapitiya U, Dissanayake VHW. Novel mutation in the SLC12A3 gene in a Sri Lankan family with Gitelman syndrome & coexistent diabetes: a case report. *BMC Nephrol* 2017; **18**: 140 [PMID: 28446151 DOI: 10.1186/s12882-017-0563-0]

10 **Peng X**, Jiang L, Chen C, Qin Y, Yuan T, Wang O, Xing X, Li X, Nie M, Chen L. Increased urinary prostaglandin E2 metabolite: A potential therapeutic target of Gitelman syndrome. *PLoS One* 2017; **12**: e0180811 [PMID: 28700713 DOI: 10.1371/journal.pone.0180811]

11 **Kusuda T**, Hosoya T, Mori T, Ihara K, Nishida H, Chiga M, Sohara E, Rai T, Koike R, Uchida S, Kohsaka H. Acquired Gitelman Syndrome in an Anti-SSA Antibody-positive Patient with a SLC12A3 Heterozygous Mutation. *Intern Med* 2016; **55**: 3201-3204 [PMID: 27803420 DOI: 10.2169/internalmedicine.55.6390]

12 **Peng X**, Zhao B, Zhang L, Jiang L, Yuan T, Wang Y, Wang H, Ma J, Li N, Zheng K, Nie M, Li X, Xing X, Chen L. Hydrochlorothiazide Test as a Tool in the Diagnosis of Gitelman Syndrome in Chinese Patients. *Front Endocrinol (Lausanne)* 2018; **9**: 559 [PMID: 30319542 DOI: 10.3389/fendo.2018.00559]

13 **Al-Shibli A**, Yusuf M, Abounajab I, Willems PJ. Mixed Bartter-Gitelman syndrome: an inbred family with a heterogeneous phenotype expression of a novel variant in the CLCNKB gene. *Springerplus* 2014; **3**: 96 [PMID: 24711981 DOI: 10.1186/2193-1801-3-96]

14 **Makino S**, Tajima T, Shinozuka J, Ikumi A, Awaguni H, Tanaka S, Maruyama R, Imashuku S. Gitelman Syndrome in a School Boy Who Presented with Generalized Convulsion and Had a R642H/R642W Mutation in the SLC12A3 Gene. *Case Rep Pediatr* 2014; **2014**: 279389 [PMID: 25140267 DOI: 10.1155/2014/279389]

15 **Fujimura J**, Nozu K, Yamamura T, Minamikawa S, Nakanishi K, Horinouchi T, Nagano C, Sakakibara N, Nakanishi K, Shima Y, Miyako K, Nozu Y, Morisada N, Nagase H, Ninchoji T, Kaito H, Iijima K. Clinical and Genetic Characteristics in Patients With Gitelman Syndrome. *Kidney Int Rep* 2018; **4**: 119-125 [PMID: 30596175 DOI: 10.1016/j.ekir.2018.09.015]

16 **Gug C**, Mihaescu A, Mozos I. Two mutations in the thiazide-sensitive NaCl co-transporter gene in a Romanian Gitelman syndrome patient: case report. *Ther Clin Risk Manag* 2018; **14**: 149-155 [PMID: 29403282 DOI: 10.2147/TCRM.S150483]

17 **Mishima E**, Mori T, Sohara E, Uchida S, Abe T, Ito S. Inherited, not acquired, Gitelman syndrome in a patient with Sjögren's syndrome: importance of genetic testing to distinguish the two forms. *CEN Case Rep* 2017; **6**: 180-184 [PMID: 28819721 DOI: 10.1007/s13730-017-0271-4]

18 **Yang W**, Zhao S, Xie Y, Mo Z. A novel SLC12A3 homozygous c2039delG mutation in Gitelman syndrome with hypocalcemia. *BMC Nephrol* 2018; **19**: 362 [PMID: 30558554 DOI: 10.1186/s12882-018-1163-3]

19 **Balavoine AS**, Bataille P, Vanhille P, Azar R, Noël C, Asseman P, Soudan B, Wémeau JL, Vantyghem MC. Phenotype-genotype correlation and follow-up in adult patients with hypokalaemia of renal origin suggesting Gitelman syndrome. *Eur J Endocrinol* 2011; **165**: 665-673 [PMID: 21753071 DOI: 10.1530/EJE-11-0224]

World Journal of Clinical Cases

Submit a Manuscript: https://www.f6publishing.com

World J Clin Cases 2019 June 26; 7(12): 1529-1534

DOI: 10.12998/wjcc.v7.i12.1529

ISSN 2307-8960 (online)

CASE REPORT

Thoracotomy of an asymptomatic, functional, posterior mediastinal paraganglioma: A case report

Yi-Yu Yin, Bin Yang, Yeni Ait Ahmed, Hua Xin

ORCID number: Yi-Yu Yin (0000-0003-0351-4077); Bin Yang (0000-0001-6839-6388); Yeni Ait Ahmed (0000-0002-7726-9417); Hua Xin (0000-0001-6144-1908).

Author contributions: Yin YY contributed to study design and manuscript preparation and revision; Yang B contributed to literature research and clinical studies; Ahmed YA contributed to manuscript editing and language polishing; Xin H contributed to manuscript final version approval.

Informed consent statement: All study participants, or their legal guardian, provided informed written consent prior to study enrollment

Conflict-of-interest statement: None.

CARE Checklist (2016) statement: The authors have read the CARE Checklist (2016), and the manuscript was prepared and revised according to the CARE Checklist (2016).

Yi-Yu Yin, Bin Yang, Hua Xin, Department of Thoracic Surgery, China-Japan Union Hospital of Jilin University, Changchun 130000, Jilin Province, China

Yeni Ait Ahmed, National Institutes on Alcohol Abuse and Alcoholism, National Institutes of Health, Bethesda, MD 20892, United States

Corresponding author: Hua Xin, MD, PhD, Chief Doctor, Professor, Chief, Department of Thoracic Surgery, China-Japan Union Hospital of Jilin University, 126 Xiantai Street, Changchun 130000, Jinlin Province, China. yinjie17@mails.jlu.edu.cn
Telephone: +86-431-84995999
Fax: +86-431-84995999

Abstract

BACKGROUND

Paragangliomas in the mediastinum are rare, accounting for only 1%-2% of all paragangliomas and < 0.3% of all mediastinal tumors. Most paragangliomas are nonfunctional, therefore, asymptomatic functional paragangliomas in the left posterior mediastinum are extremely rare. Perioperative management including preoperative preparation, careful intraoperative procedures, and strict postoperative care is important, and one-stage surgical resection should be performed only after appropriate perioperative measures are undertaken. Because those tumors are rare, it is necessary to report known cases to raise awareness regarding them.

CASE SUMMARY

We report the case of a 47-year-old male who was admitted to our hospital with the chief complaints of intermittent tearing pain on the left side of the chest and back for more than 10 mo. A chest contrast-enhanced computed tomography scan revealed a round, solid mass in the left posterior mediastinum, with low-density cystic lesions in the middle, and no enlarged lymph nodes in the hilum or mediastinum (Figure 1). After the diagnosis of paraganglioma, the patient was preoperatively given an oral adrenoceptor blocking drug (phenoxybenzamine), and intravenous fluid resuscitation for two weeks, subsequently the patient underwent a one-stage resection of lesions via left thoracotomy. The patient's blood pressure increased to 220/120 mmHg when the tumor was touched, which could be relieved by symptomatic treatment such as accelerating liquid transfusion or other intervention to lower blood pressure. The patient recovered uneventfully after surgery, with no abnormal blood pressure or recurrence during one year of follow-up visits.

Manuscript source: Unsolicited manuscript

Received: January 11, 2019
Peer-review started: January 11, 2019
First decision: March 10, 2019
Revised: March 21, 2019
Accepted: April 18, 2019
Article in press: April 19, 2019
Published online: June 26, 2019

P-Reviewer: Takura T, Tu WJ
S-Editor: Ji FF
L-Editor: Wang TQ
E-Editor: Wu YXJ

CONCLUSION
Surgical resection is the preferred treatment for asymptomatic functional paragangliomas.

Key words: Mediastinal tumor; Paraganglioma; Pheochromocytoma; Hypertension; Case report

Core tip: We present a patient with paraganglioma located in the left posterior mediastinum. After the diagnosis of paraganglioma, the patient was preoperatively given an oral adrenoceptor blocking drug, along with intravenous fluid resuscitation for two weeks, and then underwent one-stage resection of lesions via left thoracotomy. The patient recovered after surgery, with no abnormal blood pressure or recurrence during one year of follow-up visits.

Citation: Yin YY, Yang B, Ahmed YA, Xin H. Thoracotomy of an asymptomatic, functional, posterior mediastinal paraganglioma: A case report. *World J Clin Cases* 2019; 7(12): 1529-1534
URL: https://www.wjgnet.com/2307-8960/full/v7/i12/1529.htm
DOI: https://dx.doi.org/10.12998/wjcc.v7.i12.1529

INTRODUCTION

Ninety percent of neuroendocrine tumors arise from chromaffin cells in the adrenal medulla and are commonly known as pheochromocytomas. The remaining 10% originate from neural crest progenitors located outside of the adrenal gland, and are called paragangliomas[1]. The paragangliomas that occur in the mediastinum are extremely rare, accounting for only 1%-2% of all paragangliomas and < 0.3% of all mediastinal tumors[2], with only about 150 cases reported in the literature[3]. Paragangliomas can be classified as functional or non-functional ones based on their ability to synthesize and release catecholamines[4]. Most paragangliomas are nonfunctional[2], therefore asymptomatic functional posterior mediastinal paragangliomas are very rare. According to documented cases[2,5,6], perioperative interventions including oral administration of alpha-receptor blocker (phenoxybenzamine) and full intravenous fluid resuscitation for two weeks, intraoperative avoidance of tumor irritation, and postoperative close monitoring are all necessary.

CASE PRESENTATION

Chief complaints

Intermittent tearing pain on the left side of the chest and back for more than 10 mo in a 47-year-old man.

History of present illness

The patient was admitted to our hospital for physical examination revealing lesions in the left posterior mediastinum space 6 d previously. On admission, the patient's blood pressure was 120/80 mmHg, pulse was 82 beats/min, breathing was 18 beats/min, and body temperature was 36.5 °C without headaches, palpitations, night sweats, weight loss, facial flushing, *etc*.

History of past illness

The patient had no history of hypertension.

Personal and family history

He had no history of cigarette smoking or alcohol use, and there were no similar cases in the family.

Physical examination upon admission

Physical examination was unremarkable.

Laboratory examinations

Plasma test of catecholamines yielded the following: Epinephrine 83 pg/mL, norepinephrine 420 pg/mL, and dopamine 82.6 pg/mL. Urine test showed epinephrine 3.22 μg/24 h, norepinephrine 224 μg/24 h, and dopamine 130.5 μg/24 h, suggesting that the tumor had neuroendocrine function.

Imaging examinations

A chest contrast-enhanced computed tomography (CT) scan revealed a round, solid mass in the left posterior mediastinum, with low-density cystic lesions in the middle, and no enlarged lymph nodes in the hilum or mediastinum (Figure 1). No multiple metastases were detected on the whole-body bone scan, which suggested a benign tumor. Preoperative ultrasound-guided biopsy result also indicated a paraganglioma.

FINAL DIAGNOSIS

The pathological diagnosis was paraganglioma with a tumor size of 6.5 cm × 6 cm × 4 cm and the capsule was incomplete. Immunohistochemistry analysis revealed the tumors to be: CK (-), EMA (-), vimentin (+), inhibinα (-), CD34 (-), S-100 (-), CD56 (+), CgA (+), SyN (+), and Ki-67 (<5%+) (Figure 2).

TREATMENT

The patient was placed in the right lateral decubitus position after general anesthesia with double-lumen endotracheal intubation. A 7 cm × 6 cm × 4 cm dark red mass was found on the left side, adjoining the T7-T8 vertebral body, with a clear border, rich blood supply, and incomplete capsule. The mass invaded the posterior chest wall and descending aorta adventitia. The patient's blood pressure increased to 220/120 mmHg paroxysmally when we touched the tumor. After accelerating the liquid transfusion and reducing blood pressure immediately, the patient's blood pressure became stable. Subsequently, the capsule of the tumor was peeled off sharply and bluntly. Resection of the tumor was achieved after transecting the nutrient artery derived from the descending aorta (Figure 3). The patient's blood pressure varied between 115/70 and 120/75 mmHg. The postoperative pathologic tests reported the lesion as a mass with a size of 6.5 cm × 6 cm × 4 cm. The gray-and-red section was soft, with a little capsule about 0.1 cm thick, and a pale-edged cystic degeneration of 2.5 cm-diameter in the central part (Figure 4).

OUTCOME AND FOLLOW-UP

The patient recovered uneventfully after surgery, and his serum catecholamine level recovered to the normal level on postoperative day 3, with no abnormal blood pressure or recurrence during one year of follow-up visits.

DISCUSSION

Paragangliomas most frequently occur in patients with an average age of 49 years irrespective of gender and only 3% of these tumors secrete catecholamines. Meanwhile, paravertebral paragangliomas occur in younger people, with an average age of 29 years and almost half of these tumors synthesize catecholamines[7]. Paragangliomas mainly occur in areas where the parasympathetic nerves are abundant in the body, such as the head, neck, mediastinum, adrenal glands, retroperitoneum, and even the bladder, duodenum, and thyroid[8]. Mediastinal paraganglioma is mainly concentrated in two areas: the aortic sinus sympathetic ganglion of the posterior mediastinum or the autonomic ganglion of the superior or middle mediastinum[9]. About 25% to 70% of extra-adrenal paraganglioma patients are characterized by symptoms and signs of excessive catecholamine secretion[10], mainly manifested as hypertension, facial flushing, palpitations, night sweats, *etc*. But the patient in the present case had no symptoms of excessive secretion of catecholamines and belonged to a normotensive pheochromocytoma patient. Such cases are rare. Detection of plasma biochemical markers (epinephrine, norepinephrine, and Chromogranin A) is the preferred laboratory test for pheochromocytoma and suspected paraganglioma[11]. For the localized and qualitative diagnosis of

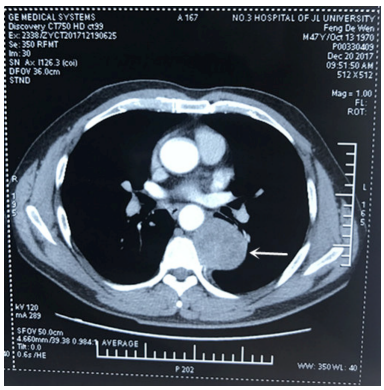

Figure 1 Chest-enhanced computed tomography image revealing a round, solid mass in the left posterior mediastinum, with low-density cystic lesions in the middle.

paraganglioma, CT and magnetic resonance imaging (MRI) are important imaging examination methods. CT scans of paragangliomas show isodensity or slightly lower density, and enhanced CT shows a significant enhancement. MRI T1W1 shows equal or low signal. T2W1 shows medium, high, or non-uniform mixed signals. DW1 shows a high signal. The enhanced scan shows a significant enhancement of the tumor mass[12]. When physical examinations reveal lesions in the posterior mediastinum, in addition to considering common neurogenic tumors such as schwannomas, rare ectopic tumors should also be considered to avoid misdiagnosis.

Surgical resection is the preferred treatment for paraganglioma. Thoracoscopic surgery can perfectly expose the operative field and show the fine structure of the lesions. In addition, compared with the traditional thoracic surgery, thoracoscopic surgery has the following benefits: Less trauma, less postoperative pain, speedy recovery, and shorter hospitalization[13]. However, because the tumor invades the posterior chest wall and the adventitia of the descending aorta, the thoracoscopic resection of the left posterior mediastinal functional paraganglioma has rarely been reported. Furthermore, cases of successful resection of the tumor in the first stage have rarely been reported, so we preferred a one-stage thoracotomy for safety reasons. Ma *et al*[14] also believe that although thoracoscopic surgery has been successfully applied in their reports, thoracotomy is still the best choice for tumors with abundant blood supply. Perioperative management is also extremely important, including adequate preoperative preparation, careful intraoperative procedures, and strict postoperative care. In the present case, the following procedures were undertaken: (1) Sufficient peripheral vasodilation before surgery, applying α-adrenoceptor blockers (phenoxybenzamine 40 mg/d, 3 times orally) for 2 wk; (2) Volume expansion, applying low molecular dextran 500 mL/d infusion for 2 wk; (3) Preoperative blood preparation; (4) Real-time monitoring of blood pressure fluctuations during the operation; (5) Closely monitoring blood pressure and heart rate changes after surgery, and maintaining water electrolyte balance; and (6) Review of relevant laboratory indexes after surgery.

Most of the paragangliomas are benign, with only 10% being malignant, and it is difficult to differentiate the benign and malignant tumors just based on their morphology[15]. The signs of malignant paraganglioma are metastasis and invasion into surrounding tissues, thus, pathological examination cannot determine the nature. Long-term follow-up visits are necessary to judge the effect of surgery.

CONCLUSION

Paraganglioma is a rare type of tumor, and asymptomatic functional paragangliomas occurring in the left posterior mediastinum are extremely rare. Surgical resection is the preferred method. In the management of such patients, adequate perioperative examination should be undertaken for an accurate diagnosis. One-stage surgical resection should only be performed after implementing suitable perioperative management. Because of the rarity of such tumors, it is necessary to report these cases to raise awareness regarding them.

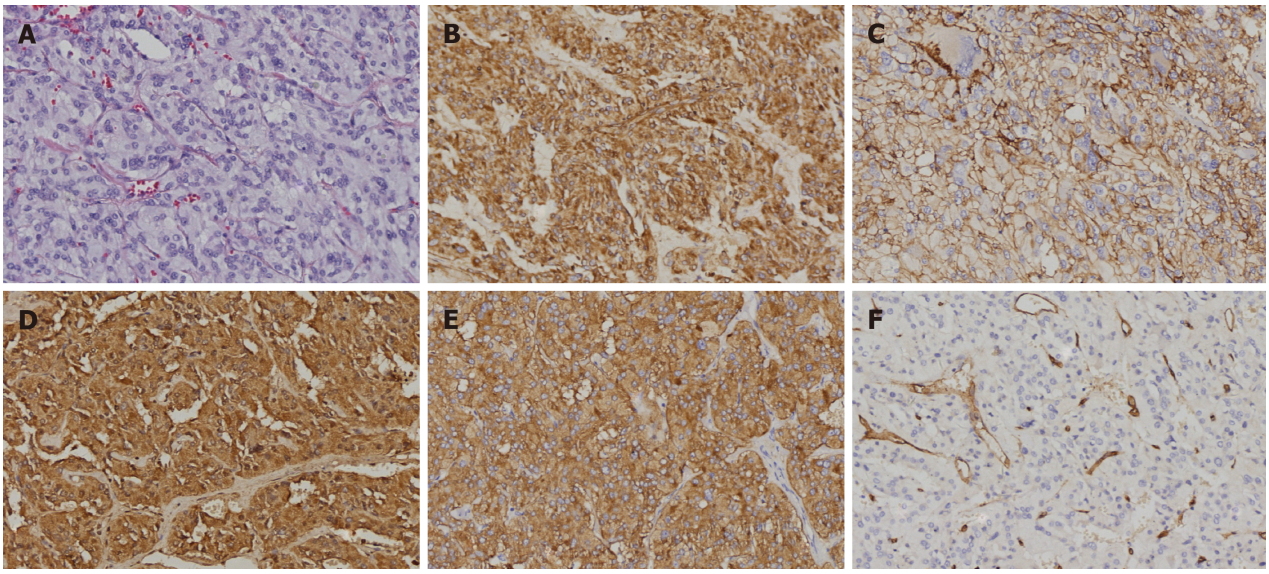

Figure 2 Pathology results. A: Routine hematoxylin and eosin staining; B-F: Immunohistochemical staining; B: Vimentin (+); C: CD56 (+); D: CgA Chromogranin A (+); E: Synaptophysin (+); F: CD34 (vessel+). Original magnification 200×.

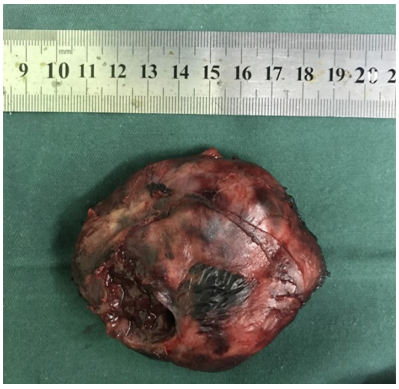

Figure 3 The tumor had a clear border, incomplete capsule.

Figure 4 The gray-and-red section was soft, with a little capsule whose thickness was about 0.1 cm, and the 2.5 cm-diameter pale-edged cystic degeneration in the central part.

REFERENCES

1 **Gunawardane PTK**, Grossman A. Phaeochromocytoma and Paraganglioma. *Adv Exp Med Biol* 2017; **956**: 239-259 [PMID: 27888488 DOI: 10.1007/5584_2016_76]
2 **Muñoz-Largacha JA**, Glocker RJ, Moalem J, Singh MJ, Litle VR. Incidental posterior mediastinal

paraganglioma: The safe approach to management, case report. *Int J Surg Case Rep* 2017; **35**: 25-28 [PMID: 28427002 DOI: 10.1016/j.ijscr.2017.03.040]
3 **Buchanan SN**, Radecki KM, Chambers LW. Mediastinal Paraganglioma. *Ann Thorac Surg* 2017; **103**: e413-e414 [PMID: 28431713 DOI: 10.1016/j.athoracsur.2016.10.031]
4 **Lack EE**, Cubilla AL, Woodruff JM. Paragangliomas of the head and neck region. A pathologic study of tumors from 71 patients. *Hum Pathol* 1979; **10**: 191-218 [PMID: 422190 DOI: 10.1016/S0046-8177(79)80008-8]
5 **Ulchaker JC**, Goldfarb DA, Bravo EL, Novick AC. Successful outcomes in pheochromocytoma surgery in the modern era. *J Urol* 1999; **161**: 764-767 [PMID: 10022680 DOI: 10.1016/S0022-5347(01)61762-2]
6 **Xia M**, Li HZ, Liu GH. Clinical experience with preoperative preparation for pheochromocytoma (report of 286 cases). *Zhonghua Miniao Waike Zazhi* 2014; 12
7 **Soomro NH**, Zahid AB, Zafar AA. Non-functional paraganglioma of the mediastinum. *J Pak Med Assoc* 2016; **66**: 609-611 [PMID: 27183947]
8 **Treglia G**, Giovanella L, Caldarella C, Bertagna F. A rare case of thyroid paraganglioma detected by ^{1}F-FDG PET/CT. *Rev Esp Med Nucl Imagen Mol* 2014; **33**: 320-321 [PMID: 24559939 DOI: 10.1016/j.remn.2013.11.004]
9 **Rakovich G**, Ferraro P, Therasse E, Duranceau A. Preoperative embolization in the management of a mediastinal paraganglioma. *Ann Thorac Surg* 2001; **72**: 601-603 [PMID: 11515906 DOI: 10.1016/S0003-4975(00)02293-1]
10 **Chen J**. [Clinicopathologic study of paraganglioma]. *Zhonghua Bing Li Xue Za Zhi* 2006; **35**: 494-496 [PMID: 17069706]
11 **Mazzaglia PJ**, Monchik JM. Limited value of adrenal biopsy in the evaluation of adrenal neoplasm: a decade of experience. *Arch Surg* 2009; **144**: 465-470 [PMID: 19451490 DOI: 10.1001/archsurg.2009.59]
12 **Huang X**, Liang QL, Jiang L, Liu QL, Ou WT, Li DH, Zhang HJ, Yuan GL. Primary Pulmonary Paraganglioma: A Case Report and Review of Literature. *Medicine (Baltimore)* 2015; **94**: e1271 [PMID: 26252294 DOI: 10.1097/MD.0000000000001271]
13 **Goto T**, Kadota Y, Mori T, Yamashita S, Horio H, Nagayasu T, Iwasaki A. Video-assisted thoracic surgery for pneumothorax: republication of a systematic review and a proposal by the guideline committee of the Japanese association for chest surgery 2014. *Gen Thorac Cardiovasc Surg* 2015; **63**: 8-13 [PMID: 25182971 DOI: 10.1007/s11748-014-0468-9]
14 **Ma L**, Mei J, Liu L. Thoracoscopic resection of functional posterior mediastinal paraganglioma: a case report. *J Thorac Dis* 2014; **6**: 1861-1864 [PMID: 25589992 DOI: 10.3978/j.issn.2072-1439.2014.12.30]
15 **Suh YJ**, Choe JY, Park HJ. Malignancy in Pheochromocytoma or Paraganglioma: Integrative Analysis of 176 Cases in TCGA. *Endocr Pathol* 2017; **28**: 159-164 [PMID: 28386672 DOI: 10.1007/s12022-017-9479-2]

Published By Baishideng Publishing Group Inc
7041 Koll Center Parkway, Suite 160, Pleasanton, CA 94566, USA
Telephone: +1-925-2238242
Fax: +1-925-2238243
E-mail: bpgoffice@wjgnet.com
Help Desk:https://www.f6publishing.com/helpdesk
https://www.wjgnet.com